

Neutral and ionic *N*-methyl phenylazo-3,5-(di-2-pyridyl)pyrazole photoswitches: Probes for reversible pH modulation by light

Sapna Singh,[‡] Archana Velloth,[‡] Rajani, Manu Goyal, Navneet Kaur, Sanjay Singh,* and Sugumar Venkataramani*

Department of Chemical Sciences, Indian Institute of Science Education and Research (IISER) Mohali.
Sector 81, SAS Nagar, Knowledge City, Manauli – 140306, Punjab, INDIA.

E-mail: sanjaysingh@iisermohali.ac.in and sugumarv@iisermohali.ac.in

[‡]Equally contributed.

Contents

| | | |
|-----------|---|----------|
| S1 | General methods | S2-S3 |
| S2 | Synthesis and characterization | S4-S10 |
| S3 | Analysis of photoswitching and thermal stability | S11-S27 |
| S4 | Kinetics studies | S28-S49 |
| S5 | Computational details | S50-S69 |
| S6 | pH modulation | S70-S85 |
| S7 | Compound characterization (¹ H and ¹³ C{ ¹ H} NMR) data | S86-S94 |
| S8 | References | S95-S96 |
| S9 | Cartesian coordinates | S97-S103 |

S1. General methods

Reagents and solvents: All the reagents (AR or LR grade) and solvents were purchased from commercially available sources such as Sigma Aldrich, Merck, Avra, Rankem, Spectrochem, and TCI, etc., and used without further purification. Dry solvents such as acetonitrile, etc was obtained from MBraun-SPS solvent purification system. HPLC or UV spectroscopic grade solvents have been used for photoswitching and kinetics studies. Milli-Q water was used for all spectroscopic studies in water. For column chromatography, pre-distilled solvents have been utilized.

Chromatography: Thin layer chromatography was performed on Merck Silica gel 60 F254 TLC plates, and the plates were visualized using UV chamber ($\lambda = 254$ nm). Column chromatography were performed over (100-200 mesh) silica gel and neutral alumina (Brockmann I grade).

NMR spectroscopy: ^1H , ^{19}F , ^{11}B , and ^{13}C NMR spectra were recorded in the deuterated solvents (CDCl_3 , D_2O , and $\text{DMSO}-d_6$) using Bruker Avance-III 400 MHz spectrometer with operational frequencies 400, 376.5, 128.3, and 100 MHz, respectively. All the spectra have been recorded with 16 scans for ^1H NMR and 512 scans for ^{13}C NMR. Chemical shift (δ) values are reported in parts per million (ppm) and coupling constants (J) are reported in Hz. Signals of residual solvent signals of CDCl_3 (7.26 ppm), D_2O (4.79 ppm), and $\text{DMSO}-d_6$ (2.50 ppm) have been used for internal calibration in ^1H NMR, whereas, the spectra have been calibrated using the corresponding signals of CDCl_3 (77.16 ppm) and $\text{DMSO}-d_6$ (39.52 ppm) in ^{13}C NMR. The signal multiplicities are abbreviated as singlet (s), doublet (d), triplet (t), quartet (q), doublet of doublets (dd), doublet of triplets (dt), triplet of doublets (td), triplet of doublets of doublets (tdd), doublet of doublet of doublets of doublets (dddd), multiplet (m), and broad (br).

HRMS: High resolution mass spectra (HRMS) have been recorded using Waters Synapt G2-Si Q-TOF or Synapt XS mass spectrometer. The ionization for those samples has been done using electrospray ionization (ESI) method, and the detections were done in both positive and negative modes.

M. P.: Melting points were recorded on SMP20 melting point apparatus and are uncorrected.

FT-IR studies: FT-IR spectra were recorded as a neat solid or neat liquid on a Bruker Alpha ZnSe ATR spectrometer, or as a KBr pellet on a Perkin Elmer Spectrum Two FTIR spectrometer.

UV-vis spectroscopic studies: UV-vis spectroscopic studies in the solution state have been carried out using an Agilent Cary 3500 and Cary 60 UV-vis NIR spectrophotometer at 1 nm resolution using quartz cuvettes.

Photoswitching studies and light sources: The analysis of photoswitching, and kinetics, measurements have been carried out using an Agilent Cary 60 UV-vis spectrophotometer connected with peltier and Bruker Avance-III 400 MHz spectrometer. For forward isomerization step (*E-Z*), samples were irradiated (in a quartz cuvette or quartz NMR tube) using a LED light source (SX-20 Applied Photophysics) or a KiloArc 1000W Xenon UV Lamp with a monochromator (1200 l/mm grating; slit width = 4 mm). The reverse photoisomerization (*Z-E*) has been induced by using SX-20 LED light source from Applied Photophysics and/or Kessil PR160L LED light sources of different wavelengths (427 and 525

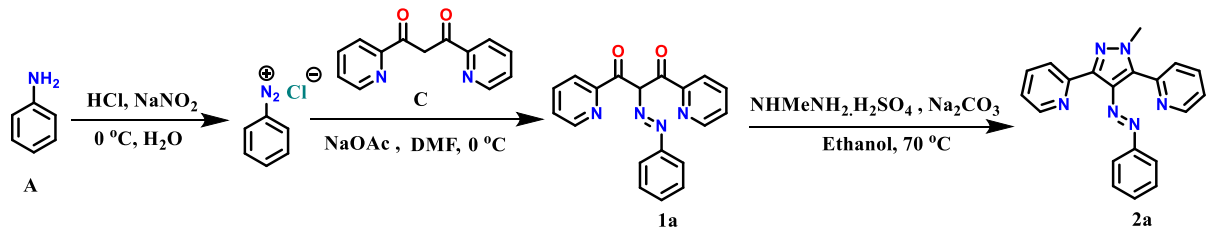
nm, FWHM = ~ 20 nm). PSS has been established by irradiating the sample for prolonged time such that no further spectral change is observed. For estimation of PSS composition, the samples have been irradiated in a quartz tube (NMR) or cuvette (UV-vis) using the above-mentioned light sources, and then immediately transferred to the spectrometers for measurement. For photoswitching experiments, different wavelengths were screened based on the $\pi-\pi^*$ and $n-\pi^*$ of the azo chromophore absorption bands, for forward and reverse isomerization steps, respectively. After screening and standardizing conditions, experiments were also conducted and analyzed by ^1H -NMR spectroscopy. For all derivatives, the PSS composition in the forward (*E*-*Z*) and reverse (*Z*-*E*) photoisomerization steps were determined in DMSO-*d*₆ and D₂O by ^1H -NMR spectroscopy. The excellent isomerization conversion in forward (*E*-*Z*) and moderate-to excellent recovery in reverse (*Z*-*E*) steps were observed.

Kinetics studies: Kinetics studies have done both using an Agilent Cary 60 UV-vis spectrophotometer with a Peltier controller for variable temperature. For kinetic studies, *E*-isomer was photoisomerized to *Z* isomer in quartz cuvette using 365 nm wavelength of light. After reaching to PSS, sample was placed in spectrometer and temperature was controlled by Peltier in UV-vis spectrometer at a constant temperature.

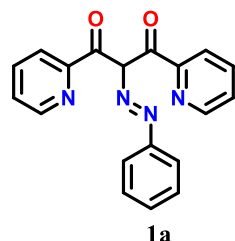
pH studies (buffers and adjusting various pH and measurement of pH): Buffer solutions ranging from pH 6-10.8 were prepared by adding NaOH (10 M) to solutions of phosphate buffer (pH = 7.4) and from pH 2.8-6 by adding standard 12 M HCl. The pH of the prepared solutions was measured with a Metrohm 913 pH Meter. All solution were prepared in Milli-Q water.

S2 Synthesis and Characterisation

S2.1. General procedures and characterisation data

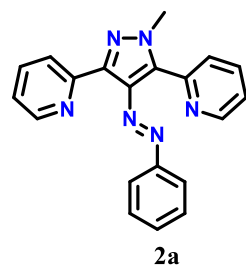


(E)-2-(Phenyldiazenyl)-1,3-di(pyridin-2-yl) propane-1,3-dione (1a): Aniline **A** (0.5 g, 5.37 mmol) was mixed in 2 ml of distilled water. To this mixture 37 % HCl (1.3ml) was added dropwise over 15 min at rt, then aq. NaNO₂ (0.46 g, 6.71 mmol) solution was slowly added at 0 °C. In other flask NaOAc (1.70 g, 21.48 mmol) and 1,3 di-pyridine propane-1,3-dione **C** (1.2 g, 5.37 mmol) were dissolved in DMF. Diazonium salt of aniline was added dropwise to the solution of **C** at 0 °C. Reaction was kept at room temperature for 2 hr. Reaction mixture was filtered and washed with 1:1 ethanol-H₂O mixture to get pure **1a**. Orange solid, 60% yield.



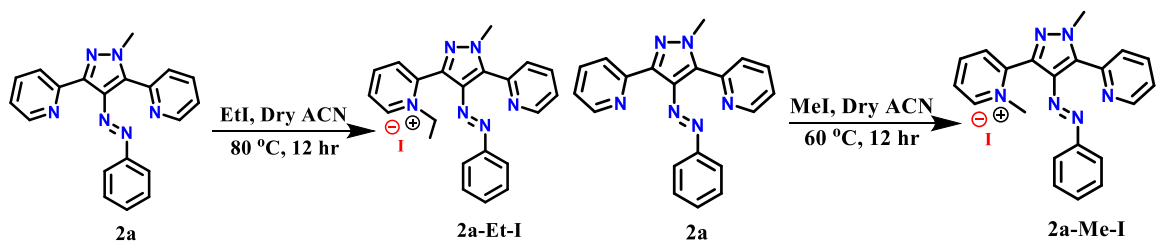
M. P. = 166-167 ¹H NMR (400 MHz, CDCl₃): δ 7.12 (t, *J* = 7.2 Hz, 1H), 7.19 (dd, *J* = 8.8, 7.6, 4.8, 1.0 Hz, 2H), 7.35 (t, *J* = 7.3 Hz, 2H), 7.42 (d, *J* = 7.6 Hz, 2H), 7.75 (tdd, *J* = 7.7, 3.7, 1.6 Hz, 2H), 8.03 (d, *J* = 7.8 Hz, 1H), 8.17 (d, *J* = 7.9 Hz, 1H), 8.22 (d, *J* = 4.2 Hz, 1H), 8.33 (d, *J* = 4.7 Hz, 1H), 13.87 (br, 1H) ppm; ¹³C{¹H} (100 MHz, CDCl₃): δ 116.0, 123.06, 123.11, 124.8, 125.7, 126.2, 129.5, 134.7, 136.7, 137.0, 142.2, 147.8, 148.3, 154.2, 155.4, 187.6, 189.2 ppm; HRMS-ESI: m/z C₁₉H₁₅N₄O₂ [M+H]⁺ calc. 330.1117, obs. 330.1120.

(E)-2,2'-(1-Methyl-4-(phenyldiazenyl)-1*H*-pyrazole-3,5-diyl)dipyridine (2a): The dione derivative **1a** (1.2 g, 3.76 mmol) was added into a mixture of *N*-methyl hydrazine sulphate (0.82 g, 5.64 mmol), and sodium carbonate (0.46 g, 5.64 mmol) in 15 ml ethanol. The reaction mixture was refluxed for 6-8 hrs and monitored by TLC. Upon completion, solvent was evaporated and the compound was purified by column chromatography by using neutral alumina and (20:80) ethyl acetate-hexane mixture as an eluent. Orange sticky liquid, 75% yield.

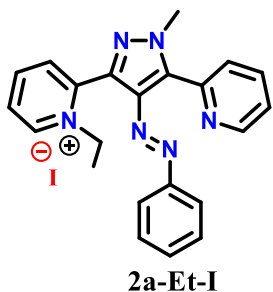


¹H NMR (400 MHz, DMSO-d₆): δ 4.04 (s, 3H), 7.46 (br, 6H), 7.54 (ddd, *J* = 7.5, 5.0, 0.9 Hz, 1H), 7.80 (d, *J* = 7.9 Hz, 1H), 7.84 (d, *J* = 7.8 Hz, 1H), 7.94 (td, *J* = 7.7, s1.4 Hz, 1H), 8.01 (td, *J* = 7.8, 1.7 Hz, 1H), 8.64 (d, *J* = 2.7 Hz, 1H), 8.80 (d, *J* = 4.2 Hz, 1H) ppm; ¹³C{¹H} (100 MHz, DMSO-d₆): δ 38.7, 121.9, 123.2, 124.0, 124.1, 126.9, 129.4, 130.7, 135.0, 136.4, 136.8, 137.1, 143.3, 147.9, 149.2, 149.5, 151.7, 152.2 ppm. HRMS-ESI: m/z C₂₀H₁₇N₆ [M+H]⁺ calc. 340.1436, obs. 341.1499; FT-IR (KBr, cm⁻¹): 690, 744, 794, 1426, 1456, 1588, 2946, 3049.

Synthesis of 2a-Et-I and 2a-Me-I: The solution of the compounds **2a** (0.34 g, 1 mmol) in dry MeCN has been charged in to an RB flask. Ethyl iodide or methyl iodide (1.5-3.0 eq.) was added to the solution and the reaction mixture was heated at 80-60 °C for 12 h. Reaction was monitored by TLC. After completion, the reaction was cooled to room temperature and diethyl ether was added to the reaction mixture and the resulting suspension was kept in refrigerator overnight. Afterwards, the precipitate was filtered and thoroughly washed with excess amount of diethyl ether. The filtered solid was passed through a neutral alumina column using MeOH-ethyl acetate (20:80) to yield the pure product. Yellow solid, 60-75 % yield.

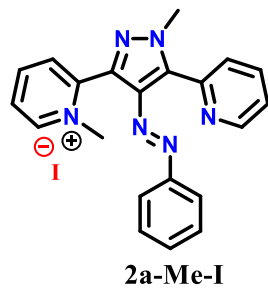


Iodide salt of (*E*)-1-ethyl-2-(1-methyl-4-(phenyldiazenyl)-5-(pyridin-2-yl)-1*H*-pyrazol-3-yl) pyridin-1-ium



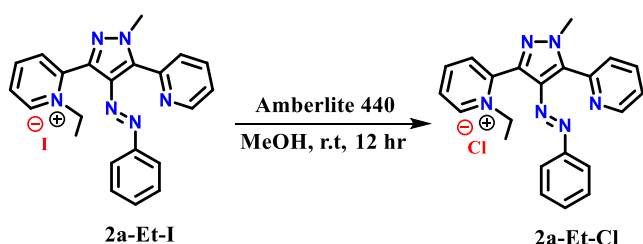
M. P. = 238-240 °C, ^1H (400 MHz, DMSO- d_6): δ 1.38 (t, J = 7.2 Hz, 3H), 4.27 (s, 3H), 4.51(q, J = 7.2 Hz, 2H), 7.35-7.41(m, 2H), 7.44-7.51 (m, 3H), 7.62-7.68 (m, 1H), 8.10-8.17 (m, 2H), 8.20(d, J = 7.9 Hz, 1H), 8.34(t, J = 7.4 Hz, 1H), 8.69 (t, J = 7.9 Hz, 1H), 8.90 (d, J = 4.7 Hz, 1H), 9.34 (d, J = 6.1 Hz, 1H) ppm; $^{13}\text{C}\{\text{H}\}$ (100 MHz, DMSO- d_6): δ 15.8, 40.0, 54.1, 122.1 (2C), 124.7, 127.4, 128.4, 129.4, 129.5, 130.7, 131.7, 135.4, 137.4, 142.0, 145.8, 146.2, 147.7, 149.7, 151.3 ppm. HRMS-ESI: m/z $C_{22}\text{H}_{21}\text{N}_6^+$ [M $^+$] calc. 369.1822, obs. 369.1815, [I] calc. 126.9050, obs. 126.9025; FT-IR (KBr, cm $^{-1}$): 691, 1014, 1102, 1164, 1457, 1477, 1581, 1624, 2932, 2987, 3005, 3039.

Iodide salt of (*E*)-1-methyl-2-(1-methyl-4-(phenyldiazenyl)-5-(pyridin-2-yl)-1*H*-pyrazol-3-yl) pyridin-1-ium

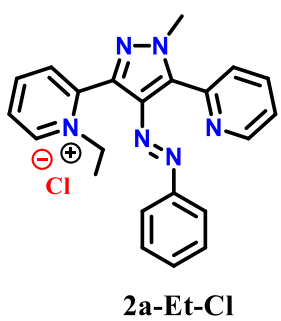


M. P. = 202-204 °C, ^1H (400 MHz, DMSO- d_6): δ 4.11 (s, 3H), 4.26 (s, 3H), 7.37-7.44 (m, 2H), 7.46-7.52 (m, 3H), 7.62-7.67 (m, 1H), 8.08-8.17 (m, 2H), 8.22 (d, J = 7.8 Hz, 1H), 8.30 (t, J = 6.5 Hz, 1H), 8.70 (t, J = 7.6 Hz, 1H), 8.89 (d, J = 4.6 Hz, 1H), 9.25 (d, J = 6.1 Hz, 1H) ppm; $^{13}\text{C}\{\text{H}\}$ (100 MHz, DMSO- d_6): δ 46.1, 53.0, 122.3, 124.8, 127.5, 128.0, 129.3, 129.6, 130.1, 131.0, 135.8, 137.5, 142.2, 146.0, 146.3, 147.1, 148.1, 149.9, 151.5; HRMS-ESI:m/z $C_{21}\text{H}_{19}\text{N}_6^+$ [M $^+$] calc. 355.1666, obs. 355.1298, [I] calc. 126.9050 , obs. 126.9033; IR (KBr, cm $^{-1}$): 690, 991, 1018, 1094, 1150, 1427, 1456, 1588, 2946, 3050.

Synthesis of 2a-Et-Cl: In a 5ml RBF, 2a-Et-I (0.37 g, 1.0 mmol) was dissolved in methanol (2 ml) and Amberlite 440° (0.34 g) was added. Reaction was stirred overnight at room temperature and filtered, dried to yield the desired product. Pale orange solid.

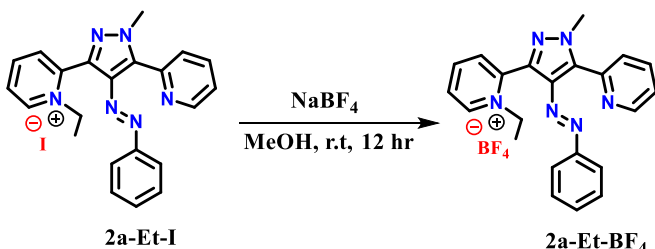


Chloride salt of (*E*)-1-ethyl-2-(1-methyl-4-(phenyldiazenyl)-5-(pyridin-2-yl)-1*H*-pyrazol-3-yl) pyridin-1-ium

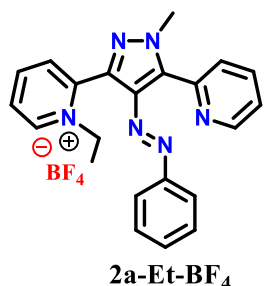


M. P. = 232-234 °C, ^1H (400 MHz, DMSO- d_6): δ 1.38 (t, J = 7.1 Hz, 3H), 4.27 (s, 3H), 4.51 (q, J = 7.1 Hz, 2H), 7.36-7.41 (m, 2H), 7.45-7.51 (m, 3H), 7.62-7.67 (m, 1H), 8.09-8.17 (m, 2H), 8.20 (d, J = 7.9 Hz, 1H), 8.34 (t, J = 7.0 Hz, 1H), 8.69 (t, J = 7.8 Hz, 1H), 8.90 (d, J = 4.4 Hz, 1H), 9.35 (d, J = 6.1 Hz, 1H), $^{13}\text{C}\{\text{H}\}$ (100 MHz, DMSO- d_6): δ 15.8, 40.0, 54.1, 122.1 (2C), 124.7, 127.4, 128.4, 129.4, 129.5, 130.7, 131.7, 135.4, 137.4, 142.0, 145.8, 146.2, 147.7, 149.7, 151.3 ppm; HRMS-ESI: m/z C₂₂H₂₁N₆⁺ [M⁺] calc. 369.1822, obs. 369.1842, [Cl⁻] calc. 34.9694, obs. 34.9698 ; IR (KBr, cm⁻¹): 622, 693, 1015, 1104, 1163, 1396, 1455, 1477, 1581, 1624, 2898, 2947, 3038.

Synthesis of 2a-Et-BF₄: In a 5ml RBF, **2a-Et-I** (0.37 g, 1 mmol) was dissolved in methanol (2 ml) and sodium tetrafluoroborate (0.33g, 3 mmol) was added. The reaction mixture was stirred at room temp overnight. Afterwards, the reaction mixture was filtered off and dried. Further DCM was added to dissolve the product and excess sodium salt was filtered off. Solvent was evaporated to yield the desired product as dark orange solid.

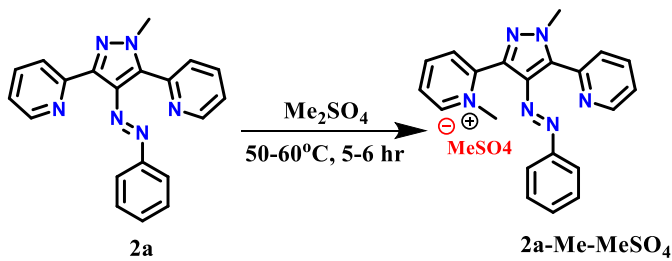


Tetrafluoroborate salt of (*E*)-1-ethyl-2-(1-methyl-4-(phenyldiazenyl)-5-(pyridin-2-yl)-1*H*-pyrazol-3-yl)pyridin-1-i um

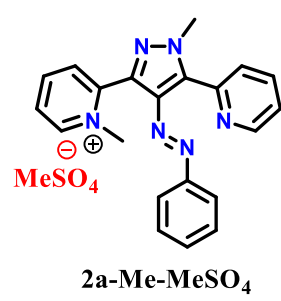


M. P. = 240-241 °C, ^1H NMR (400 MHz, DMSO- d_6): δ 1.38 (t, J = 7.2 Hz, 3H), 4.27 (s, 3H), 4.51 (q, J = 7.2 Hz, 2H), 7.35-7.40 (m, 2H), 7.45-7.50 (m, 3H), 7.62-7.67 (m, 1H), 8.10-8.17 (m, 2H), 8.20 (d, J = 7.8 Hz, 1H), 8.34 (t, J = 7.4 Hz, 1H), 8.69 (t, J = 7.8 Hz, 1H), 8.89 (d, J = 4.8 Hz, 1H), 9.33 (d, J = 6.1 Hz, 1H) ppm; $^{13}\text{C}\{\text{H}\}$ (100 MHz, DMSO- d_6): δ 15.9, 40.0, 54.2, 122.2, 124.7, 127.5, 128.4, 129.6, 130.7, 131.8, 135.5, 137.4, 138.8, 142.0, 145.9 (2C), 146.2, 147.8, 149.8, 151.3 ppm; ^{19}F NMR (376.5 MHz, DMSO- d_6): δ -148.2 ppm; ^{11}B NMR (128.3 MHz, DMSO- d_6): δ -1.3 ppm; HRMS-ESI: m/z C₂₂H₂₁N₆⁺ [M⁺] calc. 369.1822, obs. 369.1830, [BF₄⁻] calc. 87.0035, obs. 87.0017; IR (KBr, cm⁻¹): 533, 622, 691, 1063, 1083, 1164, 1458, 1478, 1581, 1624, 2856, 2929, 3040.

Synthesis of 2a-Me-MeSO₄: The solution of **2a** (0.34 g, 1 mmol) in dry MeCN has been charged in to a RB flask. Dimethyl sulfate (0.9 mmol) was added to the solution and the reaction mixture was then heated at 50-60 °C for 5-6 h. The reaction was monitored by TLC. After completion, the reaction mixture was cooled to room temperature and diethyl ether was added to the reaction mixture and the resulting suspension was kept in a refrigerator overnight. Afterwards, the precipitate was filtered and thoroughly washed with excess amount of diethyl ether. The filtered solid was passed through a neutral alumina column using MeOH-ethyl acetate (20:80) to give the pure product of **2a-Me-MeSO₄**. Orange sticky liquid, 55% yield.

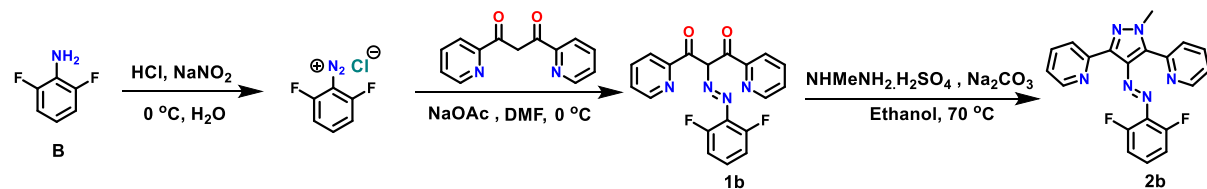


Methylsulfate salt of (*E*)-1-methyl-2-(1-methyl-4-(phenyldiazenyl)-5-(pyridin-2-yl)-1*H*-pyrazol-3-yl)pyridin-1-ium

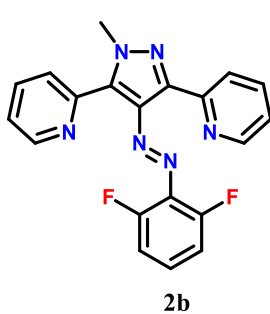


¹H (400 MHz, DMSO-d₆): δ 3.37 (s, 3H), 4.12 (s, 3H), 4.26(s, 3H), 7.37-7.44 (m, 2H), 7.46-7.52(m, 3H), 7.62-7.67 (m, 1H), 8.08-8.17(m, 2H), 8.22(d, J = 7.8 Hz, 1H), 8.30 (t, J = 6.5 Hz, 1H), 8.70 (t, J = 7.6 Hz, 1H), 8.89 (d, J = 4.6 Hz, 1H), 9.25 (d, J = 5.4 Hz, 1H) ppm; ¹³C{¹H} (100 MHz, DMSO-d₆): δ 40.0, 46.1, 53.0, 122.3, 124.8, 127.5, 128.0, 129.3, 129.6, 130.1, 131.0, 135.8, 137.5, 142.2, 146.0, 146.3, 147.1, 148.1, 149.9, 151.5 ppm; HRMS-ESI: m/z C₂₁H₁₉N₆⁺ [M⁺] calc. 355.1666, obs. 355.1648, [MeSO₄⁻] calc. 110.9752, obs. 110.9722 ; FT-IR (KBr, cm⁻¹): 584, 619, 692, 749, 799, 1016, 1100, 1260, 1461, 1626, 2854, 2925, 2961.

Synthesis of 2b:

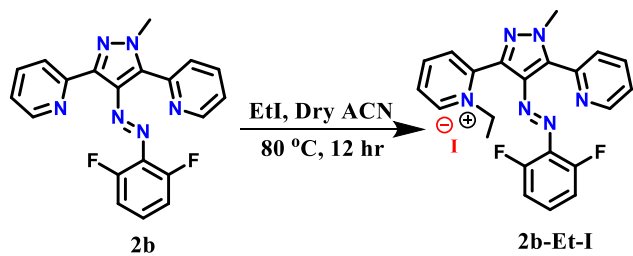


(*E*)-2,2'-(4-((2,6-difluorophenyl)diazenyl)-1-methyl-1*H*-pyrazole-3,5-diyl)dipyridine (2b): Similar procedure was adapted as **2a** for diazotization of 2,6 difluoro aniline **B**. Reaction was proceeded further without isolation of **1b**. Reaction mixture was filtered and washed with 1:1 ethanol-H₂O mixture to get pure **2b**. Pale orange solid, 85% yield.

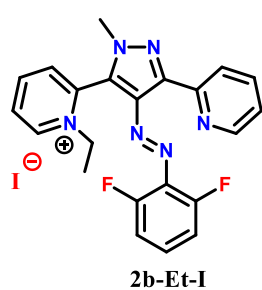


M. P. = 144-146 °C, ¹H (400 MHz, DMSO-d₆): δ 4.02 (s, 3H), 7.20-7.27 (m, 1H), 7.31-7.46 (m, 3H), 7.52-7.58 (m, 1H), 7.78-7.86 (m, 2H), 7.90 (t, J = 8 Hz, 1H), 8.01 (t, J = 7.8 Hz, 1H), 8.62 (d, J = 4 Hz, 1H), 8.79 (d, J = 4.2 Hz, 1H) ppm; ¹³C{¹H} (100 MHz, DMSO-d₆): δ 38.7, 103.2 (d, J = 24.8 Hz), 118.5 (dd, J = 11.1, 3.6 Hz), 118.8 (dd, J = 17.9, 2.9 Hz), 123.3, 124.2 (2C), 127.1, 135.1, 136.4, 136.9, 137.9, 140.6 (d, J = 5.9 Hz), 140.7 (d, J = 6.1 Hz), 143.9, 147.5, 149.5 (d, J = 31.1 Hz), 151.3, 155.2 (dd, J = 252.9, 2.26 Hz) 158.4 (dd, J = 243.4, 2.17 Hz) ppm; ¹⁹F NMR (376.5 MHz, DMSO-d₆): δ -116.7 (d, J = 16.2 Hz), -129.3 (d, J = 16.4 Hz) ppm; HRMS-ESI: m/z C₂₀H₁₅F₂N₆⁺ [M+H⁺] calc. 377.1404, obs. 377.1453.

Synthesis of 2b-Et-I: The procedure followed for the synthesis of **2a-Et-I** and **2a-Me-I** was followed to synthesize the desired product **2b-Et-I**. Dark orange solid. Yield = 75%.



Iodide salt of (*E*)-2-((2,6-difluorophenyl) diazenyl)-1-methyl-3-(pyridin-2-yl)-1*H*-pyrazol-5-yl)-1-ethylpyridin-1-ium



¹H (400 MHz, DMSO-*d*₆): δ 1.36 (t, *J* = 7.2 Hz, 3H), 4.28 (s, 3H), 4.48(d, *J* = 7.2 Hz, 2H), 7.28-7.34 (m, 1H), 7.38-7.46 (m, 2H), 8.13-8.21 (m, 3H), 8.29-8.35 (m, 1H), 8.69 (t, *J* = 7.8 Hz, 1H), 8.90 (d, *J* = 4.6 Hz, 1H), 9.36 (d, *J* = 6.1 Hz, 1H) ppm; ¹³C{¹H} (100 MHz, DMSO-*d*₆): δ 15.8, 54.0, 59.7, 103.0 (d, *J* = 24.9 Hz), 115.2, 118.7 (dd, *J* = 30.6, 22.4 Hz), 120.0 (dd, *J* = 32.5, 24.7 Hz), 124.9, 127.7, 128.3, 129.4, 130.4, 131.0, 135.8, 137.6, 142.8, 146.0 (d, *J* = 17.2 Hz), 147.4, 149.8, 155.4 (dd, *J* = 256.0, 1.8 Hz), 158.3 (dd, *J* = 246.6, 2.4 Hz), 162.3 ppm; ¹⁹F NMR (376.5 MHz, DMSO-*d*₆): δ -115.5 (d, *J* = 16.5 Hz), -116.2 (d, *J* = 16.1 Hz), -126.0 (d, *J* = 17.0 Hz), -129.9 (d, *J* = 15.8 Hz) ppm; HRMS-ESI: m/z C₂₂H₁₉F₂N₆⁺ [M⁺] calc. 405.1634, obs. 405.1448; [I⁻] calc. 126.9050, obs. 126.9043; FT-IR (KBr, cm⁻¹): 1014, 1102, 1164, 1457, 1478, 1581, 1624, 2932, 2987, 3005, 3039.

S2.2 Crystallographic data and refinement details of complexes **2a-Et-I** and **2a-Me-I**

Single crystal X-ray diffraction data for complexes **2a-Et-I** and **2a-Me-I** were acquired employing a Rigaku XtaLAB mini diffractometer outfitted with a Mercury375M CCD detector. MoK α radiation ($\lambda = 0.71073 \text{ \AA}$) was utilized with omega scans. Throughout data collection, the detector distance remained constant at 49.9 mm (constant), while the detector was positioned at $2\theta = 29.85^\circ$ (fixed) for all datasets. Data collection and reduction were performed using CrysAlisPro 1.171.38.46, and crystal structures were resolved utilizing the OLEX2¹ package with SHELXT² and the structures were refined using SHELXL³. All atoms, excluding hydrogen, underwent anisotropic refinement. All visual representations were crafted using Mercury 2020.3.0.

Table S2.1: Crystallographic data for complexes **2a-Et-I and **2a-Me-I****

| Compound | 2a-Et-I | 2a-Me-I |
|---|--------------------|--------------------|
| Chemical formula | $C_{22}H_{21}IN_6$ | $C_{21}H_{19}IN_6$ |
| Molar mass | 496.35 | 482.32 |
| Crystal system | monoclinic | Monoclinic |
| Space group | P2 ₁ /c | P2 ₁ /c |
| T [K] | 250.00(10) | 293(2) |
| a [\AA] | 11.6528(9) | 9.2634(3) |
| b [\AA] | 18.0105(10) | 11.5165(4) |
| c [\AA] | 10.8343(8) | 19.7935(9) |
| α [$^\circ$] | 90 | 90 |
| β [$^\circ$] | 106.939(8) | 95.013(3) |
| γ [$^\circ$] | 90 | 90 |
| V [\AA^3] | 2175.2(3) | 2103.53(14) |
| Z | 4 | 4 |
| ρ (calcd.) [$\text{g}\cdot\text{cm}^{-3}$] | 1.516 | 1.523 |
| $\mu(\text{Mo-K}\alpha)$ [mm^{-1}] | 1.492 | 1.540 |
| Reflections collected | 15732 | 23386 |
| Independent reflections | 3841 | 7403 |
| Data/restraints/parameters | 3841/0/264 | 7403/0/256 |
| R1, wR ₂ [I>2 σ (I)] ^[a] | 0.0366, 0.0776 | 0.0541, 0.1603 |
| R1, wR ₂ (all data) ^[a] | 0.0540, 0.0905 | 0.0734, 0.1922 |
| GOF | 1.073 | 1.070 |

[a] $R1 = \sum |F_O| - |F_C| | / \sum |F_O|$, $wR_2 = [\sum w (|F_O|^2 - |F_C|^2)^2 / \sum w |F_O|^2]^1/2$

Crystallographic details:

The solid-state structure of complexes **2a-Et-I** and **2a-Me-I** were determined by the single-crystal X-ray diffraction method. Complexes **2a-Et-I** and **2a-Me-I** crystallized from methanol solution in open-air condition and needle shaped crystals were obtained. Compounds **2a-Et-I** and **2a-Me-I** crystallized in the monoclinic system with $P2_1/c$ space group. The single-crystal X-ray structure showed that in complex **2a-Et-I**, the ethyl group and in complex **2a-Me-I**, the methyl group are connected to N-atom of the respective pyridine moiety and overall net cationic charge was neutralized with the iodide counter anion. The azo group in both the complexes showed the E-configuration.

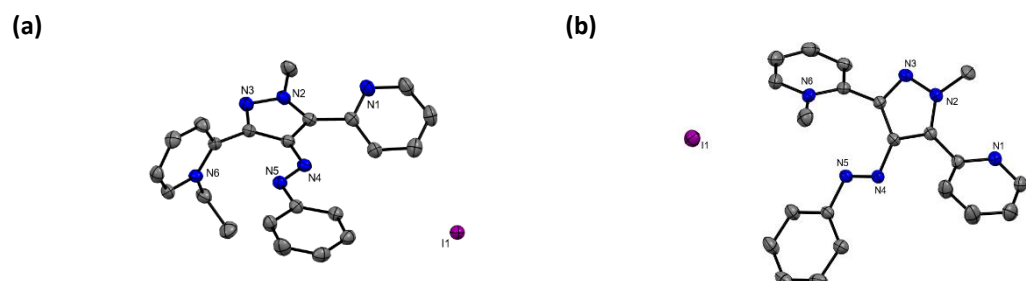


Figure S2.1. (a) Solid-state structure of complex **2a-Et-I**. All hydrogen atoms have been omitted for clarity. Selected bond lengths [\AA] and bond angles [$^\circ$]: N5-N4 1.366(5), N3-N2 1.257(4), N1-C2 1.514(5), N1-C3 1.352(5), N1-C7 1.353(5), C7-N1-C2 122.2(3), C3-N1-C7 120.8(4), C3-N1-C2 116.9(4), N2-N3-C9 113.6(3), N3-N2-C17 114.4(3); (b) Solid state structure of complex **2a-Me-I**. Selected bond lengths [\AA] and bond angles [$^\circ$]: N5-N4 1.263(3), N3-N2 1.355(3), N1-C1 1.338(4), N1-C5 1.341(3), N2-C7 1.459(3), C1-N1-C5 117.2(3), C6-N2-N3 112.96(18), N3-N2-C7 117.6(2), N4-N5-C16 114.7(2).

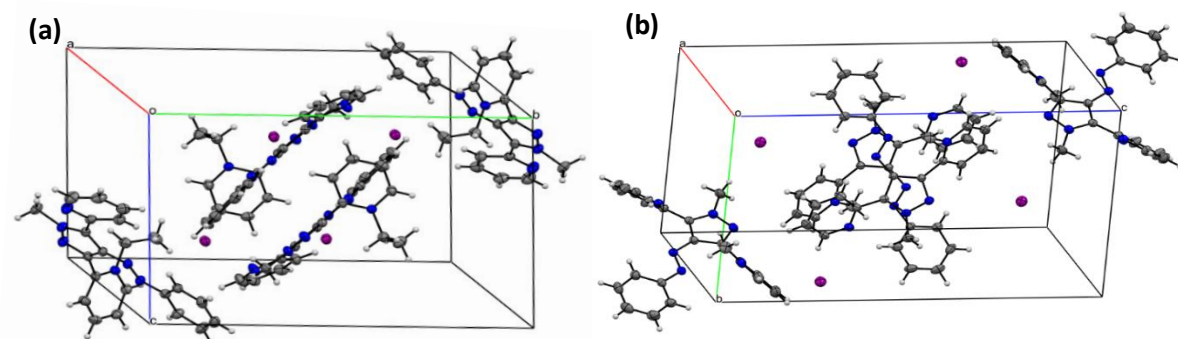


Figure S2.2. (a) Packing arrangement of complex **2a-Et-I** in the unit cell. (b) Packing arrangement of complex **2a-Me-I** in the unit cell.

S3. Analysis of photoswitching and thermal stability

S3.1 UV-vis spectroscopic studies

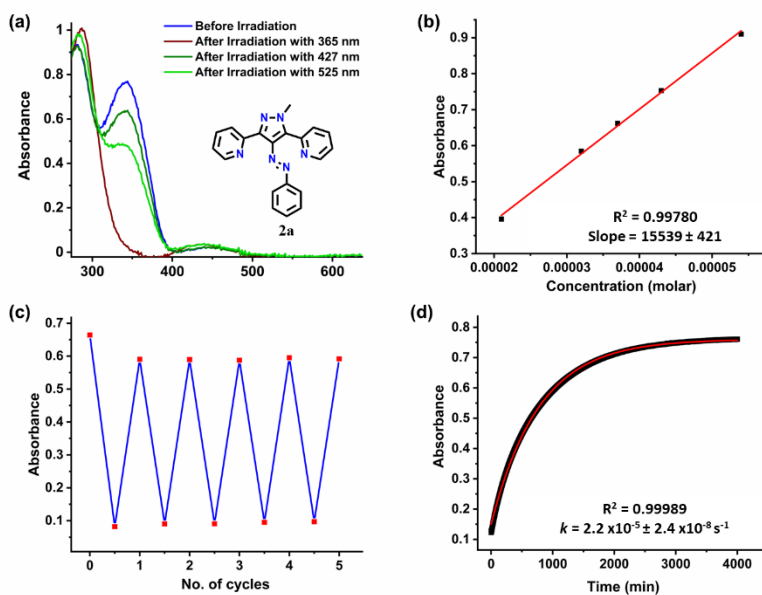


Figure S3.1. UV-Vis spectroscopic data of **2a**: (a) Photoswitching studies performed in DMSO (51 μM) (forward with 365 nm in brown and 525 nm in light green in color); (b) Estimation of the molar absorption coefficient for $\pi-\pi^*$ absorption maxima; (c) Photoswitching stability test upto five cycles in DMSO (forward isomerization step: 365 nm; reverse isomerization step: 427 nm) and (d) First order thermal reverse isomerization kinetics plot and exponential fit at 70 °C.

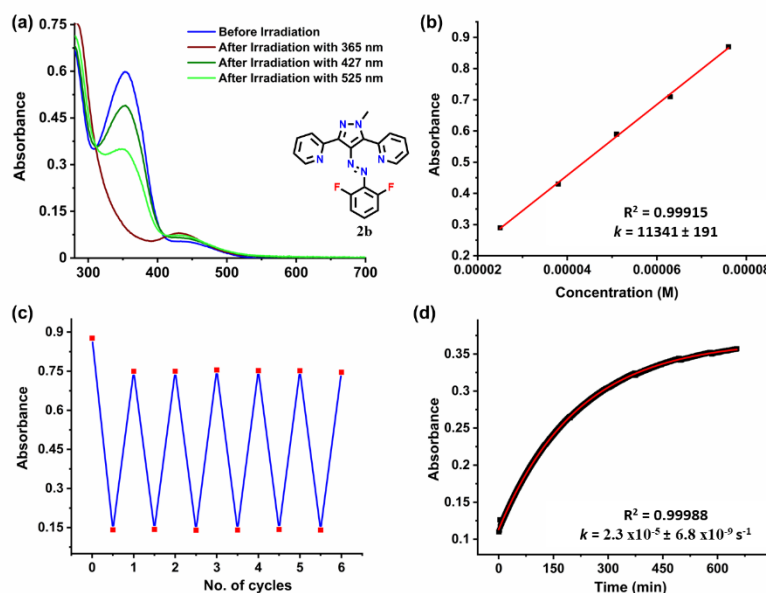


Figure S3.2. UV-Vis spectroscopic data of **2b**: (a) Photoswitching studies performed in DMSO (53 μM) (forward with 365 nm in brown and 525 nm in light green in color); (b) Estimation of the molar absorption coefficient for $\pi-\pi^*$ absorption maxima; (c) Photoswitching stability test upto six cycles in DMSO (forward isomerization step: 365 nm; reverse isomerization step: 427 nm) and (d) First order thermal reverse isomerization kinetics plot and exponential fit at 70 °C.

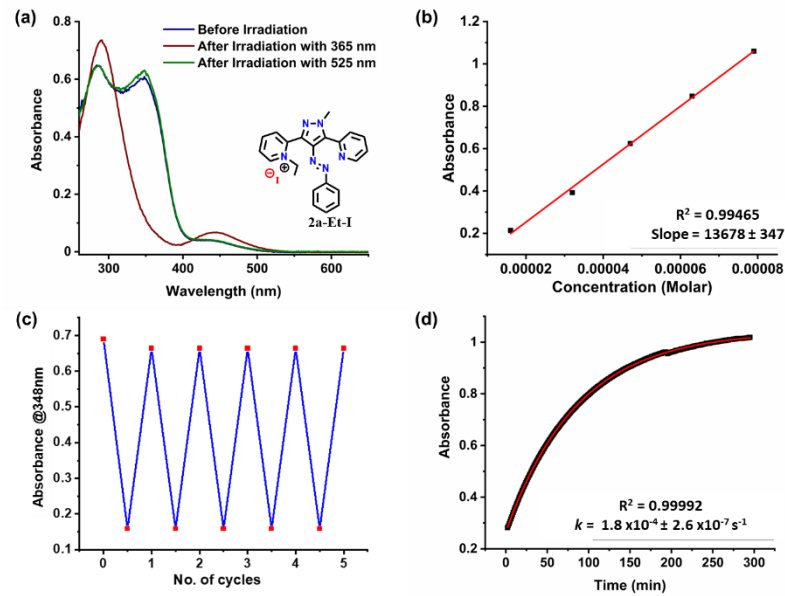


Figure S3.3. UV-Vis spectroscopic data of **2a-Et-I**: (a) Photoswitching studies performed in DMSO (43 μM); (b) Estimation of the molar absorption coefficient for $\pi-\pi^*$ absorption maxima; (c) Photoswitching stability test upto five cycles in DMSO (forward isomerization step: 365 nm; reverse isomerization step: 525 nm) and (d) First order thermal reverse isomerization kinetics plot and exponential fit at 70 °C.

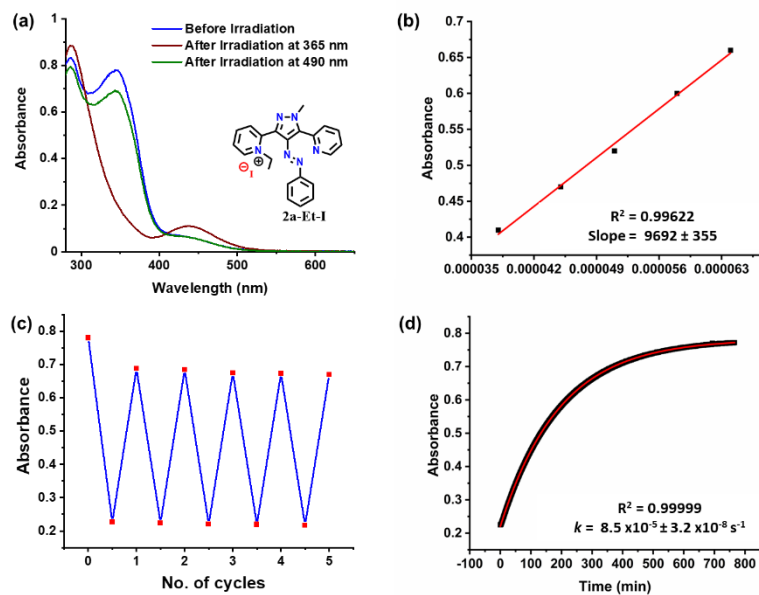


Figure S3.4. UV-Vis spectroscopic data of **2a-Et-I**: (a) Photoswitching studies performed in H_2O (77 μM); (b) Estimation of the molar absorption coefficient for $\pi-\pi^*$ absorption maxima; (c) Photoswitching stability test upto five cycles in H_2O (forward isomerization step: 365 nm; reverse isomerization step: 525 nm) and (d) First order thermal reverse isomerization kinetics plot and exponential fit at 70 °C.

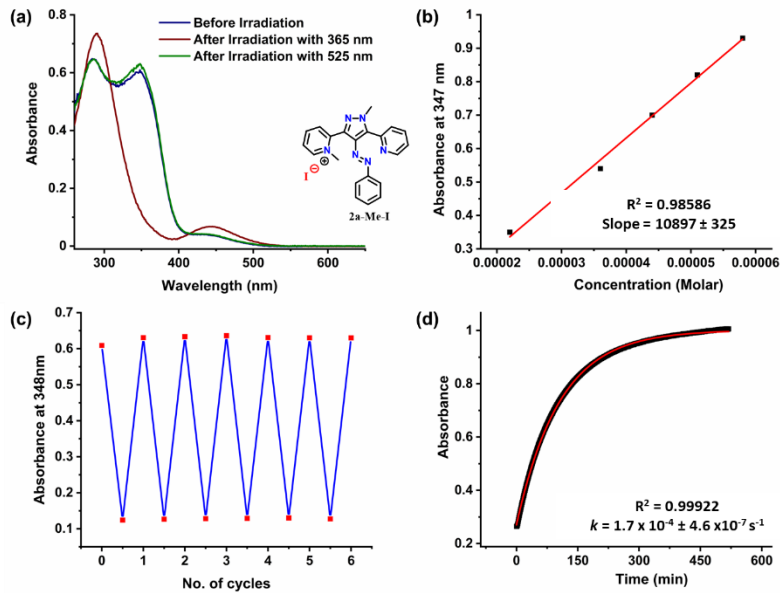


Figure S3.5. UV-Vis spectroscopic data of **2a-Me-I**: (a) Photoswitching studies performed in DMSO (56 μM); (b) Estimation of the molar absorption coefficient for $\pi-\pi^*$ absorption maxima; (c) Photoswitching stability test upto five cycles in DMSO (forward isomerization step: 365 nm; reverse isomerization step: 525 nm) and (d) First order thermal reverse isomerization kinetics plot and exponential fit at 70 °C.

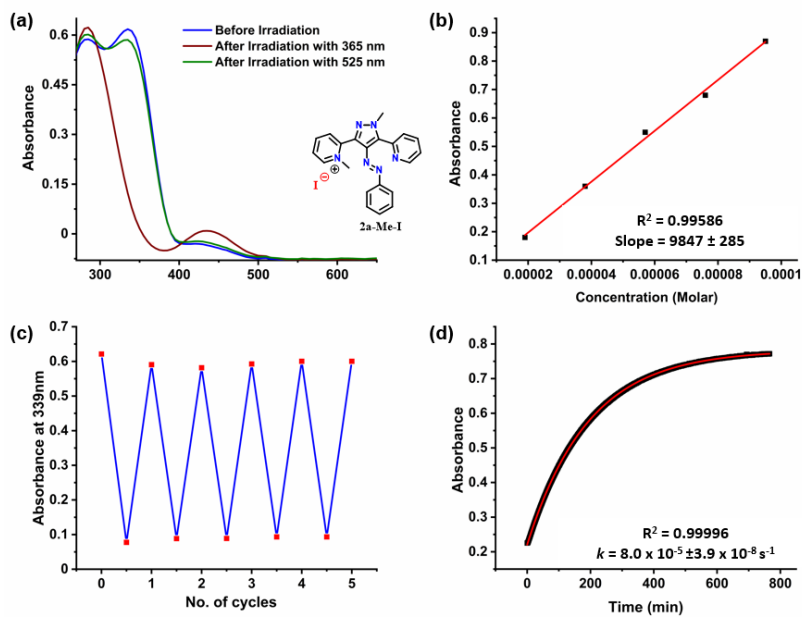


Figure S3.6. UV-Vis spectroscopic data of **2a-Me-I**: (a) Photoswitching studies performed in H₂O (61 μM); (b) Estimation of the molar absorption coefficient for $\pi-\pi^*$ absorption maxima; (c) Photoswitching stability test upto five cycles in H₂O (forward isomerization step: 365 nm; reverse isomerization step: 525 nm) and (d) First order thermal reverse isomerization kinetics plot and exponential fit at 70 °C

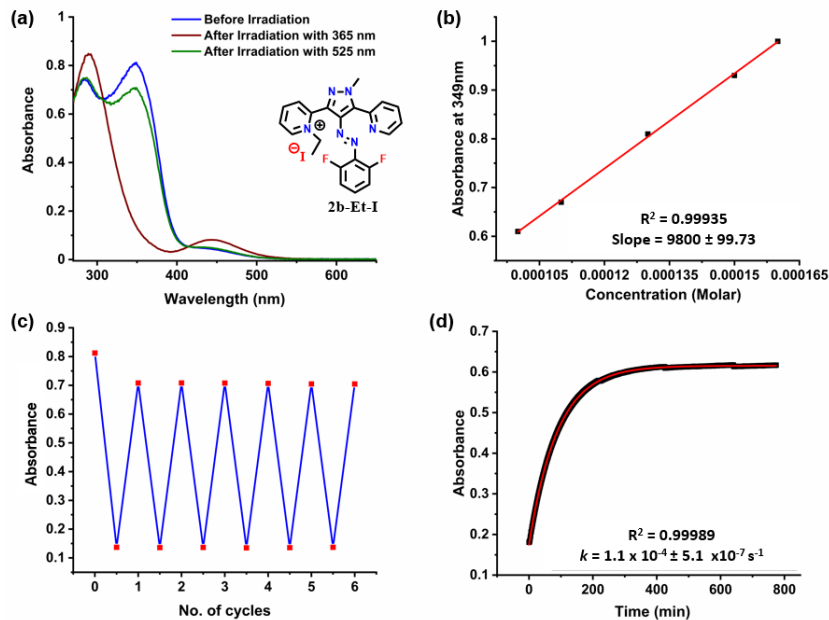


Figure S3.7. UV-Vis spectroscopic data of **2b-Et-I**: (a) Photoswitching studies performed in H_2O (81 μM); (b) Estimation of the molar absorption coefficient for $\pi-\pi^*$ absorption maxima; (c) Photoswitching stability test upto five cycles in H_2O (forward isomerization step: 365 nm; reverse isomerization step: 525 nm) and (d) First order thermal reverse isomerization kinetics plot and exponential fit at 70 $^\circ\text{C}$.

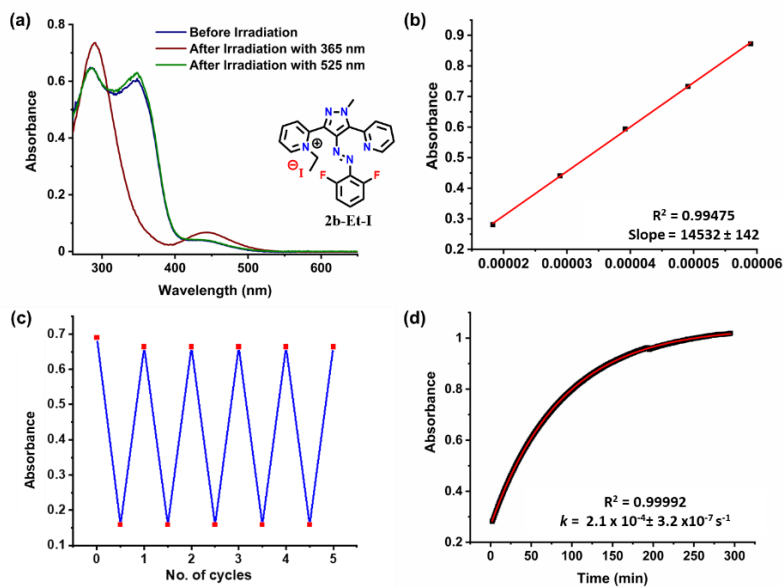


Figure S3.8. UV-Vis spectroscopic data of **2b-Et-I**: (a) Photoswitching studies performed in DMSO (42 μM); (b) Estimation of the molar absorption coefficient for $\pi-\pi^*$ absorption maxima; (c) Photoswitching stability test upto five cycles in DMSO (forward isomerization step: 365 nm; reverse isomerization step: 525 nm) and (d) First order thermal reverse isomerization kinetics plot and exponential fit at 70 $^\circ\text{C}$.

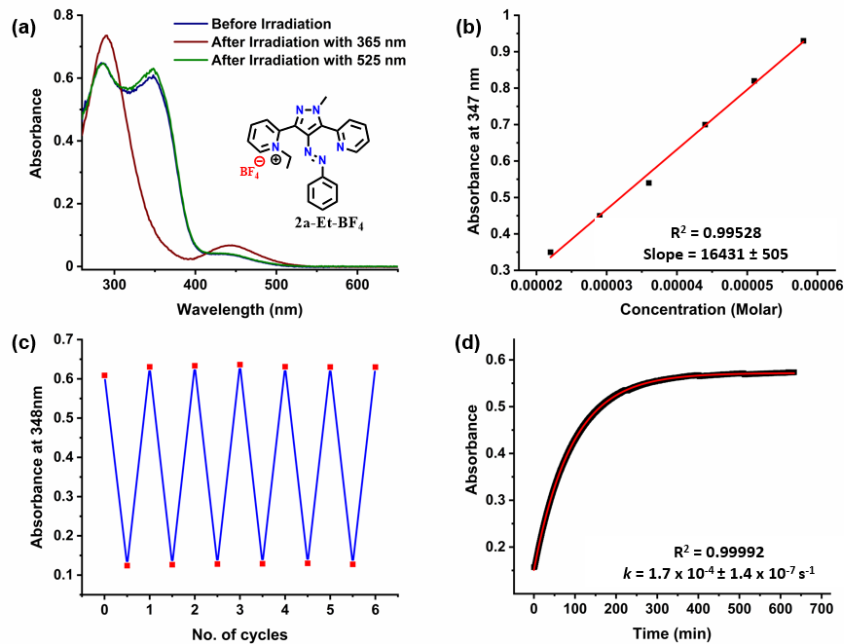


Figure S3.9. UV-Vis spectroscopic data of **2a-Et-BF₄**: (a) Photoswitching studies performed in DMSO (40 μM); (b) Estimation of the molar absorption coefficient for $\pi-\pi^*$ absorption maxima; (c) Photoswitching stability test upto five cycles in DMSO (forward isomerization step: 365 nm; reverse isomerization step: 525 nm) and (d) First order thermal reverse isomerization kinetics plot and exponential fit at 70 °C.

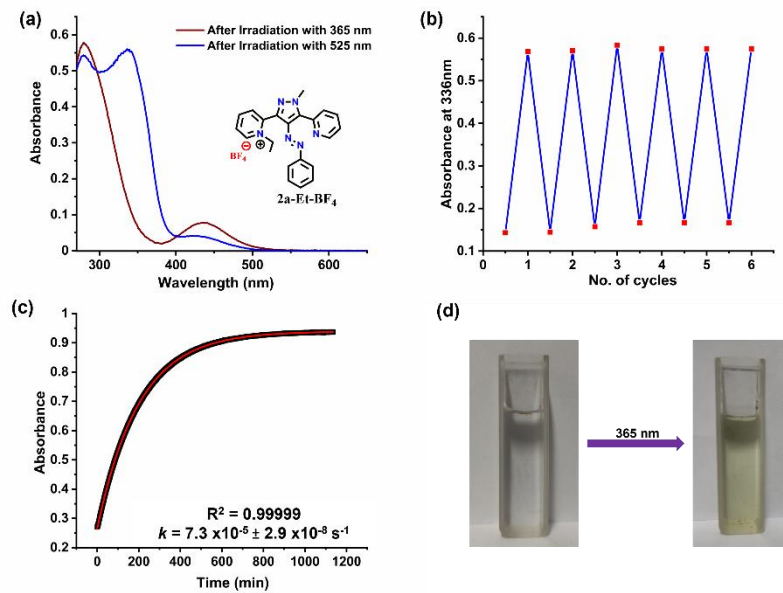


Figure S3.10. UV-Vis spectroscopic data of **2a-Et-BF₄**: (a) Photoswitching studies performed in H₂O; (b) Photoswitching stability test upto five cycles in H₂O (forward isomerization step: 365 nm; reverse isomerization step: 525 nm) and (c) First order thermal reverse isomerization kinetics plot and exponential fit at 70 °C. (Due to insolubility of *trans* isomer, the molar extinction coefficient could not be calculated in water) (d) Upon irradiation at 365 nm, the sample was partially dissolved and the soluble portion was used for reversible cycles, which is depicted.

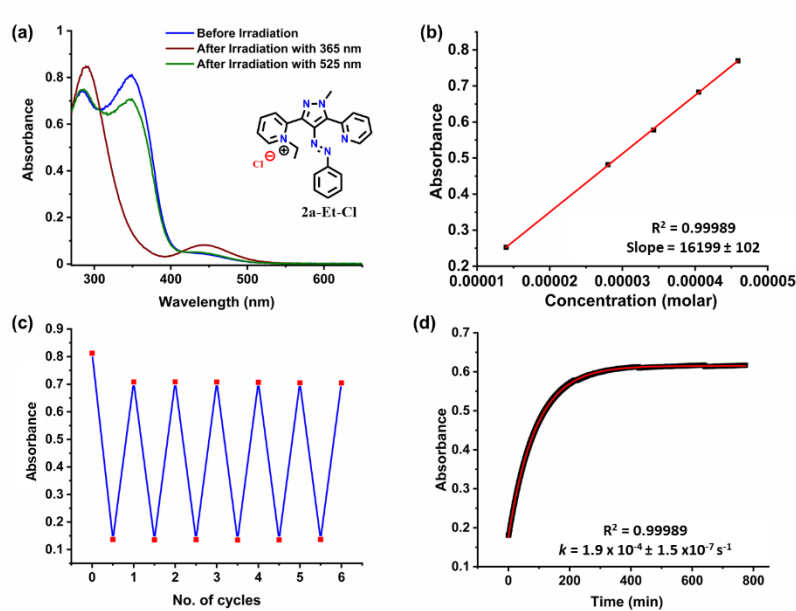


Figure S3.11. UV-Vis spectroscopic data of **2a-Et-Cl**: (a) Photoswitching studies performed in DMSO ($77 \mu\text{M}$); (b) Estimation of the molar absorption coefficient for $\pi-\pi^*$ absorption maxima; (c) Photoswitching stability test upto five cycles in DMSO (forward isomerization step: 365 nm; reverse isomerization step: 525 nm) and (d) First order thermal reverse isomerization kinetics plot and exponential fit at 70°C .

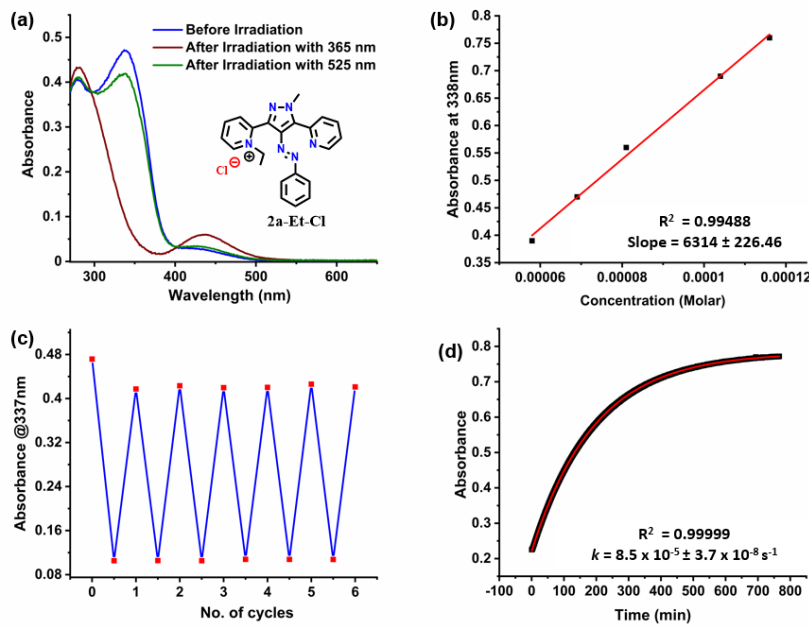


Figure S3.12. UV-Vis spectroscopic data of **2a-Et-Cl**: (a) Photoswitching studies performed in H_2O ($71 \mu\text{M}$); (b) Estimation of the molar absorption coefficient for $\pi-\pi^*$ absorption maxima; (c) Photoswitching stability test upto five cycles in H_2O (forward isomerization step: 365 nm; reverse isomerization step: 525 nm) and (d) First order thermal reverse isomerization kinetics plot and exponential fit at 70°C .

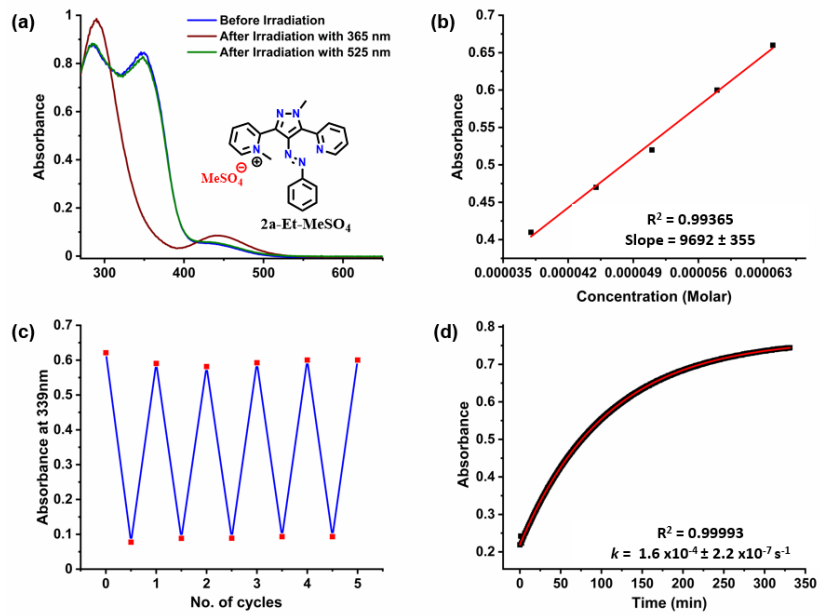


Figure S3.13. UV-Vis spectroscopic data of **2a-Me-MeSO₄**: (a) Photoswitching studies performed in DMSO ($68 \mu\text{M}$); (b) Estimation of the molar absorption coefficient for $\pi-\pi^*$ absorption maxima; (c) Photoswitching stability test upto five cycles in DMSO (forward isomerization step: 365 nm; reverse isomerization step: 525 nm) and (d) First order thermal reverse isomerization kinetics plot and exponential fit at 70 °C.

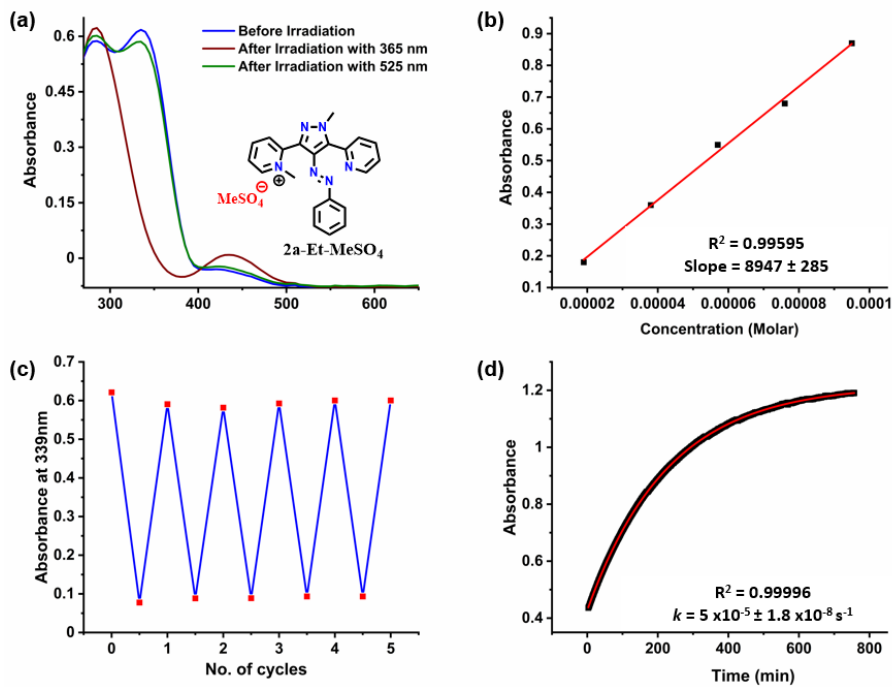


Figure S3.14. UV-Vis spectroscopic data of **2a-Me-MeSO₄**: (a) Photoswitching studies performed in H₂O ($67 \mu\text{M}$); (b) Estimation of the molar absorption coefficient for $\pi-\pi^*$ absorption maxima; (c) Photoswitching stability test upto five cycles in H₂O (forward isomerization step: 365 nm; reverse isomerization step: 525 nm) and (d) First order thermal reverse isomerization kinetics plot and exponential fit at 70 °C.

S3.2 NMR spectroscopic studies

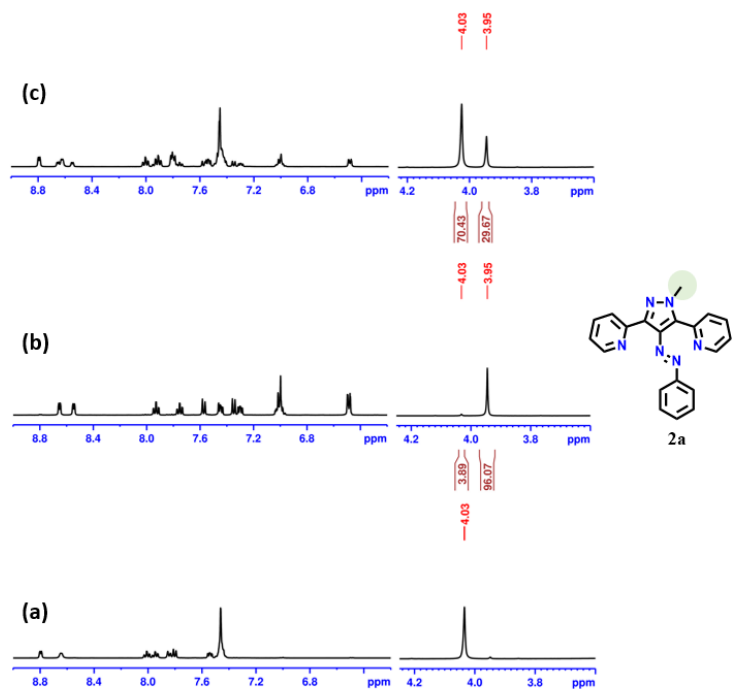


Figure S3.15. Estimation of PSS composition using ^1H NMR spectroscopy of **2a** ($\text{DMSO}-d_6$, 15 mM) (a) before irradiation; (b) after irradiation at 365 nm (2 hr); (c) after irradiation at 427 nm (3 h); (Normalized integral values of highlighted protons are indicated for *E* and *Z* isomers.)

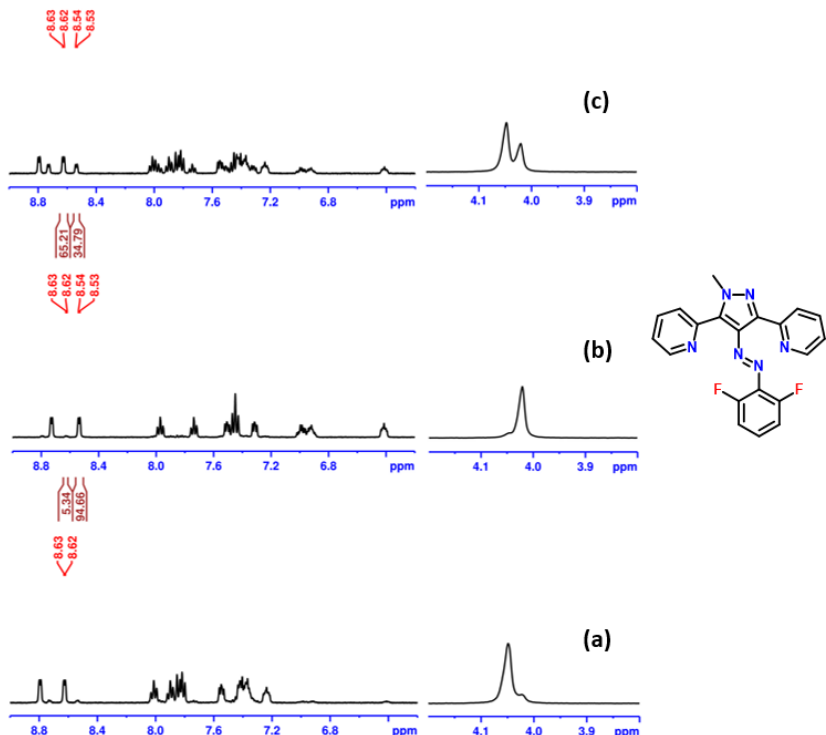


Figure S3.16. Estimation of PSS composition using ^1H NMR spectroscopy of **2b** ($\text{DMSO}-d_6$, 9.5 mM) (a) before irradiation; (b) after irradiation at 365 nm (2 hr); (c) after irradiation at 427 nm (3 h); (Normalized integral values of highlighted protons are indicated for *E* and *Z* isomers.)

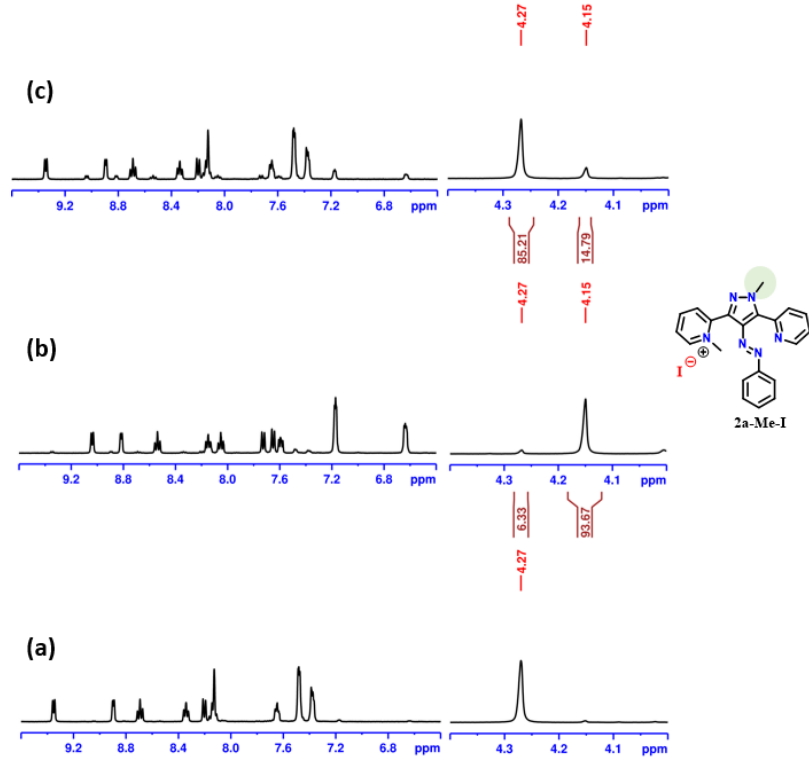


Figure S3.17. Estimation of PSS composition using ^1H NMR spectroscopy of **2a-Me-I** ($\text{DMSO}-d_6$, 9 mM) (a) before irradiation; (b) after irradiation at 365 nm (2 hr); (c) after irradiation at 490 nm (3 h); (Normalized integral values of highlighted protons are indicated for *E* and *Z* isomers.)

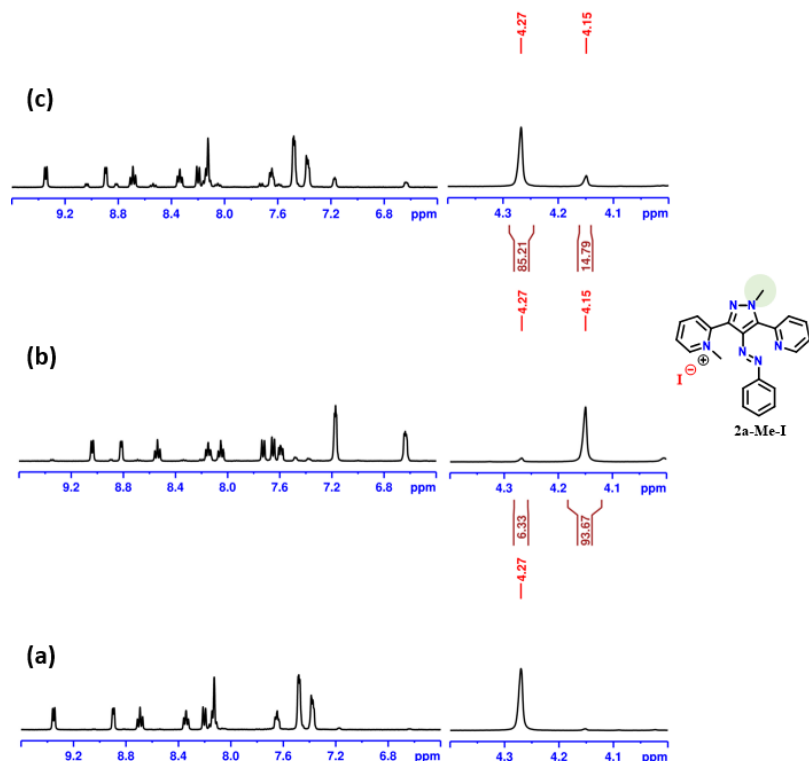


Figure S3.18. Estimation of PSS composition using ^1H NMR spectroscopy of **2a-Me-I** (D_2O_6 , 13 mM) (a) before irradiation; (b) after irradiation at 365 nm (2 hr); (c) after irradiation at 490 nm (3 h); (Normalized integral values of highlighted protons are indicated for *E* and *Z* isomers.)

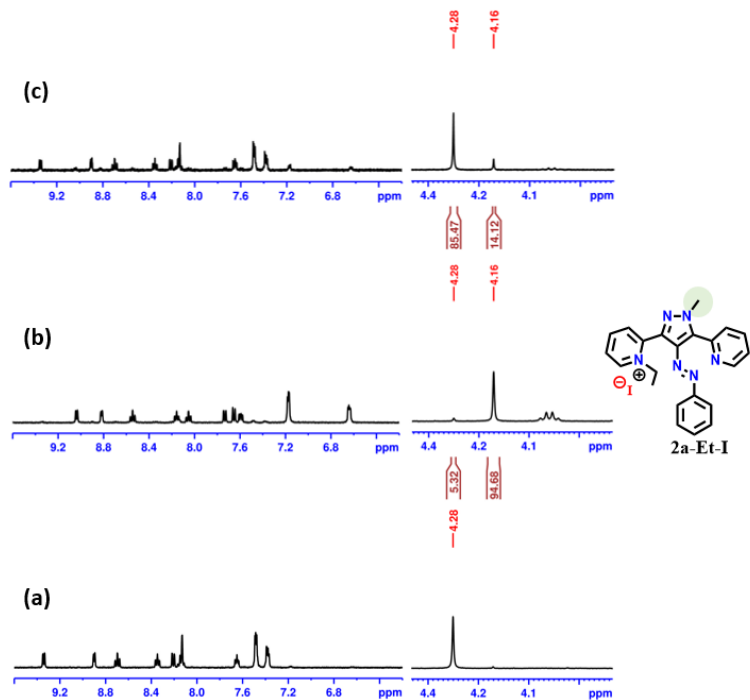


Figure S3.19. Estimation of PSS composition using ^1H NMR spectroscopy of **2a-Et-I** ($\text{DMSO}-d_6$, 7 mM) (a) before irradiation; (b) after irradiation at 365 nm (2 hr); (c) after irradiation at 490 nm (3 h); (Normalized integral values of highlighted protons are indicated for *E* and *Z* isomers.)

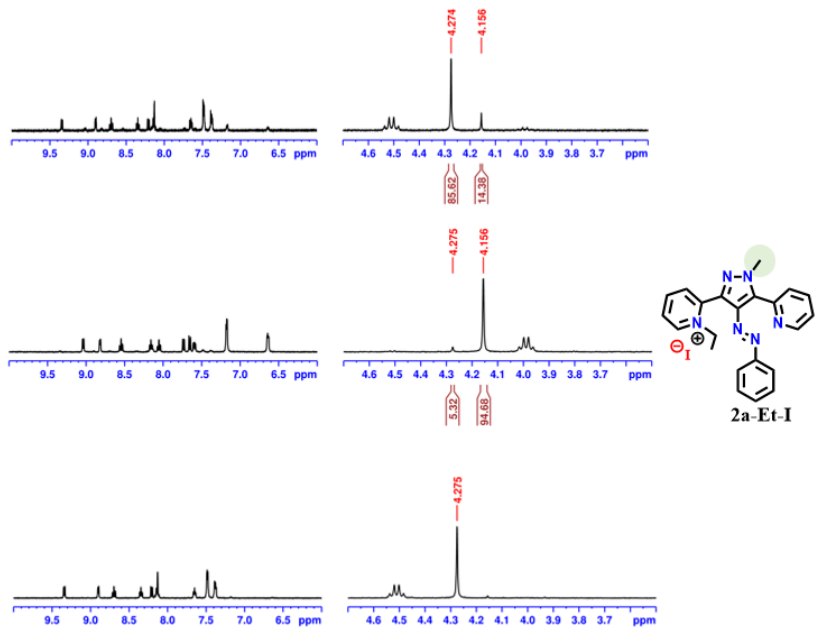


Figure S3.20. Estimation of PSS composition using ^1H NMR spectroscopy of **2a-Et-I** (D_2O , 12 mM) (a) before irradiation; (b) after irradiation at 365 nm (2 hr); (c) after irradiation at 490 nm (3 h); (Normalized integral values of highlighted protons are indicated for *E* and *Z* isomers.)

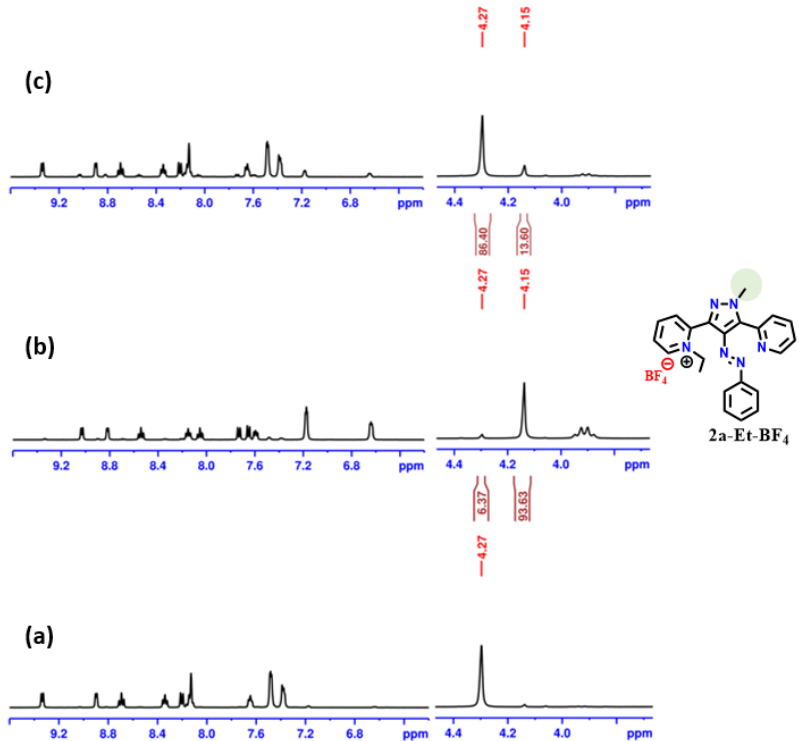


Figure S3.21. Estimation of PSS composition using ^1H NMR spectroscopy of **2a-Et-BF₄** (DMSO- d_6 , 10 mM) (a) before irradiation; (b) after irradiation at 365 nm (2 hr); (c) after irradiation at 490 nm (3 h); (Normalized integral values of highlighted protons are indicated for *E* and *Z* isomers.)

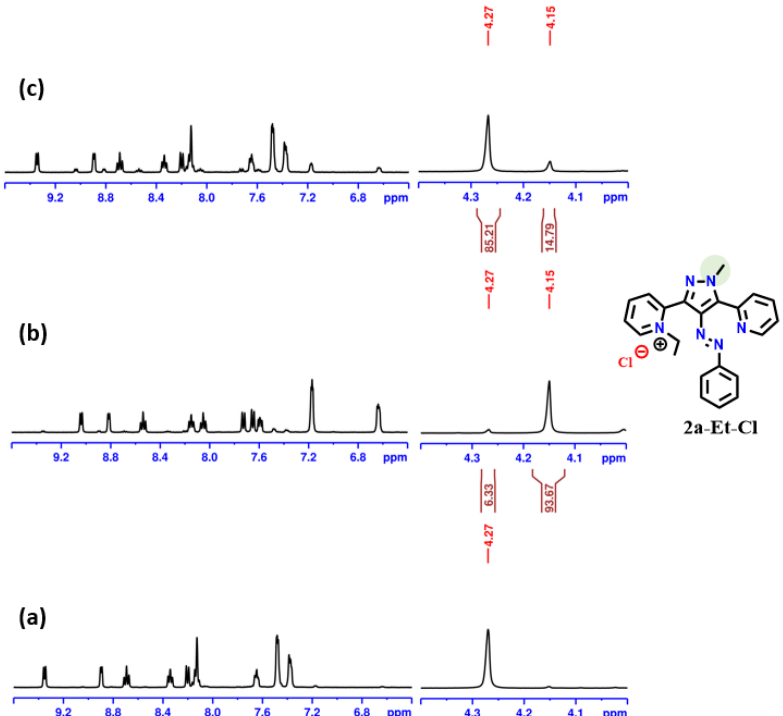


Figure S3.22. Estimation of PSS composition using ^1H NMR spectroscopy of **2a-Et-Cl** (DMSO- d_6 , 11.5 mM) (a) before irradiation; (b) after irradiation at 365 nm (2 hr); (c) after irradiation at 490 nm (3 h); (Normalized integral values of highlighted protons are indicated for *E* and *Z* isomers.)

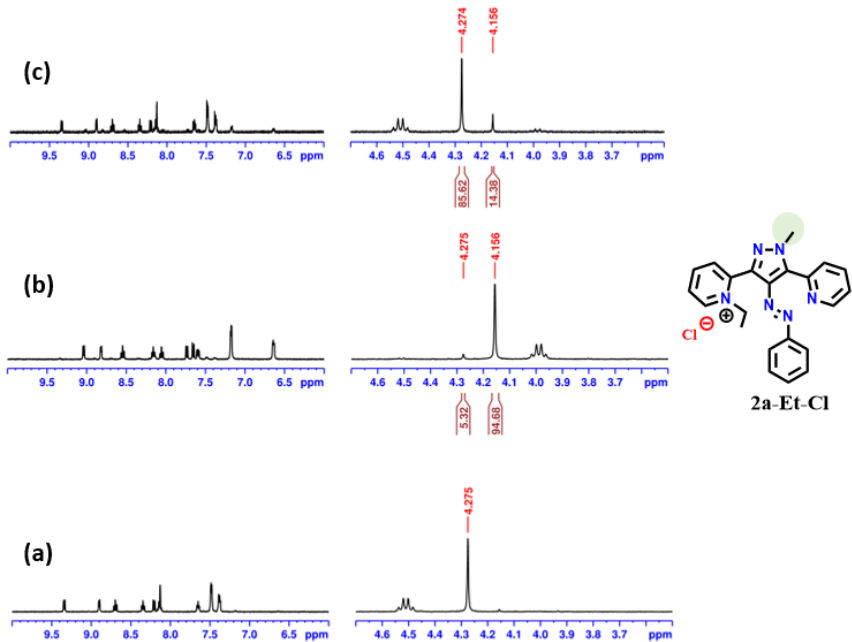


Figure S3.23. Estimation of PSS composition using ^1H NMR spectroscopy of **2a-Et-Cl** (D_2O , 15 mM) (a) before irradiation; (b) after irradiation at 365 nm (2 hr); (c) after irradiation at 490 nm (3 h); (Normalized integral values of highlighted protons are indicated for *E* and *Z* isomers.)

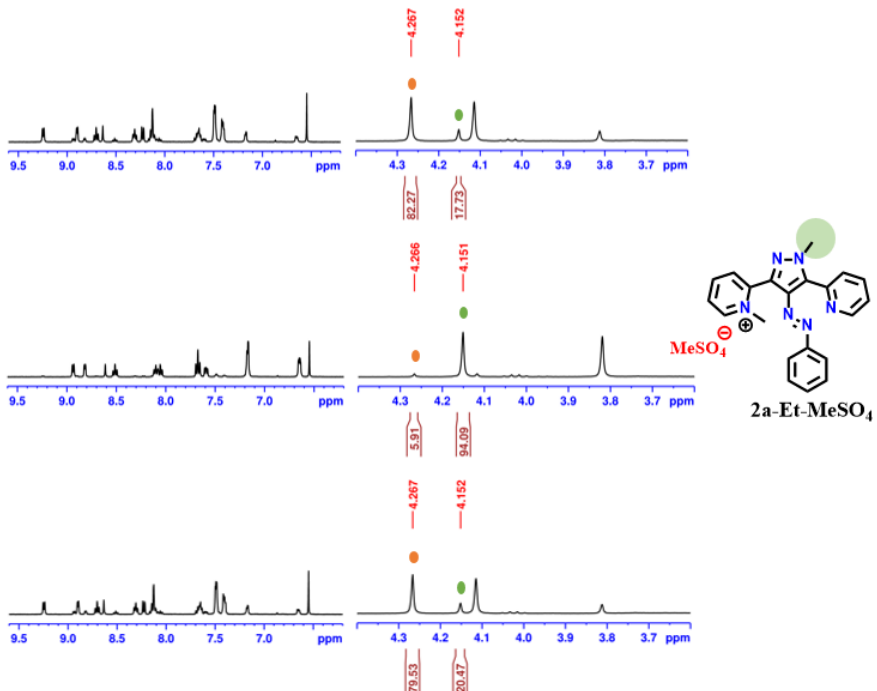


Figure S3.24. Estimation of PSS composition using ^1H NMR spectroscopy of **2a-Et-MeSO₄** ($\text{DMSO}-d_6$, 11 mM) (a) before irradiation; (b) after irradiation at 365 nm (2 hr); (c) after irradiation at 490 nm (3 h); (Normalized integral values of highlighted protons are indicated for *E* and *Z* isomers.)

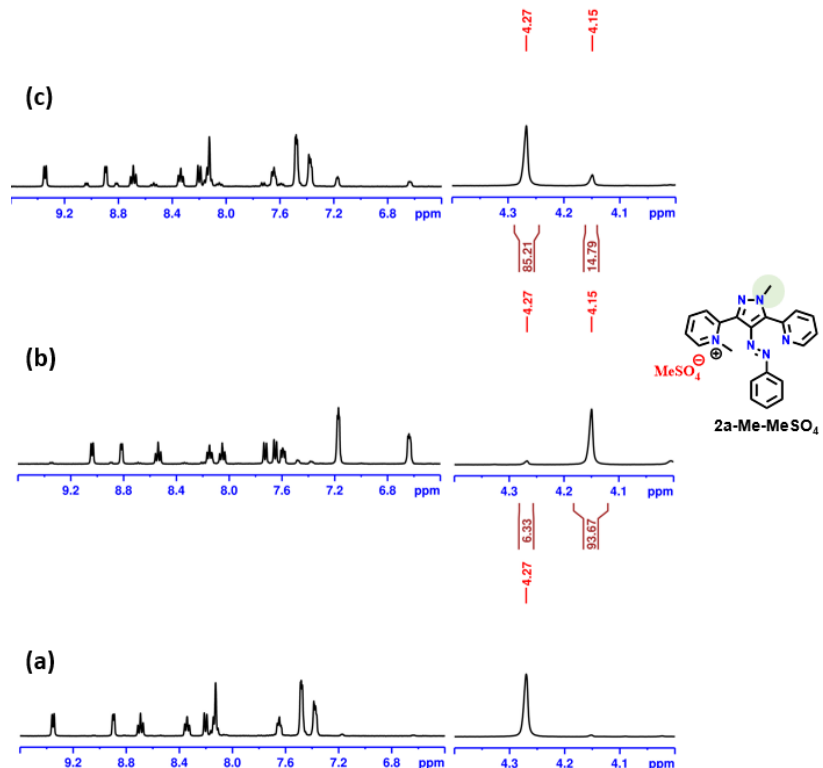


Figure S3.25. Estimation of PSS composition using ^1H NMR spectroscopy of **2a-Me-MeSO₄** (D_2O , 15 mM) (a) before irradiation; (b) after irradiation at 365 nm (2 hr); (c) after irradiation at 490 nm (3 h); (Normalized integral values of highlighted protons are indicated for *E* and *Z* isomers.)

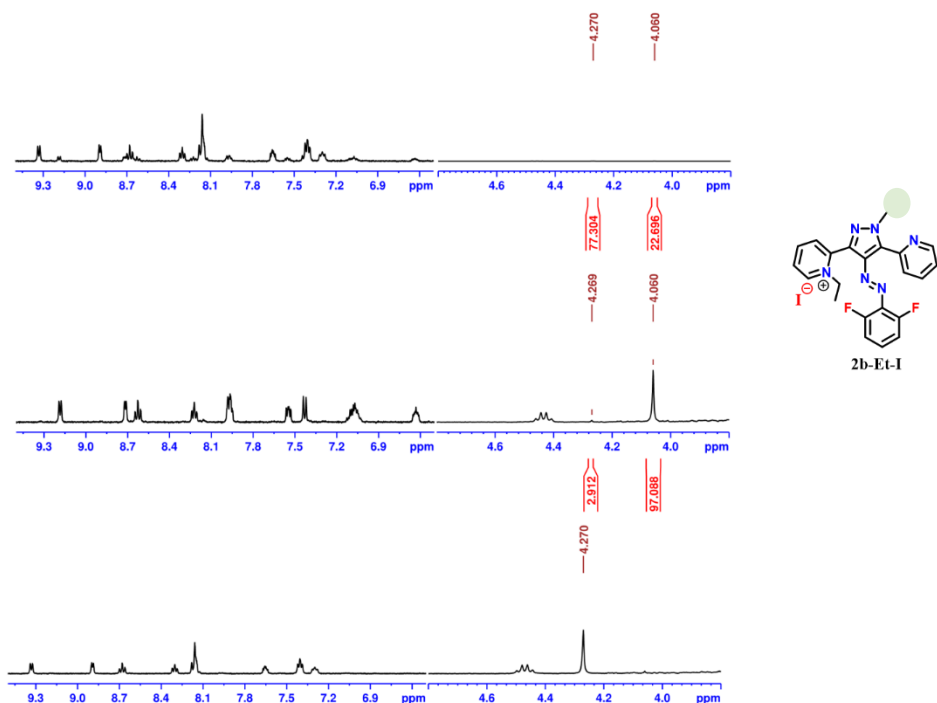


Figure S3.26. Estimation of PSS composition using ^1H NMR spectroscopy of **2b-Et-I** ($\text{DMSO}-d_6$, 12 mM) (a) before irradiation; (b) after irradiation at 365 nm (2 h); (c) after irradiation at 490 nm (3 h); (Normalized integral values of highlighted protons are indicated for *E* and *Z* isomers.)

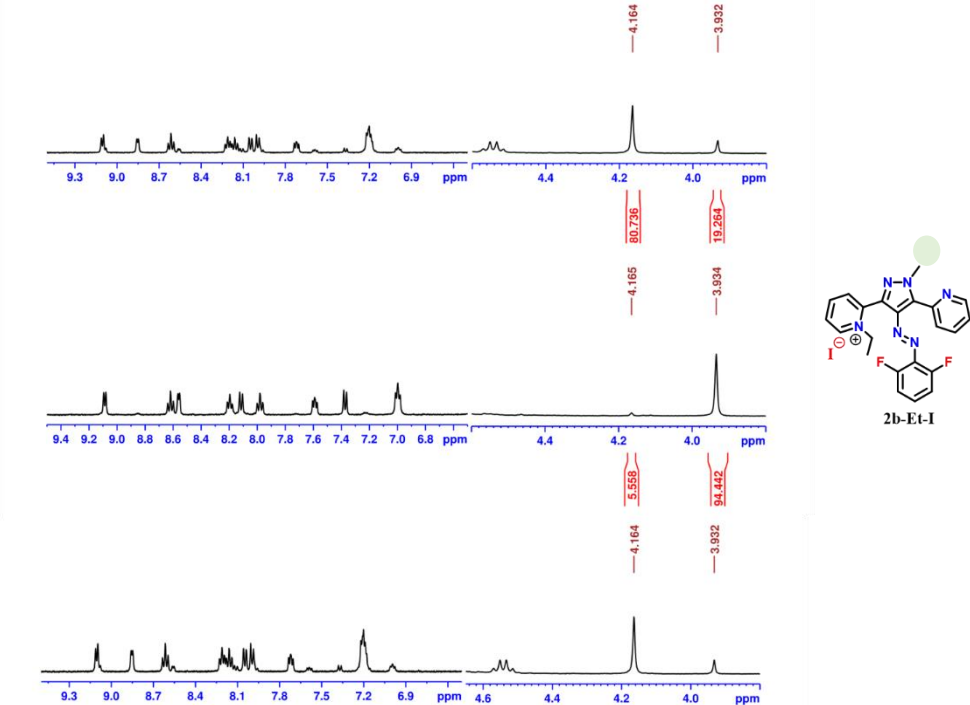


Figure S3.27. Estimation of PSS composition using ^1H NMR spectroscopy of **2b-Et-I** (D_2O , 20 mM) (a) before irradiation; (b) after irradiation at 365 nm (2 h); (c) after irradiation at 490 nm (3 h); (Normalized integral values of highlighted protons are indicated for *E* and *Z* isomers.)

S3.3 Estimation of quantum yields of photoisomerization

Photoisomerization quantum yields were calculated using previously reported method.³

The rate of a forward photoisomerization reaction is given by equation (1):

$$r_{E \rightarrow Z} = \frac{q_{in}\phi_{E \rightarrow Z}}{V} (1 - 10^{-\varepsilon_E}[A]l) \quad (1)$$

Using the following equations (2) and (3) and the measurable properties of the sample, the quantum yield $\phi_{E \rightarrow Z}$ can be estimated.

$$r_{E \rightarrow Z} = \frac{q_{in}\phi_{E \rightarrow Z}\varepsilon_E l}{V}[A] \quad (2)$$

$$\phi_{E \rightarrow Z} = \frac{kV}{q_{in}\varepsilon_E l \ln 10} \quad (3)$$

where ϕ = quantum yield; k = rate constant (obtained from the exponential fit of a graph of A vs. time); V = sample volume; ε_E = molar extinction coefficient; l = pathlength; and q_{in} = molar photon flux (calculated using the formula $\frac{P\lambda}{hcN_A}$).

Similarly, the quantum yield $\phi_{Z \rightarrow E}$ of reverse photoisomerization reaction can be estimated using the following equation.

$$\phi_{Z \rightarrow E} = \frac{kV}{q_{in}\varepsilon_Z l \ln 10} \quad (4)$$

Extinction coefficient for the Z-isomer at irradiation wavelength (ϵ_Z) can be obtained by following equation.⁴

$$\epsilon_Z = \frac{A_{PSS} - A_0 \chi_E}{C_0 \chi_Z} \quad (5)$$

Where, A_{PSS} = Absorbance at observation wavelength at 365 nm irradiation, A_0 = Absorbance at observation wavelength before irradiation, C_0 = Concentration of the solution, χ_E = E isomer ratio at 365 nm PSS (obtained by ^1H NMR), and χ_Z = Z isomer ratio at 365 nm PSS (obtained by ^1H NMR).

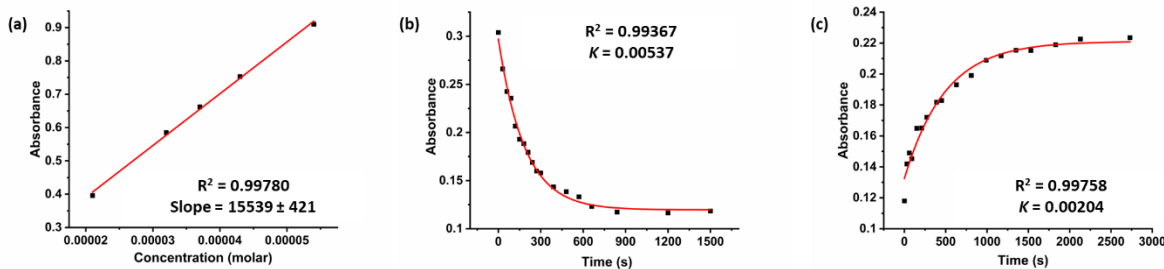


Figure S3.28. UV-vis spectroscopic studies for the quantum yields of derivative **2a** in DMSO. (a) Estimation of molar absorption coefficient at λ_{\max} of $\pi-\pi^*$ absorbance band; Kinetics plots of (b) forward E-Z photoisomerization at 365 nm irradiation, and (c) reverse Z-E photoisomerization at 427 nm irradiation.

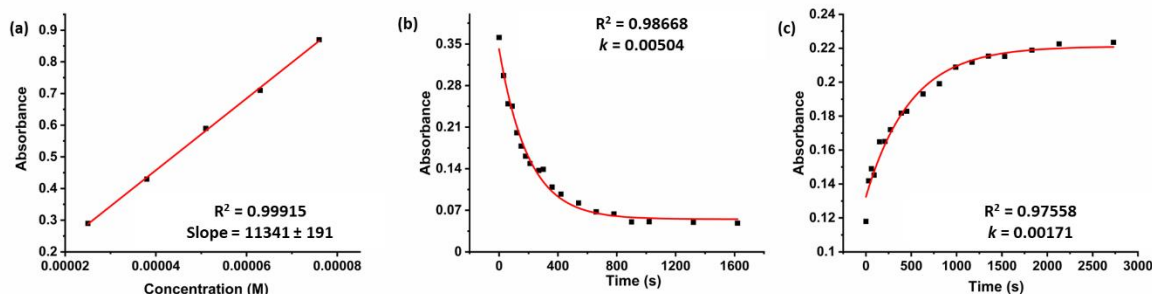


Figure S3.29. UV-vis spectroscopic studies for the quantum yields of derivative **2b** in DMSO. (a) Estimation of molar absorption coefficient at λ_{\max} of $\pi-\pi^*$ absorbance band; Kinetics plots of (b) forward E-Z photoisomerization at 365 nm irradiation, and (c) reverse Z-E photoisomerization at 427 nm irradiation.

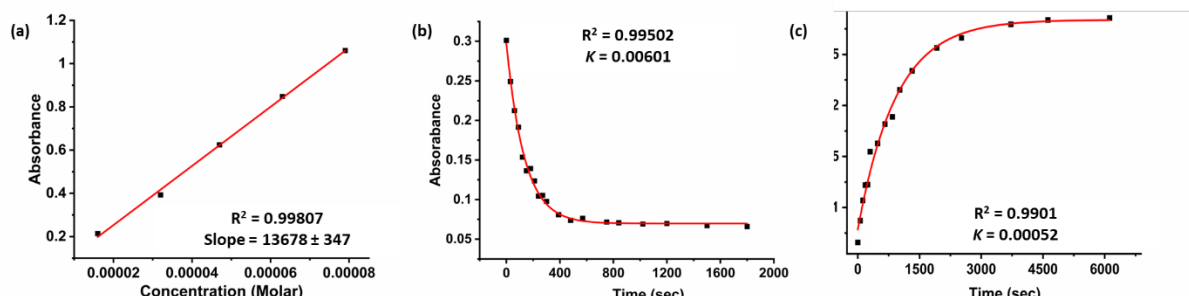


Figure S3.30. UV-vis spectroscopic studies for the quantum yields of derivative **2a-Et-I** in DMSO. (a) Estimation of molar absorption coefficient at λ_{\max} of $\pi-\pi^*$ absorbance band; Kinetics plots of (b) forward E-Z photoisomerization at 365 nm irradiation, and (c) reverse Z-E photoisomerization at 490 nm irradiation.

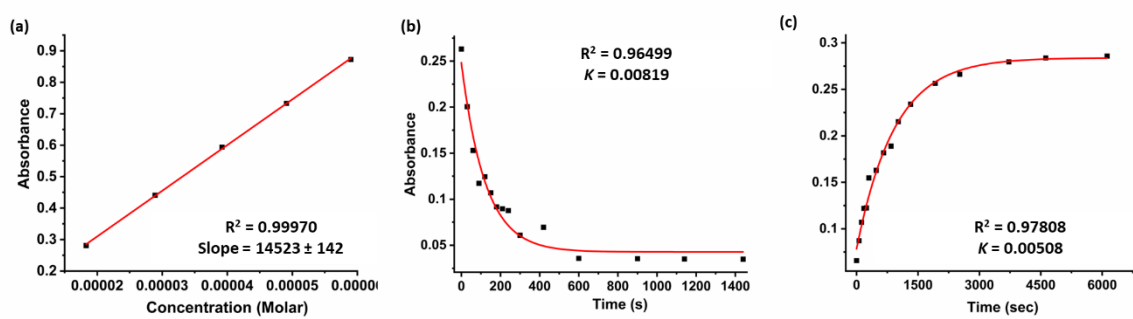


Figure S3.31. UV-vis spectroscopic studies for the quantum yields of derivative **2b-Et-I** in DMSO. (a) Estimation of molar absorption coefficient at λ_{max} of $\pi-\pi^*$ absorbance band; Kinetics plots of (b) forward *E-Z* photoisomerization at 365 nm irradiation, and (c) reverse *Z-E* photoisomerization at 490 nm irradiation.

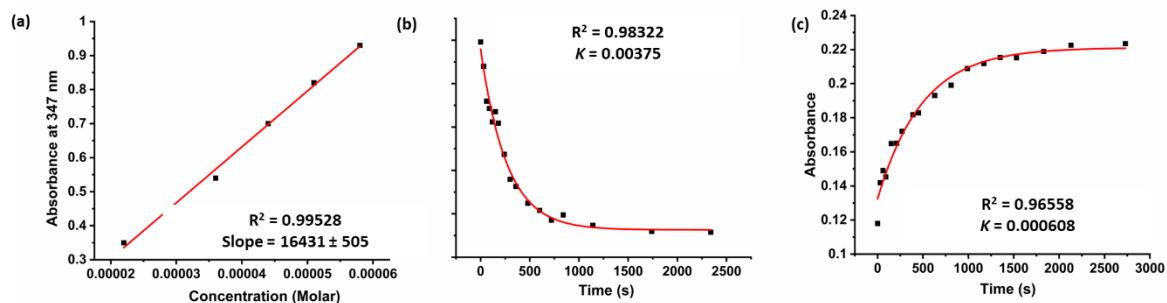


Figure S3.32. UV-vis spectroscopic studies for the quantum yields of derivative **2a-Et-BF₄** in DMSO. (a) Estimation of molar absorption coefficient at λ_{max} of $\pi-\pi^*$ absorbance band; Kinetics plots of (b) forward *E-Z* photoisomerization at 365 nm irradiation, and (c) reverse *Z-E* photoisomerization at 490 nm irradiation.

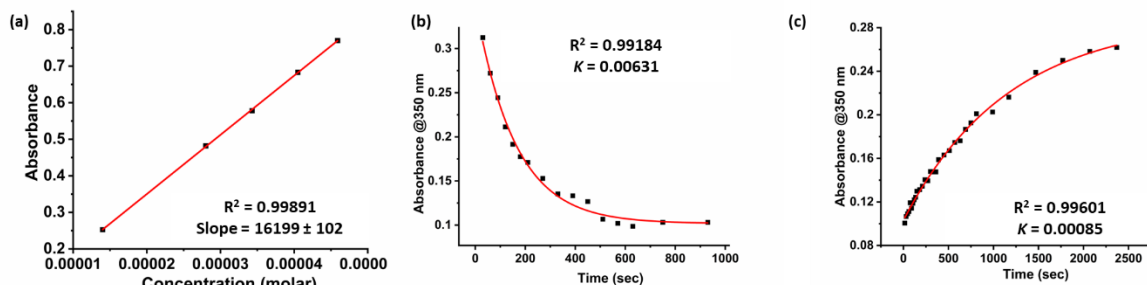


Figure S3.33. UV-vis spectroscopic studies for the quantum yields of derivative **2a-Et-Cl** in DMSO. (a) Estimation of molar absorption coefficient at λ_{max} of $\pi-\pi^*$ absorbance band; Kinetics plots of (b) forward *E-Z* photoisomerization at 365 nm irradiation, and (c) reverse *Z-E* photoisomerization at 490 nm irradiation.

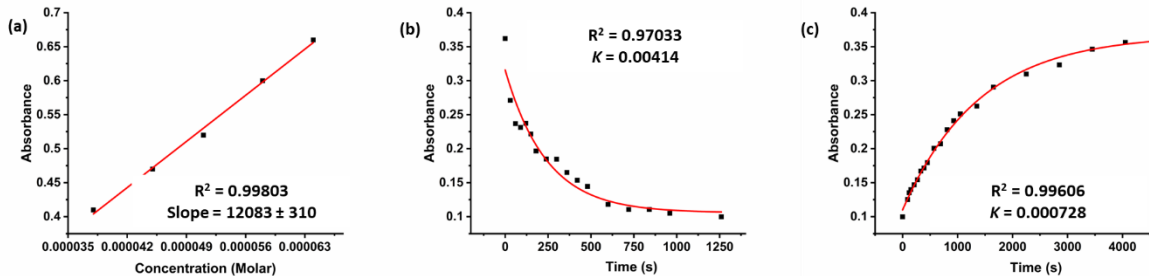


Figure S3.34. UV-vis spectroscopic studies for the quantum yields of derivative **2a-Me-MeSO₄** in DMSO. (a) Estimation of molar absorption coefficient at λ_{max} of $\pi-\pi^*$ absorbance band; Kinetics plots of (b) forward *E-Z* photoisomerization at 365 nm irradiation, and (c) reverse *Z-E* photoisomerization at 490 nm irradiation.

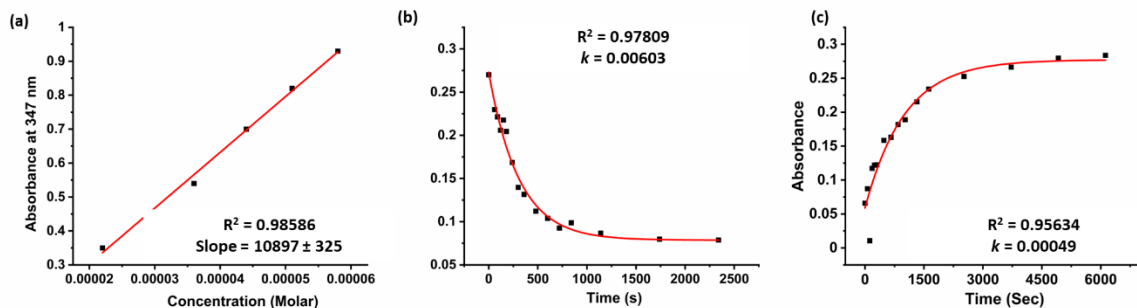


Figure S3.35. UV-vis spectroscopic studies for the quantum yields of derivative **2a-Me-I** in DMSO. (a) Estimation of molar absorption coefficient at λ_{max} of $\pi-\pi^*$ absorbance band; Kinetics plots of (b) forward *E-Z* photoisomerization at 365 nm irradiation, and (c) reverse *Z-E* photoisomerization at 490 nm irradiation.

Table S3.1. Estimation of quantum yields of forward *E-Z* photoisomerization in DMSO.

| Compound | Wavelength (nm) | ε_E ($M^{-1}cm^{-1}$) | Rate kinetics (s^{-1}) | Power (10^{-4}) (W) | Photon Flux (10^{10}) | Quantum yield |
|-------------------------------|-----------------|-------------------------------------|----------------------------|-------------------------|---------------------------|-----------------|
| 2a | 365 | 11076 | 0.00537 | 1.70 | 5.21 | 0.40 ± 0.03 |
| 2a-Et-I | 365 | 11583 | 0.00341 | 1.01 | 3.06 | 0.42 ± 0.02 |
| 2a-Et-BF₄ | 365 | 13342 | 0.00375 | 1.30 | 3.22 | 0.38 ± 0.03 |
| 2a-Et-Cl | 365 | 13336 | 0.00631 | 1.75 | 5.36 | 0.38 ± 0.01 |
| 2a-Me-MeSO₄ | 365 | 10097 | 0.00414 | 1.48 | 4.54 | 0.39 ± 0.04 |
| 2b | 365 | 10198 | 0.00504 | 1.55 | 4.75 | 0.45 ± 0.05 |
| 2b-Et-I | 365 | 14412 | 0.00819 | 1.75 | 5.40 | 0.46 ± 0.03 |
| 2a-Me-I | 365 | 9991 | 0.00603 | 1.76 | 5.36 | 0.48 ± 0.03 |

Table S3.2. Estimation of quantum yields of reverse *Z-E* photoisomerization in DMSO.

| Compound | Wavelength (nm) | ε_Z ($M^{-1}cm^{-1}$) | Rate kinetics (s^{-1}) | Power (10^{-4}) (W) | Photon Flux (10^{10}) | Quantum yield |
|-------------------------------|-----------------|-------------------------------------|----------------------------|-------------------------|---------------------------|-----------------|
| 2a | 427 | 1858 | 0.00204 | 2.30 | 8.24 | 0.58 ± 0.03 |
| 2a-Et-I | 490 | 593 | 0.00052 | 1.73 | 7.12 | 0.53 ± 0.02 |
| 2a-Et-BF₄ | 490 | 549 | 0.000608 | 2.06 | 8.48 | 0.57 ± 0.04 |
| 2a-Et-Cl | 490 | 650 | 0.00065 | 2.02 | 8.32 | 0.53 ± 0.02 |
| 2a-Me-MeSO₄ | 490 | 575 | 0.000728 | 2.16 | 8.89 | 0.62 ± 0.05 |
| 2b | 427 | 1700 | 0.00170 | 2.10 | 7.53 | 0.57 ± 0.02 |
| 2b-Et-I | 490 | 463 | 0.000508 | 2.10 | 8.64 | 0.51 ± 0.04 |
| 2a-Me-I | 490 | 501 | 0.00049 | 2.08 | 8.56 | 0.50 ± 0.03 |

Power of the light source was determined using power meter (Newport/Model 843-R).

S4 Kinetics studies

S4.1 Variable temperature kinetics studies

The rate constants, thermal half-lives (at room temperature), and activation parameters for *Z-E* thermal reverse isomerization deduced from the variable temperature kinetics studies using Arrhenius and Eyring plots in DMSO and Water.

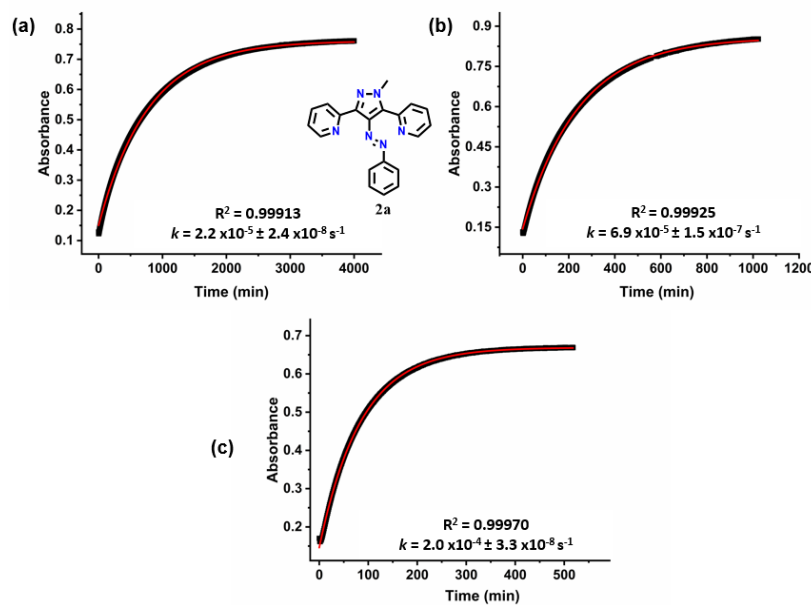


Figure S4.1. Reverse *Z-E* isomerization kinetics of **2a** in DMSO at (a) 70 °C; (b) 80 °C, and (c) 90 °C.

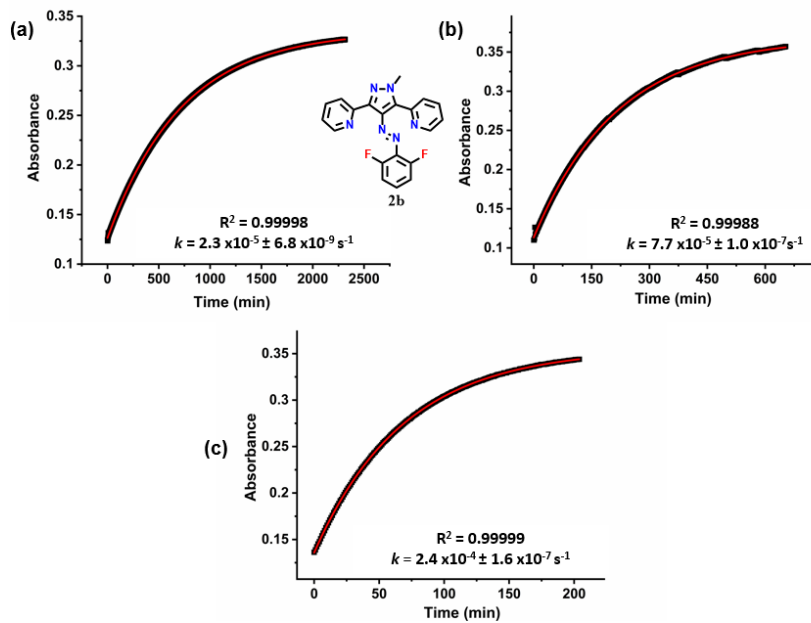


Figure S4.2. Reverse *Z-E* isomerization kinetics of **2b** in DMSO at (a) 70 °C; (b) 80 °C, and (c) 90 °C.

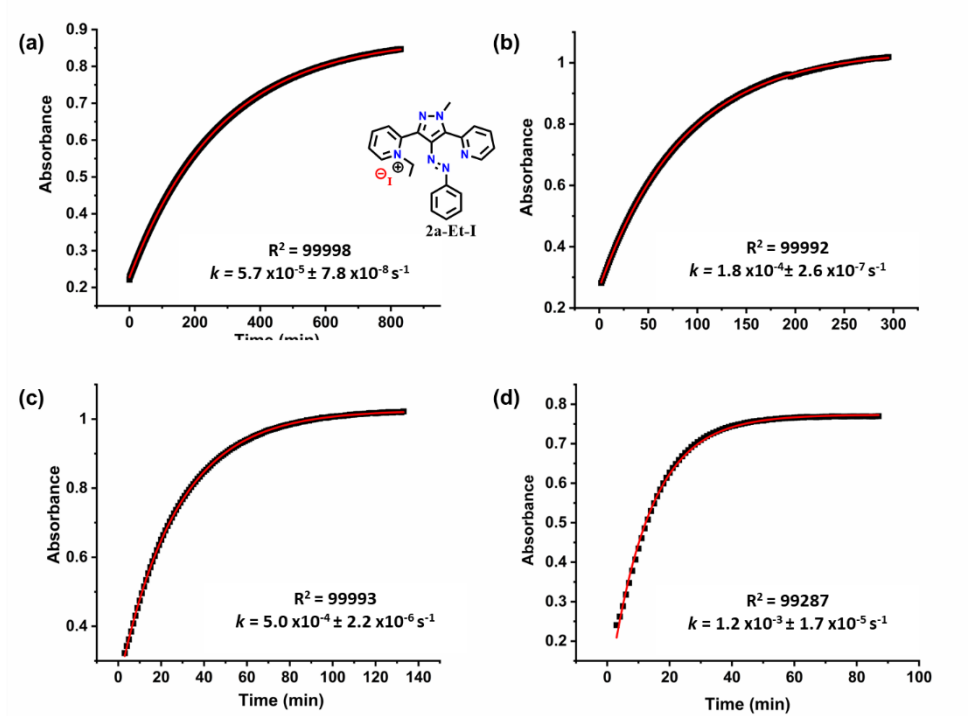


Figure S4.3. Reverse Z-E isomerization kinetics of **2a-Et-I** in DMSO at (a) 60 °C; (b) 70 °C; (c) 80 °C, and (d) 90 °C.

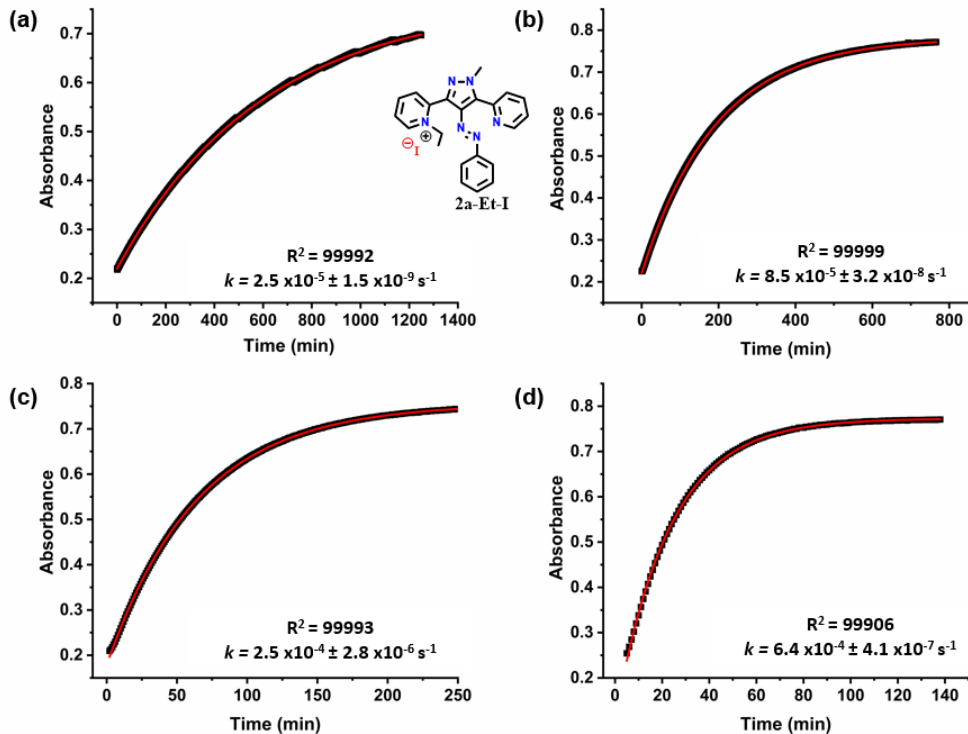


Figure S4.4. Reverse Z-E isomerization kinetics of **2a-Et-I** in H₂O at (a) 60 °C; (b) 70 °C; (c) 80 °C, and (d) 90 °C.

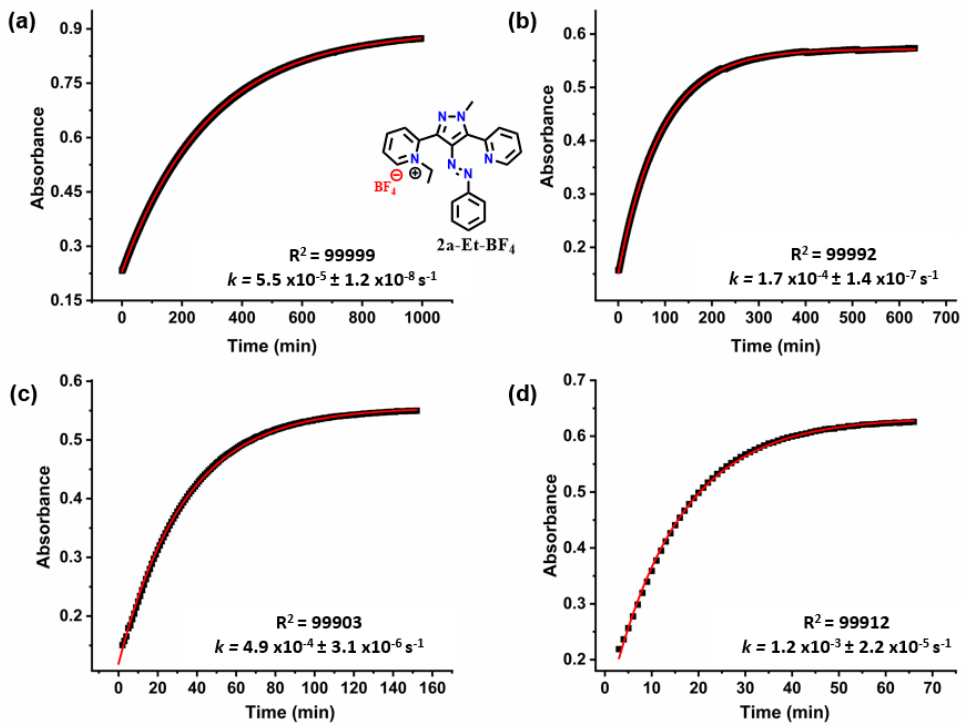


Figure S4.5. Reverse Z-E isomerization kinetics of **2a-Et-BF₄** DMSO at (a) 60 °C; (b) 70 °C; (c) 80 °C, and (d) 90 °C.

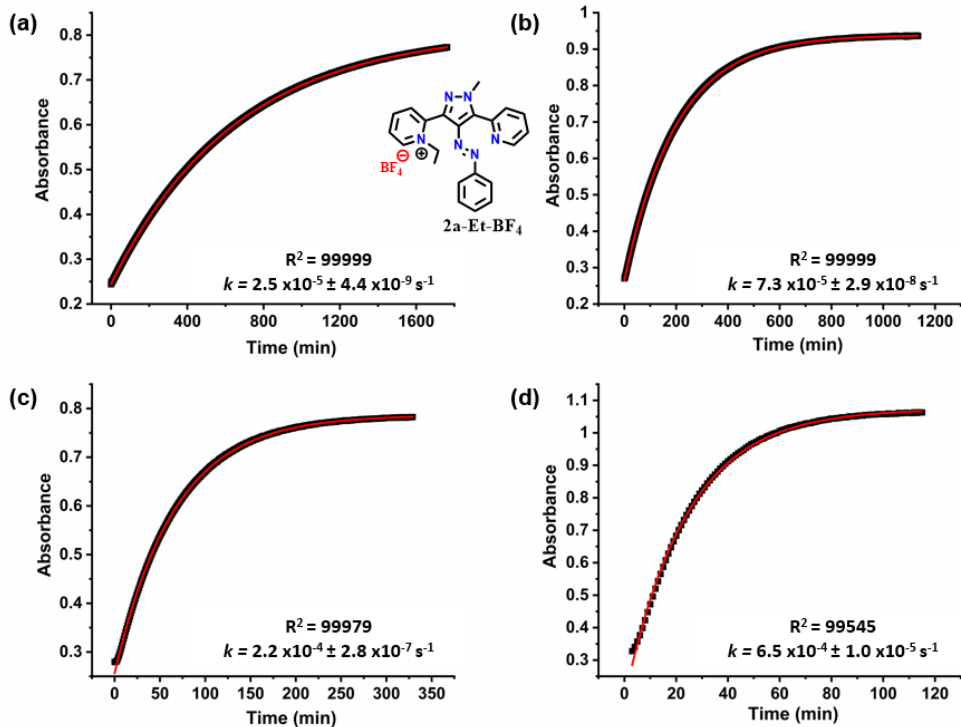


Figure S4.6. Reverse Z-E isomerization kinetics of **2a-Et-BF₄** H₂O at (a) 60 °C; (b) 70 °C; (c) 80 °C, and (d) 90 °C.

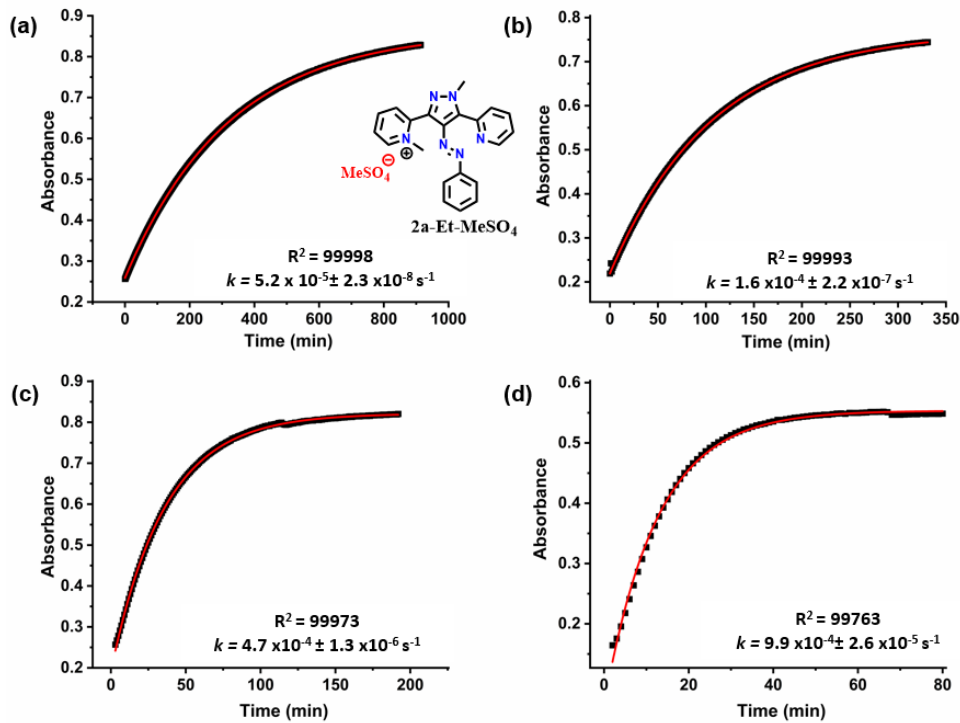


Figure S4.7. Reverse Z-E isomerization kinetics of **2a-Me-MeSO₄** DMSO at (a) 60 °C; (b) 70 °C; (c) 80 °C, and (d) 90 °C.

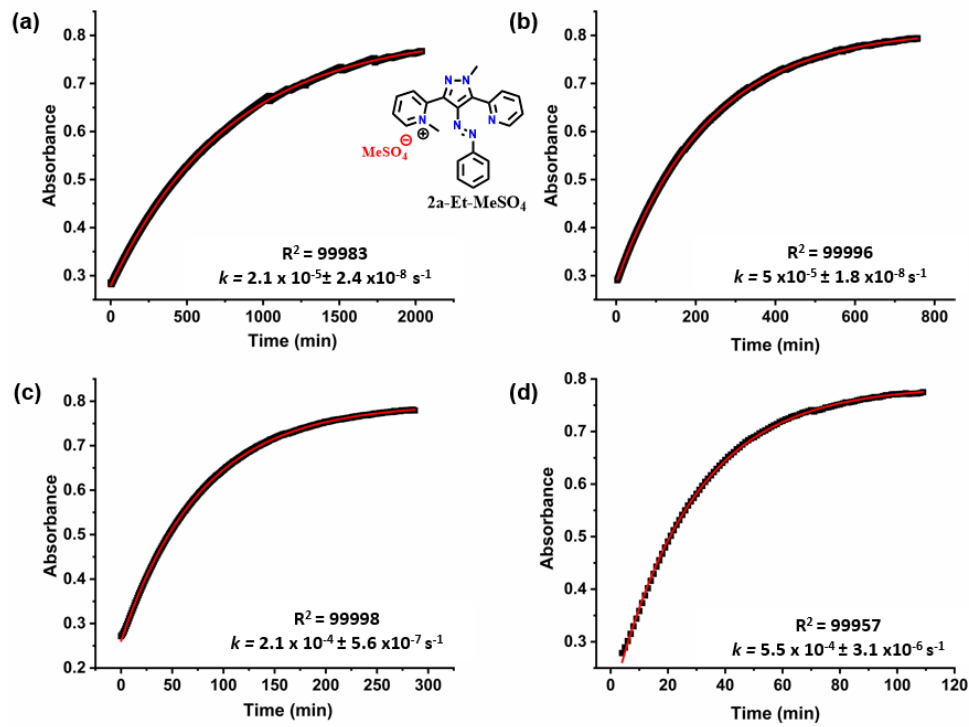


Figure S4.8. Reverse Z-E isomerization kinetics of **2a-Me-MeSO₄** H₂O at (a) 60 °C; (b) 70 °C; (c) 80 °C, and (d) 90 °C.

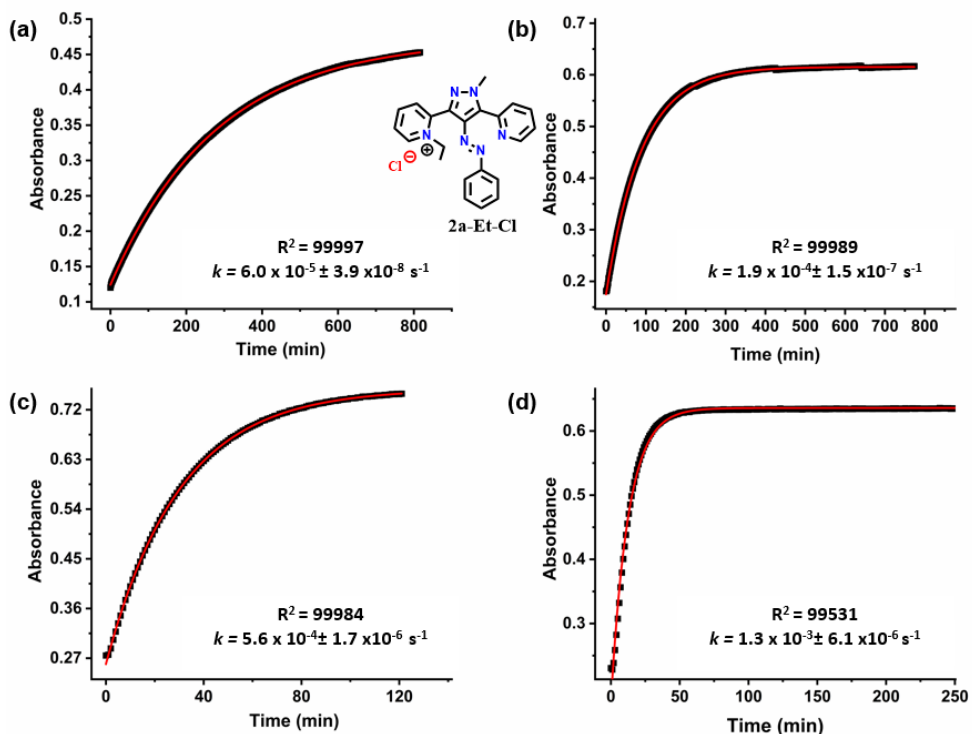


Figure S4.9. Reverse Z-E isomerization kinetics of **2a-Et-Cl** DMSO at (a) 60 °C; (b) 70 °C; (c) 80 °C, and (d) 90 °C.

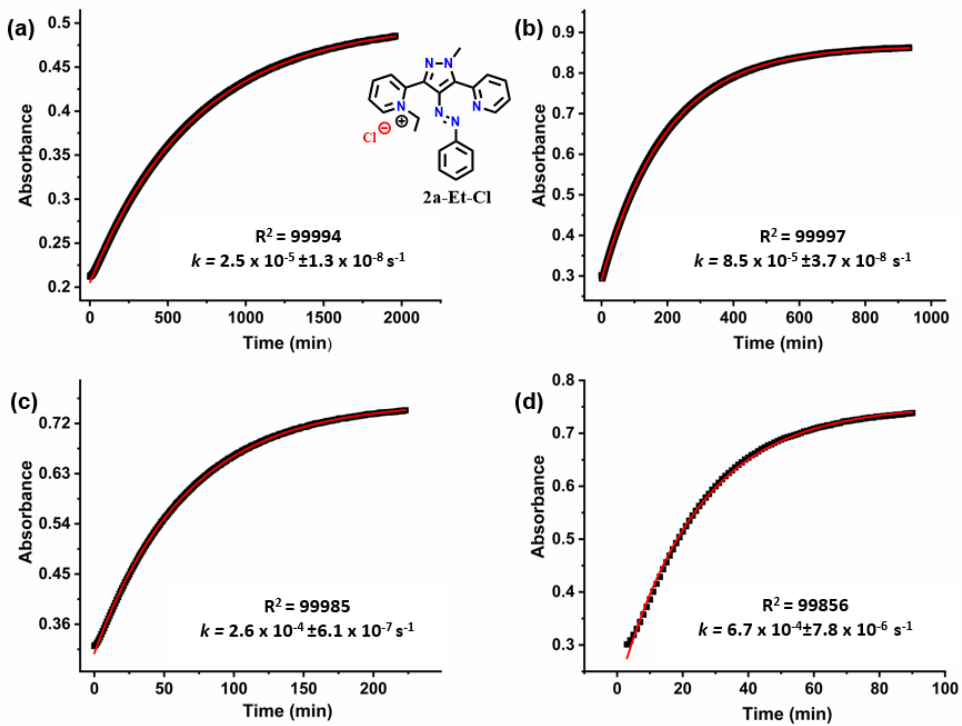


Figure S4.10. Reverse Z-E isomerization kinetics of **2a-Et-Cl** in H_2O at (a) 60 °C; (b) 70 °C; (c) 80 °C, and (d) 90 °C.

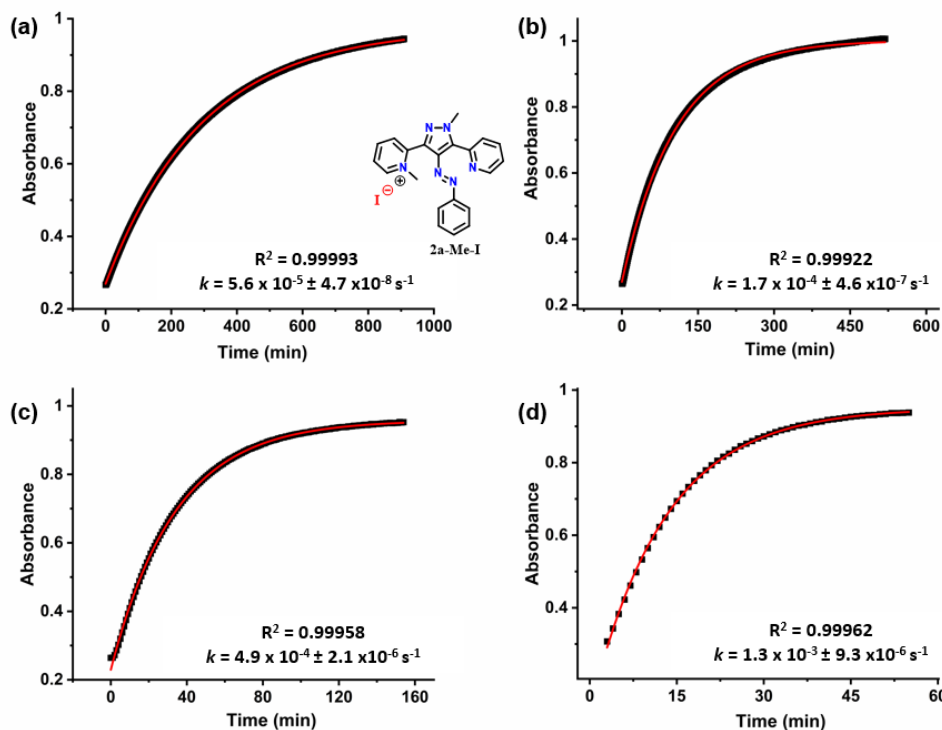


Figure S4.11. Reverse Z-E isomerization kinetics of **2a-Me-I** in DMSO at (a) 60 °C; (b) 70 °C; (c) 80 °C, and (d) 90 °C.

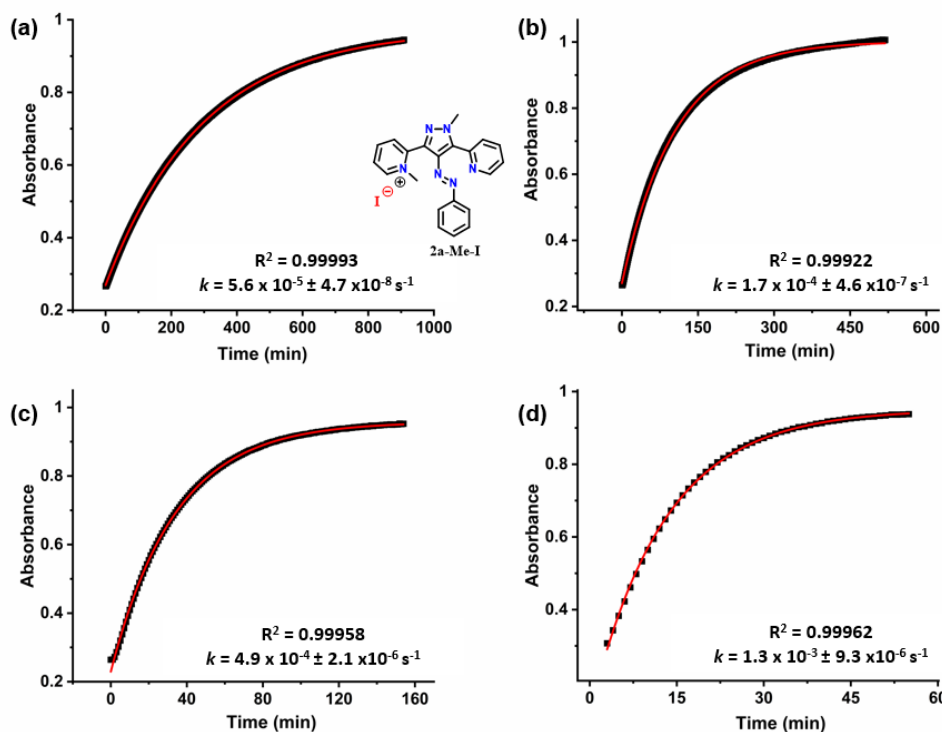


Figure S4.12. Reverse Z-E isomerization kinetics of **2a-Me-I** in H₂O at (a) 60 °C; (b) 70 °C; (c) 80 °C, and (d) 90 °C.

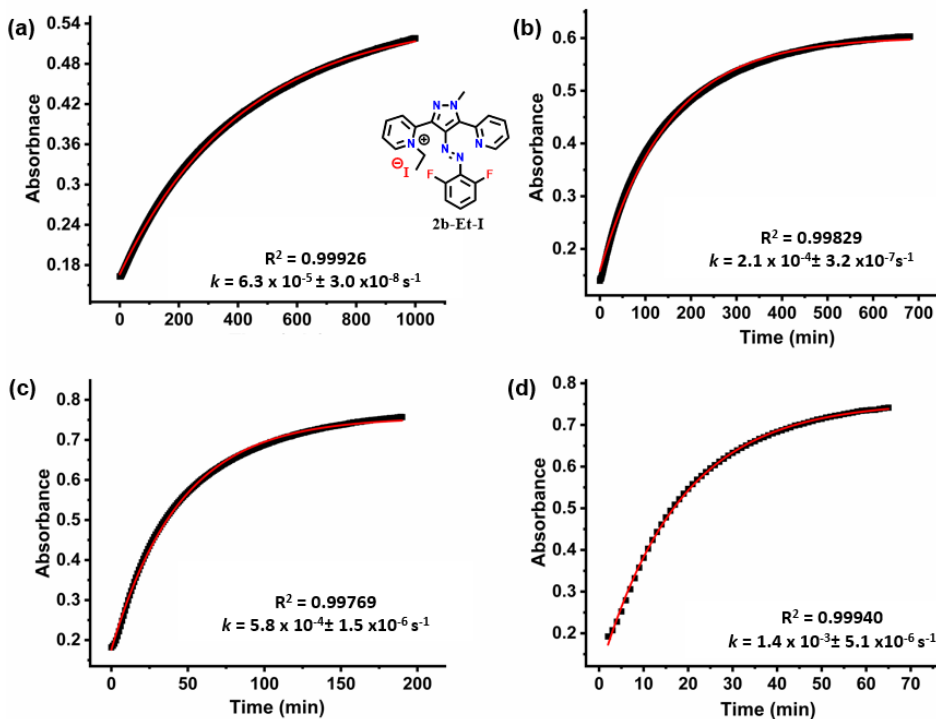


Figure S4.13. Reverse Z-E isomerization kinetics of **2b-Et-I** in DMSO at (a) 60 °C; (b) 70 °C; (c) 80 °C, and (d) 90 °C.

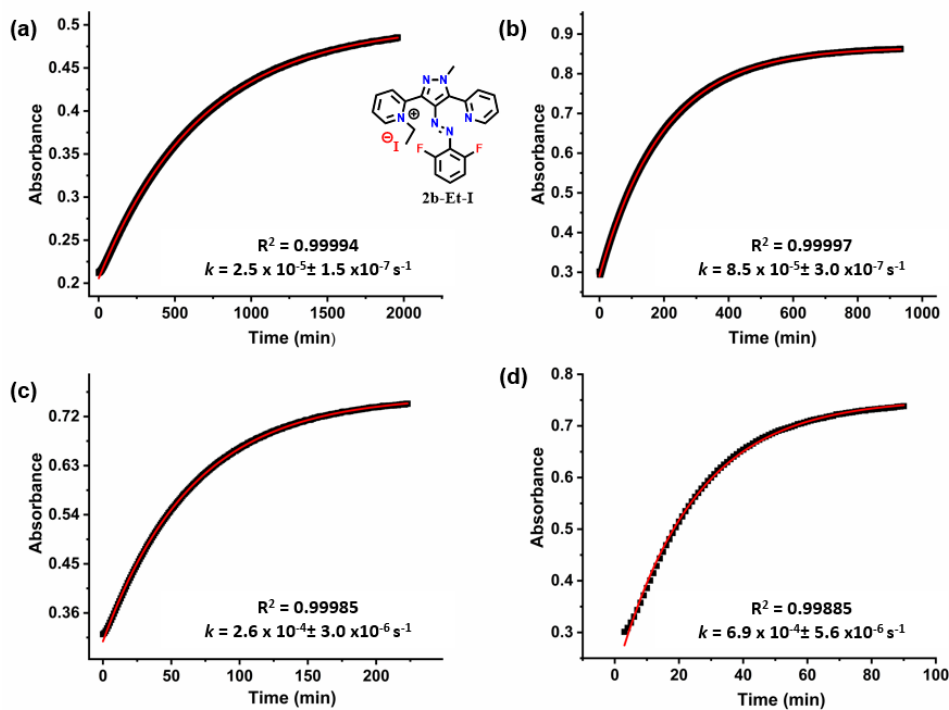


Figure S4.14. Reverse Z-E isomerization kinetics of **2b-Et-I** in H_2O at (a) 60 °C; (b) 70 °C; (c) 80 °C, and (d) 90 °C.

S4.2 Evaluation of activation parameters and determination of rates and half-life at room temperature

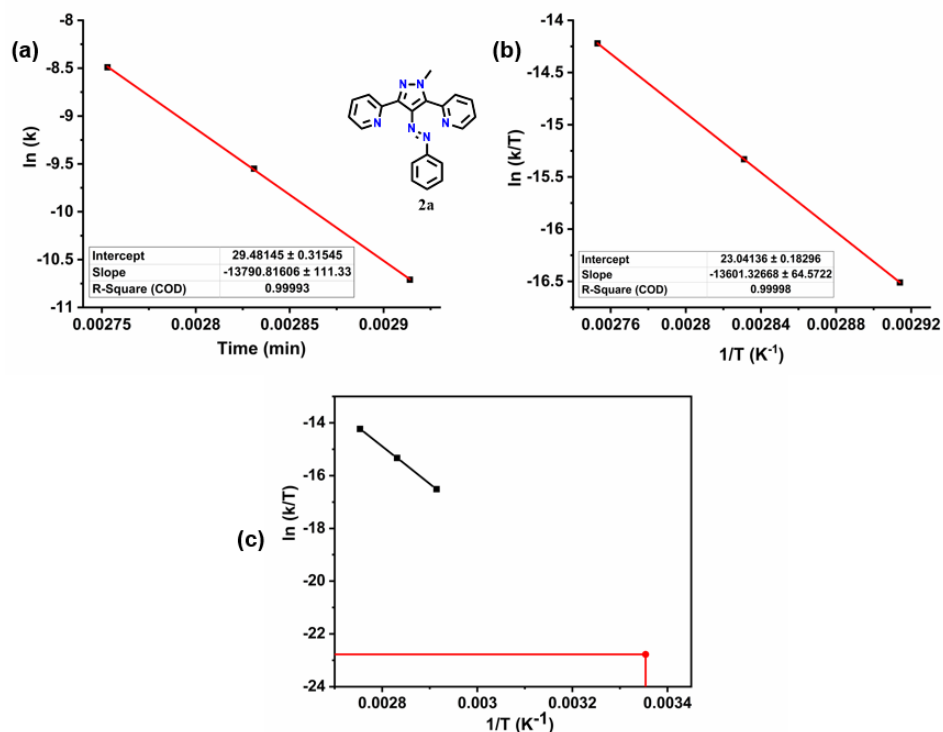


Figure S4.15. (a) Arrhenius plot, and (b) Eyring plot for **2a** in DMSO; (c) Linear extrapolation of Eyring plot for **2a** in DMSO to room temperature (298 K).

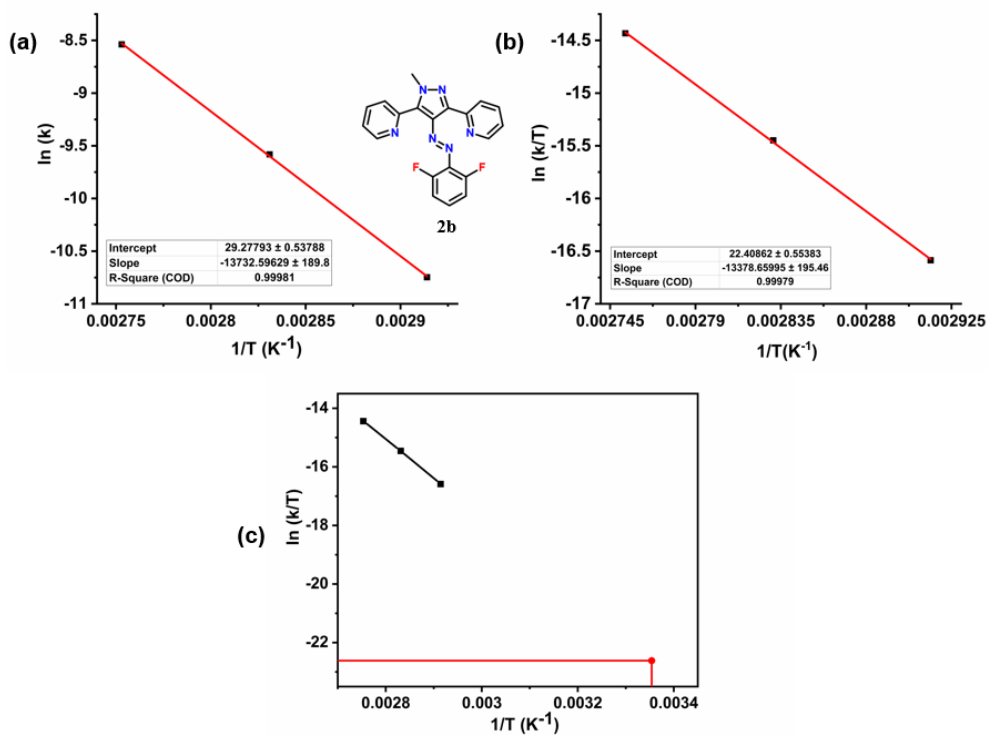


Figure S4.16. (a) Arrhenius plot, and (b) Eyring plot for **2b** in DMSO; (c) Linear extrapolation of Eyring plot for **2b** in DMSO to room temperature (298 K).

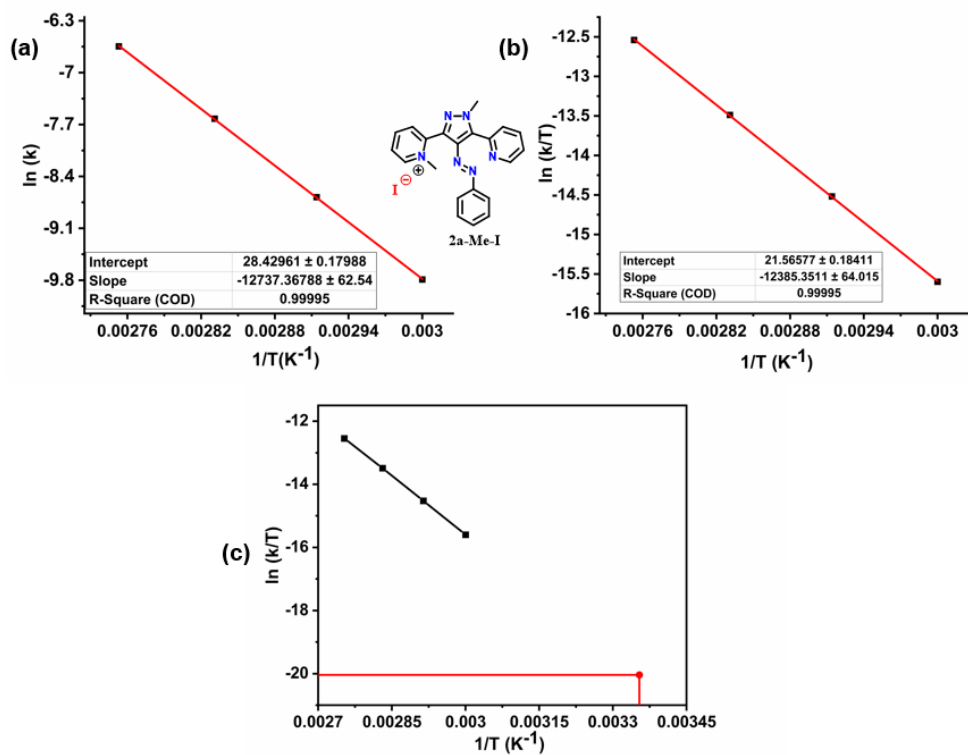


Figure S4.17. (a) Arrhenius plot, and (b) Eyring plot for **2a-Me-I** in DMSO; (c) Linear extrapolation of Eyring plot for **2a-Me-I** in DMSO to room temperature (298 K).

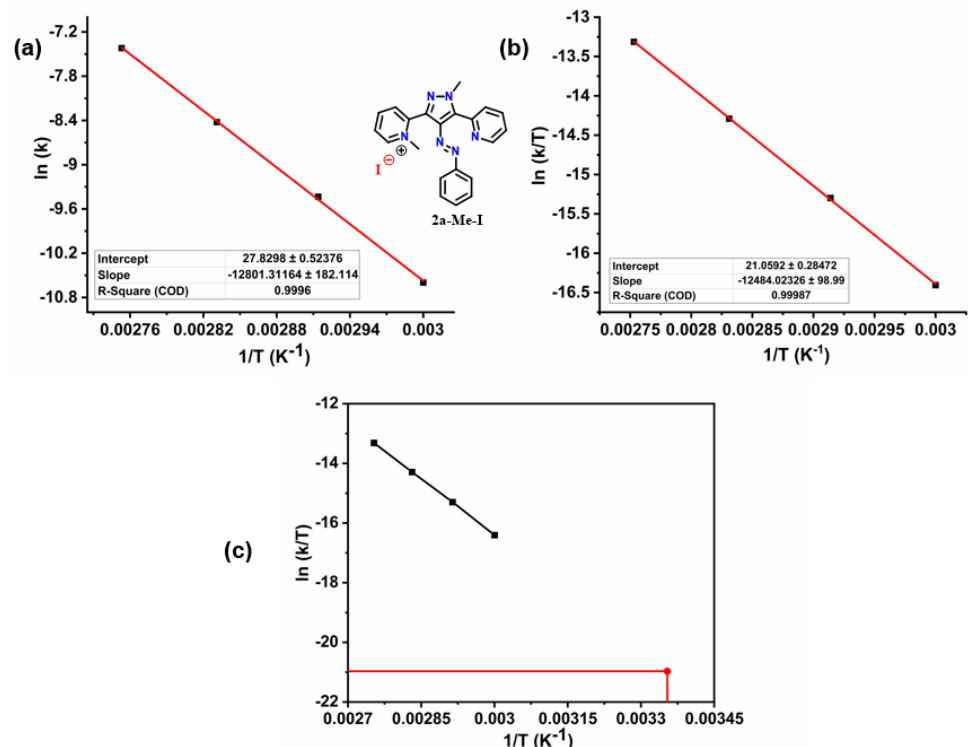


Figure S4.18. (a) Arrhenius plot, and (b) Eyring plot for **2a-Me-I** in H₂O; (c) Linear extrapolation of Eyring plot for **2a-Me-I** in H₂O to room temperature (298 K).

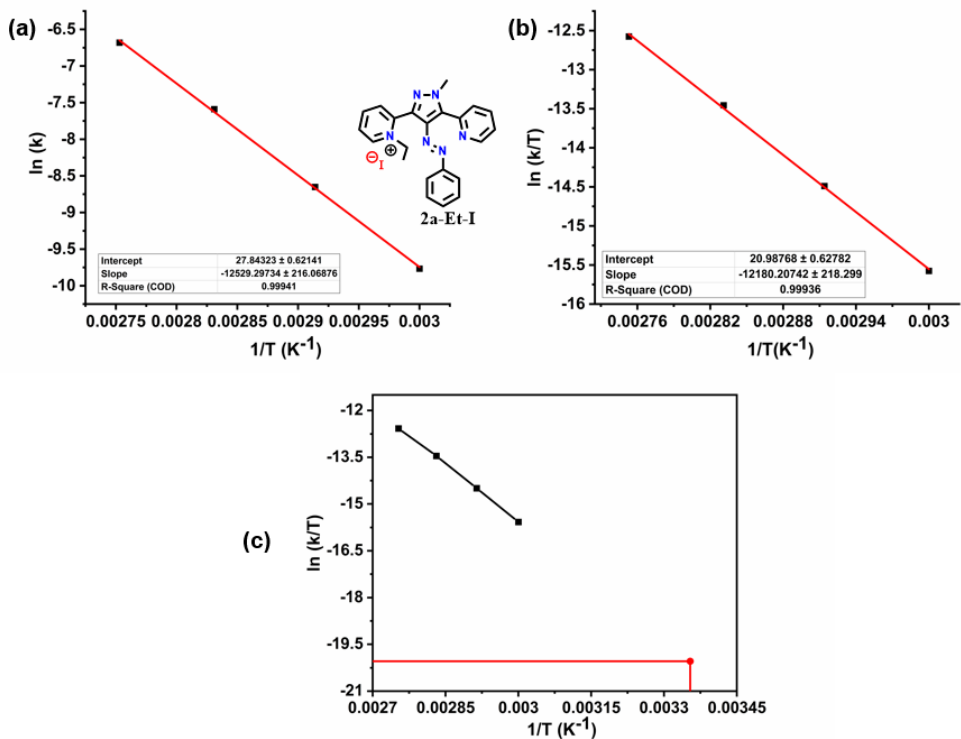


Figure S4.19. (a) Arrhenius plot, and (b) Eyring plot for **2a-Et-I** in DMSO; (c) Linear extrapolation of Eyring plot for **2a-Et-I** in DMSO to room temperature (298 K).

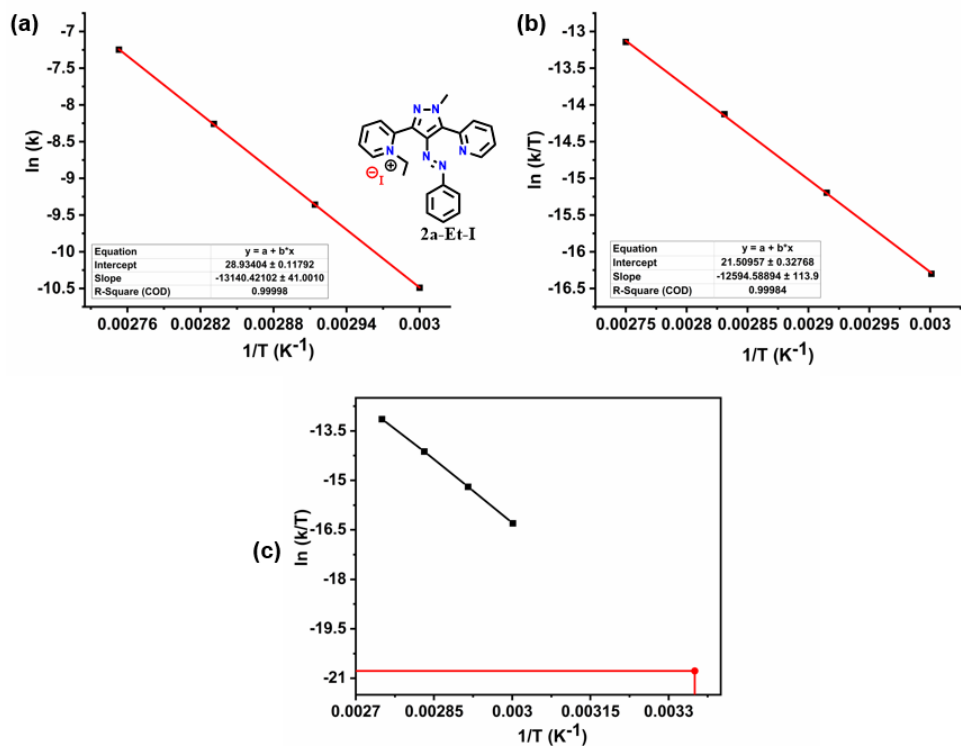


Figure S4.20. (a) Arrhenius plot, and (b) Eyring plot for **2a-Et-I** in H_2O ; (c) Linear extrapolation of Eyring plot for **2a-Et-I** in H_2O to room temperature (298 K).

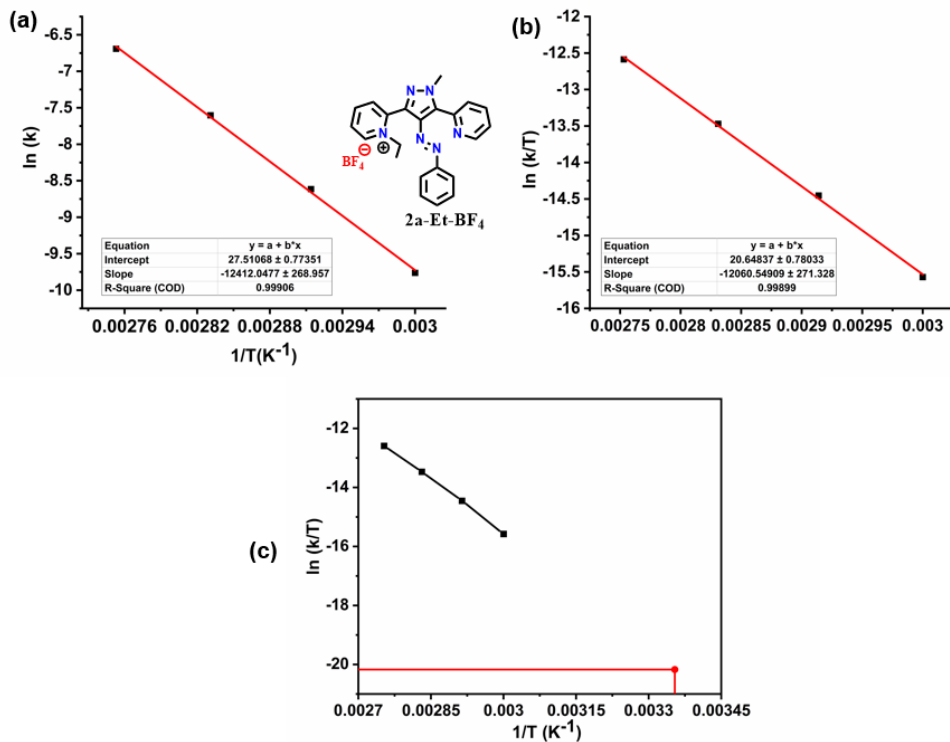


Figure S4.21. (a) Arrhenius plot, and (b) Eyring plot for **2a-Et-BF₄** in DMSO; (c) Linear extrapolation of Eyring plot for **2a-Et-BF₄** in DMSO to room temperature (298 K).

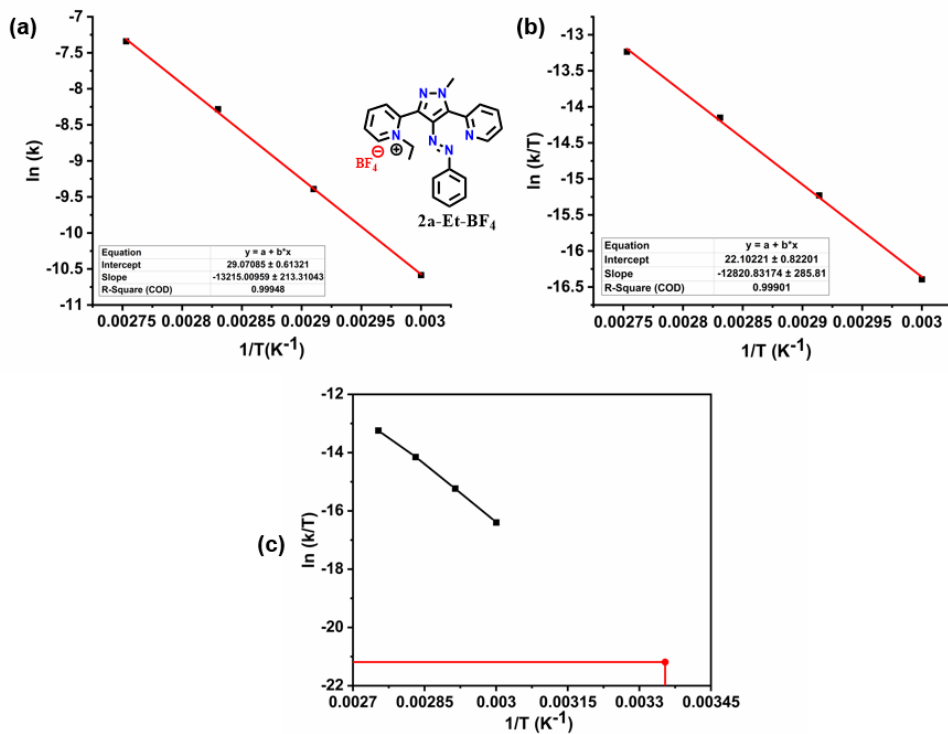


Figure S4.22. (a) Arrhenius plot, and (b) Eyring plot for **2a-Et-BF₄** in H₂O; (c) Linear extrapolation of Eyring plot for **2a-Et-BF₄** in H₂O to room temperature (298 K).

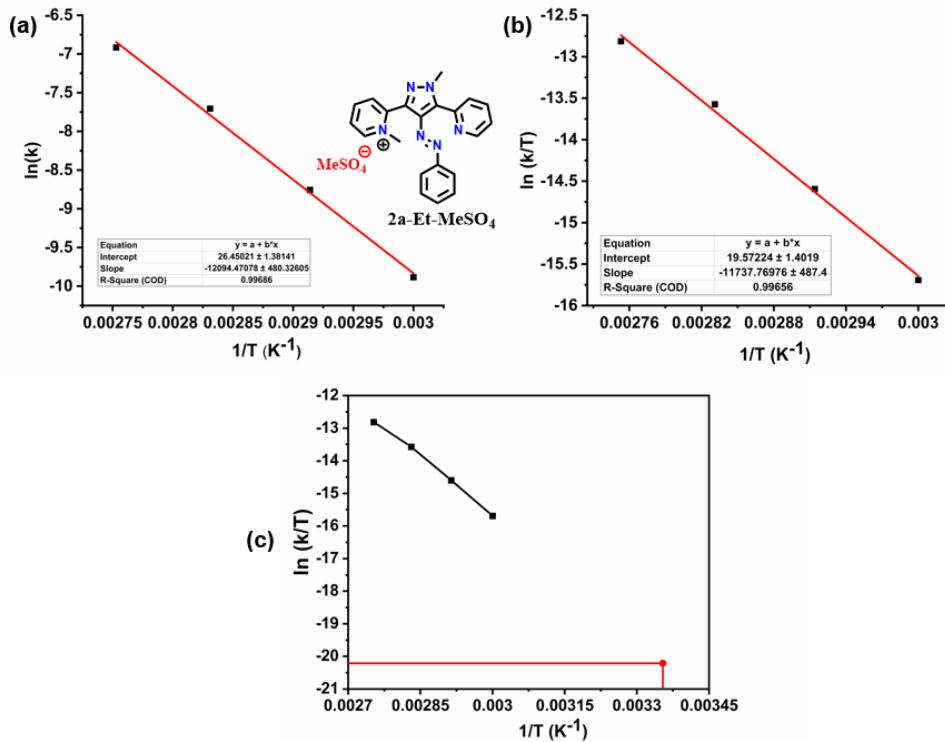


Figure S4.23. (a) Arrhenius plot, and (b) Eyring plot for **2a-Me-MeSO₄** in DMSO; (c) Linear extrapolation of Eyring plot for **2a-Me-MeSO₄** in DMSO to room temperature (298 K).

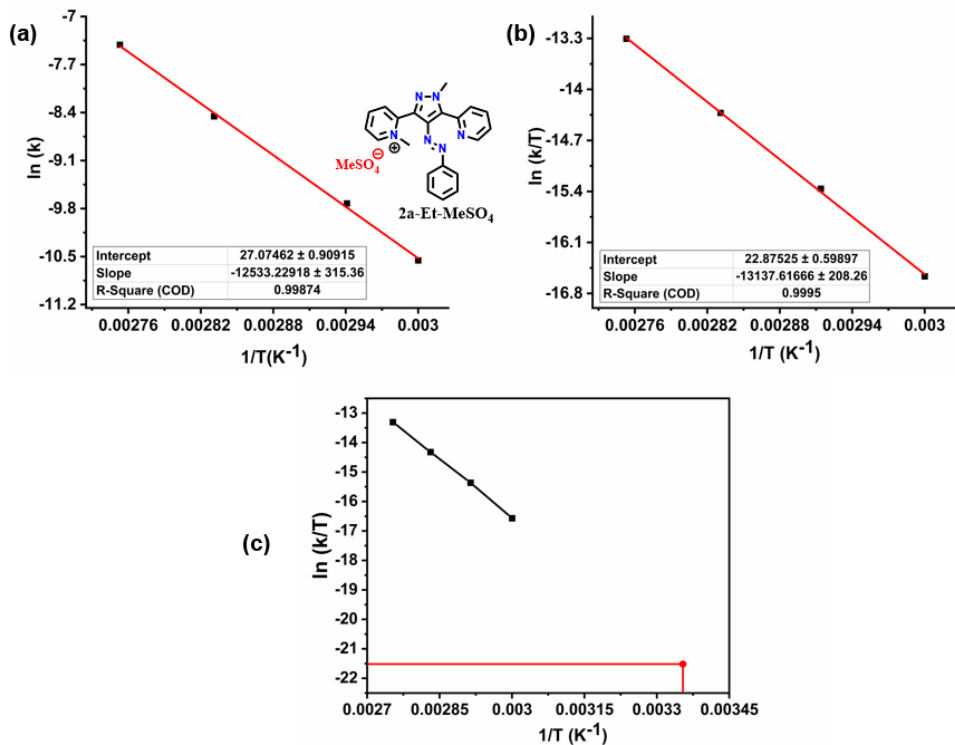


Figure S4.24. (a) Arrhenius plot, and (b) Eyring plot for **2a-Me-MeSO₄** in H₂O; (c) Linear extrapolation of Eyring plot for **2a-Me-MeSO₄** in H₂O to room temperature (298 K).

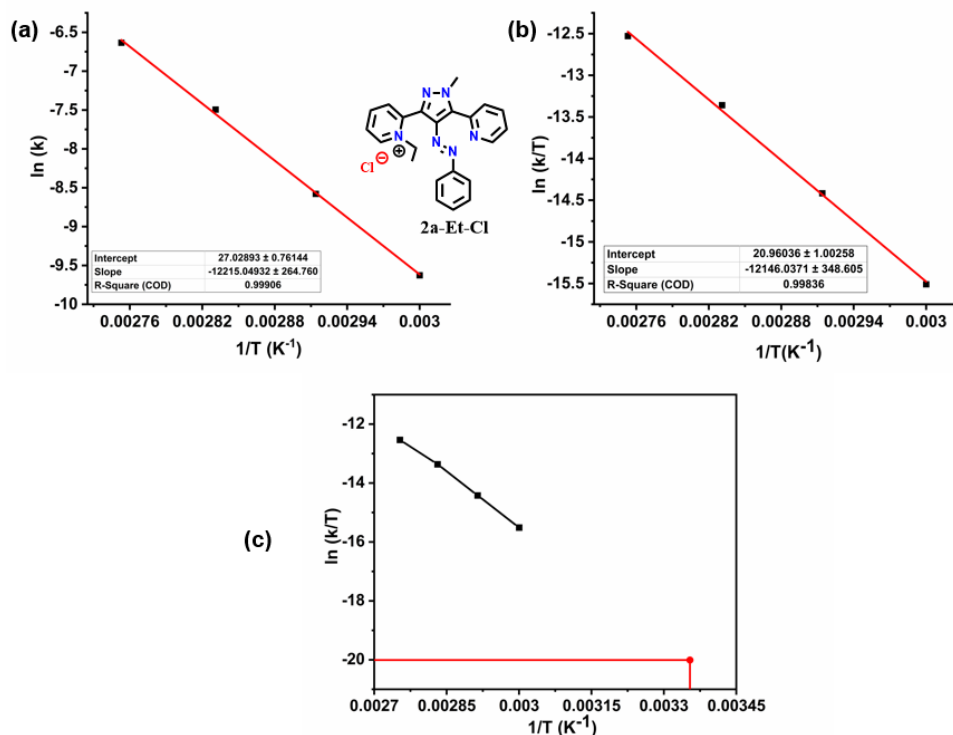


Figure S4.25. (a) Arrhenius plot, and (b) Eyring plot for **2a-Et-Cl** in DMSO; (c) Linear extrapolation of Eyring plot for **2a-Et-Cl** in DMSO to room temperature (298 K).

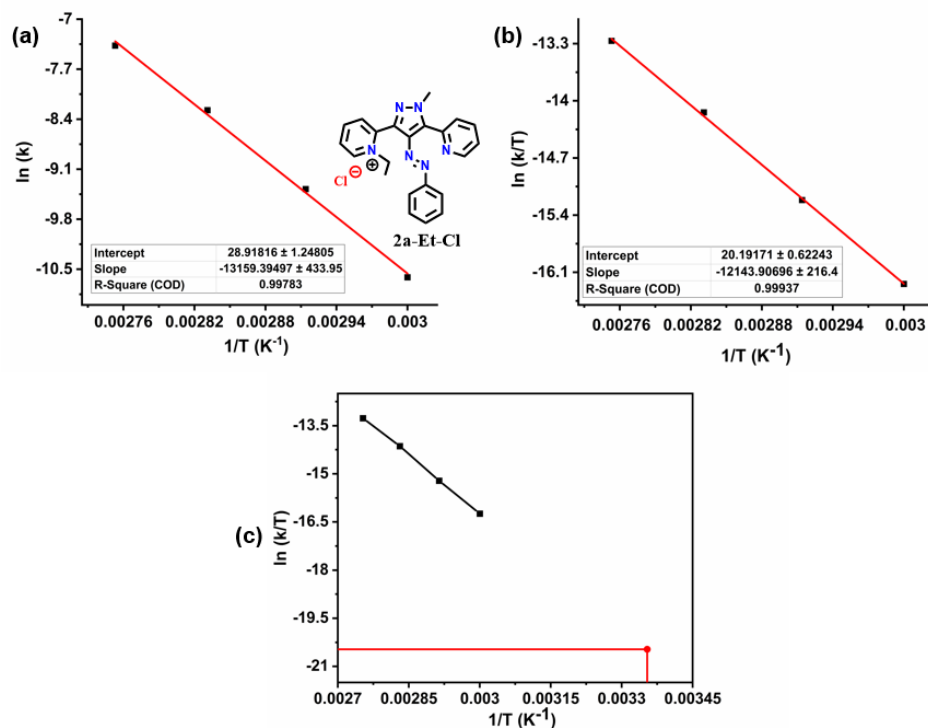


Figure S4.26. (a) Arrhenius plot, and (b) Eyring plot for **2a-Et-Cl** in H_2O ; (c) Linear extrapolation of Eyring plot for **2a-Et-Cl** in H_2O to room temperature (298 K).

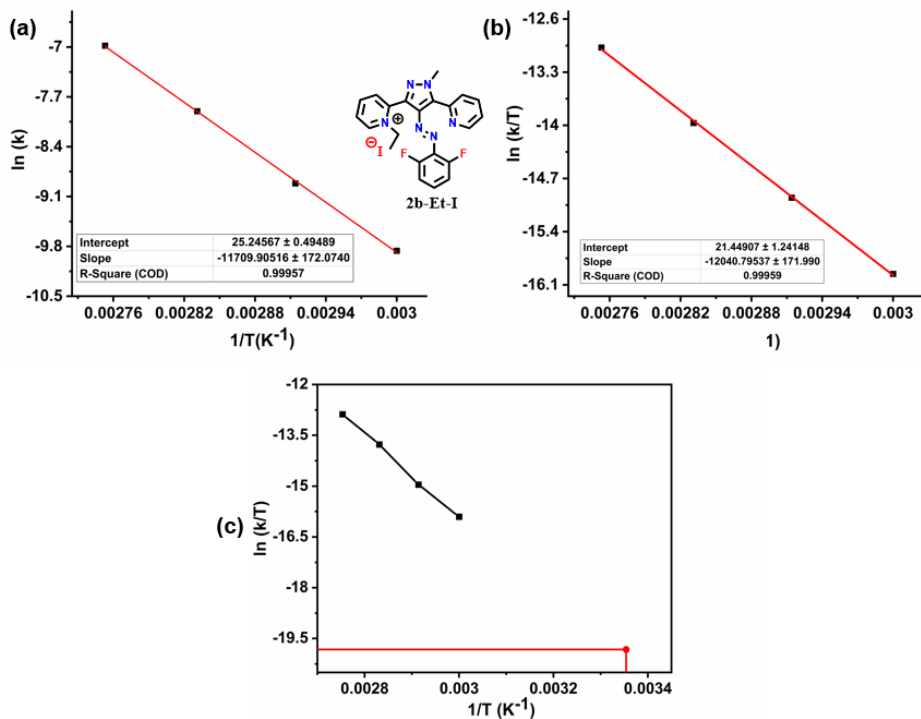


Figure S4.27. (a) Arrhenius plot, and (b) Eyring plot for **2b-Et-I** in DMSO; (c) Linear extrapolation of Eyring plot for **2b-Et-I** in DMSO to room temperature (298 K).

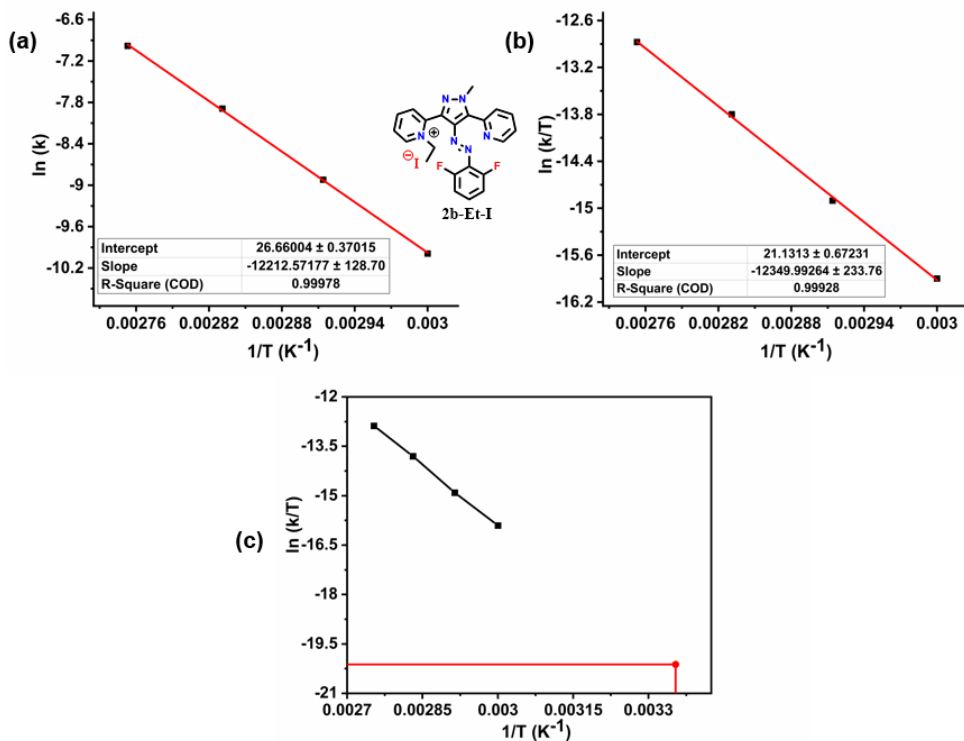


Figure S4.28. (a) Arrhenius plot, and (b) Eyring plot for **2b-Et-I** in H_2O ; (c) Linear extrapolation of Eyring plot for **2b-Et-I** in H_2O to room temperature (298 K).

Table S4.1. Comparison of rate constants and half-lives of thermal Z-E isomerization of all the targets in DMSO and water at 70 °C.

| S.No. | Compound | Rate Constant (k) in DMSO | Half Life in DMSO | Rate Constant (k) in water | Half Life in water |
|----------|-------------------------------|---------------------------|-------------------|----------------------------|--------------------|
| 1 | 2a | 1.3×10^{-3} | 537 | - | - |
| 2 | 2b | 1.4×10^{-3} | 500 | - | - |
| 3 | 2a-Et-I | 1.1×10^{-2} | 64 | 5.0×10^{-3} | 138 |
| 4 | 2a-Et-BF4 | 1.0×10^{-2} | 66 | 4.4×10^{-3} | 158 |
| 5 | 2a-Et-Cl | 1.1×10^{-2} | 61 | 5.1×10^{-3} | 136 |
| 6 | 2a-Me-MeSO₄ | 9.5×10^{-3} | 73 | 3.5×10^{-3} | 200 |
| 7 | 2b-Et-I | 1.3×10^{-2} | 56 | 6.7×10^{-3} | 103 |
| 8 | 2a-Me-I | 1.0×10^{-2} | 66 | 4.8×10^{-3} | 145 |

Rate constants are expressed in min⁻¹ and the half-lives are indicated in minutes.

S4.3 pH dependent thermal reverse isomerisation

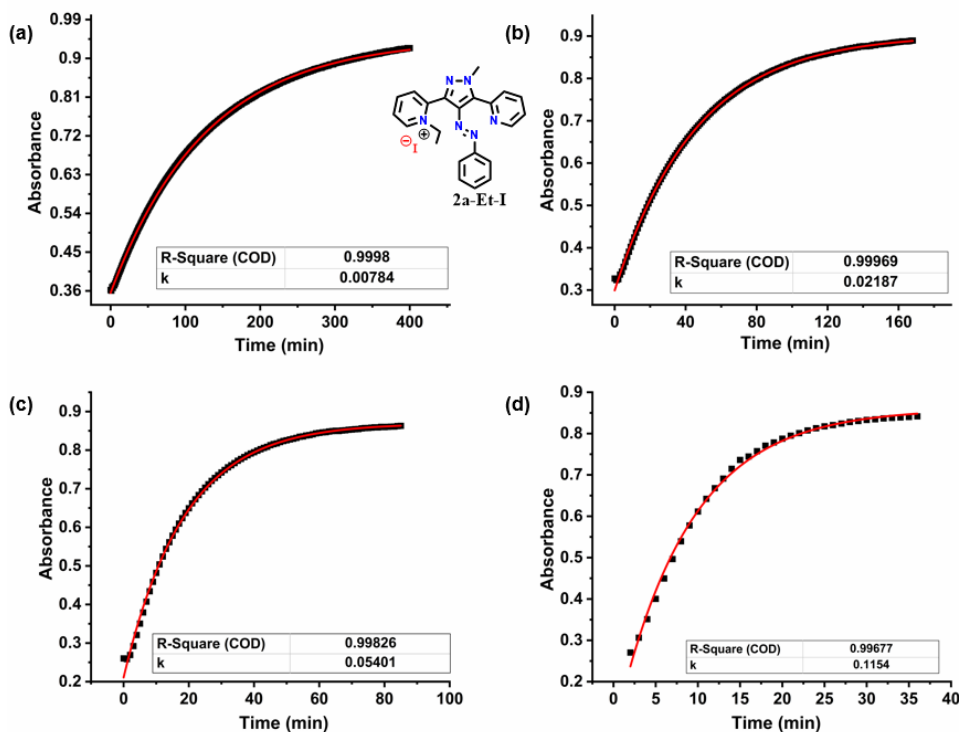


Figure S4.29. Reverse Z-E isomerization kinetics of **2a-Et-I** in phosphate buffer (pH = 2.8) at (a) 60 °C; (b) 70 °C; (c) 80 °C, and (d) 90 °C.

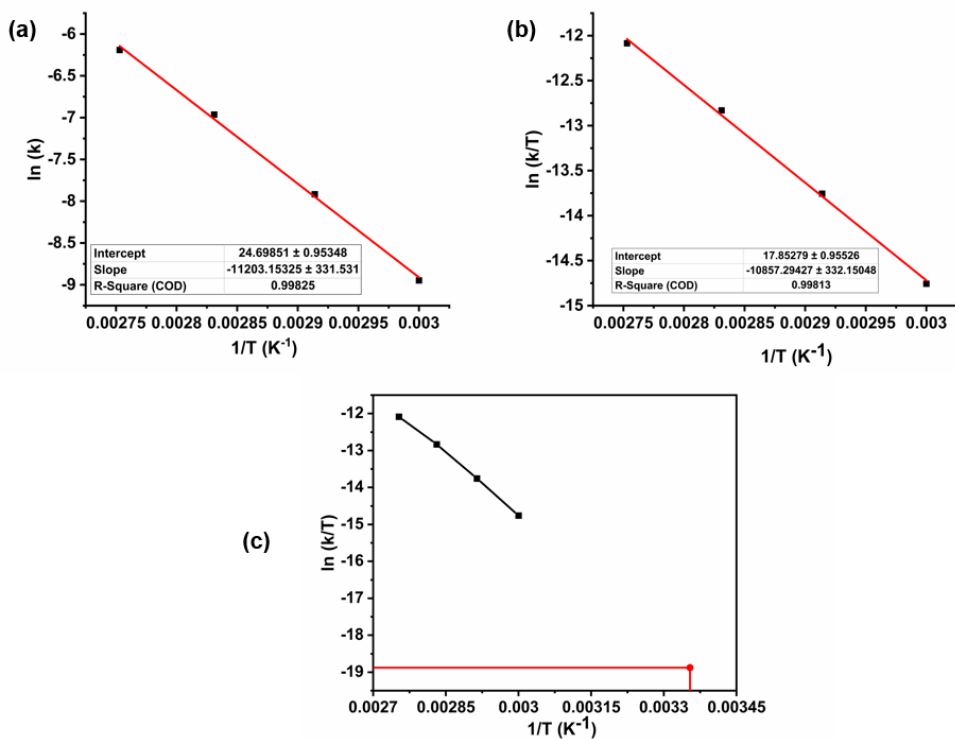


Figure S4.30. (a) Arrhenius plot, (b) Eyring plot for **2a-Et-I** in phosphate buffer ($\text{pH} = 2.8$), and (c) linear extrapolation of Eyring plot for **2a-Et-I** to room temperature (298 K).

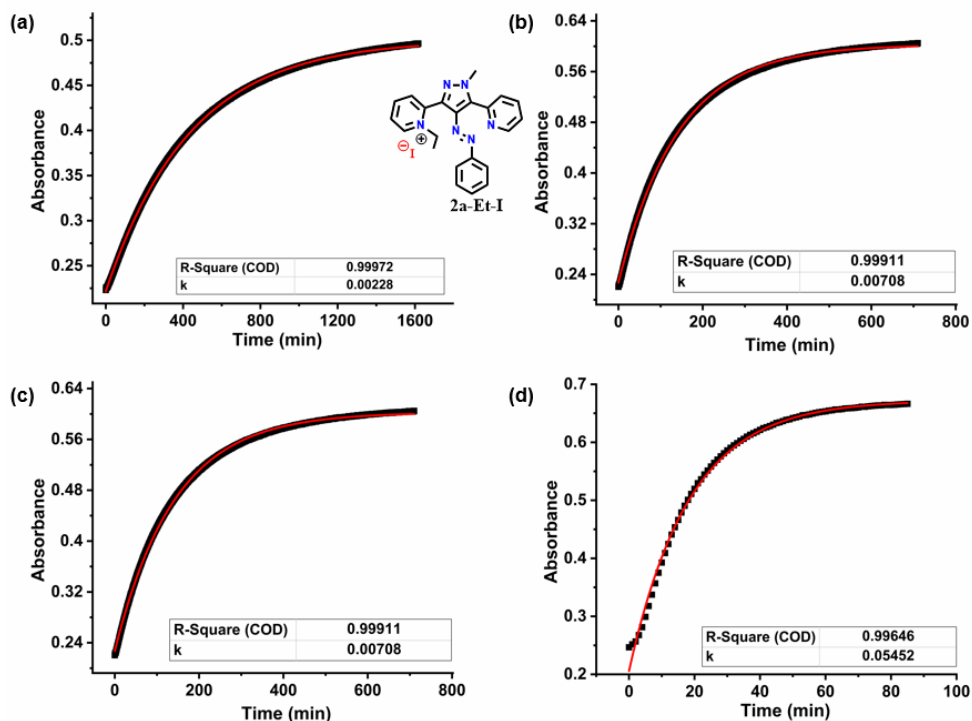


Figure S4.31. Reverse *Z-E* isomerization kinetics of **2a-Et-I** in phosphate buffer ($\text{pH} = 8.0$) at (a) 60 °C; (b) 70 °C; (c) 80 °C, and (d) 90 °C.

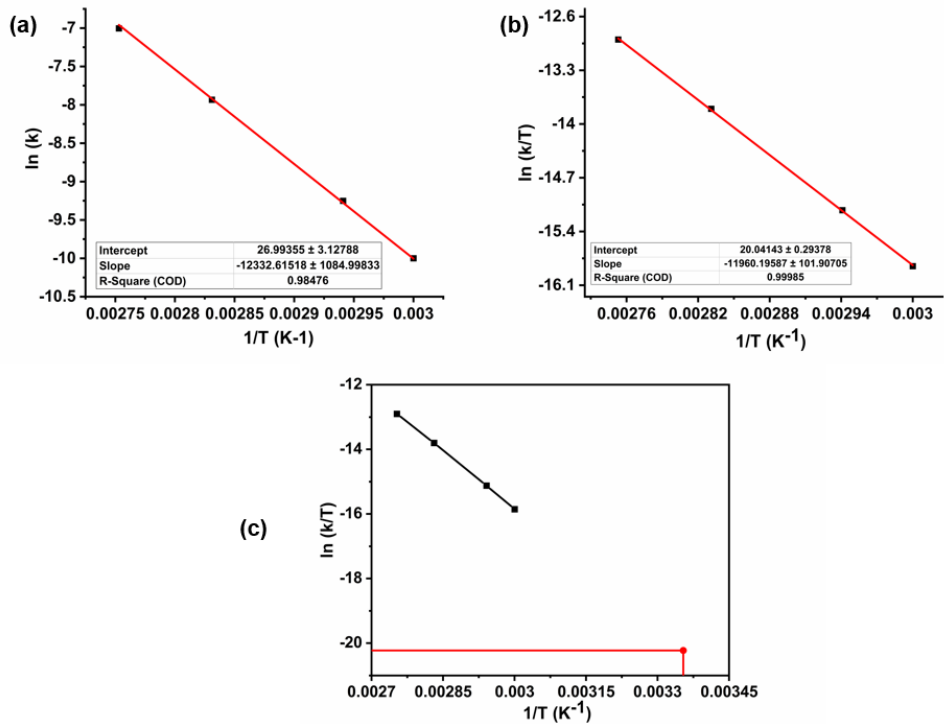


Figure S4.32. (a) Arrhenius plot, (b) Eyring plot for **2a-Et-I** in phosphate buffer (pH = 8.0) and (c) linear extrapolation of Eyring plot for **2a-Et-I** to room temperature (298 K).

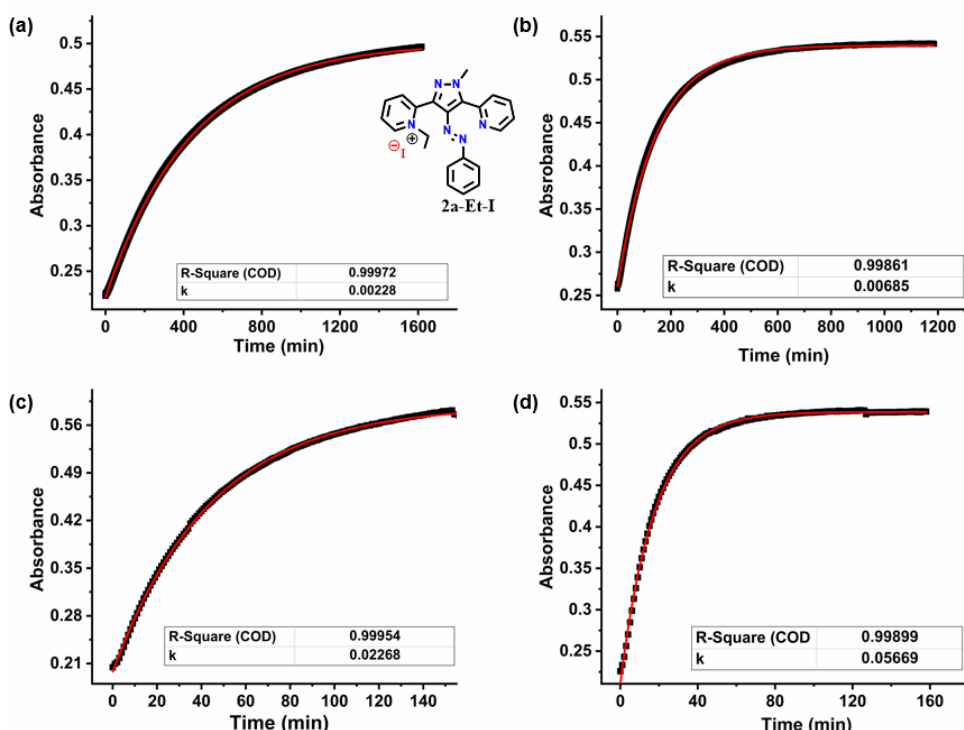


Figure S4.33. Reverse Z-E isomerization kinetics of **2a-Et-I** in phosphate buffer (pH = 7.4) at (a) 60 °C; (b) 70 °C; (c) 80 °C, and (d) 90 °C.

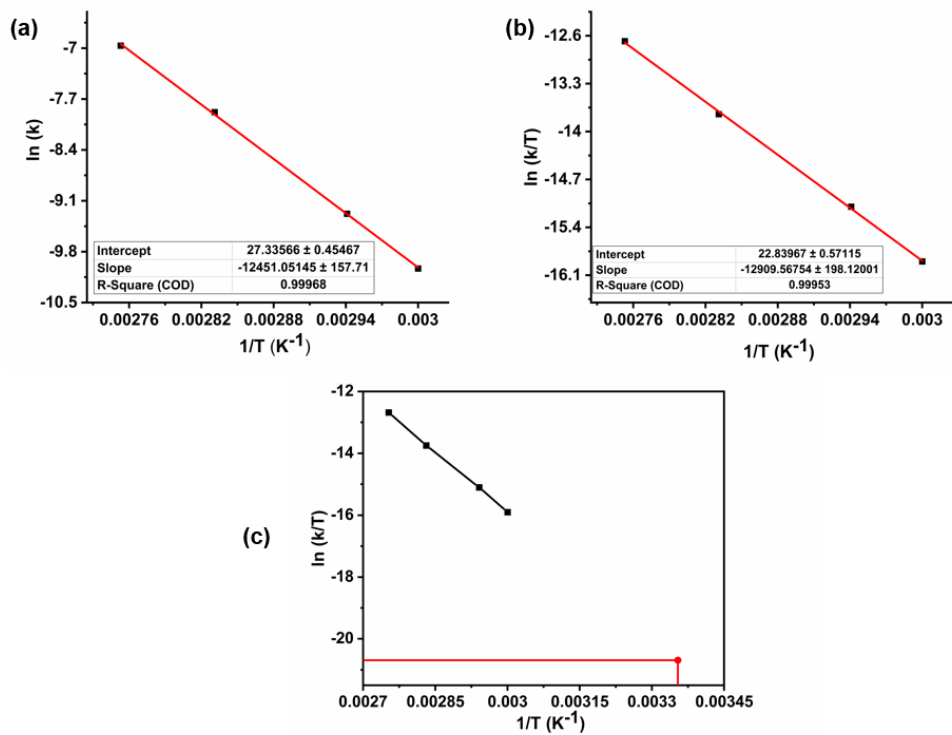


Figure S4.34. (a) Arrhenius plot, (b) Eyring plot for **2a-Et-I** in phosphate buffer ($pH = 7.4$) and (c) linear extrapolation of Eyring plot for **2a-Et-I** to room temperature (298 K)

Table S4.2. Activation parameters deduced from the variable temperature kinetics studies using Arrhenius and Eyring plots

| S. No. | Compound | E_a (kJ/mol) | ΔG^\ddagger (kJ/mol) | ΔH^\ddagger (kJ/mol) | ΔS^\ddagger (J/K mol) | k^a at 25 °C (s ⁻¹) | $t_{1/2}$ (Min) | $\Delta G^{\ddagger b}$ (kcal/mol) |
|-----------|-------------------------------|-------------------|---------------------------------|---------------------------------|----------------------------------|--------------------------------------|--------------------|---------------------------------------|
| 1 | 2a | 114.6 ± 0.9 | 114.9 ± 3.0 | 113.1 ± 0.53 | -6.2 ± 4.6 | 3.8 x 10 ⁻⁸ | 3,03,947 | 27.5 27.8 |
| 2 | 2b | 114.2 ± 1.6 | 114.5 ± 3.0 | 111.2 ± 4.6 | -11.5 ± 4.6 | 4.5 x 10 ⁻⁸ | 2,57,238 | 27.4 |
| 3 | 2a-Me-I | 105.9 ± 5.2 | 108.5 ± 1.0 | 102.7 ± 5.3 | -18.5 ± 1.5 | 5.9 x 10 ⁻⁷ | 19,676 | 25.9 |
| 4 | 2a-Me-I | 106.4 ± 1.5 | 110.5 ± 1.5 | 103.8 ± 8.2 | -22.7 ± 2.4 | 2.3 x 10 ⁻⁷ | 39,965 | 26.4 |
| 5 | 2a-Et-I | 104.2 ± 2.2 | 108.0 ± 3.3 | 101.3 ± 1.8 | -21.8 ± 5.2 | 5.9 x 10 ⁻⁷ | 19,604 | 25.8 25.7 |
| 6 | 2a-Et-I | 109.4 ± 3.6 | 110.3 ± 1.5 | 104.7 ± 9.5 | -18.7 ± 2.7 | 3.1 x 10 ⁻⁷ | 37,574 | 26.4 25.7 |
| 7 | 2b-Et-I | 97.3 ± 1.4 | 106.1 ± 4.4 | 100.1 ± 1.4 | -19.5 ± 10.3 | 7.33 x 10 ⁻⁷ | 15,757 | 25.3 |
| 8 | 2b-Et-I | 101.5 ± 1.1 | 109.2 ± 3.8 | 102.7 ± 1.9 | -22.1 ± 5.6 | 5.4 x 10 ⁻⁷ | 21,192 | 26.1 |
| 9 | 2a-Et-BF₄ | 103.2 ± 2.23 | 108.1 ± 4.2 | 100.3 ± 2.3 | -26.1 ± 6.5 | 5.2 x 10 ⁻⁷ | 22,331 | 25.8 25.9 |
| 10 | 2a-Et-BF₄ | 107.2 ± 2.1 | 110.9 ± 0.8 | 108.2 ± 9.5 | -9.2 ± 2.7 | 2.1 x 10 ⁻⁷ | 55,263 | 26.5 26.0 |
| 11 | 2a-Me-MeSO₄ | 100.5 ± 2.1 | 108.3 ± 1.5 | 97.6 ± 3.3 | -34.8 ± 11.7 | 4.9 x 10 ⁻⁷ | 23,338 | 25.9 25.8 |
| 12 | 2a-Me-MeSO₄ | 111.5 ± 2.9 | 111.5 ± 2.9 | 109.2 ± 1.7 | -7.6 ± 4.0 | 1.4 x 10 ⁻⁷ | 85,555 | 26.6 26.0 |
| 13 | 2a-Et-Cl | 101.6 ± 2.2 | 107.8 ± 4.3 | 101.0 ± 2.9 | -23.5 ± 8.3 | 6.3 x 10 ⁻⁷ | 18,383 | 25.8 25.2 |
| 14 | 2a-Et-Cl | 109.4 ± 3.6 | 109.7 ± 3.3 | 101.0 ± 1.8 | -29.9 ± 5.2 | 3.8 x 10 ⁻⁷ | 30,078 | 25.7 25.2 |
| 15 | 2a-Et-I @ pH = 2.8 | 93.1 ± 2.8 | 105.0 ± 2.1 | 90.3 ± 2.8 | -49.4 ± 8.0 | 1.9 x 10 ⁻⁶ | 6,111 | 21.6 |
| 16 | 2a-Et-I @ pH = 7.4 | 103.5 ± 1.3 | 109.9 ± 3.1 | 107.3 ± 1.6 | -7.9 ± 4.7 | 3.2 x 10 ⁻⁷ | 35,700 | 26.3 |
| 17 | 2a-Et-I @ pH = 8 | 102.5 ± 9.0 | 108.9 ± 9.3 | 99.4 ± 0.8 | -31.2 ± 2.4 | 4.8 x 10 ⁻⁷ | 23,592 | 23.7 |

^aThe rate constants (*k*) at room temperature (25 °C) were estimated based on extrapolation. ΔG^\ddagger values in kcal/mol (Normal text represent experimental values and bold text represent computational values obtained at B3LYP-D3/6-311++G(d,p) level of theory); The corresponding data in H₂O and buffer at specified pH are represented with blue and green shades, respectively. Those data without shading are estimated in DMSO.

Table S4.3. Rate constants and half-lives at variable temperature

| Compound | Temp. (° C) | Rate Constant <i>k</i> (s ⁻¹) | Half-life (min) | Compound | Temp. (° C) | Rate Constant <i>k</i> (s ⁻¹) | Half-life (min) |
|-----------------------------|----------------|--|--------------------|-------------------------------|----------------|--|--------------------|
| 2a | 90 | $2.0 \times 10^{-4} \pm 3.3 \times 10^{-8}$ | 60 | 2a @pH = 2.8 | 80 | $1.3 \times 10^{-3} \pm 8.5 \times 10^{-5}$ | 9 |
| | 80 | $6.9 \times 10^{-5} \pm 1.5 \times 10^{-7}$ | 167 | 2a @pH = 5 | 80 | $1.0 \times 10^{-4} \pm 7.4 \times 10^{-8}$ | 113 |
| | 70 | $2.2 \times 10^{-5} \pm 2.4 \times 10^{-8}$ | 536 | 2a @pH = 7.4 | 80 | $8.7 \times 10^{-5} \pm 2.9 \times 10^{-8}$ | 133 |
| | 25 | 3.8×10^{-8} | 3,03,947 | 2a-Et-I | 90 | $6.4 \times 10^{-4} \pm 4.1 \times 10^{-7}$ | 18 |
| 2b | 90 | $2.4 \times 10^{-4} \pm 1.6 \times 10^{-7}$ | 48 | | 80 | $2.5 \times 10^{-4} \pm 2.8 \times 10^{-6}$ | 46 |
| | 80 | $7.7 \times 10^{-5} \pm 1.0 \times 10^{-7}$ | 149 | | 70 | $8.5 \times 10^{-5} \pm 3.2 \times 10^{-8}$ | 138 |
| | 70 | $2.3 \times 10^{-5} \pm 6.8 \times 10^{-9}$ | 500 | | 60 | $2.5 \times 10^{-5} \pm 1.5 \times 10^{-9}$ | 456 |
| | 25 | 4.5×10^{-8} | 2,57,238 | | 25 | 3.1×10^{-7} | 37,574 |
| 2a-Et-I | 90 | $1.2 \times 10^{-3} \pm 1.7 \times 10^{-5}$ | 9 | 2a-Et-BF₄ | 90 | $6.5 \times 10^{-4} \pm 1.0 \times 10^{-5}$ | 18 |
| | 80 | $5.0 \times 10^{-4} \pm 2.2 \times 10^{-6}$ | 23 | | 80 | $2.2 \times 10^{-4} \pm 2.8 \times 10^{-7}$ | 52 |
| | 70 | $1.8 \times 10^{-4} \pm 2.6 \times 10^{-7}$ | 64 | | 70 | $7.3 \times 10^{-5} \pm 2.9 \times 10^{-8}$ | 158 |
| | 60 | $5.7 \times 10^{-5} \pm 7.8 \times 10^{-8}$ | 201 | | 60 | $2.5 \times 10^{-5} \pm 4.4 \times 10^{-9}$ | 467 |
| | 25 | 5.9×10^{-7} | 19,604 | | 25 | 2.1×10^{-7} | 55,263 |
| 2a-Et-BF₄ | 90 | $1.2 \times 10^{-3} \pm 2.2 \times 10^{-5}$ | 9 | 2a-Me-MeSO₄ | 90 | $5.5 \times 10^{-4} \pm 3.1 \times 10^{-6}$ | 28 |
| | 80 | $4.9 \times 10^{-4} \pm 3.1 \times 10^{-6}$ | 23 | | 80 | $2.1 \times 10^{-4} \pm 5.6 \times 10^{-7}$ | 54 |
| | 70 | $1.7 \times 10^{-4} \pm 1.4 \times 10^{-7}$ | 66 | | 70 | $5 \times 10^{-5} \pm 1.8 \times 10^{-8}$ | 200 |
| | 60 | $5.5 \times 10^{-5} \pm 1.2 \times 10^{-8}$ | 208 | | 60 | $2.1 \times 10^{-5} \pm 2.4 \times 10^{-8}$ | 541 |
| | 25 | 5.2×10^{-7} | 22,331 | | 25 | 1.3×10^{-7} | 85,555 |

| | | | | | | | |
|-------------------------------|----|---|--------|---------------------------|----|---|--------|
| 2a-Me MeSO₄ | 90 | $9.9 \times 10^{-4} \pm 2.6 \times 10^{-5}$ | 12 | 2a-Et-Cl | 90 | $6.7 \times 10^{-4} \pm 7.8 \times 10^{-6}$ | 16 |
| | 80 | $4.7 \times 10^{-4} \pm 1.3 \times 10^{-6}$ | 27 | | 80 | $2.6 \times 10^{-4} \pm 6.1 \times 10^{-7}$ | 45 |
| | 70 | $1.6 \times 10^{-4} \pm 2.2 \times 10^{-7}$ | 73 | | 70 | $8.5 \times 10^{-5} \pm 3.7 \times 10^{-8}$ | 136 |
| | 60 | $5.2 \times 10^{-5} \pm 2.3 \times 10^{-8}$ | 223 | | 60 | $2.5 \times 10^{-5} \pm 1.3 \times 10^{-8}$ | 450 |
| | 25 | 4.9×10^{-7} | 23,338 | | 25 | 3.8×10^{-7} | 30,078 |
| 2a-Et-Cl* | 90 | $1.3 \times 10^{-3} \pm 6.1 \times 10^{-6}$ | 9 | 2a-Et-I @ pH = 2.5 | 90 | $1.9 \times 10^{-3} \pm 5.1 \times 10^{-6}$ | 6 |
| | 80 | $5.6 \times 10^{-4} \pm 1.7 \times 10^{-6}$ | 21 | | 80 | $9.5 \times 10^{-4} \pm 2.8 \times 10^{-6}$ | 12 |
| | 70 | $1.9 \times 10^{-4} \pm 1.5 \times 10^{-7}$ | 61 | | 70 | $3.6 \times 10^{-4} \pm 1.4 \times 10^{-6}$ | 32 |
| | 60 | $6.0 \times 10^{-5} \pm 3.9 \times 10^{-8}$ | 193 | | 60 | $1.3 \times 10^{-4} \pm 2.8 \times 10^{-7}$ | 88 |
| | 25 | 6.3×10^{-7} | 18,383 | | 25 | 1.9×10^{-6} | 6,111 |
| 2b-Et-I* | 90 | $1.4 \times 10^{-3} \pm 5.1 \times 10^{-6}$ | 8 | 2a-Et-I @ pH = 7.4 | 90 | $9.4 \times 10^{-4} \pm 5.0 \times 10^{-6}$ | 12 |
| | 80 | $5.8 \times 10^{-4} \pm 1.5 \times 10^{-6}$ | 20 | | 80 | $3.8 \times 10^{-4} \pm 9.7 \times 10^{-6}$ | 31 |
| | 70 | $2.1 \times 10^{-4} \pm 3.2 \times 10^{-7}$ | 56 | | 70 | $1.1 \times 10^{-4} \pm 1.6 \times 10^{-6}$ | 101 |
| | 60 | $6.3 \times 10^{-5} \pm 3.0 \times 10^{-8}$ | 182 | | 60 | $3.6 \times 10^{-5} \pm 6.8 \times 10^{-8}$ | 313 |
| | 25 | 7.33×10^{-7} | 15,757 | | 25 | 3.2×10^{-7} | 35,700 |
| 2a-Me-I* | 90 | $1.3 \times 10^{-3} \pm 9.3 \times 10^{-6}$ | 12 | 2b-Et-I | 90 | $9.3 \times 10^{-4} \pm 9.0 \times 10^{-6}$ | 12 |
| | 80 | $4.9 \times 10^{-4} \pm 2.1 \times 10^{-6}$ | 23 | | 80 | $3.7 \times 10^{-4} \pm 2.8 \times 10^{-6}$ | 31 |
| | 70 | $1.7 \times 10^{-4} \pm 4.6 \times 10^{-7}$ | 66 | | 70 | $1.1 \times 10^{-4} \pm 5.1 \times 10^{-7}$ | 103 |
| | 60 | $5.6 \times 10^{-5} \pm 4.7 \times 10^{-8}$ | 204 | | 60 | $3.7 \times 10^{-5} \pm 1.1 \times 10^{-7}$ | 314 |
| | 25 | 5.9×10^{-7} | 19,676 | | 25 | 3.2×10^{-7} | 35,543 |
| 2a-Et-I @ pH = 8 | 90 | $9.1 \times 10^{-4} \pm 1.4 \times 10^{-6}$ | 12 | 2a-Me-I | 90 | $6.0 \times 10^{-4} \pm 4.8 \times 10^{-6}$ | 19 |
| | 80 | $3.6 \times 10^{-4} \pm 1.5 \times 10^{-6}$ | 32 | | 80 | $2.6 \times 10^{-4} \pm 1.4 \times 10^{-7}$ | 49 |
| | 70 | $1.2 \times 10^{-4} \pm 1.9 \times 10^{-7}$ | 98 | | 70 | $8.0 \times 10^{-5} \pm 3.9 \times 10^{-8}$ | 145 |
| | 60 | $3.8 \times 10^{-5} \pm 4.3 \times 10^{-8}$ | 303 | | 60 | $2.5 \times 10^{-5} \pm 1.5 \times 10^{-7}$ | 470 |

| | | | | | | | |
|--|----|----------------------|--------|--|----|----------------------|--------|
| | 25 | 4.9×10^{-7} | 23,592 | | 25 | 2.9×10^{-7} | 39,965 |
|--|----|----------------------|--------|--|----|----------------------|--------|

The data obtained in DMSO are represented with blue shades, whereas those estimated in H₂O (or buffer at specified pH) are represented without shading. Those data shaded in grey correspond to estimated rate constants and half-lives at room temperature using linear extrapolation in Eyring plot.

S5. Computational details

All density functional theory (DFT) calculations were performed using the Gaussian16 (Revision C.01) suite of quantum chemical programs.⁵ The geometry optimizations of *Z*, *E*, and transition states (*TS*) were carried out using hybrid generalized gradient approximation, B3LYP functional⁶ including Grimme's dispersion correction⁷ (D3) with Becke Johns damping and 6-311++G(d,p) basis set⁸ for all the other atoms. Relativistic effective core potential SDD⁹ was used for the I atom. Vibrational frequency analyses were performed on all the *E* and *Z* isomers to ensure that the stationary points were local minima on the potential energy surface. Transition states were identified using the Berny algorithm and were confirmed with only one imaginary frequency that corresponds to the inversion mechanism.¹⁰ Potential energy surface (PES) scan calculations were performed to obtain transition state barriers for inversion mechanisms by varying the N=N-C_{phenyl}/N=N-C_{pyrazole} bond angle and C-N-N-C dihedral angle for rotational mechanisms. Solvent effects (DMSO and water) were considered using the linear-response integral equation formalism-polarizable continuum model (LR-IEF-PCM) approach.¹¹ The rate constant for the isomerization at 298.15 K was calculated based on the Eyring equation.

$$k(T) = \frac{k_B T}{hc_0} e^{\frac{-\Delta G^\ddagger}{RT}}$$

where k_B is the Boltzmann constant, h is Planck's constant and R is the gas constant. For all the calculations c_0 is considered to be one. The ΔG^\ddagger is the free energy change between the transition state and the *Z* isomer.

The topological investigation of the electron density distribution was carried out using Bader's atoms in molecules (AIM) formalism¹² using Multiwfn software.¹³ Espinosa's formulation¹⁴ was used to determine the strength of weak interatomic interactions in different *E*, *Z* isomers, and *TS*'s. VMD software¹⁵ was used to acquire isosurfaces of the non-covalent interaction (NCI)¹⁶ and reduced density gradient (RDG) from the Multiwfn outputs. The RDG analysis uses the sign of λ_2 and electron density ρ to distinguish between repulsive and attractive interactions. In this analysis, the function sign (λ_2) ρ is defined as a product of the signal (λ_2) with ρ . Positive values correspond to nonbonding interactions (red surfaces), while negative values (λ_2) ρ indicate attractive interactions (blue surfaces), such as hydrogen bonds or dipole-dipole interactions. Green surfaces with a sign (λ_2) ρ approaching 0 are caused by van der Waals (vdW) interactions.

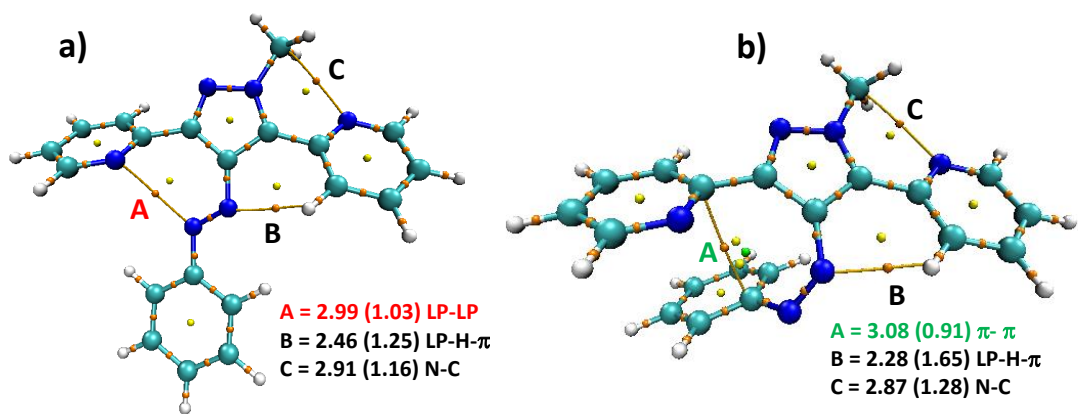


Figure S5.1. The optimized a) *E* and b) *Z* isomers of **2a** in the gas phase and AIM computed topological diagrams. The atomic contacts representing various NCIs are in Å, and the corresponding electron densities ($\rho \times 10^{-2}$ au) at the bond critical points are given in parentheses and the type of interaction is represented for each BCP. (Color code:- gold: bond critical point; yellow: ring critical point, and green: cage critical point).

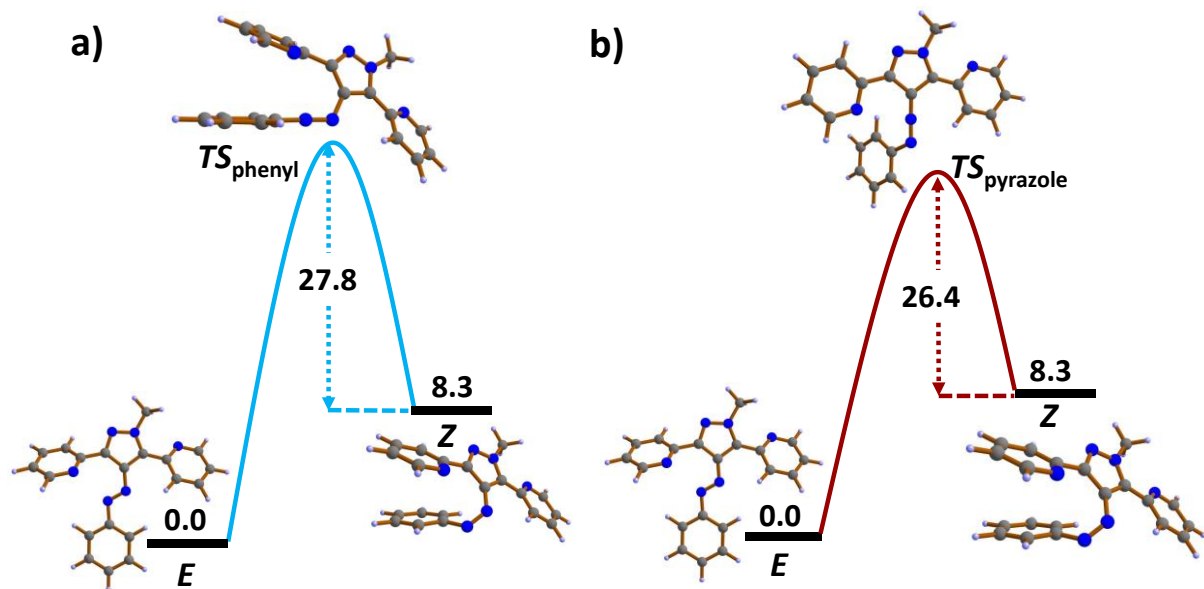


Figure S5.2. Inversion barriers along the azo nitrogen connected to a) phenyl and b) pyrazole ring, respectively for *Z* to *E* conversion of **2a** in DMSO.

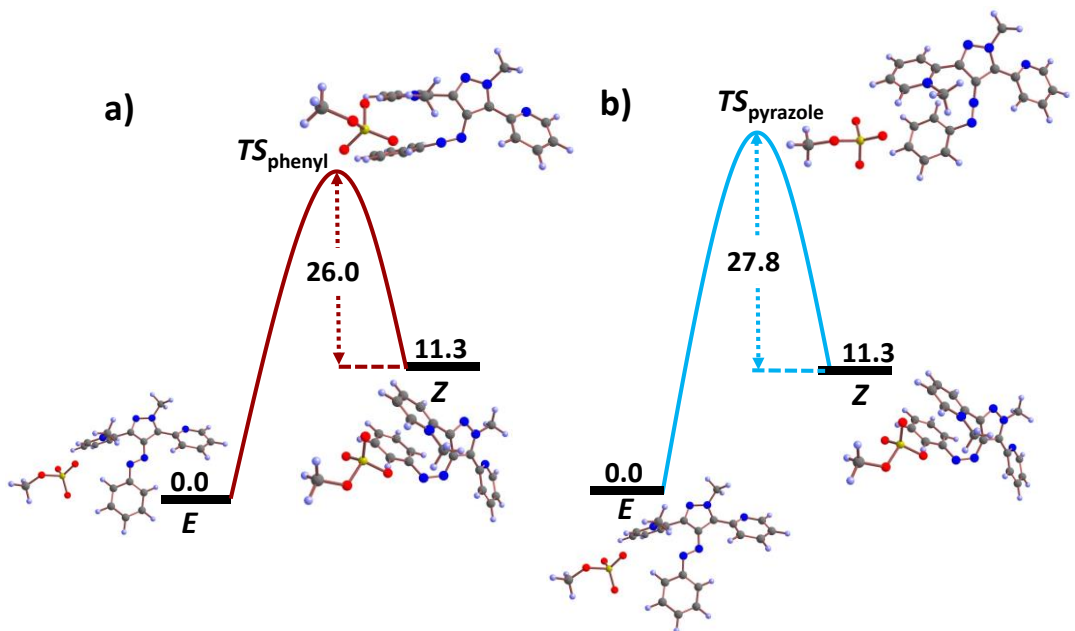


Figure S5.3. Inversion barriers along the azo nitrogen connected to a) phenyl and b) pyrazole ring, respectively for *Z* to *E* conversion of **2a**-Me-MeSO₄ in water.

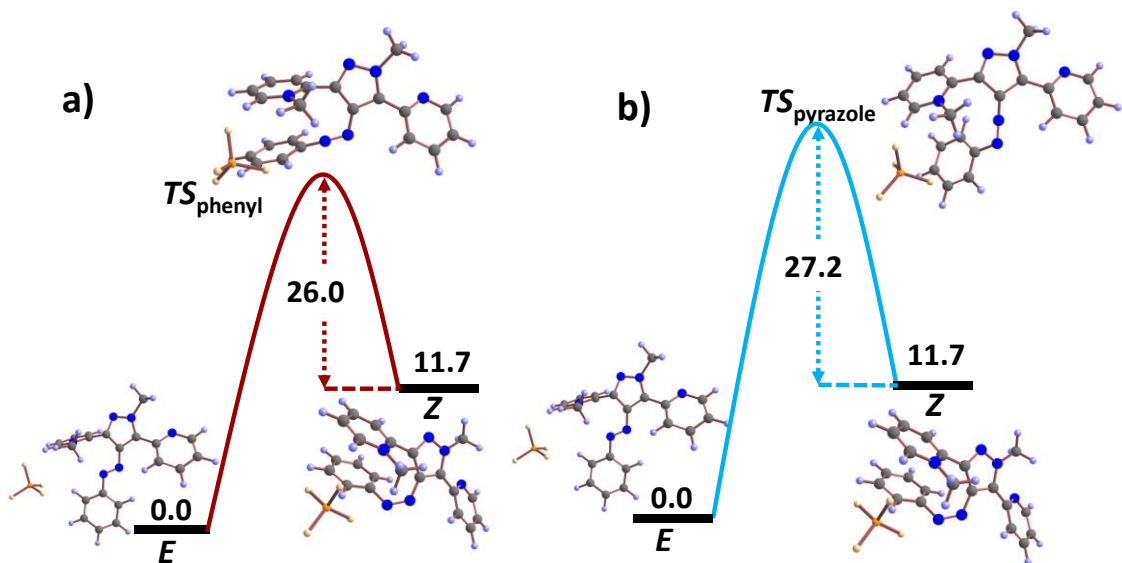


Figure S5.4. Inversion barriers along the azo nitrogen connected to a) phenyl and b) pyrazole ring, respectively for *Z* to *E* conversion of **2a**-Me-BF₄ in water.

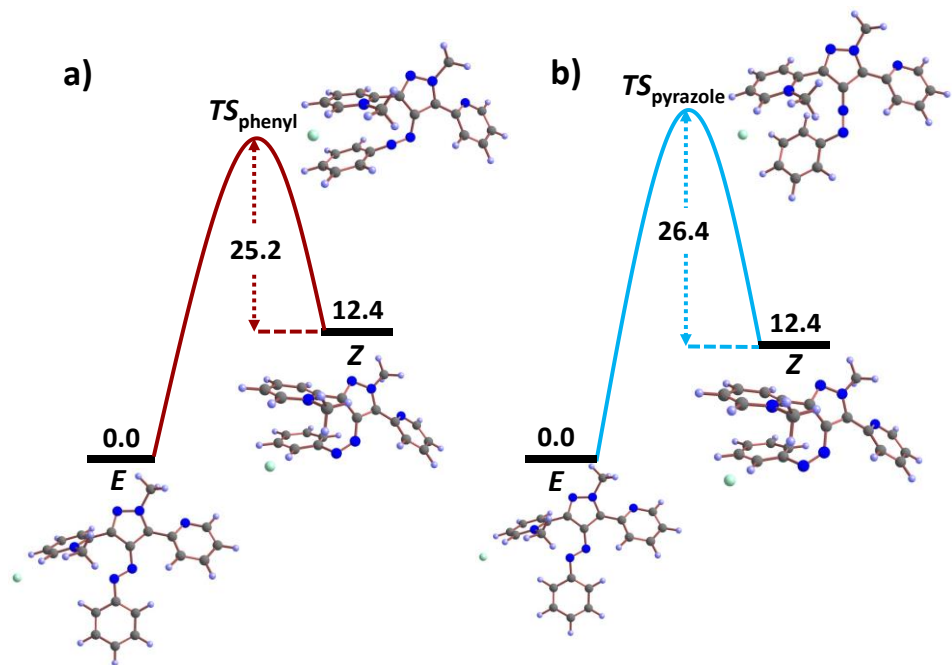


Figure S5.5. Inversion barriers along the azo nitrogen connected to a) phenyl and b) pyrazole ring, respectively for *Z* to *E* conversion of **2a-Me-Cl** in water.

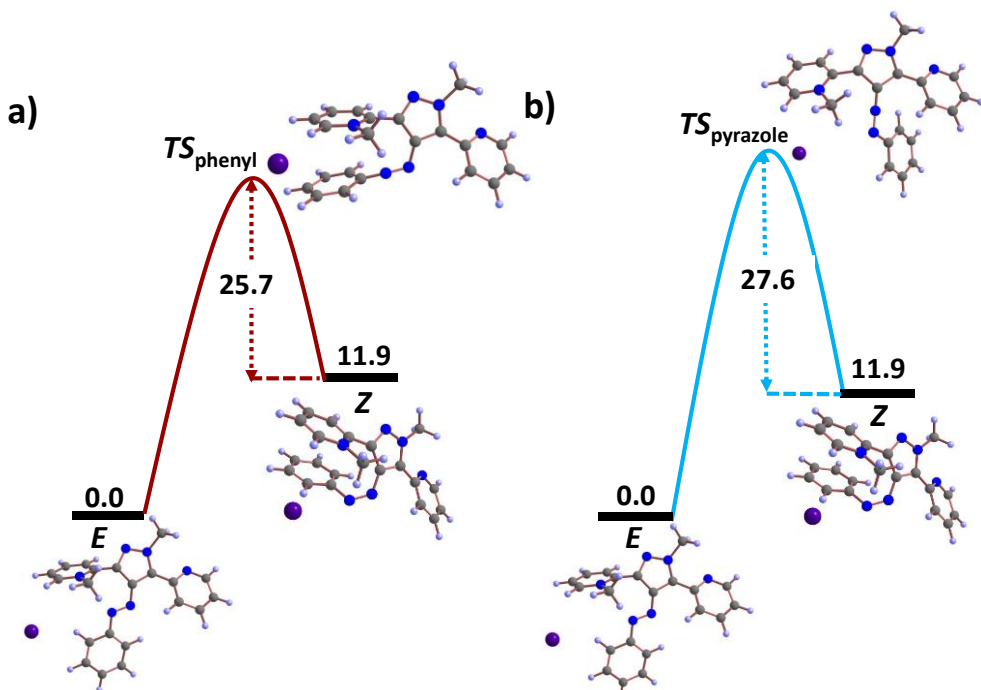


Figure S5.6. Inversion barriers along the azo nitrogen connected to a) phenyl and b) pyrazole ring, respectively for *Z* to *E* conversion of **2a-Me-I** in water.

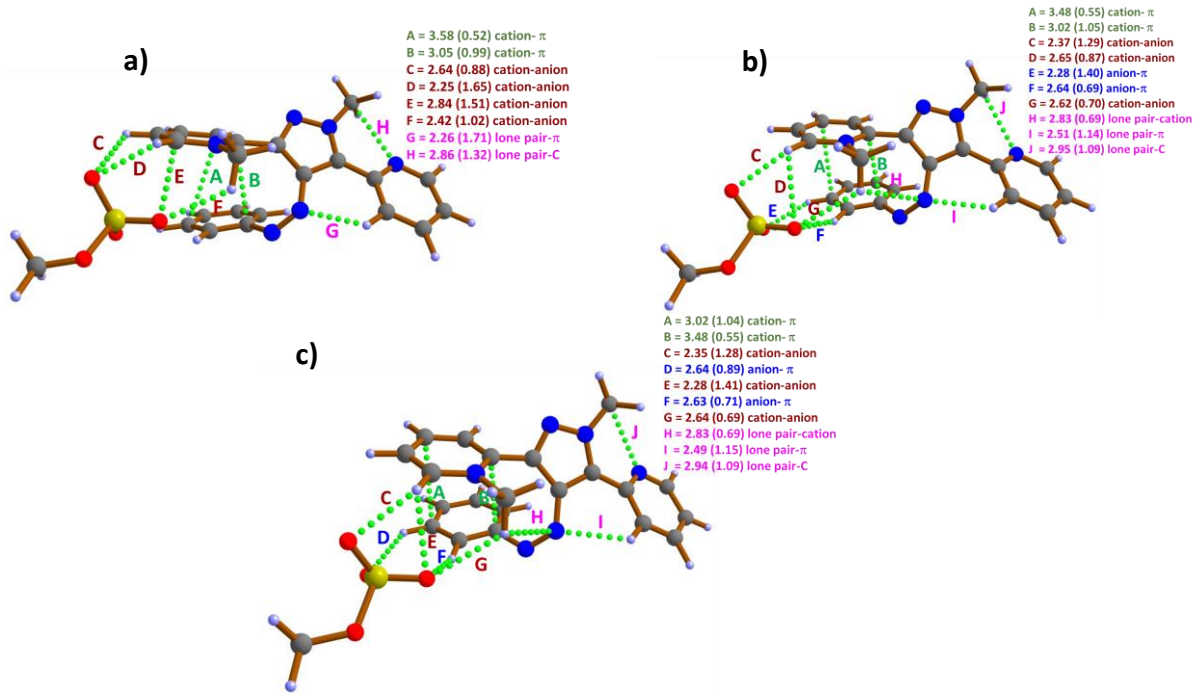


Figure S5.7. The optimized Z isomer of **2a-Me-MeSO₄** in a) gas phase, b) water, and c) DMSO and their non-covalent interactions. The atomic contacts (green color) representing various NCIs are in Å, and the corresponding electron densities ($\rho \times 10^{-2}$ au) at the bond critical points are given in parentheses.

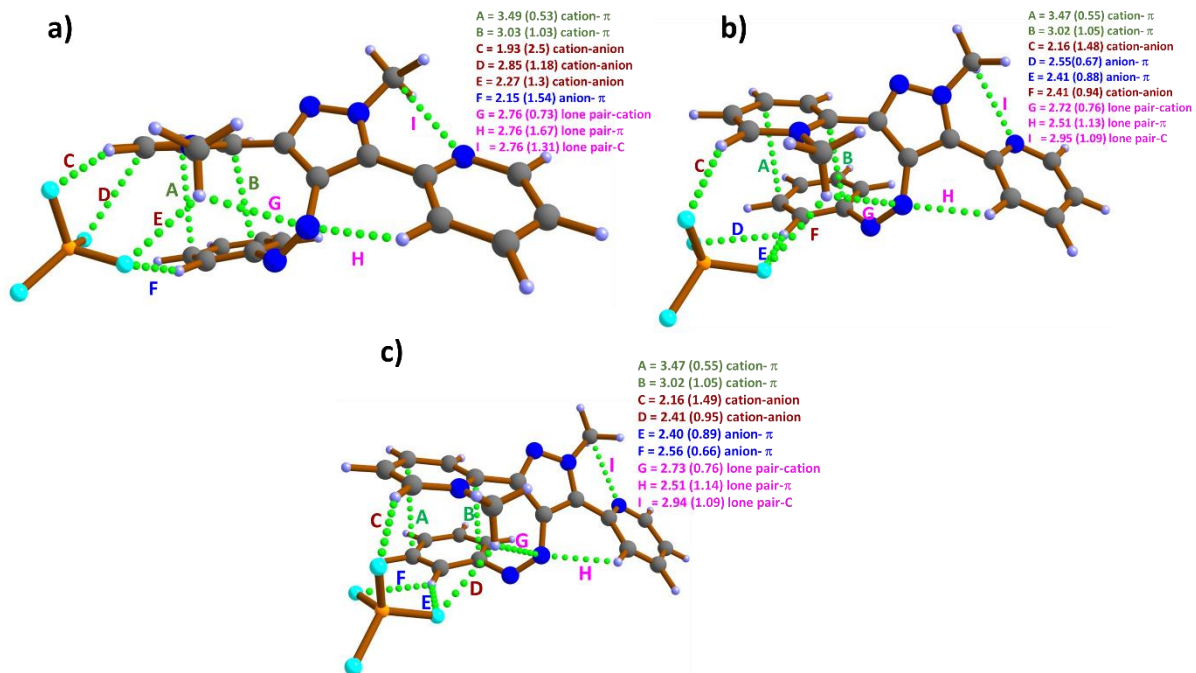


Figure S5.8. The optimized Z isomer of **2a-Me-BF₄** in a) gas phase, b) water, and c) DMSO and their non-covalent interactions. The atomic contacts (green color) representing various NCIs are in Å, and the corresponding electron densities ($\rho \times 10^{-2}$ au) at the bond critical points are given in parentheses.

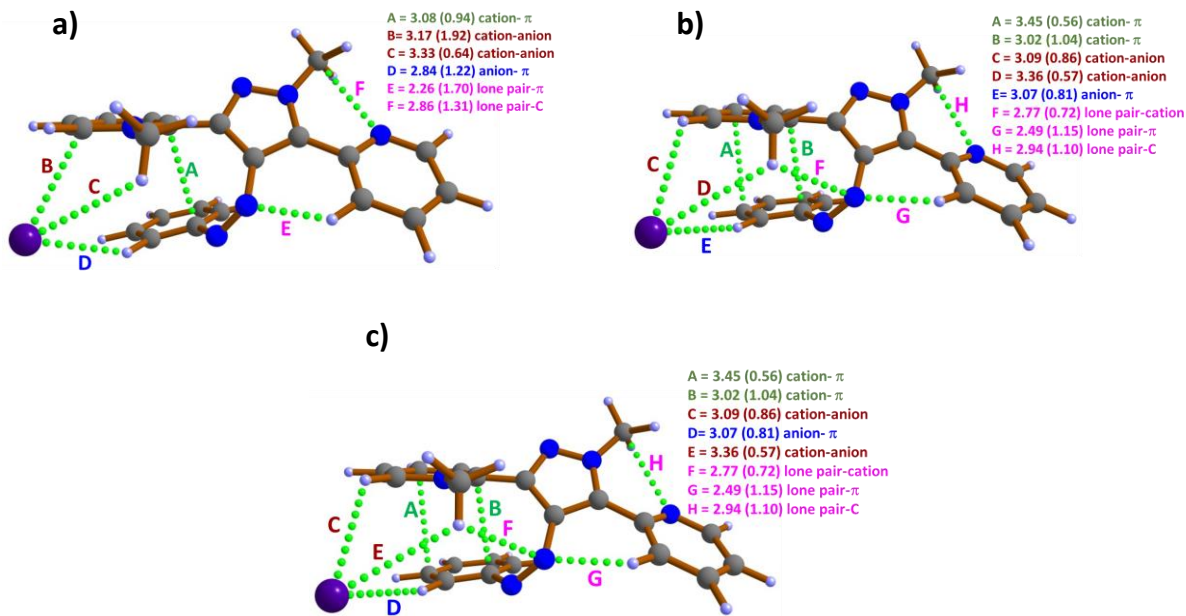


Figure S5.9. The optimized Z isomer of **2a-Me-I** in a) gas phase, b) water, and c) DMSO and their non-covalent interactions. The atomic contacts (green color) representing various NCIs are in Å, and the corresponding electron densities ($\rho \times 10^{-2}$ au) at the bond critical points are given in parentheses.

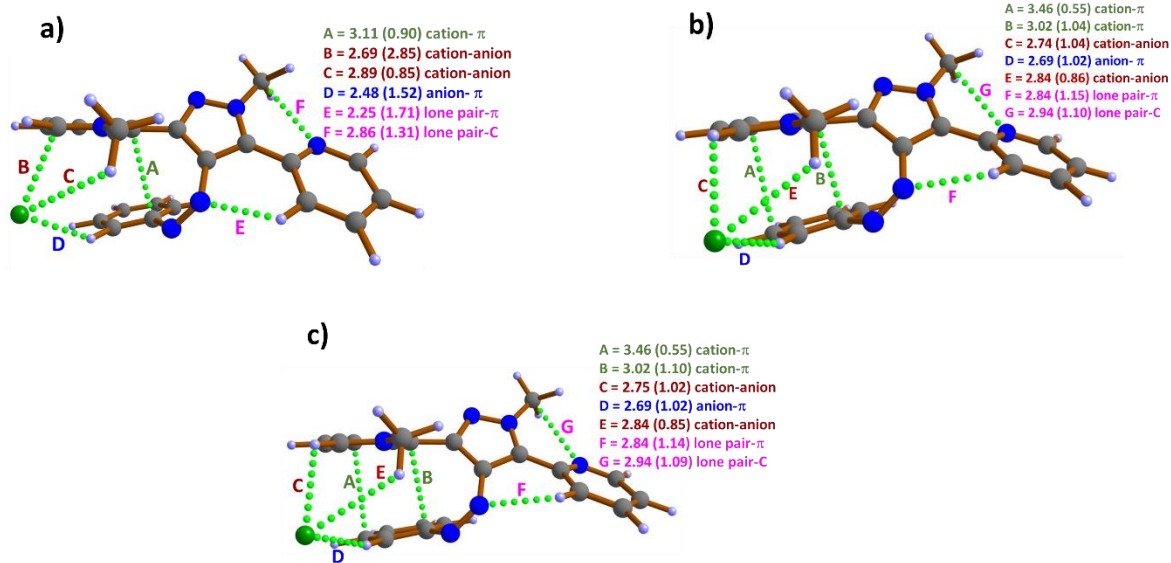


Figure S5.10. The optimized Z isomer of **2a-Me-Cl** in a) gas phase, b) water, and c) DMSO and their non-covalent interactions. The atomic contacts (green color) representing various NCIs are in Å, and the corresponding electron densities ($\rho \times 10^{-2}$ au) at the bond critical points are given in parentheses.

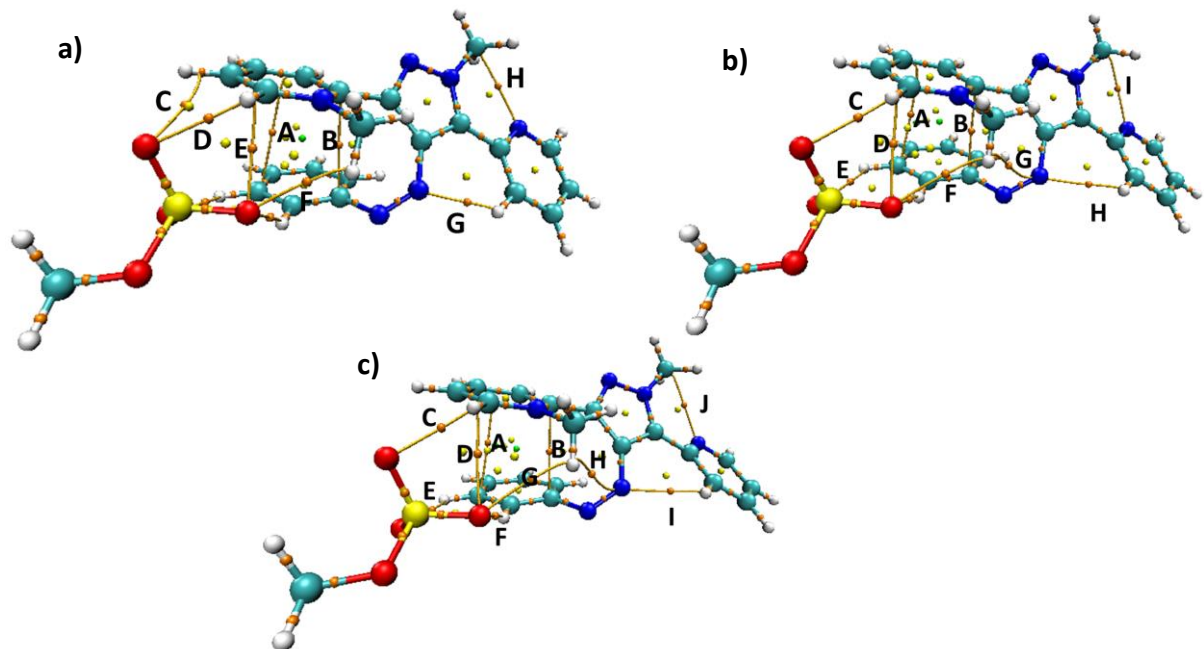


Figure S5.11. AIM computed topological diagrams for the *Z* isomer of **2a-Me-MeSO₄** in a) gas phase, b) water, and c) DMSO and their non-covalent interactions. (Color code:- gold: bond critical point; yellow: ring critical point, and green: cage critical point).

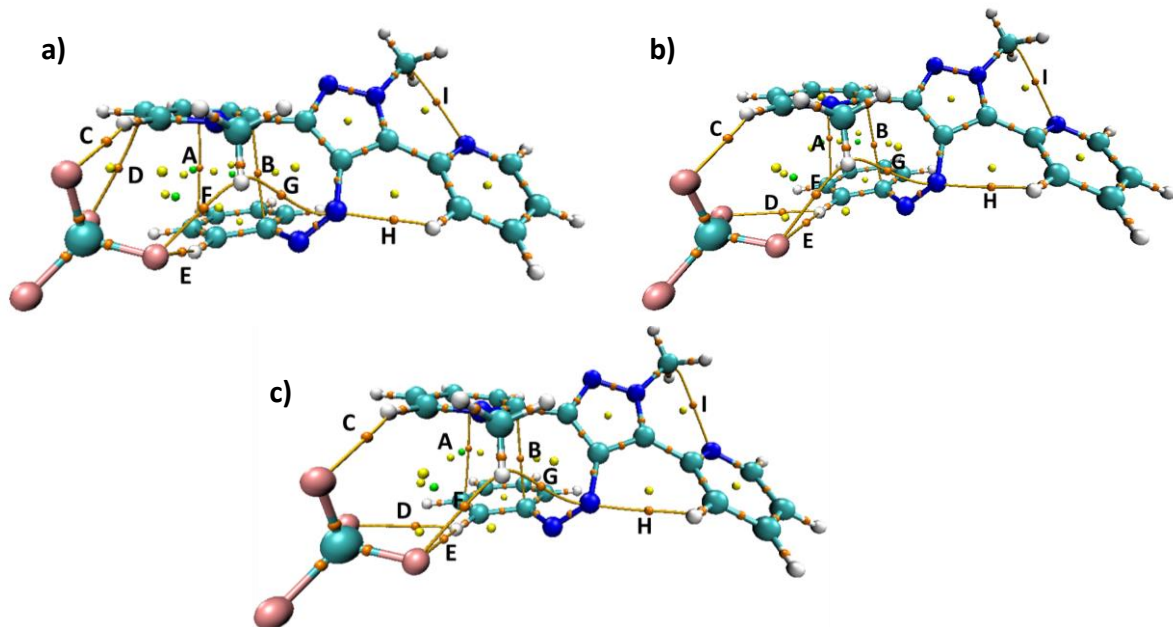


Figure S5.12. AIM computed topological diagrams for the *Z* isomer of **2a-Me-BF₄** in a) gas phase, b) water, and c) DMSO and their non-covalent interactions. (Color code:- gold: bond critical point; yellow: ring critical point, and green: cage critical point).

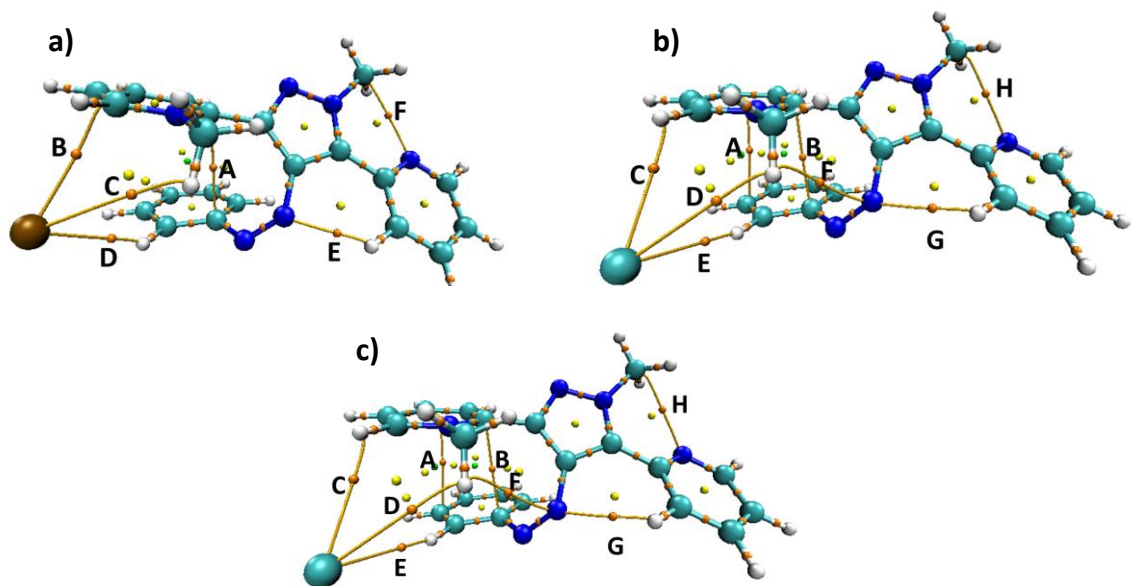


Figure S5.13. AIM computed topological diagrams for the *Z* isomer of **2a-Me-I** in a) gas phase, b) water, and c) DMSO and their non-covalent interactions. (Color code:- gold: bond critical point; yellow: ring critical point, and green: cage critical point).

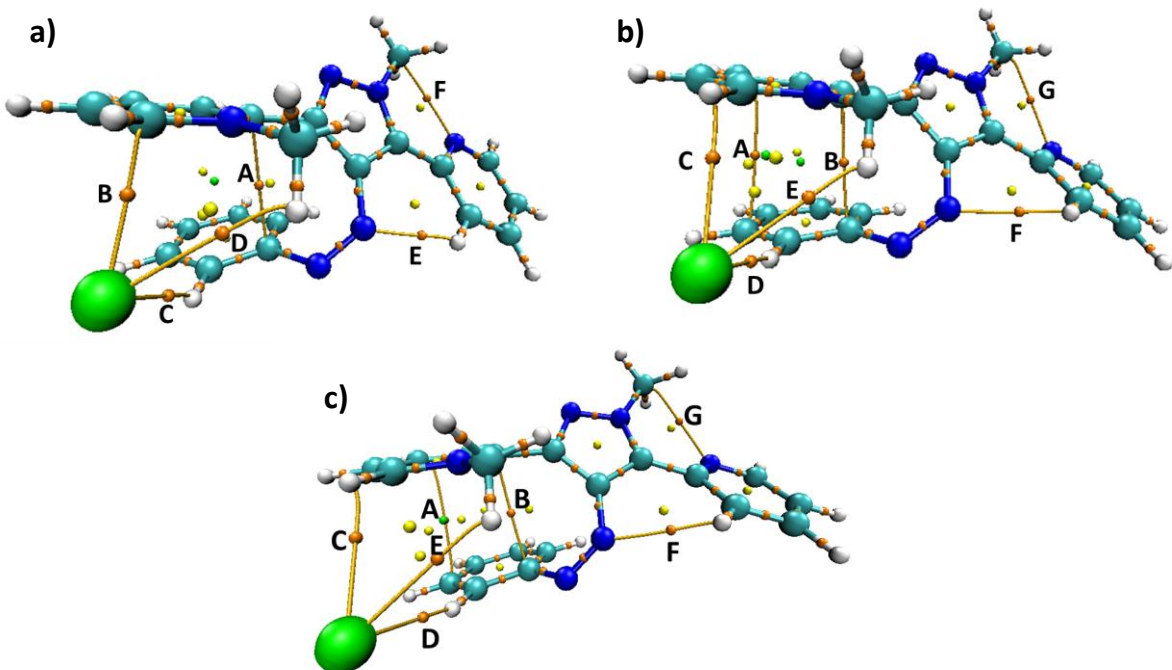


Figure S5.14. AIM computed topological diagrams for the *Z* isomer of **2a-Me-Cl** in a) gas phase, b) water, and c) DMSO and their non-covalent interactions. (Color code:- gold: bond critical point; yellow: ring critical point, and green: cage critical point).

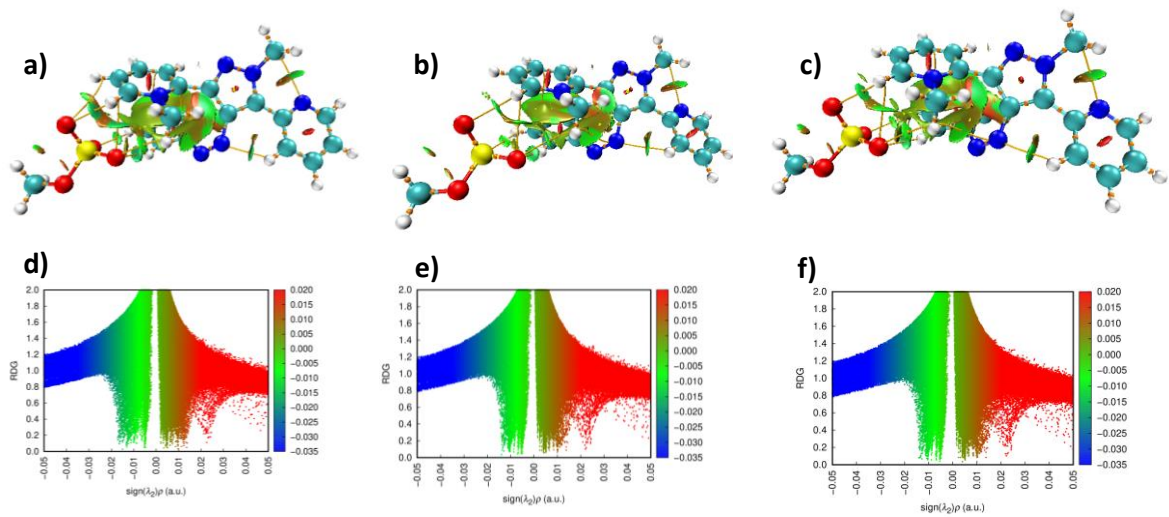


Figure S5.15. a-c) Non-covalent interaction (NCI) plots, and d-f) reduced density gradient (RDG) scatter plots of Z isomers of **2a**-Me-MeSO₄ in a) gas phase, b) water, and c) DMSO (The blue-colored spikes in the negative region of the scatter plot correspond to the hydrogen bonds, the red colored spikes represent the strong repulsive interactions, and the green region indicates the van der Waals interaction).

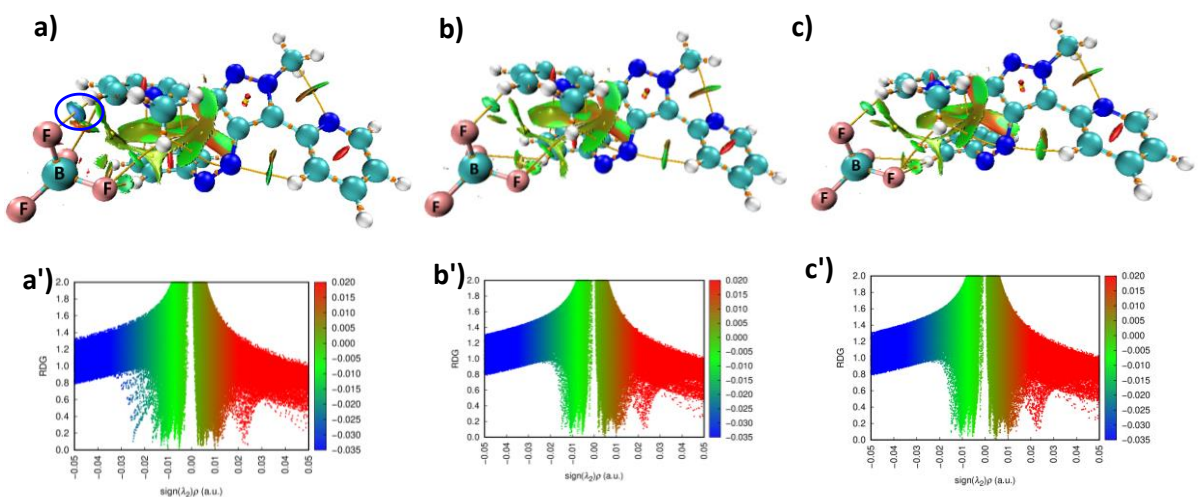


Figure S5.16. a-c) Non-covalent interaction (NCI) plots and d-f) reduced density gradient (RDG) scatter plots of Z isomers of **2a**-Me-BF₄ in a) gas phase, b) water, and c) DMSO (The blue-colored spikes in the negative region of the scatter plot correspond to the hydrogen bonds, the red colored spikes represent the strong repulsive interactions, and the green region indicates the van der Waals interaction).

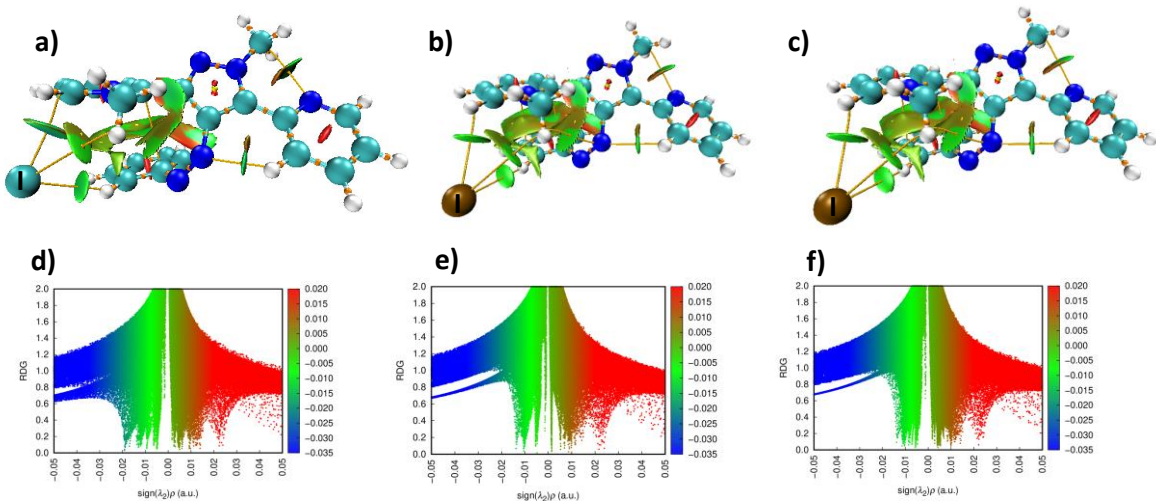


Figure S5.17. a-c) Non-covalent interaction (NCI) plots and d-f) reduced density gradient (RDG) scatter plots of Z isomers of **2a-Me-I** in a) gas phase, b) water, and c) DMSO (The blue-colored spikes in the negative region of the scatter plot correspond to the hydrogen bonds, the red colored spikes represent the strong repulsive interactions, and the green region indicates the van der Waals interaction).

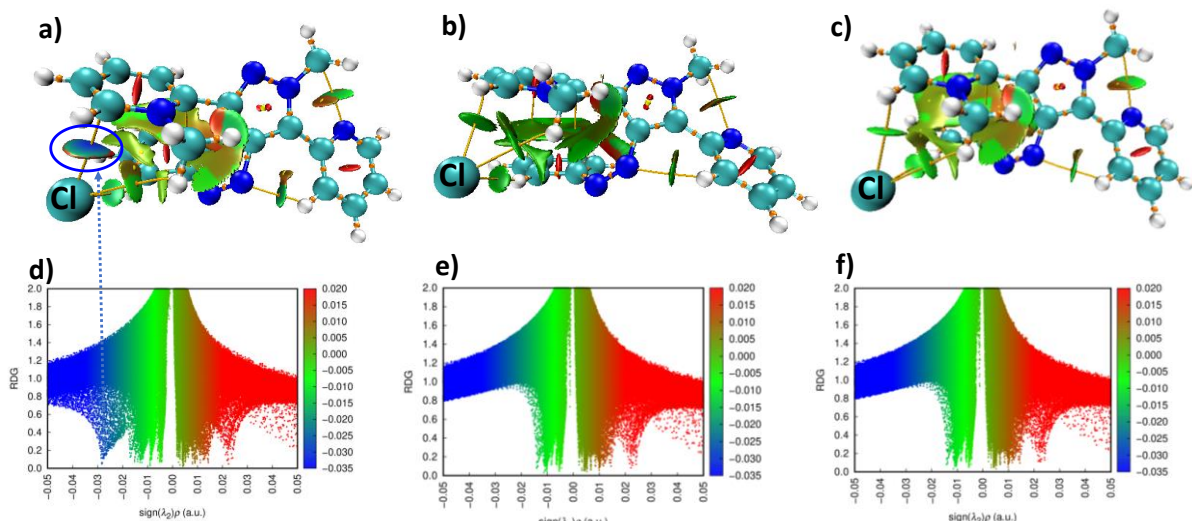


Figure S5.18. a-c) Non-covalent interaction (NCI) plots, and d-f) reduced density gradient (RDG) scatter plots of Z isomers of **2a-Me-Cl** in a) gas phase, b) water, and c) DMSO (The blue-colored spikes in the negative region of the scatter plot correspond to the hydrogen bonds, the red colored spikes represent the strong repulsive interactions, and the green region indicates the van der Waals interaction).

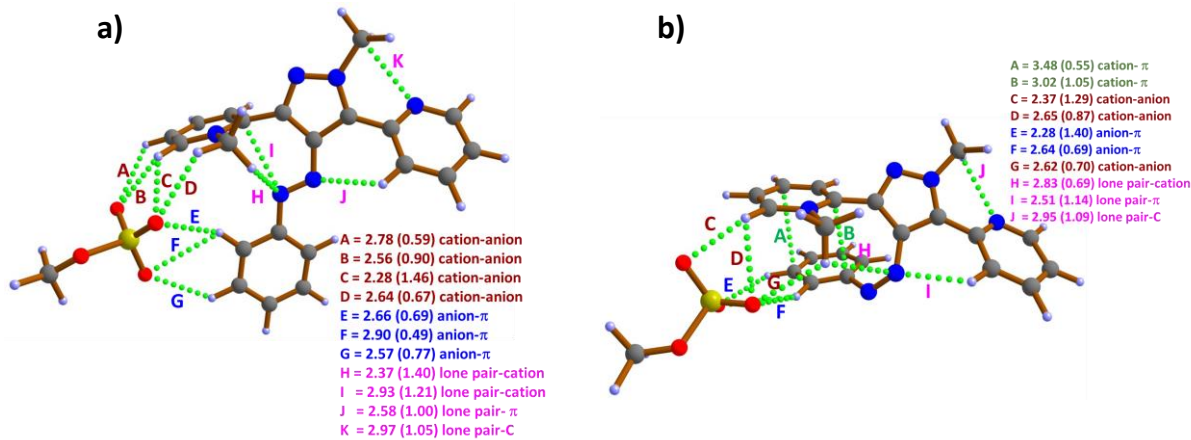


Figure S5.19. The optimized a) *E* isomer and b) *Z* isomer of **2a-Me-MeSO₄** and their non-covalent interactions. The atomic contacts (green color) representing various NCIs are in Å, and the corresponding electron densities ($\rho \times 10^{-2}$ au) at the bond critical points are given in parentheses.

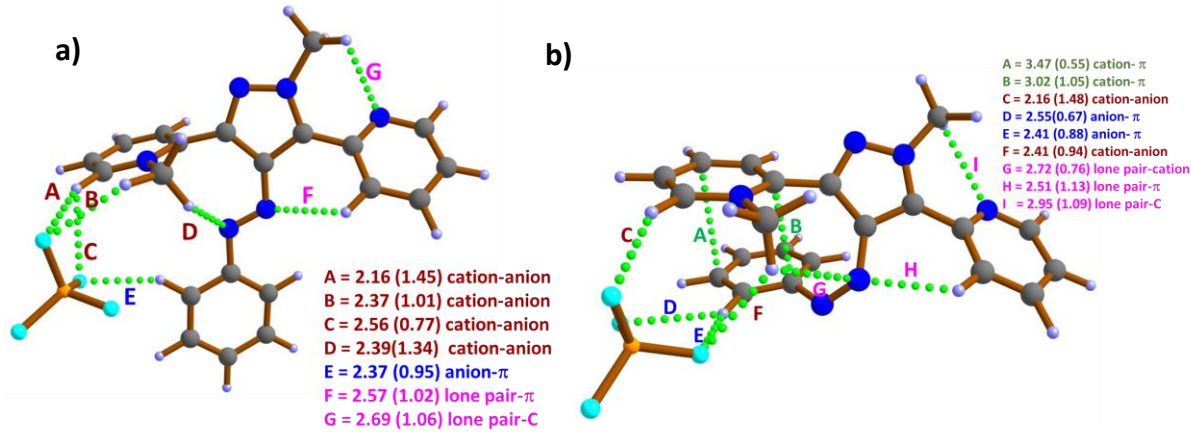


Figure S5.20. The optimized a) *E* isomer and b) *Z* isomer of **2a-Me-BF₄** and their non-covalent interactions. The atomic contacts (green color) representing various NCIs are in Å, and the corresponding electron densities ($\rho \times 10^{-2}$ au) at the bond critical points are given in parentheses.

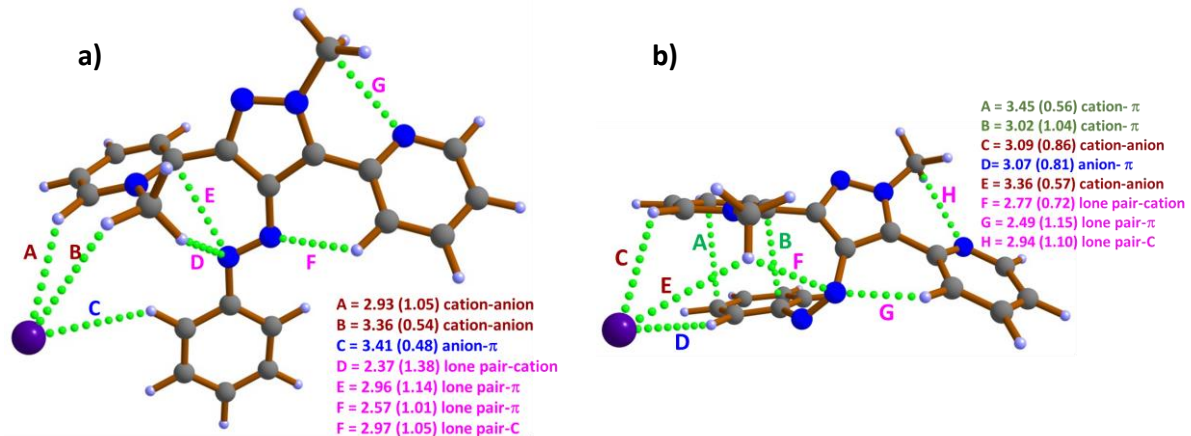


Figure S5.21. The optimized a) *E* isomer and b) *Z* isomer of **2a-Me-I** and their non-covalent interactions. The atomic contacts (green color) representing various NCIs are in Å, and the corresponding electron densities ($\rho \times 10^{-2}$ au) at the bond critical points are given in parentheses.

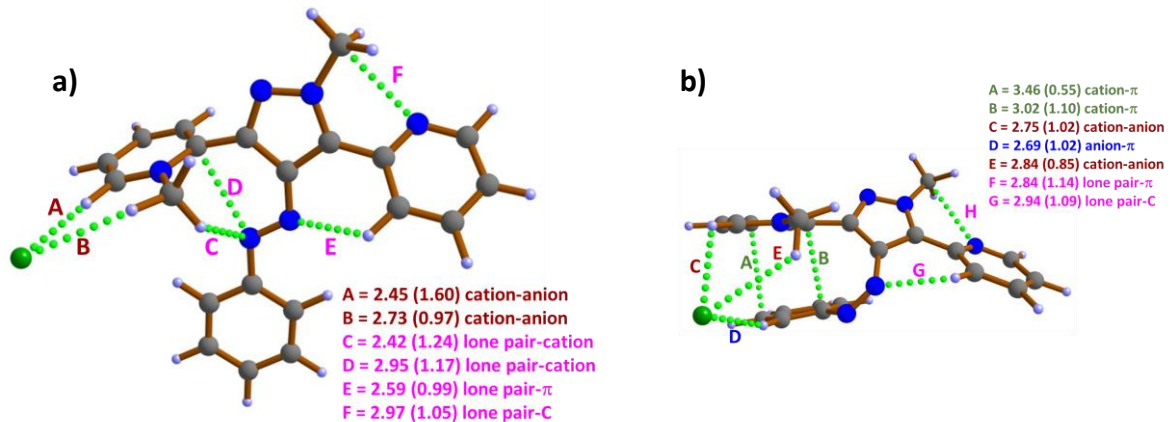


Figure S5.22. The optimized a) *E* isomer and b) *Z* isomer of **2a-Me-Cl** and their non-covalent interactions. The atomic contacts (green color) representing various NCIs are in Å, and the corresponding electron densities ($\rho \times 10^{-2}$ au) at the bond critical points are given in parentheses.

Table S5.1. Important structural parameters of the experimental and DFT optimized geometry of **2a-Me-I**

| 2a-Me-I | Experimental (Å) | DFT optimized (Å) |
|--|------------------|-------------------|
| C_{phenyl}-N_{azo}-N_{azo}-C_{pyrazole} | 175.387 | 176.949 |
| N_{azo}=N_{azo} | 1.262 | 1.259 |
| N_{azo}=N_{azo}-C_{phenyl} | 114.621 | 115.997 |
| N_{azo}=N_{azo}-C_{pyrazole} | 112.872 | 113.449 |

Table S5.2. Computed transition state inversion barriers ($TS_{\text{Phenyl (Z-E)}}$ and $TS_{\text{Pyrazole (Z-E)}}$) corresponding to *Z-E* thermal reverse isomerization of various **2a-Me-X** in the gas phase (normal font), in **water** (in bold) and in *DMSO* (in italics) at B3LYP/6-311++G(d,p) level of theory (solvent effect were incorporated using PCM model).

| S. No. | Compound | $TS_{\text{Phenyl(Z-E)}}$ (kcal/mol) | $TS_{\text{Pyrazole(Z-E)}}$ (kcal/mol) |
|--------|-------------------------------|---|---|
| 1 | 2a-Me-MeSO₄ | 26.5/ 26.0 /25.8 | 27.4/ 27.8 /27.5 |
| 2 | 2a-Me-BF₄ | 26.8/ 26.0 /25.9 | 26.9/ 27.2 /27.3 |
| 3 | 2a-Me-I | 27.7/ 25.7 /25.7 | 26.8/ 27.6 /27.5 |
| 4 | 2a-Me-Cl | 27.4/ 25.2 /25.2 | 28.3/ 26.4 /26.4 |
| 5 | 2a | 27.3/-/27.8 | 24.0/-/26.4 |
| 6 | 2a-N-H⁺ | 27.6/-/27.7 | 25.3/-/27.1 |
| 7 | 2a-N-Me⁺ | 25.5/ 25.7 /-- | 25.4/ 27.0 /-- |

Table S5.3. Topological parameters of different conformers at the bond critical point of ionic and neutral species. electron density [$\rho(r)$], Laplacian of electron density [$\nabla^2\rho(r)$], local electronic kinetic energy density [G(r)], local electronic potential energy density [V(r)], and interaction energy (E) values are indicated. The values for $\rho(r)$, $\nabla^2\rho(r)$, G(r), and V(r) are given in atomic units and for E, in kcal/mol.

| | BCP and type of interaction | Contact distance Å | $\rho(r)$ (au) | $\nabla^2\rho(r)$ (au) | G(r) (au) | V(r) (au) | E (kcal/mol) |
|---|-----------------------------|--------------------|----------------|------------------------|-----------|-----------|--------------|
| Z-2a-Me-MeSO₄ : gas phase | | | | | | | |
| 1 | cation-π | 3.579 | 5.184E-03 | 0.0140 | 0.0028 | -0.0021 | -0.6484 |
| 2 | cation-π | 3.052 | 9.957E-03 | 0.0314 | 0.0066 | -0.0053 | -1.6590 |
| 3 | anion-π | 2.640 | 8.754E-03 | 0.0334 | 0.0067 | -0.0049 | -1.5514 |
| 4 | anion-π | 2.254 | 1.645E-02 | 0.0598 | 0.0130 | -0.0111 | -3.4938 |
| 5 | anion-π | 2.842 | 1.508E-02 | 0.0538 | 0.0116 | -0.0098 | -3.0764 |
| 6 | cation-anion | 2.422 | 1.025E-02 | 0.0377 | 0.0077 | -0.0059 | -1.8637 |
| 7 | LP-π | 2.256 | 1.715E-02 | 0.0595 | 0.0132 | -0.0115 | -3.6225 |
| 8 | C-N | 2.857 | 1.320E-02 | 0.0528 | 0.0109 | -0.0087 | -2.7189 |
| Z-2a-Me-MeSO₄ : water | | | | | | | |
| 1 | cation-π | 3.475 | 5.45E-03 | 0.0148 | 0.0030 | -0.0022 | -0.6934 |
| 2 | cation-π | 3.021 | 1.05E-02 | 0.0330 | 0.0069 | -0.0056 | -1.7706 |
| 3 | cation-anion | 2.346 | 1.29E-02 | 0.0435 | 0.0093 | -0.0077 | -2.4241 |
| 4 | cation-anion | 2.649 | 8.71E-03 | 0.0310 | 0.0062 | -0.0047 | -1.4820 |
| 5 | anion-π | 2.278 | 1.40E-02 | 0.0454 | 0.0099 | -0.0085 | -2.6593 |
| 6 | anion-π | 2.642 | 6.93E-03 | 0.0236 | 0.0047 | -0.0034 | -1.0751 |
| 7 | cation-anion | 2.623 | 7.07E-03 | 0.0253 | 0.0050 | -0.0036 | -1.1366 |
| 8 | LP-cation | 2.835 | 6.88E-03 | 0.0230 | 0.0046 | -0.0034 | -1.0557 |
| 9 | LP-π | 2.507 | 1.14E-02 | 0.0387 | 0.0081 | -0.0066 | -2.0552 |
| 10 | C-N | 2.946 | 1.09E-02 | 0.0435 | 0.0088 | -0.0067 | -2.1079 |
| Z-2a-Me-MeSO₄ : DMSO | | | | | | | |
| 1 | cation-π | 3.476 | 5.45E-03 | 0.0148 | 0.0029 | -0.0022 | -0.6926 |
| 2 | cation-π | 3.021 | 1.04E-02 | 0.0330 | 0.0069 | -0.0056 | -1.7690 |
| 3 | anion-pi | 2.349 | 1.28E-02 | 0.0434 | 0.0093 | -0.0077 | -2.4134 |
| 4 | anion-pi | 2.635 | 8.94E-03 | 0.0318 | 0.0064 | -0.0049 | -1.5307 |
| 5 | anion-pi | 2.627 | 7.13E-03 | 0.0241 | 0.0048 | -0.0035 | -1.1126 |
| 6 | anion-pi | 2.275 | 1.41E-02 | 0.0458 | 0.0100 | -0.0086 | -2.6830 |
| 7 | Electrostatic | 2.637 | 6.89E-03 | 0.0248 | 0.0049 | -0.0035 | -1.1025 |
| 8 | LP-π | 2.832 | 6.92E-03 | 0.0231 | 0.0046 | -0.0034 | -1.0615 |
| 9 | LP-π | 2.500 | 1.15E-02 | 0.0391 | 0.0082 | -0.0067 | -2.0871 |
| 10 | C-N | 2.943 | 1.09E-02 | 0.0438 | 0.0089 | -0.0068 | -2.1245 |
| E-2a-Me-MeSO₄ : gas phase | | | | | | | |
| 1 | Cation-anion | 2.565 | 9.13E-03 | 0.0356 | 0.0071 | -0.0053 | -1.6583 |
| 2 | Cation-anion | 2.337 | 1.43E-02 | 0.0527 | 0.0112 | -0.0093 | -2.9040 |
| 3 | Cation-anion | 2.200 | 1.88E-02 | 0.0681 | 0.0152 | -0.0134 | -4.1960 |
| 4 | Cation-anion | 2.313 | 1.29E-02 | 0.0481 | 0.0101 | -0.0081 | -2.5438 |
| 5 | anion-π | 2.266 | 1.44E-02 | 0.0461 | 0.0101 | -0.0087 | -2.7425 |
| 6 | anion-π | 2.458 | 9.49E-03 | 0.0333 | 0.0068 | -0.0052 | -1.6433 |

| | | | | | | | |
|---|---------------|-------|----------|--------|--------|---------|---------|
| 7 | LP-cation | 2.429 | 1.27E-02 | 0.0392 | 0.0085 | -0.0073 | -2.2865 |
| 8 | LP-cation | 2.885 | 1.33E-02 | 0.0475 | 0.0101 | -0.0083 | -2.5890 |
| 9 | LP- π | 2.376 | 1.38E-02 | 0.0473 | 0.0102 | -0.0086 | -2.6829 |
| 10 | C-N | 2.884 | 1.24E-02 | 0.0496 | 0.0102 | -0.0080 | -2.5040 |
| E-2a-Me-MeSO₄: water | | | | | | | |
| 1 | Cation-anion | 2.779 | 5.91E-03 | 0.0232 | 0.0044 | -0.0031 | -0.9609 |
| 2 | Cation-anion | 2.562 | 9.03E-03 | 0.0327 | 0.0066 | -0.0050 | -1.5671 |
| 3 | Cation-anion | 2.283 | 1.46E-02 | 0.0495 | 0.0108 | -0.0092 | -2.8823 |
| 4 | Cation-anion | 2.644 | 6.72E-03 | 0.0243 | 0.0048 | -0.0034 | -1.0729 |
| 5 | anion- π | 2.659 | 6.94E-03 | 0.0210 | 0.0042 | -0.0032 | -1.0089 |
| 6 | anion- π | 2.904 | 4.89E-03 | 0.0178 | 0.0034 | -0.0023 | -0.7215 |
| 7 | anion- π | 2.569 | 7.72E-03 | 0.0260 | 0.0052 | -0.0039 | -1.2277 |
| 8 | LP- π | 2.373 | 1.40E-02 | 0.0443 | 0.0097 | -0.0084 | -2.6262 |
| 9 | LP-cation | 2.932 | 1.21E-02 | 0.0432 | 0.0090 | -0.0073 | -2.2816 |
| 10 | LP- π | 2.578 | 1.00E-02 | 0.0347 | 0.0071 | -0.0056 | -1.7532 |
| 11 | C-N | 2.969 | 1.05E-02 | 0.0415 | 0.0084 | -0.0064 | -2.0024 |
| E-2a-Me-MeSO₄: DMSO | | | | | | | |
| 1 | Cation-anion | 2.783 | 5.87E-03 | 0.0232 | 0.0044 | -0.0030 | -0.9553 |
| 2 | Cation-anion | 2.552 | 9.17E-03 | 0.0332 | 0.0067 | -0.0051 | -1.5978 |
| 3 | Cation-anion | 2.283 | 1.47E-02 | 0.0496 | 0.0108 | -0.0092 | -2.8887 |
| 4 | Cation-anion | 2.630 | 6.90E-03 | 0.0249 | 0.0049 | -0.0035 | -1.1075 |
| 5 | anion- π | 2.651 | 7.05E-03 | 0.0213 | 0.0043 | -0.0033 | -1.0276 |
| 6 | anion- π | 2.902 | 4.90E-03 | 0.0178 | 0.0034 | -0.0023 | -0.7248 |
| 7 | anion- π | 2.568 | 7.72E-03 | 0.0260 | 0.0052 | -0.0039 | -1.2292 |
| 8 | LP- π | 2.373 | 1.40E-02 | 0.0443 | 0.0097 | -0.0084 | -2.6266 |
| 9 | LP-cation | 2.930 | 1.21E-02 | 0.0433 | 0.0091 | -0.0073 | -2.2908 |
| 10 | LP- π | 2.574 | 1.01E-02 | 0.0348 | 0.0072 | -0.0056 | -1.7643 |
| 11 | C-N | 2.968 | 1.05E-02 | 0.0417 | 0.0084 | -0.0064 | -2.0104 |
| Z-2-Me-BF₄: gas phase | | | | | | | |
| 1 | cation- π | 3.497 | 5.34E-03 | 0.0143 | 0.0029 | -0.0021 | -0.6718 |
| 2 | cation- π | 3.032 | 1.03E-02 | 0.0322 | 0.0068 | -0.0055 | -1.7233 |
| 3 | Cation-anion | 1.927 | 2.50E-02 | 0.0960 | 0.0222 | -0.0203 | -6.3791 |
| 4 | Cation-anion | 2.850 | 1.18E-02 | 0.0492 | 0.0100 | -0.0076 | -2.3999 |
| 5 | anion-pi | 2.143 | 1.54E-02 | 0.0567 | 0.0122 | -0.0102 | -3.2118 |
| 6 | Cation-anion | 2.266 | 1.30E-02 | 0.0484 | 0.0101 | -0.0082 | -2.5710 |
| 7 | LP-cation | 2.765 | 7.38E-03 | 0.0243 | 0.0049 | -0.0036 | -1.1442 |
| 8 | LP- π | 2.281 | 1.67E-02 | 0.0577 | 0.0128 | -0.0111 | -3.4827 |
| 9 | C-N | 2.861 | 1.31E-02 | 0.0522 | 0.0108 | -0.0085 | -2.6793 |
| Z-2a-Me-BF₄: water | | | | | | | |
| 1 | cation- π | 3.469 | 5.48E-03 | 0.0149 | 0.0030 | -0.0022 | -0.6988 |
| 2 | cation- π | 3.018 | 1.05E-02 | 0.0331 | 0.0070 | -0.0057 | -1.7752 |
| 3 | anion- π | 2.165 | 1.48E-02 | 0.0543 | 0.0116 | -0.0097 | -3.0383 |
| 4 | anion- π | 2.553 | 6.72E-03 | 0.0255 | 0.0049 | -0.0035 | -1.1038 |
| 5 | anion- π | 2.407 | 8.86E-03 | 0.0315 | 0.0064 | -0.0048 | -1.5144 |
| 6 | Electrostatic | 2.410 | 9.38E-03 | 0.0343 | 0.0069 | -0.0053 | -1.6544 |

| | | | | | | | |
|--|---------------|-------|----------|--------|--------|---------|---------|
| 7 | LP- π | 2.724 | 7.60E-03 | 0.0252 | 0.0050 | -0.0038 | -1.1930 |
| 8 | LP- π | 2.513 | 1.13E-02 | 0.0384 | 0.0080 | -0.0065 | -2.0309 |
| 9 | C-N | 2.947 | 1.09E-02 | 0.0434 | 0.0088 | -0.0067 | -2.1066 |
| Z-2a-Me-BF₄: DMSO | | | | | | | |
| 1 | cation- π | 3.471 | 5.47E-03 | 0.0148 | 0.0030 | -0.0022 | -0.6966 |
| 2 | cation- π | 3.019 | 1.05E-02 | 0.0331 | 0.0070 | -0.0057 | -1.7733 |
| 3 | anion- π | 2.161 | 1.49E-02 | 0.0547 | 0.0117 | -0.0098 | -3.0723 |
| 4 | anion- π | 2.556 | 6.69E-03 | 0.0255 | 0.0049 | -0.0035 | -1.0987 |
| 5 | anion- π | 2.401 | 8.96E-03 | 0.0319 | 0.0064 | -0.0049 | -1.5357 |
| 6 | Electrostatic | 2.406 | 9.46E-03 | 0.0346 | 0.0070 | -0.0053 | -1.6737 |
| 7 | LP- π | 2.725 | 7.60E-03 | 0.0252 | 0.0050 | -0.0038 | -1.1922 |
| 8 | LP- π | 2.507 | 1.14E-02 | 0.0387 | 0.0081 | -0.0066 | -2.0578 |
| 9 | C-N | 2.944 | 1.09E-02 | 0.0437 | 0.0088 | -0.0068 | -2.1205 |
| E-2a-Me-BF₄: gas phase | | | | | | | |
| 1 | Cation-anion | 2.985 | 2.24E-02 | 0.0856 | 0.0194 | -0.0174 | -5.4660 |
| 2 | Cation-anion | 2.368 | 1.33E-02 | 0.0540 | 0.0111 | -0.0088 | -2.7624 |
| 3 | Cation-anion | 2.298 | 1.21E-02 | 0.0435 | 0.0091 | -0.0073 | -2.2962 |
| 4 | Cation-anion | 2.496 | 9.26E-03 | 0.0367 | 0.0073 | -0.0054 | -1.7032 |
| 5 | anion- π | 2.154 | 1.49E-02 | 0.0548 | 0.0118 | -0.0098 | -3.0758 |
| 6 | anion- π | 2.582 | 7.22E-03 | 0.0298 | 0.0058 | -0.0041 | -1.2723 |
| 7 | LP-cation | 2.522 | 1.05E-02 | 0.0323 | 0.0068 | -0.0056 | -1.7545 |
| 8 | LP-cation | 2.927 | 1.22E-02 | 0.0445 | 0.0093 | -0.0074 | -2.3336 |
| 9 | LP- π | 2.417 | 1.31E-02 | 0.0447 | 0.0096 | -0.0079 | -2.4943 |
| 10 | C-N | 2.897 | 1.20E-02 | 0.0480 | 0.0098 | -0.0077 | -2.4058 |
| E-2a-Me-BF₄: water | | | | | | | |
| 1 | cation-anion | 2.166 | 1.45E-02 | 0.0535 | 0.0114 | -0.0095 | -2.9654 |
| 2 | cation-anion | 2.370 | 1.01E-02 | 0.0357 | 0.0073 | -0.0057 | -1.7879 |
| 3 | cation-anion | 2.555 | 7.72E-03 | 0.0317 | 0.0062 | -0.0044 | -1.3780 |
| 4 | anion-pi | 2.370 | 9.52E-03 | 0.0341 | 0.0069 | -0.0053 | -1.6691 |
| 5 | LP-H | 2.392 | 1.34E-02 | 0.0419 | 0.0092 | -0.0079 | -2.4644 |
| 6 | N-H | 2.573 | 1.02E-02 | 0.0352 | 0.0073 | -0.0057 | -1.7900 |
| 7 | C-N | 2.686 | 1.06E-02 | 0.0415 | 0.0084 | -0.0064 | -2.0088 |
| E-2a-Me-BF₄: DMSO | | | | | | | |
| 1 | cation-anion | 2.164 | 1.46E-02 | 0.0538 | 0.0115 | -0.0095 | -2.9880 |
| 2 | cation-anion | 2.370 | 1.01E-02 | 0.0357 | 0.0073 | -0.0057 | -1.7881 |
| 3 | cation-anion | 2.553 | 7.76E-03 | 0.0319 | 0.0062 | -0.0044 | -1.3882 |
| 4 | anion-pi | 2.365 | 9.62E-03 | 0.0344 | 0.0070 | -0.0054 | -1.6917 |
| 5 | LP-cation | 2.393 | 1.33E-02 | 0.0418 | 0.0091 | -0.0078 | -2.4557 |
| 6 | LP-cation | 2.570 | 1.02E-02 | 0.0354 | 0.0073 | -0.0057 | -1.8007 |
| 7 | C-N | 2.968 | 1.06E-02 | 0.0416 | 0.0084 | -0.0064 | -2.0153 |
| Z-2a-Me-I: gas phase | | | | | | | |
| 1 | cation-pi | 3.084 | 9.43E-03 | 0.0302 | 0.0062 | -0.0049 | -1.5530 |
| 2 | anion-pi | 3.174 | 1.92E-02 | 0.0465 | 0.0117 | -0.0118 | -3.6957 |
| 3 | Electrostatic | 3.327 | 6.41E-03 | 0.0147 | 0.0031 | -0.0025 | -0.7861 |
| 4 | anion-pi | 2.835 | 1.22E-02 | 0.0299 | 0.0069 | -0.0062 | -1.9559 |

| | | | | | | | |
|-------------------------------|---------------|-------|----------|--------|--------|---------|---------|
| 5 | LP-H | 2.256 | 1.70E-02 | 0.0592 | 0.0131 | -0.0115 | -3.5946 |
| 6 | C-N | 2.859 | 1.31E-02 | 0.0525 | 0.0109 | -0.0086 | -2.6991 |
| Z-2a-Me-I: water | | | | | | | |
| 1 | cation-pi | 3.023 | 0.0104 | 0.0328 | 0.0069 | -0.0056 | -1.7509 |
| 2 | cation-pi | 3.452 | 0.0055 | 0.0151 | 0.0030 | -0.0023 | -0.7122 |
| 3 | anion-pi | 3.087 | 0.0086 | 0.0217 | 0.0047 | -0.0039 | -1.2235 |
| 4 | Electrostatic | 3.364 | 0.0057 | 0.0136 | 0.0028 | -0.0022 | -0.6827 |
| 5 | anion-pi | 3.069 | 0.0081 | 0.0183 | 0.0040 | -0.0034 | -1.0744 |
| 6 | cation-LP | 2.773 | 0.0072 | 0.0247 | 0.0049 | -0.0036 | -1.1286 |
| 7 | LP-pi | 2.494 | 0.0115 | 0.0391 | 0.0082 | -0.0066 | -2.0864 |
| 8 | C-N | 2.941 | 0.0110 | 0.0439 | 0.0089 | -0.0068 | -2.1402 |
| Z-2a-Me-I: DMSO | | | | | | | |
| 1 | cation-pi | 3.024 | 0.0103 | 0.0328 | 0.0069 | -0.0056 | -1.7495 |
| 2 | cation-pi | 3.454 | 0.0028 | 0.0151 | 0.0027 | -0.0016 | -0.4954 |
| 3 | anion-pi | 3.073 | 0.0088 | 0.0222 | 0.0048 | -0.0040 | -1.2629 |
| 4 | Electrostatic | 3.365 | 0.0057 | 0.0136 | 0.0028 | -0.0022 | -0.6825 |
| 5 | anion-pi | 3.070 | 0.0081 | 0.0183 | 0.0040 | -0.0034 | -1.0730 |
| 6 | cation-LP | 2.777 | 0.0071 | 0.0246 | 0.0049 | -0.0036 | -1.1253 |
| 7 | LP-pi | 2.489 | 0.0116 | 0.0394 | 0.0083 | -0.0067 | -2.1091 |
| 8 | C-N | 2.939 | 0.0111 | 0.0441 | 0.0089 | -0.0069 | -2.1506 |
| E-2a-Me-I: gas phase | | | | | | | |
| 1 | cation-anion | 3.171 | 0.0187 | 0.0421 | 0.0108 | -0.0111 | -3.4860 |
| 2 | cation-anion | 2.979 | 0.0104 | 0.0231 | 0.0053 | -0.0048 | -1.5031 |
| 3 | anion-pi | 2.874 | 0.0112 | 0.0260 | 0.0060 | -0.0054 | -1.6964 |
| 4 | LP-cation | 2.913 | 0.0125 | 0.0462 | 0.0096 | -0.0077 | -2.4252 |
| 5 | LP-pi | 2.381 | 0.0138 | 0.0470 | 0.0101 | -0.0085 | -2.6669 |
| 6 | C-N | 2.889 | 0.0122 | 0.0491 | 0.0101 | -0.0079 | -2.4650 |
| E-2a-Me-I: water | | | | | | | |
| 1 | cation-anion | 2.929 | 0.0105 | 0.0251 | 0.0056 | -0.0050 | -1.5721 |
| 2 | cation-anion | 3.367 | 0.0054 | 0.0130 | 0.0027 | -0.0021 | -0.6452 |
| 3 | anion-pi | 3.411 | 0.0048 | 0.0110 | 0.0022 | -0.0017 | -0.5322 |
| 4 | cation-LP | 2.373 | 0.0138 | 0.0438 | 0.0096 | -0.0083 | -2.5932 |
| 5 | cation-LP | 2.962 | 0.0114 | 0.0421 | 0.0087 | -0.0068 | -2.1452 |
| 6 | LP-pi | 2.574 | 0.0101 | 0.0352 | 0.0072 | -0.0057 | -1.7836 |
| 7 | C-N | 2.969 | 0.0105 | 0.0415 | 0.0084 | -0.0064 | -2.0073 |
| E-2a-Me-I: DMSO | | | | | | | |
| 1 | cation-anion | 2.922 | 0.0107 | 0.0254 | 0.0057 | -0.0051 | -1.5990 |
| 2 | cation-anion | 3.359 | 0.0055 | 0.0132 | 0.0027 | -0.0021 | -0.6563 |
| 3 | anion-pi | 3.397 | 0.0049 | 0.0112 | 0.0023 | -0.0017 | -0.5453 |
| 4 | cation-LP | 2.373 | 0.0139 | 0.0438 | 0.0096 | -0.0083 | -2.5943 |
| 5 | cation-LP | 2.962 | 0.0114 | 0.0421 | 0.0087 | -0.0068 | -2.1484 |
| 6 | LP-pi | 2.571 | 0.0102 | 0.0353 | 0.0073 | -0.0057 | -1.7934 |
| 7 | C-N | 2.967 | 0.0105 | 0.0417 | 0.0084 | -0.0064 | -2.0125 |
| Z-2a-Me-Cl : gas phase | | | | | | | |
| 1 | cation-pi | 3.111 | 0.0090 | 0.0288 | 0.0059 | -0.0047 | -1.4620 |

| | | | | | | | |
|-------------------------------|-----------------------|--------|--------|--------|--------|---------|---------|
| 2 | anion-pi | 2.695 | 0.0285 | 0.0716 | 0.0196 | -0.0212 | -6.6642 |
| 3 | anion-pi | 2.480 | 0.0152 | 0.0470 | 0.0105 | -0.0093 | -2.9263 |
| 4 | Electrostatic | 2.887 | 0.0085 | 0.0256 | 0.0053 | -0.0042 | -1.3152 |
| 5 | N _{az0} LP-H | 2.252 | 0.0171 | 0.0593 | 0.0132 | -0.0115 | -3.6002 |
| 6 | C-N | 2.862 | 0.0131 | 0.0523 | 0.0108 | -0.0086 | -2.6836 |
| Z-2a-Me-Cl : water | | | | | | | |
| 1 | cation-pi | 3.461 | 0.0055 | 0.0148 | 0.0030 | -0.0022 | -0.6967 |
| 2 | cation-pi | 3.020 | 0.0104 | 0.0330 | 0.0069 | -0.0056 | -1.7617 |
| 3 | anion-pi | 2.754 | 0.0102 | 0.0311 | 0.0066 | -0.0054 | -1.6798 |
| 4 | anion-pi | 2.844 | 0.0085 | 0.0244 | 0.0051 | -0.0041 | -1.2833 |
| 5 | Electrostatic | 2.689 | 0.0102 | 0.0289 | 0.0062 | -0.0052 | -1.6254 |
| 6 | N _{az0} LP-H | 2.500 | 0.0114 | 0.0388 | 0.0081 | -0.0066 | -2.0618 |
| 7 | C-N | 2.944 | 0.0109 | 0.0437 | 0.0088 | -0.0068 | -2.1240 |
| Z-2a-Me-Cl : DMSO | | | | | | | |
| 1 | cation-pi | 3.4625 | 0.0055 | 0.0148 | 0.0030 | -0.0022 | -0.6952 |
| 2 | cation-pi | 3.0203 | 0.0104 | 0.0330 | 0.0069 | -0.0056 | -1.7615 |
| 3 | anion-pi | 2.7397 | 0.0104 | 0.0319 | 0.0068 | -0.0055 | -1.7370 |
| 4 | anion-pi | 2.6892 | 0.0102 | 0.0289 | 0.0062 | -0.0052 | -1.6231 |
| 5 | Electrostatic | 2.8399 | 0.0086 | 0.0247 | 0.0051 | -0.0041 | -1.2972 |
| 6 | N _{az0} LP-H | 2.4949 | 0.0115 | 0.0391 | 0.0082 | -0.0067 | -2.0865 |
| 7 | C-N | 2.9419 | 0.0110 | 0.0439 | 0.0089 | -0.0068 | -2.1341 |
| E-2a-Me-Cl : gas phase | | | | | | | |
| 1 | Electrostatic | 2.690 | 0.0285 | 0.0730 | 0.0198 | -0.0214 | -6.7147 |
| 2 | Electrostatic | 2.576 | 0.0095 | 0.0284 | 0.0060 | -0.0049 | -1.5237 |
| 3 | anion-pi | 2.410 | 0.0169 | 0.0503 | 0.0116 | -0.0106 | -3.3289 |
| 4 | N _{az0} LP-H | 2.394 | 0.0137 | 0.0467 | 0.0101 | -0.0084 | -2.6488 |
| 5 | C-N | 2.892 | 0.0122 | 0.0487 | 0.0100 | -0.0078 | -2.4404 |
| E-2a-Me-Cl :water | | | | | | | |
| 1 | Electrostatic | 2.445 | 0.0160 | 0.0466 | 0.0107 | -0.0097 | -3.0587 |
| 2 | Electrostatic | 2.730 | 0.0097 | 0.0276 | 0.0059 | -0.0048 | -1.5210 |
| 3 | cation-LP | 2.425 | 0.0124 | 0.0392 | 0.0085 | -0.0071 | -2.2379 |
| 4 | cation-LP | 2.947 | 0.0117 | 0.0424 | 0.0088 | -0.0070 | -2.2020 |
| 5 | N _{az0} LP-H | 2.585 | 0.0100 | 0.0346 | 0.0071 | -0.0056 | -1.7486 |
| 6 | C-N | 2.972 | 0.0105 | 0.0413 | 0.0083 | -0.0063 | -1.9905 |
| E-2a-Me-Cl :DMSO | | | | | | | |
| 1 | Electrostatic | 2.438 | 0.0162 | 0.0472 | 0.0109 | -0.0099 | -3.1207 |
| 2 | Electrostatic | 2.725 | 0.0098 | 0.0279 | 0.0059 | -0.0049 | -1.5397 |
| 3 | cation-LP | 2.425 | 0.0124 | 0.0392 | 0.0085 | -0.0071 | -2.2368 |
| 4 | cation-LP | 2.947 | 0.0117 | 0.0424 | 0.0088 | -0.0070 | -2.2034 |
| 5 | N _{az0} LP-H | 2.582 | 0.0100 | 0.0348 | 0.0071 | -0.0056 | -1.7587 |
| 6 | C-N | 2.970 | 0.0105 | 0.0415 | 0.0084 | -0.0064 | -1.9975 |

Table S5.4. Contribution of stabilizing dispersive interaction without and with quantification through Grimme's approach, to compound **2a-Me-X** (-X = MeSO₄, Cl, I, BF₄)

| Z-E isomerization energy | ΔG_{Z-E} Without dispersion (kcal/mol) | ΔG_{Z-E} with dispersion (GD3BJ) (kcal/mol) | Difference (kcal/mol) |
|-------------------------------|--|---|--------------------------|
| 2a-Me-MeSO₄ | 18.3 | 11.9 | 6.4 |
| 2a-Me-BF₄ | 17.5 | 11.8 | 5.5 |
| 2a-Me-I | 17.4 | 11.9 | 5.5 |
| 2a-Me-Cl | 17.7 | 12.1 | 5.5 |

Table S5.5. Computational data on thermal reverse isomerization channels of the indicated targets at B3LYP-D3/6-311++G(d,p) level of theory.

| Species | Absolute Energy (Hartree) | ZPVE (Hartree) | Enthalpy (H) (Hartree) | Free Energy (G) (Hartree) | Lowest Harmonic Frequency (cm ⁻¹) |
|--------------------------------------|------------------------------|-------------------|---------------------------|------------------------------|--|
| 2a: gas phase | | | | | |
| E | -1100.258128 | 0.326074 | -1100.236140 | -1100.311476 | 15.6196 |
| Z | -1100.246269 | 0.326351 | -1100.224593 | -1100.297902 | 23.9373 |
| TS_{phenyl} | -1100.202002 | 0.324098 | -1100.180165 | -1100.254332 | -427.5644 |
| TS_{pyrazole} | -1100.207307 | 0.324310 | -1100.185671 | -1100.259582 | -407.8007 |
| 2a: DMSO | | | | | |
| E | -1100.272277 | 0.325979 | -1100.250181 | -1100.325876 | 18.4193 |
| Z | -1100.240191 | 0.326218 | -1100.239247 | -1100.312654 | 25.8599 |
| TS_{phenyl} | -1100.215765 | 0.323808 | -1100.193789 | -1100.268332 | -426.7603 |
| TS_{pyrazole} | -1100.218131 | 0.324076 | -1100.196420 | -1100.270578 | -423.2575 |
| 2a-Me⁺: gas phase | | | | | |
| E | -1139.941254 | 0.368073 | -1139.917742 | -1139.995396 | 24.1034 |
| Z | -1139.921422 | 0.368136 | -1139.898159 | -1139.974290 | 23.9193 |
| TS_{phenyl} | -1139.880293 | 0.365977 | -1139.856969 | -1139.933666 | -434.1210 |
| TS_{pyrazole} | -1139.880719 | 0.366065 | -1139.857586 | -1139.933785 | -404.4474 |
| 2a-Me⁺: water | | | | | |
| E | -1140.005184 | 0.367850 | -1139.981520 | -1140.059783 | 22.3380 |
| Z | -1139.987923 | 0.368125 | -1139.964614 | -1140.040629 | 25.6551 |
| TS_{phenyl} | -1139.946198 | 0.365829 | -1139.922739 | -1139.999624 | -448.3021 |
| TS_{pyrazole} | -1139.944419 | 0.365938 | -1139.921168 | -1139.997637 | -443.2664 |
| 2a-N-H⁺: gas phase | | | | | |
| E | -1100.661365 | 0.339964 | -1100.639808 | -1100.712590 | 27.5997 |
| Z | -1100.637212 | 0.340236 | -1100.615745 | -1100.687375 | 26.4332 |
| TS_{phenyl} | -1100.592021 | 0.338111 | -1100.570348 | -1100.643395 | -480.1096 |
| TS_{pyrazole} | -1100.595656 | 0.338422 | -1100.573990 | -1100.646935 | -478.7130 |
| 2a-N-H⁺: DMSO | | | | | |
| E | -1100.720876 | 0.340149 | -1100.699208 | -1100.772279 | 31.4990 |
| Z | -1100.699936 | 0.340225 | -1100.678141 | -1100.751096 | 30.2947 |
| TS_{phenyl} | -1100.654487 | 0.337945 | -1100.632512 | -1100.706949 | -456.3159 |
| TS_{pyrazole} | -1100.656360 | 0.338233 | -1100.634623 | -1100.707868 | -482.5433 |
| 2a-Me-I: Gas phase | | | | | |

| | | | | | |
|--|--------------|----------|--------------|--------------|-----------|
| <i>E</i> | -1151.584632 | 0.367465 | -1151.558458 | -1151.645422 | 13.0663 |
| <i>Z</i> | -1151.567286 | 0.367740 | -1151.541524 | -1151.626422 | 10.7444 |
| <i>TS_{phenyl}</i> | -1151.523319 | 0.365633 | -1151.497506 | -1151.582329 | -471.4922 |
| <i>TS_{pyrazole}</i> | -1151.525483 | 0.365736 | -1151.499849 | -1151.583700 | -414.6247 |
| 2a-Me-I: DMSO | | | | | |
| <i>E</i> | -1151.623648 | 0.367931 | -1151.597384 | -1151.685247 | 12.6054 |
| <i>Z</i> | -1151.606893 | 0.368253 | -1151.580984 | -1151.666143 | 16.4849 |
| <i>TS_{phenyl}</i> | -1151.565339 | 0.366072 | -1151.539382 | -1151.625247 | -449.2832 |
| <i>TS_{pyrazole}</i> | -1151.562128 | 0.366336 | -1151.536377 | -1151.622247 | -425.0173 |
| 2a-Me-I: water | | | | | |
| <i>E</i> | -1151.624271 | 0.367923 | -1151.597998 | -1151.685977 | 12.2555 |
| <i>Z</i> | -1151.607615 | 0.368232 | -1151.581689 | -1151.666986 | 15.4246 |
| <i>TS_{phenyl}</i> | -1151.566047 | 0.366038 | -1151.540067 | -1151.626045 | -449.2008 |
| <i>TS_{pyrazole}</i> | -1151.562878 | 0.366337 | -1151.537125 | -1151.622940 | -426.2761 |
| 2a-Me-BF₄: Gas phase | | | | | |
| <i>E</i> | -1564.735623 | 0.383348 | -1564.705910 | -1564.798894 | 16.7709 |
| <i>Z</i> | -1564.717373 | 0.383404 | -1564.687920 | -1564.779579 | 14.9982 |
| <i>TS_{phenyl}</i> | -1564.674953 | 0.381477 | -1564.645535 | -1564.736849 | -471.2939 |
| <i>TS_{pyrazole}</i> | -1564.673720 | 0.381021 | -1564.644246 | -1564.736580 | -403.6933 |
| 2a-Me-BF₄: DMSO | | | | | |
| <i>E</i> | -1564.774875 | 0.382285 | -1564.744612 | -1564.841644 | 6.4456 |
| <i>Z</i> | -1564.758217 | 0.382622 | -1564.728355 | -1564.821723 | 20.1211 |
| <i>TS_{phenyl}</i> | -1564.716049 | 0.380393 | -1564.686066 | -1564.780323 | -452.2125 |
| <i>TS_{pyrazole}</i> | -1564.713716 | 0.380312 | -1564.683865 | -1564.778257 | -445.0183 |
| 2a-Me-BF₄: water | | | | | |
| <i>E</i> | -1564.775393 | 0.382335 | -1564.745177 | -1564.841118 | 13.9309 |
| <i>Z</i> | -1564.758883 | 0.382596 | -1564.729006 | -1564.822508 | 19.3083 |
| <i>TS_{phenyl}</i> | -1564.716700 | 0.380387 | -1564.686714 | -1564.781050 | -451.6877 |
| <i>TS_{pyrazole}</i> | -1564.714424 | 0.380274 | -1564.684549 | -1564.779107 | -445.2203 |
| 2a-Me-MeSO₄: Gas phase | | | | | |
| <i>E</i> | -1879.178537 | 0.424113 | -1879.146932 | -1879.244662 | 16.0231 |
| <i>Z</i> | -1879.161499 | 0.424395 | -1879.130285 | -1879.225742 | 21.5813 |
| <i>TS_{phenyl}</i> | -1879.118888 | 0.422518 | -1879.087741 | -1879.183535 | -468.9094 |
| <i>TS_{pyrazole}</i> | -1879.116091 | 0.421605 | -1879.084644 | -1879.182072 | -418.3090 |
| 2a-Me-MeSO₄ :DMSO | | | | | |
| <i>E</i> | -1879.215867 | 0.423198 | -1879.183781 | -1879.284503 | 8.1056 |
| <i>Z</i> | -1879.199618 | 0.423478 | -1879.167880 | -1879.266082 | 11.1596 |
| <i>TS_{phenyl}</i> | -1879.158808 | 0.421657 | -1879.127170 | -1879.224947 | -455.0891 |
| <i>TS_{pyrazole}</i> | -1879.155582 | 0.421200 | -1879.123900 | -1879.222204 | -452.1031 |
| 2a-Me-MeSO₄: water | | | | | |
| <i>E</i> | -1879.216460 | 0.423192 | -1879.184372 | -1879.285080 | 8.9330 |
| <i>Z</i> | -1879.200313 | 0.423422 | -1879.168539 | -1879.267130 | 10.0160 |
| <i>TS_{phenyl}</i> | -1879.159500 | 0.421629 | -1879.127847 | -1879.225664 | -455.0705 |
| <i>TS_{pyrazole}</i> | -1879.156237 | 0.421209 | -1879.124565 | -1879.222785 | -452.5565 |
| 2a-Me-Cl: Gas phase | | | | | |
| <i>E</i> | -1600.382125 | 0.368077 | -1600.356261 | -1600.440334 | 13.6389 |
| <i>Z</i> | -1600.364636 | 0.368149 | -1600.339095 | -1600.421482 | 22.1575 |
| <i>TS_{phenyl}</i> | -1600.321046 | 0.365850 | -1600.295574 | -1600.377834 | -463.7233 |
| <i>TS_{pyrazole}</i> | -1600.318595 | 0.365855 | -1600.293004 | -1600.376416 | -436.1337 |

| 2a-Me-Cl: DMSO | | | | | |
|------------------------------|--------------|----------|--------------|--------------|-----------|
| E | -1600.426170 | 0.368242 | -1600.400133 | -1600.485880 | 19.4913 |
| Z | -1600.408493 | 0.368268 | -1600.382645 | -1600.466084 | 23.8533 |
| TS_{phenyl} | -1600.367808 | 0.366184 | -1600.341999 | -1600.425878 | -447.9874 |
| TS_{pyrazole} | -1600.365314 | 0.366298 | -1600.339609 | -1600.423994 | -451.3048 |
| 2a-Me-Cl: water | | | | | |
| E | -1600.426861 | 0.368231 | -1600.400814 | -1600.486633 | 19.2628 |
| Z | -1600.409270 | 0.368263 | -1600.383415 | -1600.466861 | 24.4964 |
| TS_{phenyl} | -1600.368570 | 0.366173 | -1600.342748 | -1600.426773 | -448.0554 |
| TS_{pyrazole} | -1600.366073 | 0.366280 | -1600.340351 | -1600.424846 | -451.8640 |

S6. pH Modulation

S6.1 Photoswitching at different pH

The pH titration was performed for **2a** followed by previously reported literature.¹⁷ A 50 μM concentration stock solution of **2a** (using 2.5×10^{-2} M in MeOH) was prepared by diluting it with 10 mM phosphate buffer. No significant changes in the UV-Vis spectral features at pH = 8 were observed, indicating the existence of target **2a** in non-protonated form. Further 1N HCl was used in small fractions to vary the pH from 8 to 1.5. A small amount (500 μL) from the stock solution of **2a** in phosphate buffer was used for photoswitching studies and the analysis were followed by UV-Vis spectroscopy for each pH variation step (Figure S6.1a). Remarkable changes in the absorption features were observed as the solution reached the pH near 4.5 (Figure S6.2). Upon following the absorption changes with the pH (by titration), a sigmoidal curve was obtained and the corresponding fitting was used to calculate the pKa values, which was found to be 4.46 and 3.39 for *trans* and *cis*, respectively (Figure S6.3). The photoswitching of **2a** and thermal relaxation of the Z isomer (at 80 °C) at various pH were also performed to understand the effect of protonation on the photoswitching characteristics and thermal stability of the Z isomer (Figure S6.1b and Figures S6.4-S6.7).

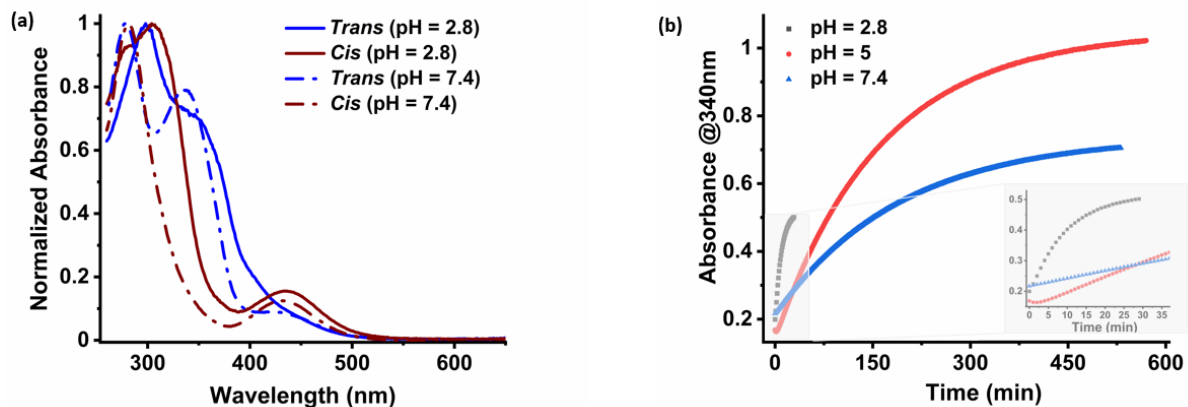


Figure S6.1. (a) Absorption spectra of **2a** and photoswitching at pH = 7.4 and pH = 2.8; (b) The effect of thermal relaxation of Z isomer at different pH.

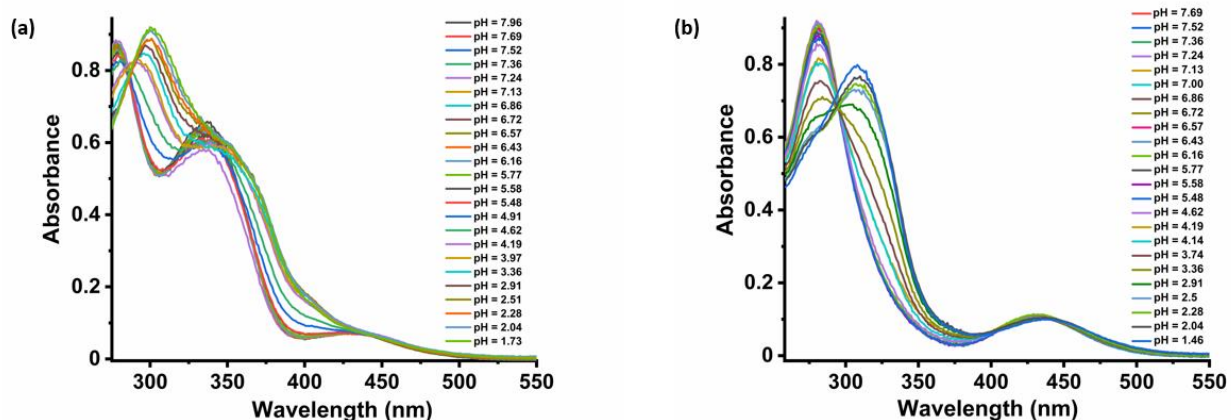


Figure S6.2. Absorption spectra of **2a**: (a) E isomer, and (b) Z isomer at different pH.

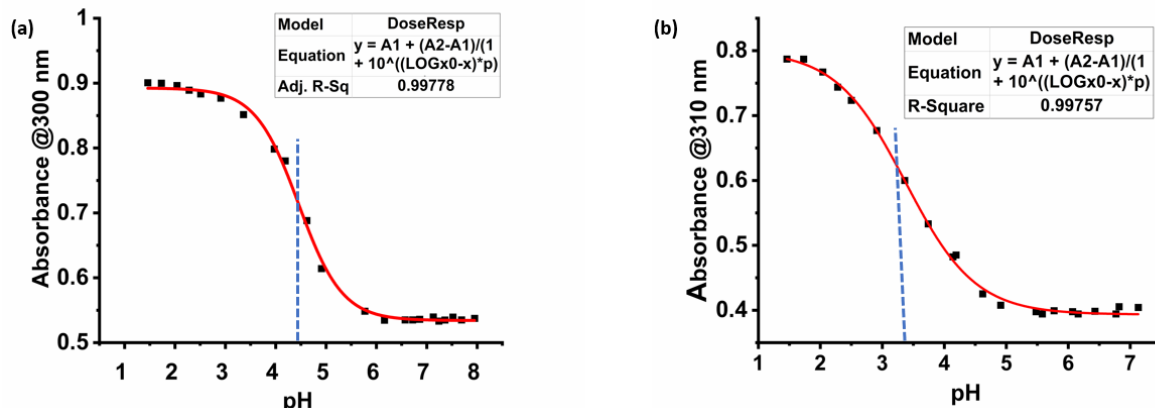


Figure S6.3. Determination of pK_a by UV-Vis spectroscopic method by following absorption changes vs pH and sigmoidal fit to the datapoints in (a) *E*, and (b) *Z* isomers of **2a**.

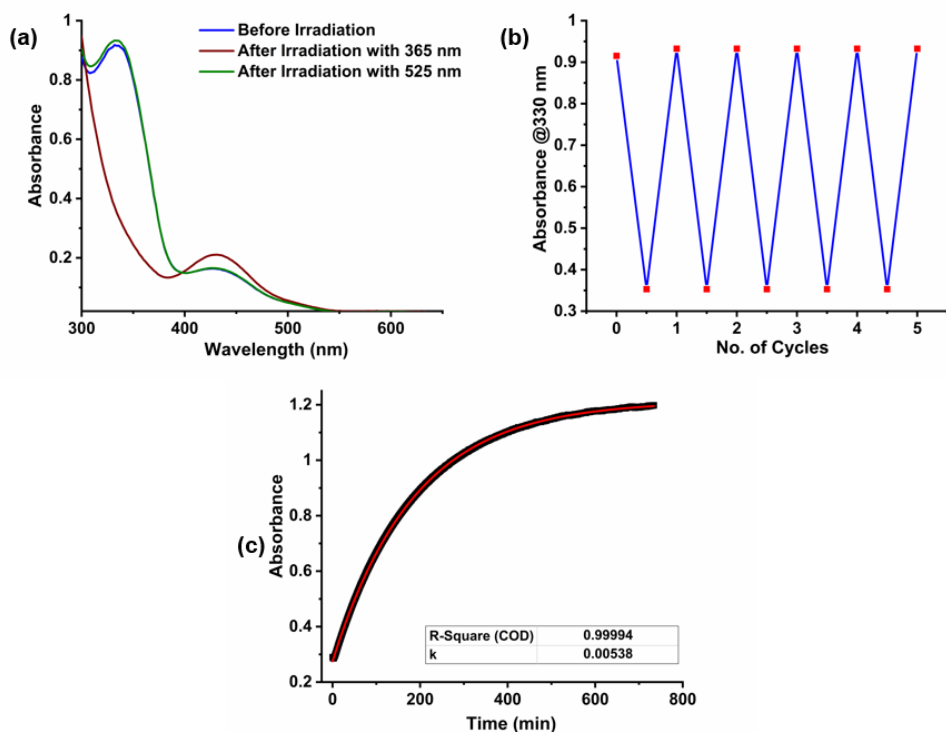


Figure S6.4. UV-Vis spectroscopic data of **2a**: (a) Photoswitching studies performed in phosphate buffer (10.8 pH); (b) Photoswitching stability test upto five cycles (forward isomerization step: 365 nm; reverse isomerization step: 525 nm) and (c) First order thermal reverse isomerization kinetics plot and exponential fit at 80 °C.

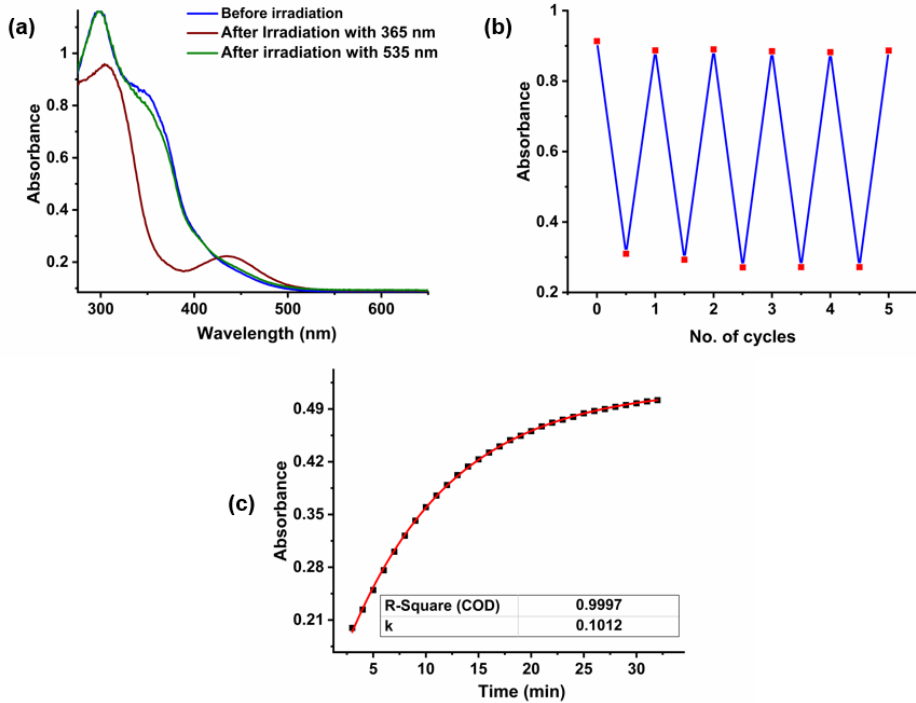


Figure S6.5. UV-Vis spectroscopic data of **2a**: (a) Photoswitching studies performed in phosphate buffer (2.89 pH); (b) Photoswitching stability test upto five cycles (forward isomerization step: 365 nm; reverse isomerization step: 525 nm) and (c) First order thermal reverse isomerization kinetics plot and exponential fit at 80 °C.

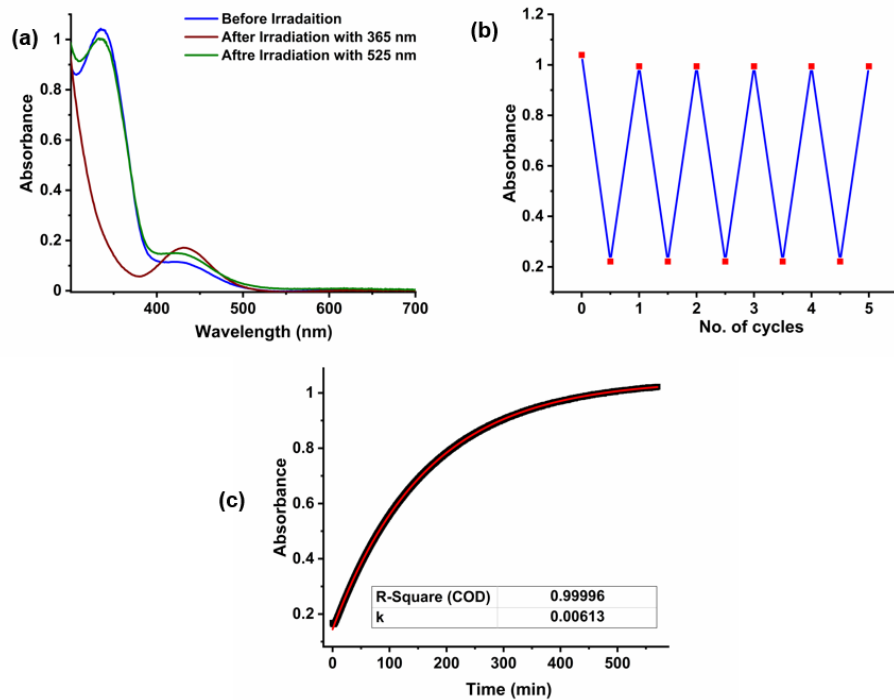


Figure S6.6. UV-Vis spectroscopic data of **2a**: (a) Photoswitching studies performed in phosphate buffer (5.03 pH); (b) Photoswitching stability test upto five cycles (forward isomerization step: 365 nm; reverse isomerization step: 525 nm) and (c) First order thermal reverse isomerization kinetics plot and exponential fit at 80 °C.

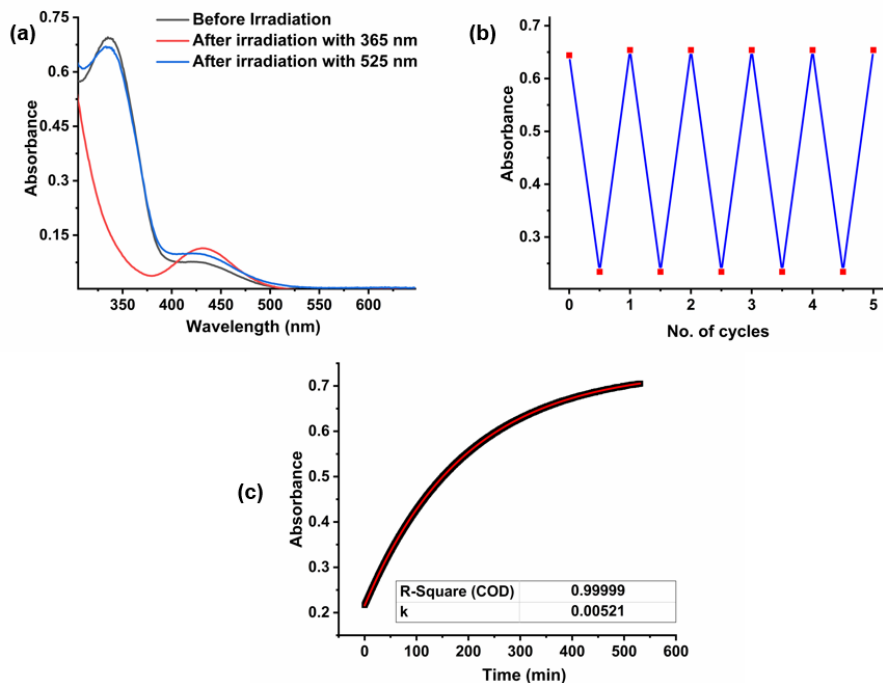


Figure S6.7. UV-Vis spectroscopic data of **2a**: (a) Photoswitching studies performed in phosphate buffer (7.4 pH); (b) Photoswitching stability test upto five cycles (forward isomerization step: 365 nm; reverse isomerization step: 525 nm) and (c) First order thermal reverse isomerization kinetics plot and exponential fit at 80 °C.

S6.2 Modulation of pH through photoisomerization

A range of pH between 4 and 6 was selected to perform pH modulation by light. The preliminary screening of pH beyond this range showed a minimal effect. In these studies, 2.5×10^{-2} M stock solution of **2a** in MeOH was prepared and diluted 1000-fold by using 10 mM phosphate buffer (\sim pH 3) to 10 mL volume to maintain a concentration of 250 μ M. The solution was kept in the dark and the pH was measured using a pH meter. Further 1N NaOH was added to adjust the pH from 3 to \sim pH 4.1. Further, pH was recorded during each forward and reverse photoisomerization step up to 5 cycles (Figure S6.9). **2a-Et-I** also tested for modulation of pH however, only a limited change was observed. Under similar conditions **2b** was not soluble in buffer.

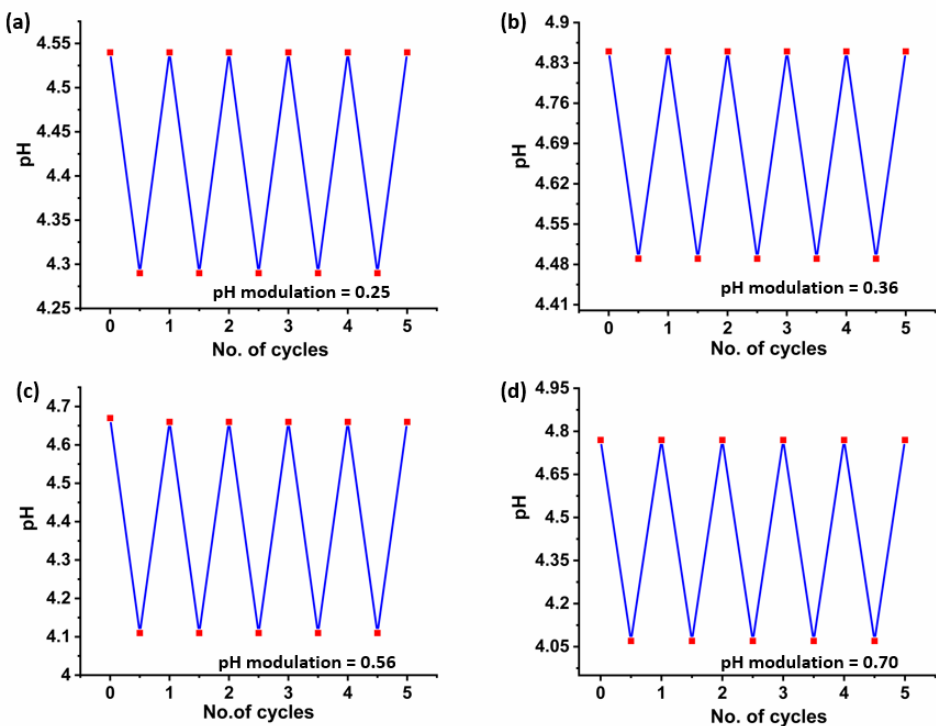


Figure S6.8. Reversible changes in pH modulation at 2 mM phosphate buffer medium during forward and reverse photoisomerization of **2a** upto five cycles at various concentrations: (a) 200 μ M, (b) 400 μ M, (c) 600 μ M, and (d) 1 mM (The effective pH modulation in each case is indicated in the plot).

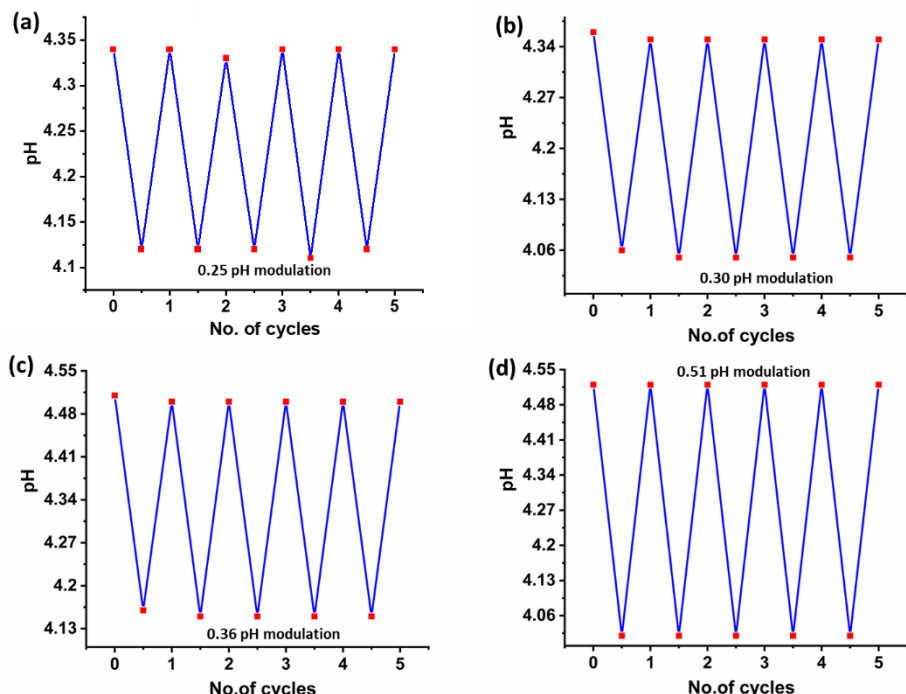


Figure S6.9. Reversible changes in pH modulation at 10 mM phosphate buffer medium during forward and reverse photoisomerization of **2a** upto five cycles at various concentrations: (a) 200 μ M, (b) 400 μ M, (c) 600 μ M, and (d) 1 mM (The effective pH modulation in each case is indicated in the plot).

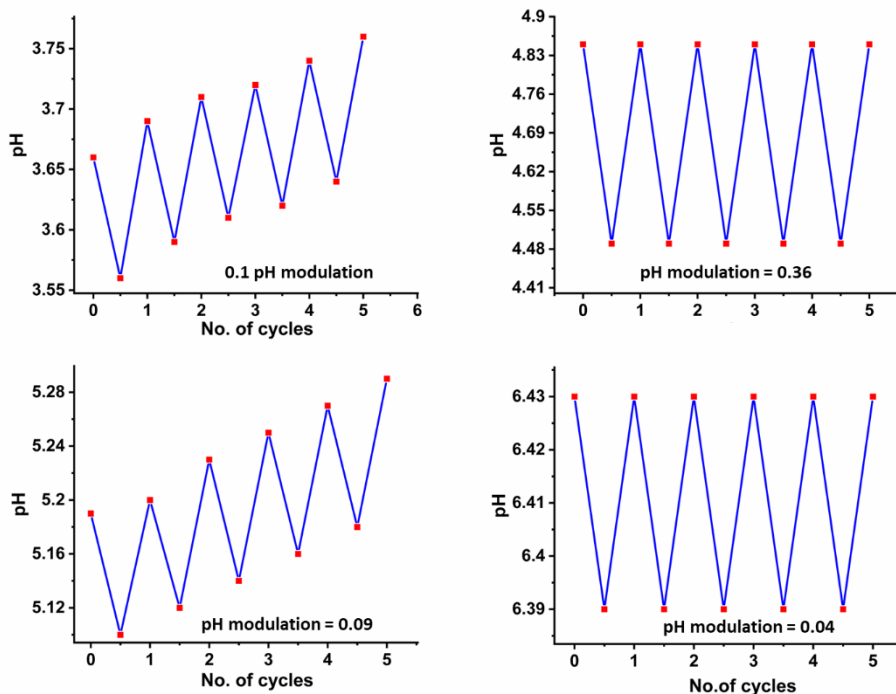


Figure S6.10. Reversible changes in pH modulation at 2 mM phosphate buffer medium during forward and reverse photoisomerization of **2a** (200 μ M) upto five cycles at various pH: (a) pH = 3.53, (b) pH = 4.45, (c) pH = 5.07, and (d) pH = 6.37 (The effective pH modulation in each case is indicated in the plot).

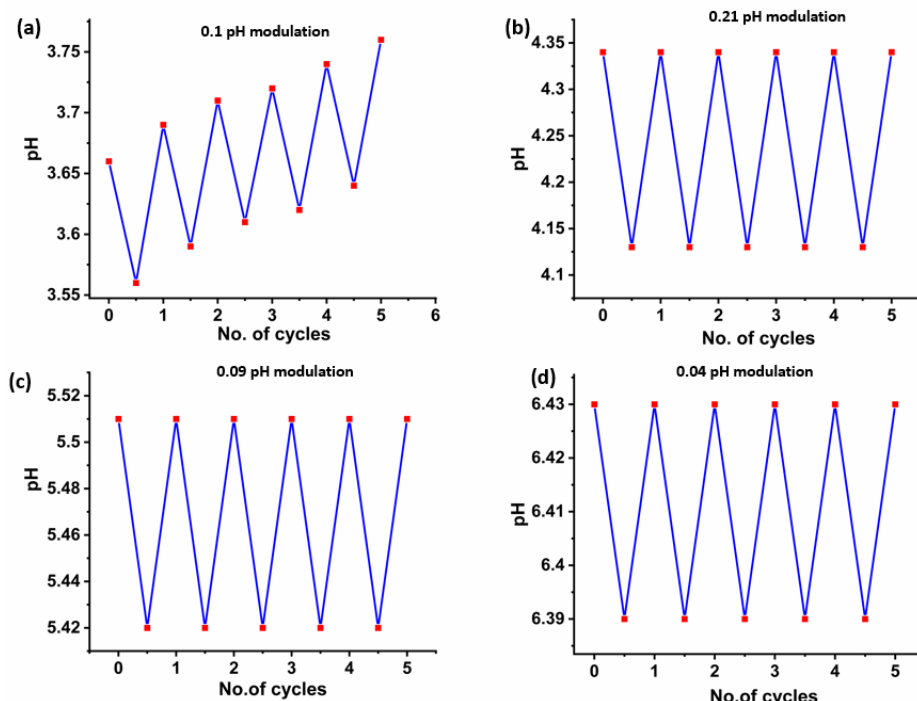


Figure S6.11. Reversible changes in pH modulation at 10 mM phosphate buffer medium during forward and reverse photoisomerization of **2a** (200 μ M) upto five cycles at various pH: (a) pH = 3.51, (b) pH = 4.10, (c) pH = 5.41, and (d) pH = 6.37 (The effective pH modulation in each case is indicated in the plot).

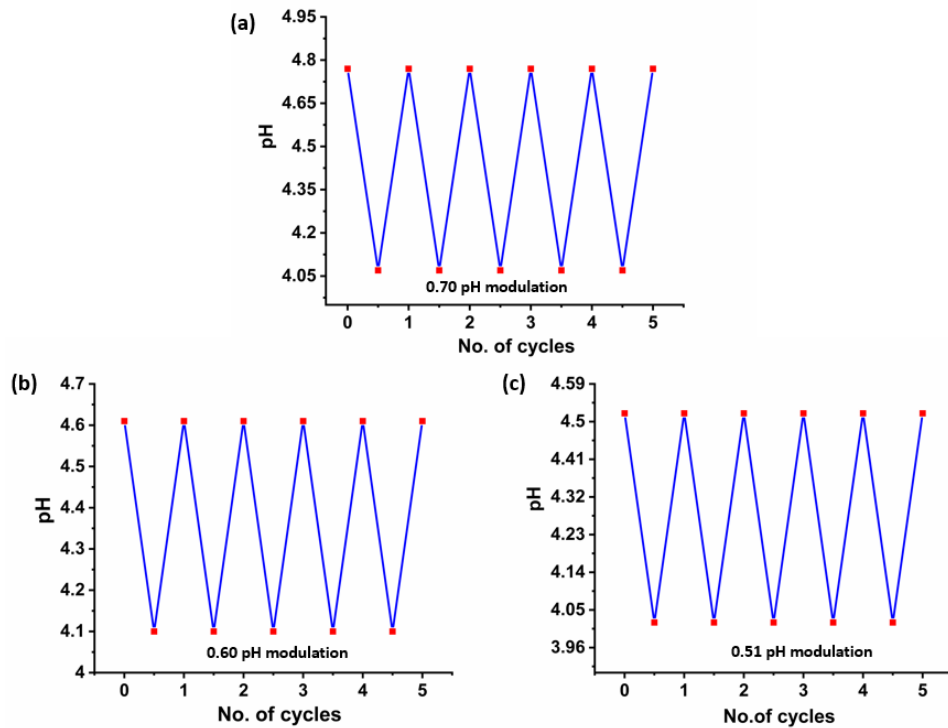


Figure S6.12. Reversible changes in pH modulation during forward and reverse photoisomerization of **2a** (1 mM) upto five cycles at pH around 4 with the different concentrations of phosphate buffer medium: (a) 2 mM, (b) 5 mM, and (c) 10 mM (The effective pH modulation in each case is indicated in the plot).

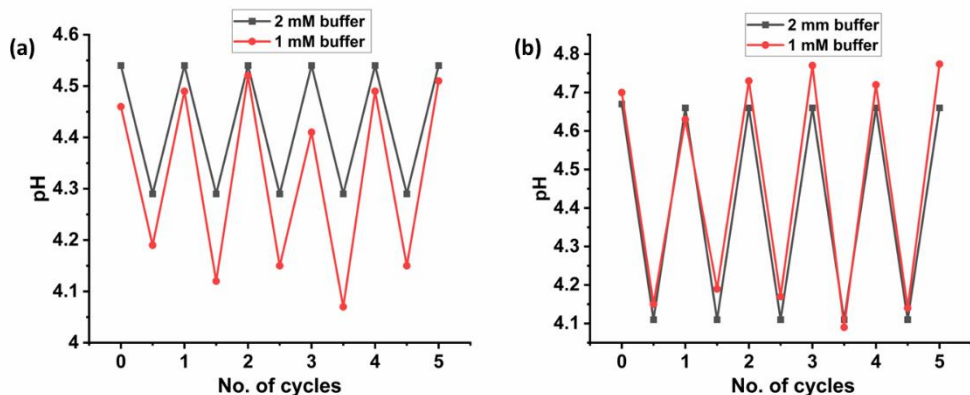


Figure S6.13. (a) Reversible changes in pH during forward and reverse photoisomerization of **2a** (600 μ M) upto five cycles at various concentrations of buffer. (Due to fluctuations, 2 mM phosphate buffer concentration was selected for comparative studies instead of 1 mM).

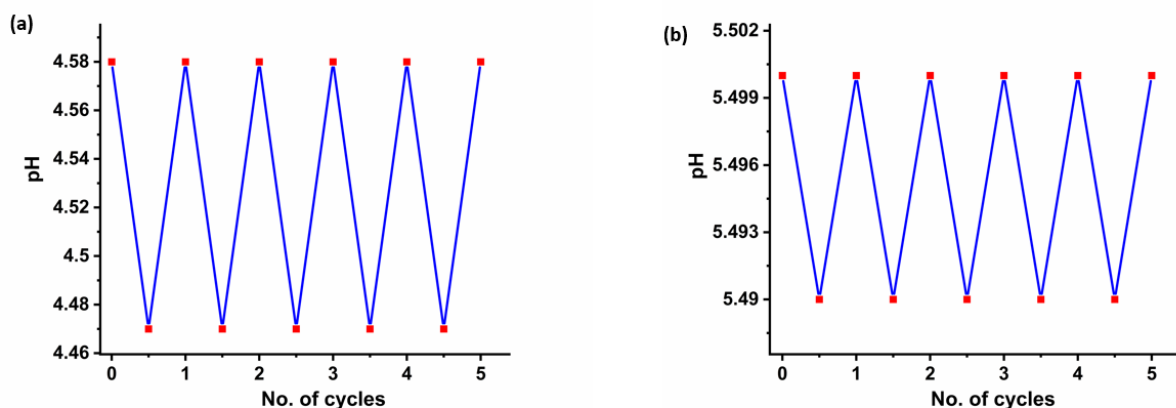


Figure S6.14. Reversible changes in the pH during forward and reverse photoisomerization of (a) **2a** (250 μM in phosphate buffer at pH = 4.45) upto five cycles; (b) **2a-Et-I** (250 μM in phosphate buffer at pH = 5.48) upto five cycles.

S.6.2 Computational studies on pH modulation

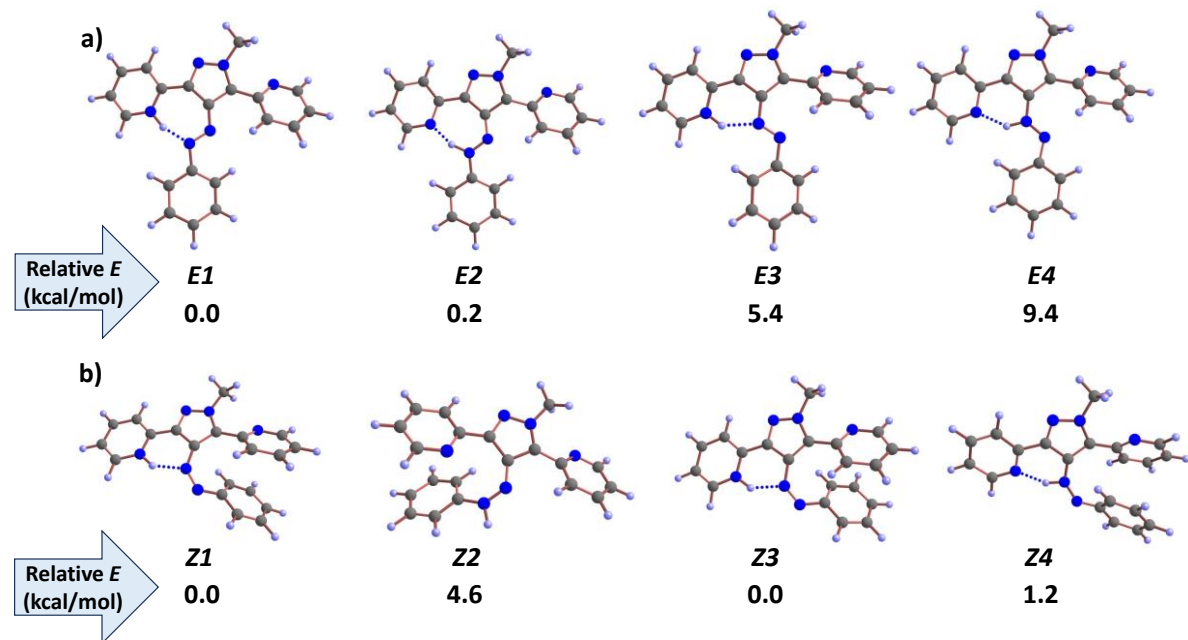


Figure S6.10. The optimized geometries of **2a** with protonation at different sites for a) E and b) Z isomers (The relative Gibbs free energies in kcal/mol relative to the most stable geometries of E and Z isomers, respectively are indicated).

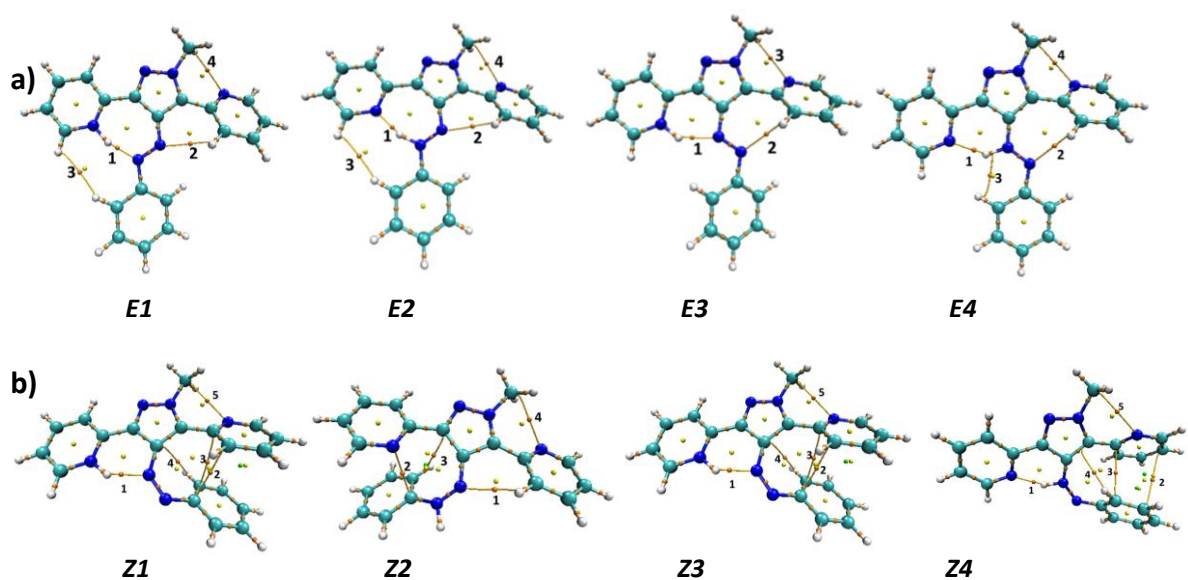


Figure S6.11. The computed topological diagrams for all possible protonated a) E isomers b) Z isomers of **2a** through AIM analysis. (Color code:- gold: bond critical point; yellow: ring critical point, and green: cage critical point).

Table S6.1. Topological parameters of different conformers at the bond critical point of ionic and neutral species. electron density [$\rho(r)$], Laplacian of electron density [$\nabla^2\rho(r)$], local electronic kinetic energy density [$G(r)$], local electronic potential energy density [$V(r)$], and interaction energy (E) values are indicated. The values for $\rho(r)$, $\nabla^2\rho(r)$, $G(r)$, and $V(r)$ are given in atomic units and for E , in kcal/mol.

| | BCP and type of interaction | Contact distance Å | $\rho(r)$ (au) | $\nabla^2\rho(r)$ (au) | $G(r)$ (au) | $V(r)$ (au) | E (kcal/mol) |
|------------------|-----------------------------|--------------------|----------------|------------------------|-------------|-------------|----------------|
| <i>E1</i> | | | | | | | |
| 1 | N-H | 1.632 | 0.0679 | 0.0950 | 0.0483 | -0.0729 | -22.8797 |
| 2 | N-H | 2.541 | 0.0112 | 0.0391 | 0.0081 | -0.0065 | -2.0376 |
| 3 | H-H | 2.799 | 0.0020 | 0.0072 | 0.0013 | -0.0008 | -0.2472 |
| 4 | C-N | 2.915 | 0.0116 | 0.0462 | 0.0094 | -0.0073 | -2.2830 |
| <i>E2</i> | | | | | | | |
| 1 | N-H | 1.617 | 0.0701 | 0.0947 | 0.0501 | -0.0764 | -23.9836 |
| 2 | N-H | 2.570 | 0.0106 | 0.0381 | 0.0078 | -0.0061 | -1.9279 |
| 3 | H-H | 2.675 | 0.0025 | 0.0088 | 0.0016 | -0.0010 | -0.3142 |
| 4 | C-N | 2.929 | 0.0113 | 0.0453 | 0.0092 | -0.0071 | -2.2221 |
| <i>E3</i> | | | | | | | |
| 1 | N-H | 1.868 | 0.0384 | 0.0984 | 0.0290 | -0.0333 | -10.4540 |
| 2 | C-N | 3.059 | 0.0101 | 0.0362 | 0.0074 | -0.0057 | -1.7982 |
| 3 | C-N | 2.946 | 0.0109 | 0.0426 | 0.0087 | -0.0067 | -2.0954 |
| <i>E4</i> | | | | | | | |
| 1 | N-H | 1.773 | 0.0490 | 0.1013 | 0.0358 | -0.0462 | -14.5032 |
| 2 | N-H | 2.642 | 0.0099 | 0.0351 | 0.0072 | -0.0056 | -1.7515 |
| 3 | N-H | 2.620 | 0.0131 | 0.0569 | 0.0116 | -0.0090 | -2.8110 |
| 4 | C-N | 2.951 | 0.0106 | 0.0432 | 0.0087 | -0.0066 | -2.0634 |
| <i>Z1</i> | | | | | | | |
| 1 | N-H | 1.789 | 0.0466 | 0.1057 | 0.0350 | -0.0435 | -13.6481 |
| 2 | C-C | 3.038 | 0.0104 | 0.0326 | 0.0069 | -0.0056 | -1.7472 |
| 3 | C-C | 3.003 | 0.0107 | 0.0339 | 0.0071 | -0.0058 | -1.8261 |
| 4 | C-H | 2.645 | 0.0103 | 0.0370 | 0.0076 | -0.0059 | -1.8489 |
| 5 | N-C | 2.926 | 0.0114 | 0.0447 | 0.0091 | -0.0071 | -2.2159 |
| <i>Z2</i> | | | | | | | |
| 1 | N-H | 2.609 | 0.0101 | 0.0370 | 0.0075 | -0.0058 | -1.8279 |
| 2 | C-N | 2.791 | 0.0152 | 0.0499 | 0.0110 | -0.0096 | -2.9964 |
| 3 | C-H | 2.712 | 0.0086 | 0.0321 | 0.0064 | -0.0048 | -1.5015 |
| 4 | N-C | 2.927 | 0.0115 | 0.0456 | 0.0093 | -0.0072 | -2.2515 |
| <i>Z3</i> | | | | | | | |
| 1 | 1 | N-H | 1.789 | 0.0466 | 0.1057 | 0.0350 | -0.0435 |
| 2 | 2 | C-C | 3.038 | 0.0104 | 0.0326 | 0.0069 | -0.0056 |
| 3 | 3 | C-C | 3.003 | 0.0107 | 0.0339 | 0.0071 | -0.0058 |
| 4 | 4 | C-H | 2.645 | 0.0103 | 0.0370 | 0.0076 | -0.0059 |
| 5 | 5 | N-C | 2.926 | 0.0114 | 0.0447 | 0.0091 | -0.0071 |
| <i>Z4</i> | | | | | | | |
| 1 | N-H | 1.750 | 0.0512 | 0.1052 | 0.0378 | -0.0493 | -15.4801 |

| | | | | | | | |
|---|-----|-------|--------|--------|--------|---------|---------|
| 2 | C-C | 2.909 | 0.0125 | 0.0394 | 0.0085 | -0.0072 | -2.2574 |
| 3 | C-C | 3.716 | 0.0040 | 0.0102 | 0.0020 | -0.0014 | -0.4496 |
| 4 | C-H | 2.676 | 0.0097 | 0.0363 | 0.0073 | -0.0056 | -1.7511 |
| 5 | N-C | 2.963 | 0.0104 | 0.0422 | 0.0085 | -0.0064 | -2.0013 |

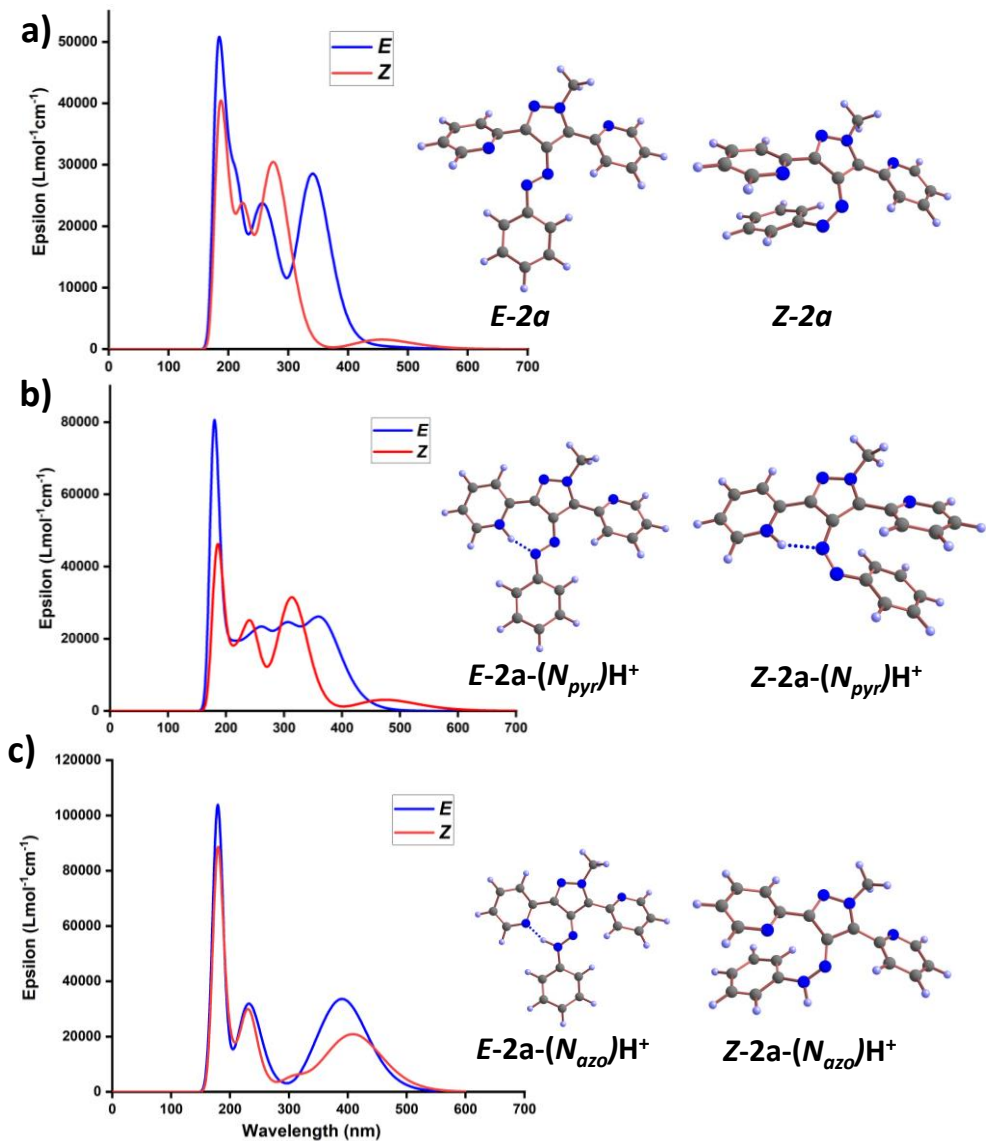


Figure S6.12. TD-DFT computed absorption spectral data of *E* and *Z* isomers of a) **2a**, b) **2a-(N_{pyr})H⁺**, and c) **2a-(N_{azo})H⁺**. The corresponding *E* and *Z* isomeric structures are included.

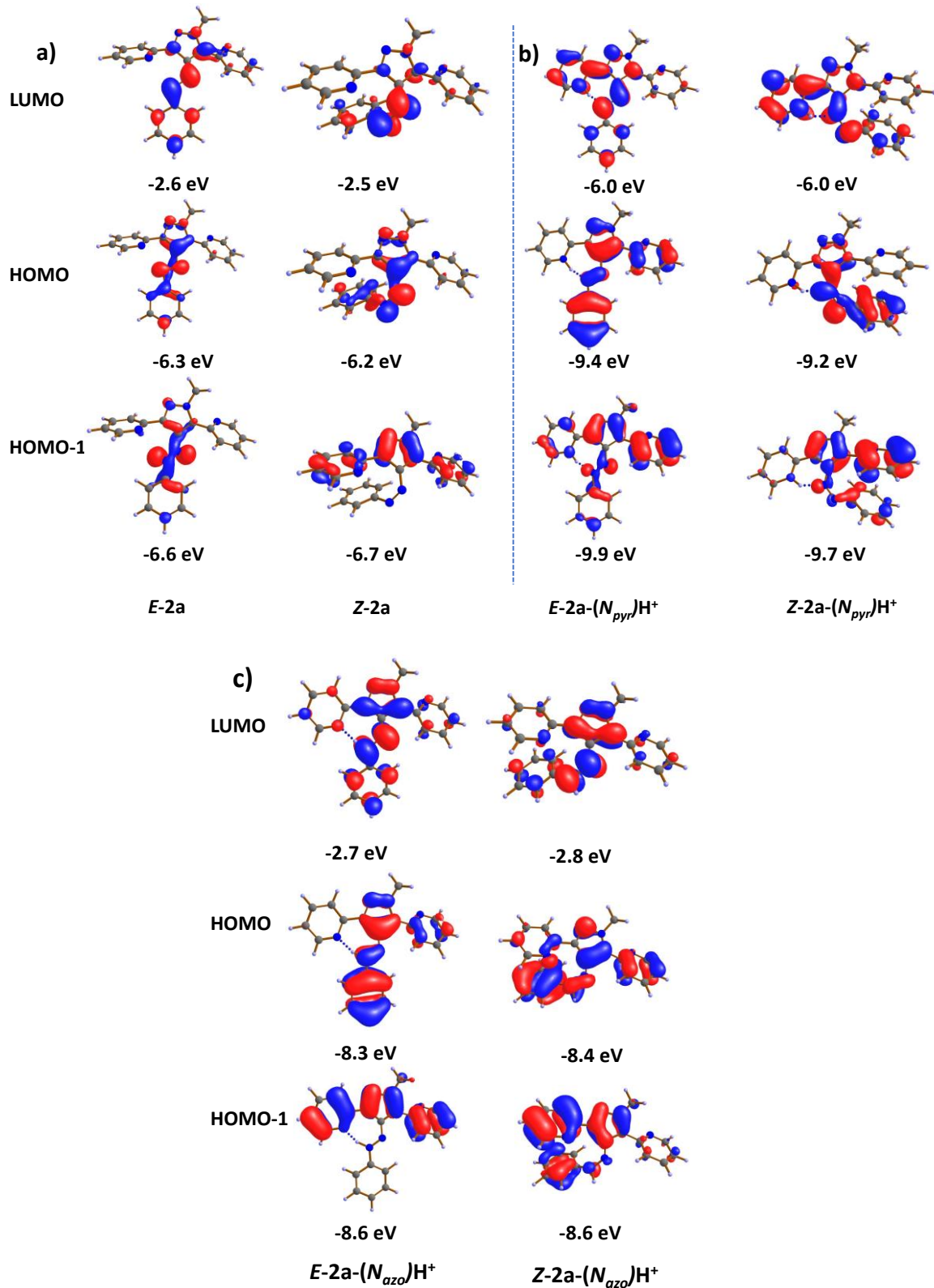


Figure S6.13. Molecular orbitals corresponding to HOMO-1, HOMO, and LUMO of a) ***E-2a*** and ***Z-2a***, b) ***E-2a-(N_{pyr})H⁺***, and ***Z-2a-(N_{pyr})H⁺***, c) ***E-2a-(N_{azo})H⁺***, and ***Z-2a-(N_{azo})H⁺***. The orbital energies (in eV) are indicated.

Table S6.2. Computed electronic spectroscopic parameters corresponding to *E* and *Z* isomers of selected species. (*E* - excitation energy, *f* - oscillator strength).

| Species | configuration | Wavelength (nm) | E (eV) | f | character | Transition |
|---|---------------|-----------------|--------|--------|----------------------------|--|
| 2a | <i>E</i> | 341.16 | 3.6342 | 0.7027 | $\pi \rightarrow \pi^*$ | H \rightarrow L (82%) |
| | | 448.06 | 2.7671 | 0.0103 | n $\rightarrow \pi^*$ | H-1 \rightarrow L (49%) H-2 \rightarrow L (24%) |
| | <i>Z</i> | 456.51 | 2.7159 | 0.0383 | n/ $\pi \rightarrow \pi^*$ | H \rightarrow L (71%) |
| | | 299.26 | 4.1431 | 0.2111 | $\pi \rightarrow \pi^*$ | H-2 \rightarrow L (32%) |
| 2a-H ⁺ protonated N _{pyridyl} | <i>E</i> | 364.74 | 3.3992 | 0.5869 | $\pi \rightarrow \pi^*$ | H \rightarrow L (84%) |
| | | 407.50 | 3.0426 | 0.0282 | n/ $\pi \rightarrow \pi^*$ | H-3 \rightarrow L (65%) |
| | <i>Z</i> | 474.20 | 2.6146 | 0.0763 | n/ $\pi \rightarrow \pi^*$ | H \rightarrow L (64%) |
| | | 319.54 | 3.8801 | 0.5898 | $\pi \rightarrow \pi^*$ | H-1 \rightarrow L (34%) |
| 2a-H ⁺ protonated N _{azo} | <i>E</i> | 352.52 | 3.5171 | 0.2994 | $\pi \rightarrow \pi^*$ | H \rightarrow L (95%) |
| | | 399.41 | 3.1042 | 0.7065 | $\pi \rightarrow \pi^*$ | H \rightarrow L (94%) |
| | <i>Z</i> | 421.39 | 2.9423 | 0.4190 | $\pi \rightarrow \pi^*$ | H \rightarrow L (79%) |
| | | 370.61 | 3.3454 | 0.2149 | $\pi \rightarrow \pi^*$ | H \rightarrow L (83%) |

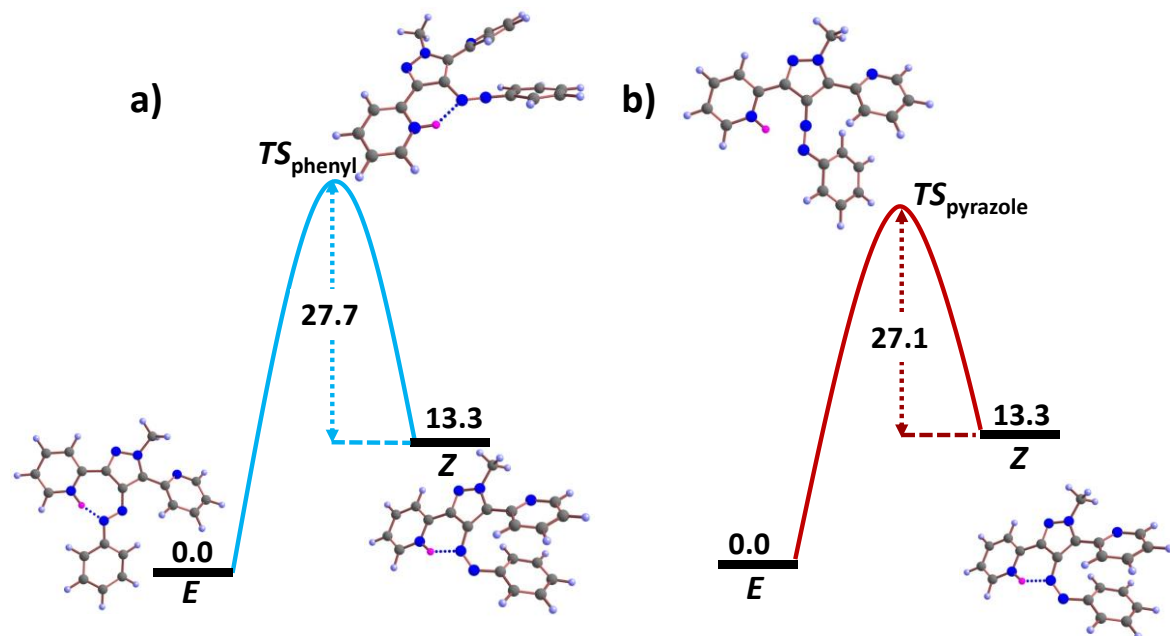


Figure S6.14. Inversion barriers along the azo nitrogen connected to a) phenyl and b) pyrazole ring, respectively for *Z* to *E* thermal conversion of 2a-H⁺ in DMSO (PCM model).

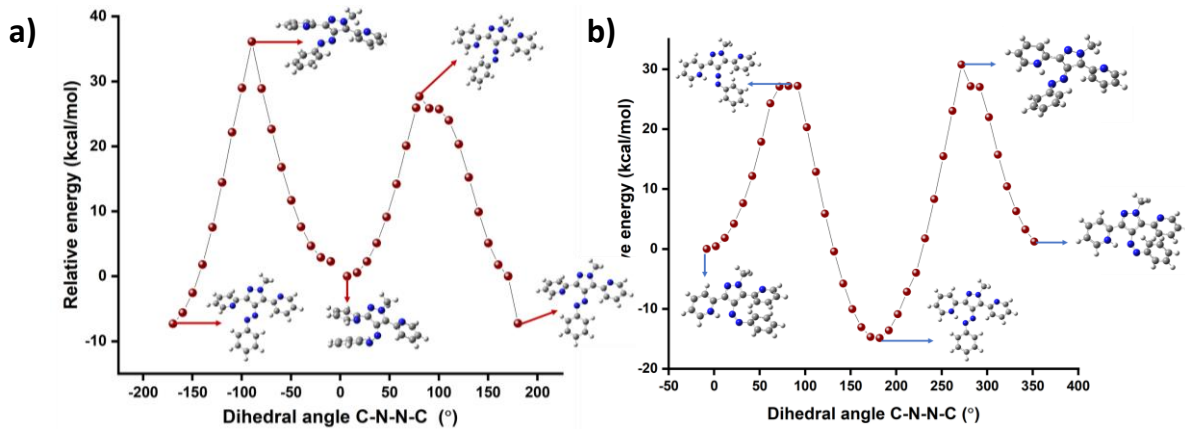


Figure S6.15. Potential energy surface scan to obtain the rotational energy barrier for *Z*-*E* isomerization in a) **2a** and b) **2a**-H⁺ (The energy dependence of the CNNC dihedral angle of **2a** and **2a**-H⁺ is depicted).

Proton affinity calculation

The gas phase proton affinities of **2a** (as shown in Figure S6.11) in *E* and *Z* forms were estimated based on DFT calculations using B3LYP-D3/6-311++G(d,p) level of theory. Since a single proton has no electrons, it cannot have its free energy determined by DFT calculations. However, the free energy can be obtained, by standard thermodynamic equations. Molar entropy can be derived from the Sackur-Tetrode equation for monoatomic ideal gas.¹⁸ At 298.15 K and 1 atm, this treatment yields a value of -6.28 kcal/mol. Several authors have employed the same method to determine the free energy of the proton and were in good agreement with the experimental observations.^{19,20} This value has been used in the present work to calculate proton affinities. Calculations predict that the gas phase proton affinity of the *E* isomer of **2a** is -257 kcal/mol and that of the *Z* isomer is -250 kcal/mol which is ~7 kcal/mol greater than *E* and is consistent with experimental observations.

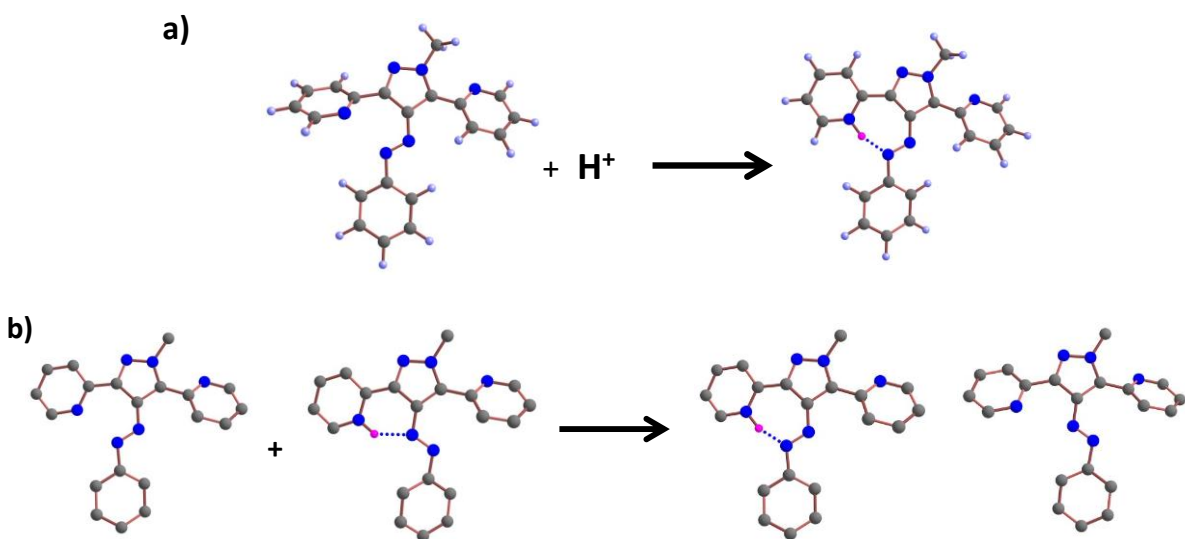


Figure S6.16. a) proton transfer in *E* isomer b) Thermodynamic cycle showing isodesmic proton transfer between *E*₁ and *E*₂.

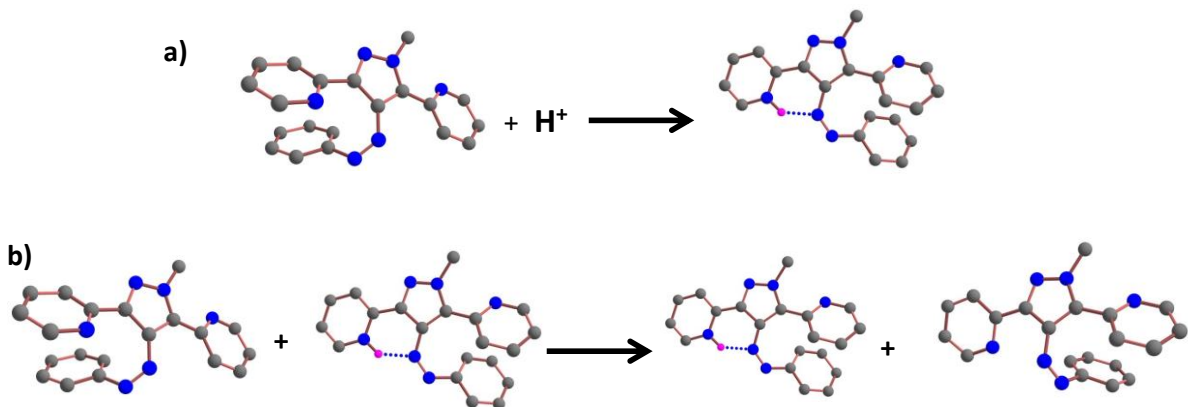


Figure S6.17. a) proton transfer in *Z* isomer b) Thermodynamic cycle showing isodesmic proton transfer between Z_1 and Z_2 .

Determination of pK_a (computational method)

DFT calculations were performed to estimate pK_a values of *E* and *Z* isomers of **2a** and its protonated derivatives.¹⁶ SMD model has been recommended for continuous representation of solvent model.^{17,18} Hence, in the present work SMD model was used for computing the aqueous free energies of these reactions using the thermodynamic cycle given in Figure S6.13, where E_1 and E_2 represent the *E* isomers of **2a** and their corresponding protonated analogues respectively. ΔG_g and ΔG_{aq} represent the free energies of the reaction in the gas phase and aqueous solution respectively. ΔG_s denotes the solvation-free energy of each species. Similar calculations were performed for the corresponding Z_1 and Z_2 isomers. Based on the DFT results a pK_a of 2.6 was obtained for **Z-2a** and pK_a of 4.8 was obtained for **E-2a** isomer.

Acidity constant is directly related to the free energy of deprotonation reaction:

$$pK_a = \frac{\Delta G_{aq}}{2.303RT}$$

According to this cycle, the free energy of the isodesmic reaction for each species can be expressed as follows:

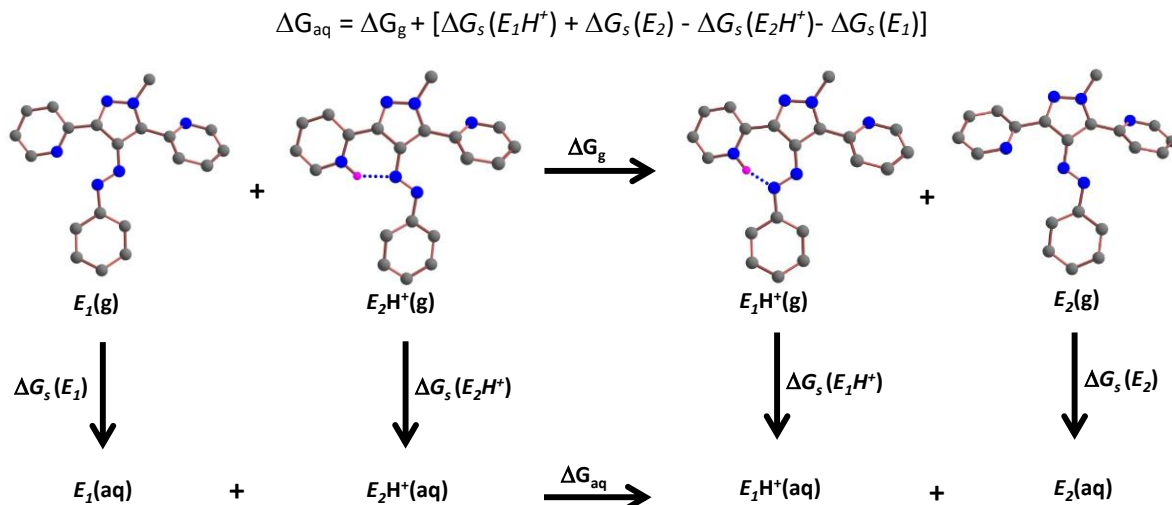


Figure S6.18. The thermodynamic cycle is used to estimate the free energy of the isodesmic reaction for the *E* isomer in the aqueous phase.

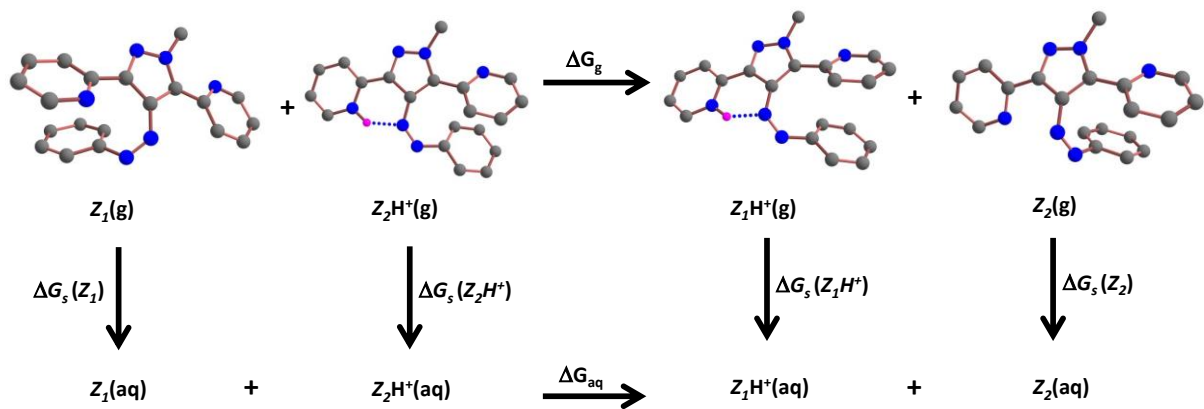


Figure S6.19. The thermodynamic cycle is used to estimate the free energy of the isodesmic reaction for the **Z** isomer in the aqueous phase.

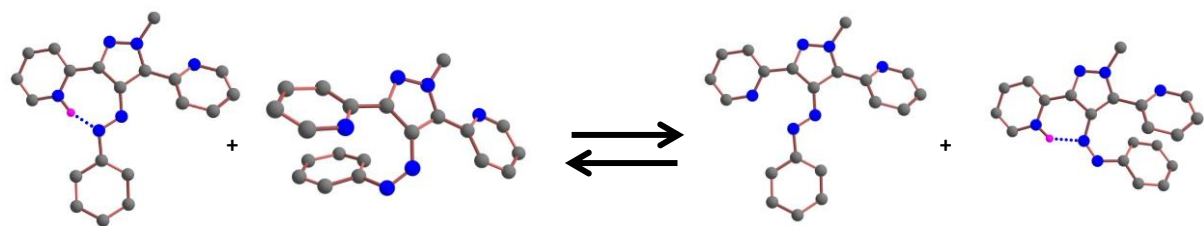


Figure S6.20. Overall proton transfer between **E-2a** and **Z-2a**. **E-2a** was taken as a reference and using experimental pKa of **E-2a** (4.4), a pK_a of 2.6 was obtained for **Z-2a** and pK_a of 4.8 was obtained for **E-2a** isomer based on DFT results.

S7. Compound characterization data

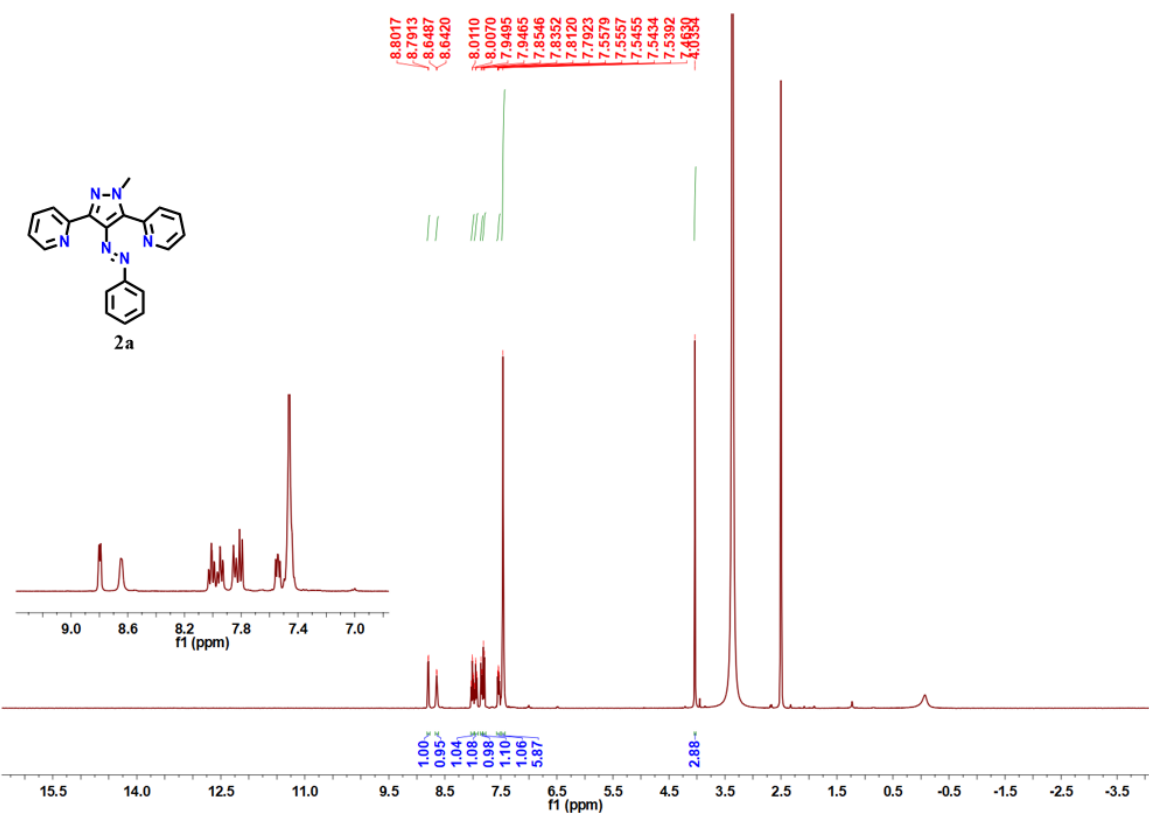


Figure S7.1. ^1H NMR (400 MHz) data of **2a** in $\text{DMSO}-d_6$.

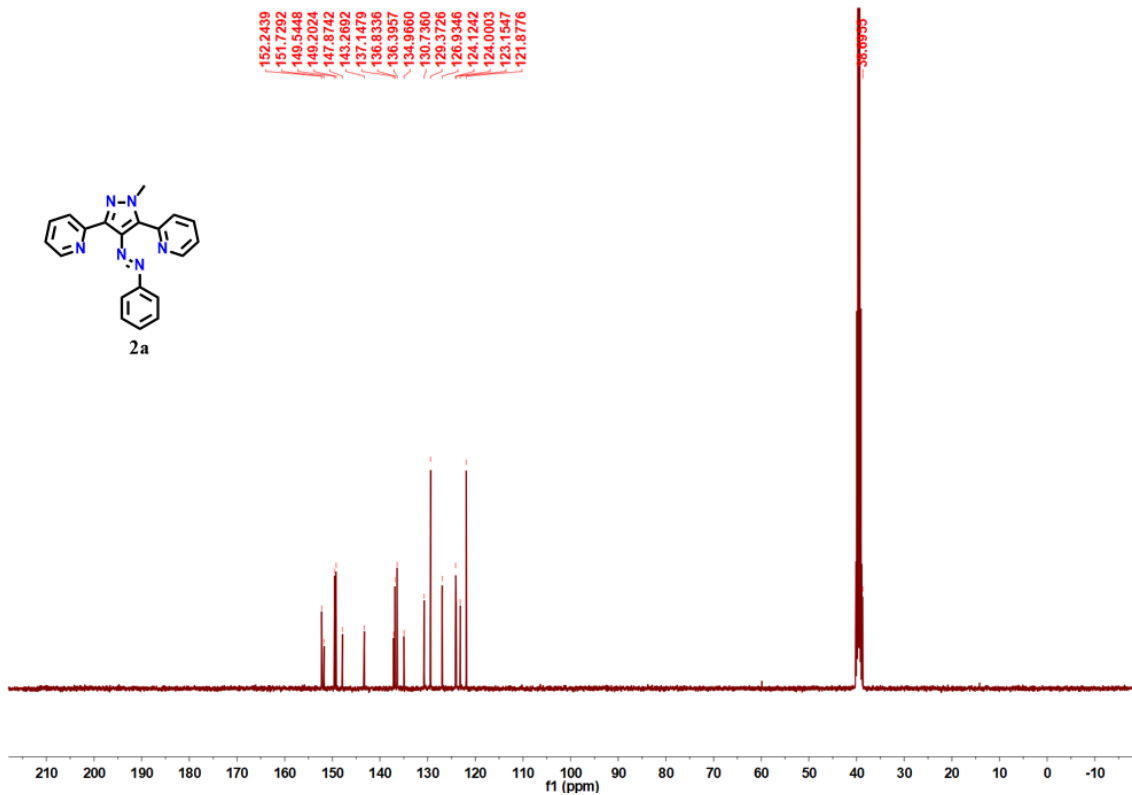


Figure S7.2. $^{13}\text{C}\{^1\text{H}\}$ NMR (100 MHz) data of **2a** in $\text{DMSO}-d_6$.

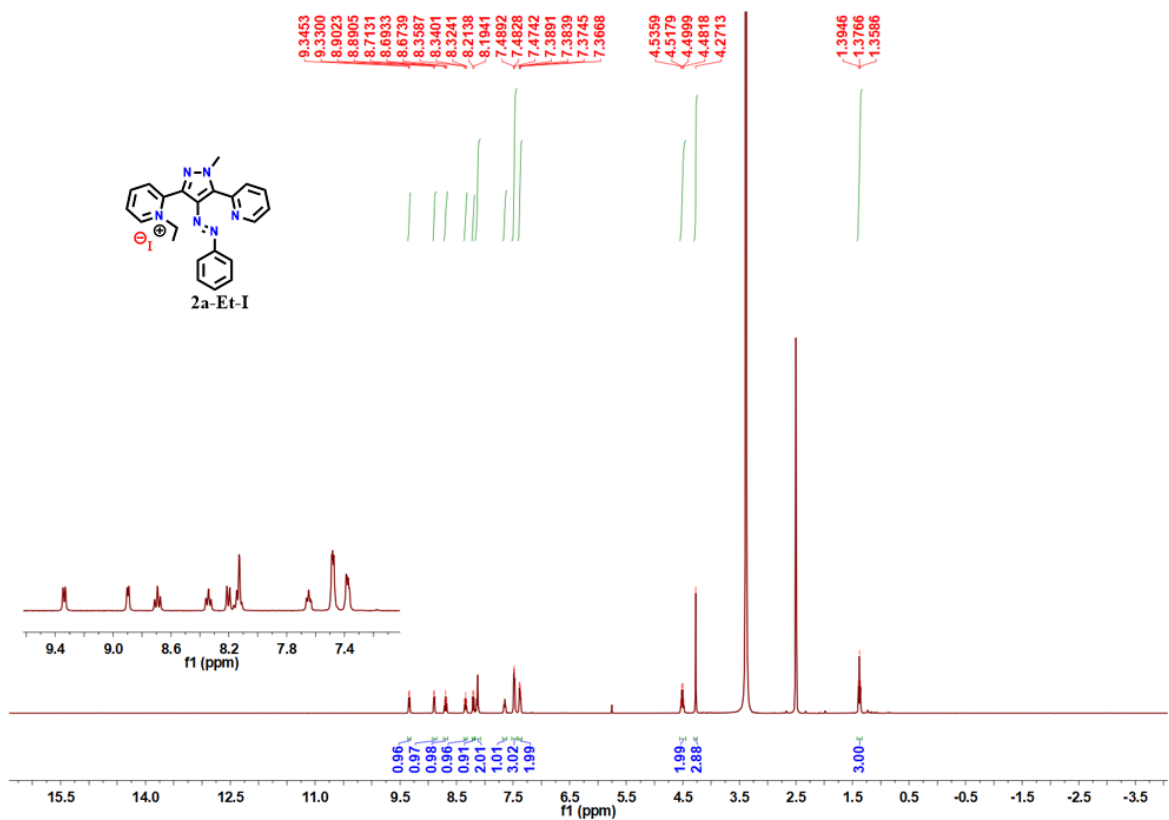


Figure S7.3. ^1H NMR (400 MHz) data of **2a-Et-I** in $\text{DMSO}-d_6$.

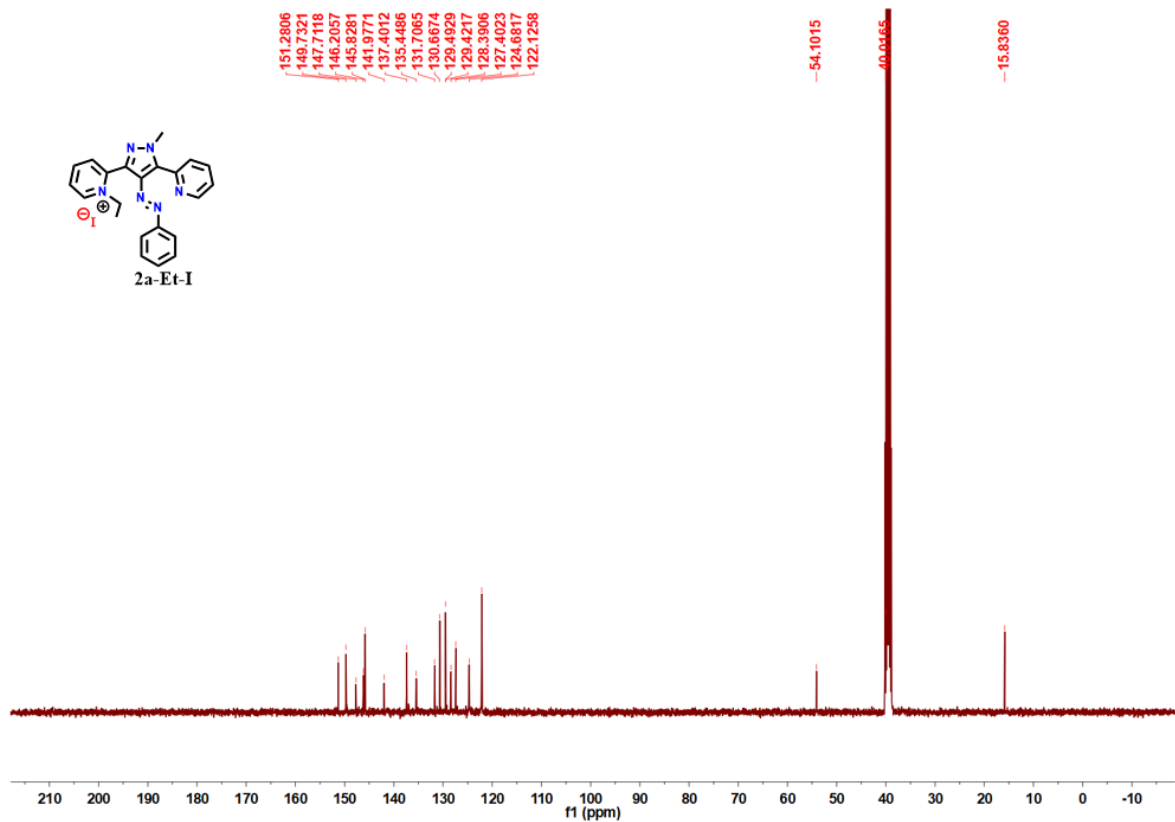


Figure S7.4. $^{13}\text{C}\{^1\text{H}\}$ NMR (100 MHz) data of **2Et-I** in $\text{DMSO}-d_6$.

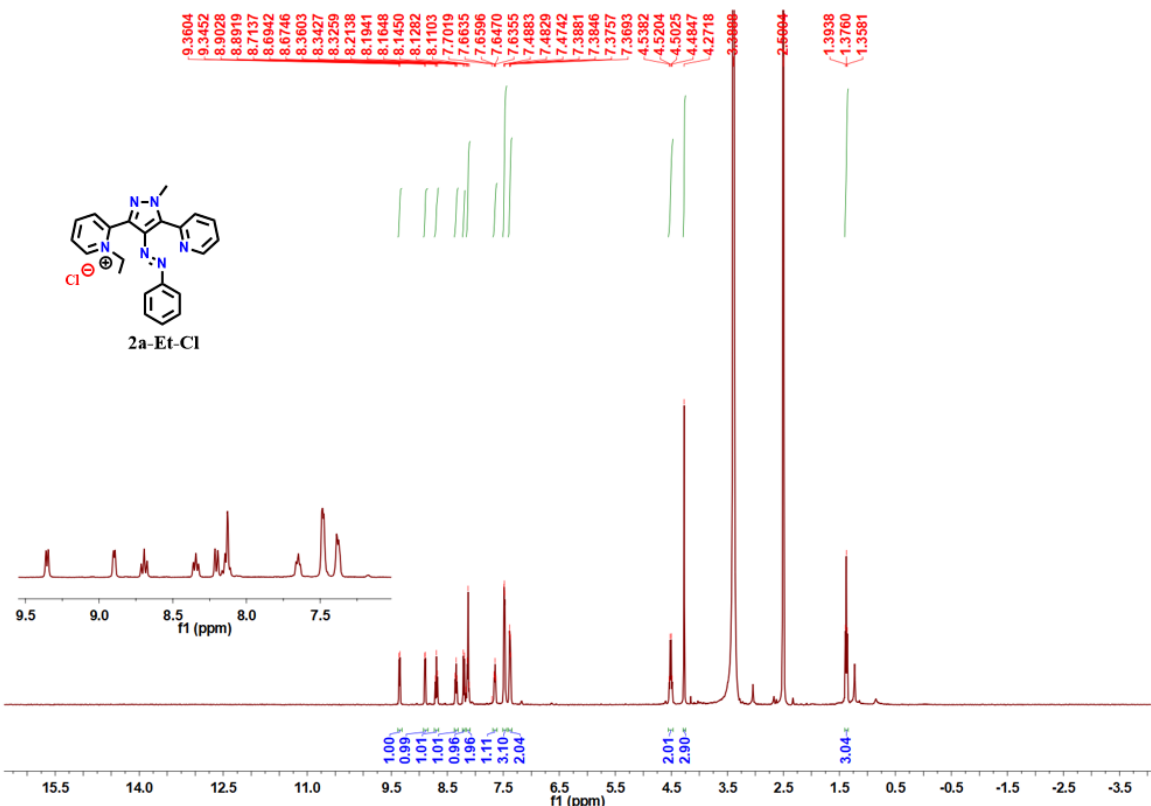


Figure S7.5. ^1H NMR (400 MHz) data of **2a-Et-Cl** in $\text{DMSO}-d_6$.

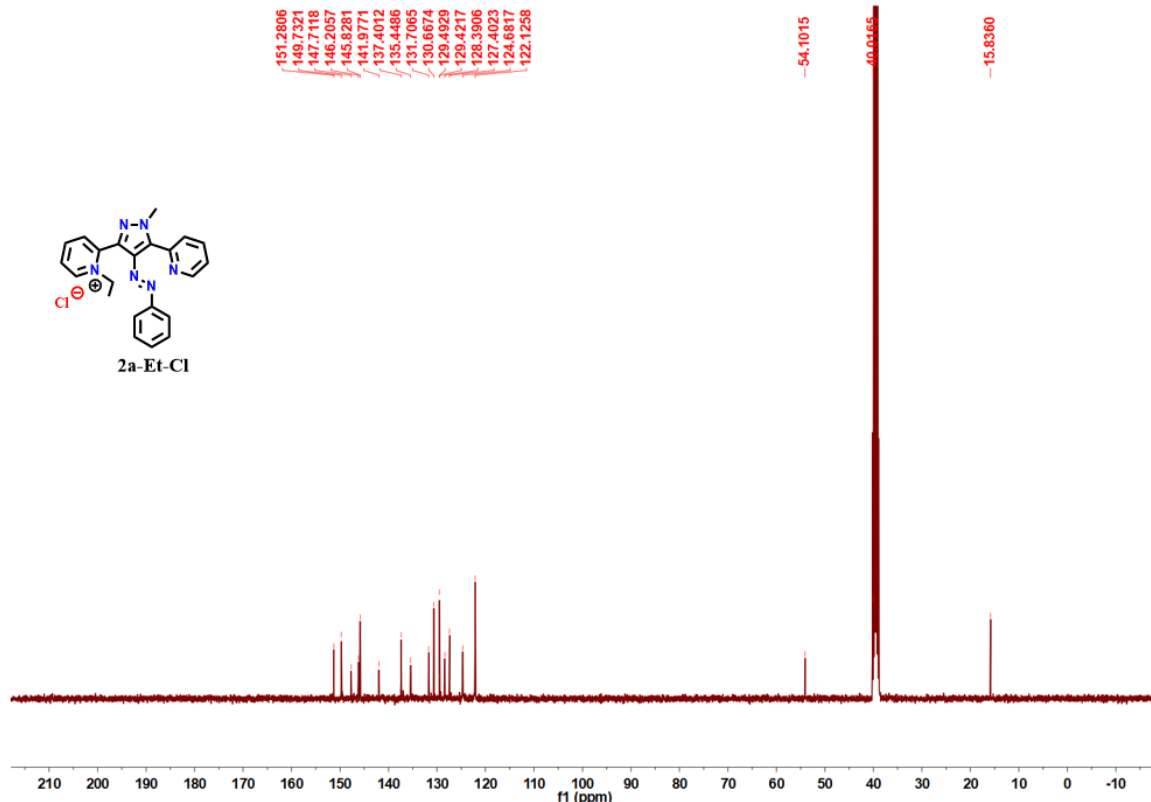


Figure S7.6. $^{13}\text{C}\{^1\text{H}\}$ NMR (100 MHz) data of **2a-Et-Cl** in $\text{DMSO}-d_6$.

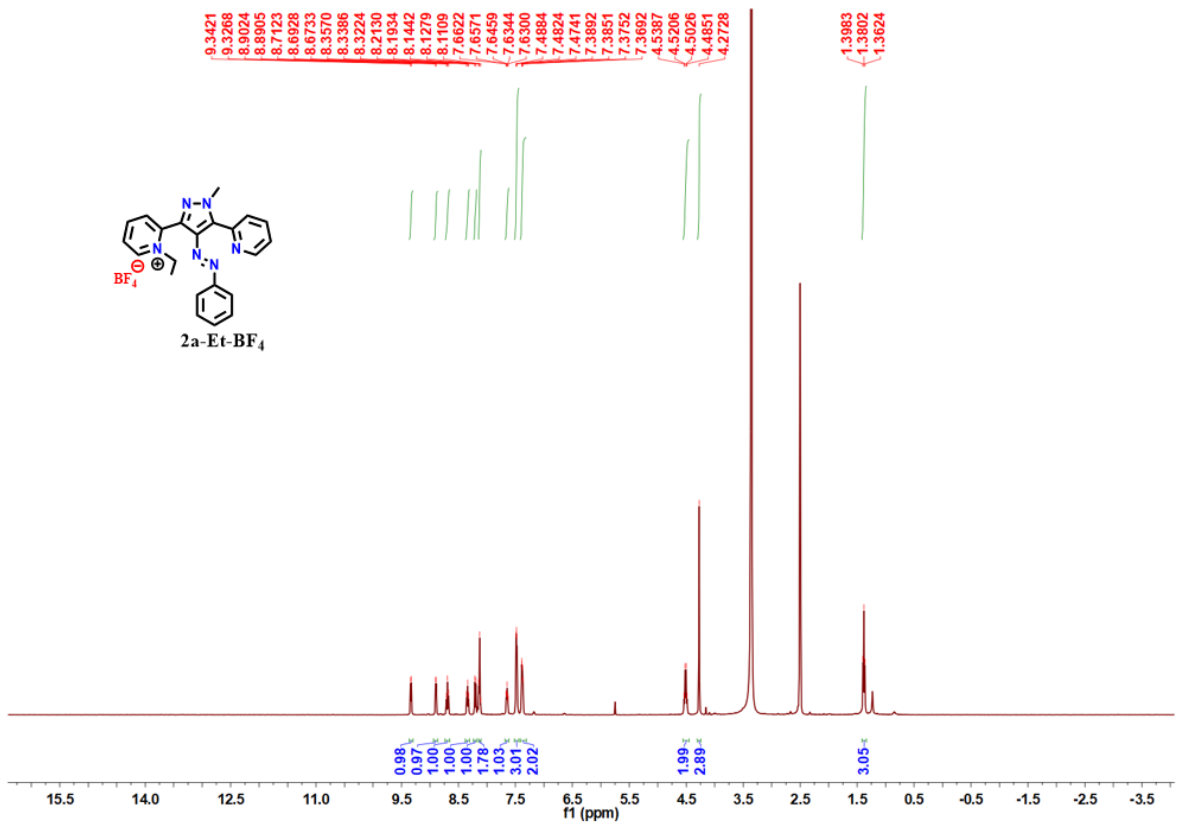


Figure S7.7. ¹H NMR (400 MHz) data of **2a-Et-BF₄** in DMSO-*d*₆.

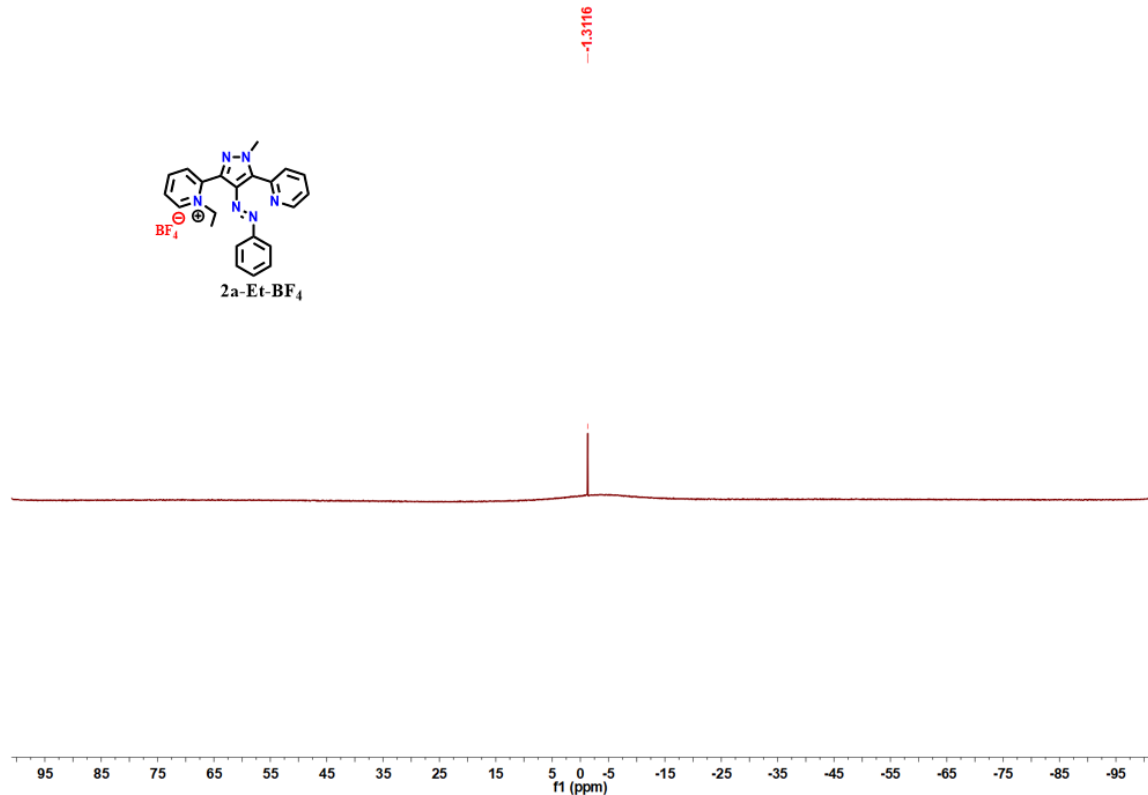


Figure S7.8. ¹¹B NMR (128.3 MHz) data of **2a-Et-BF₄** in DMSO-*d*₆.

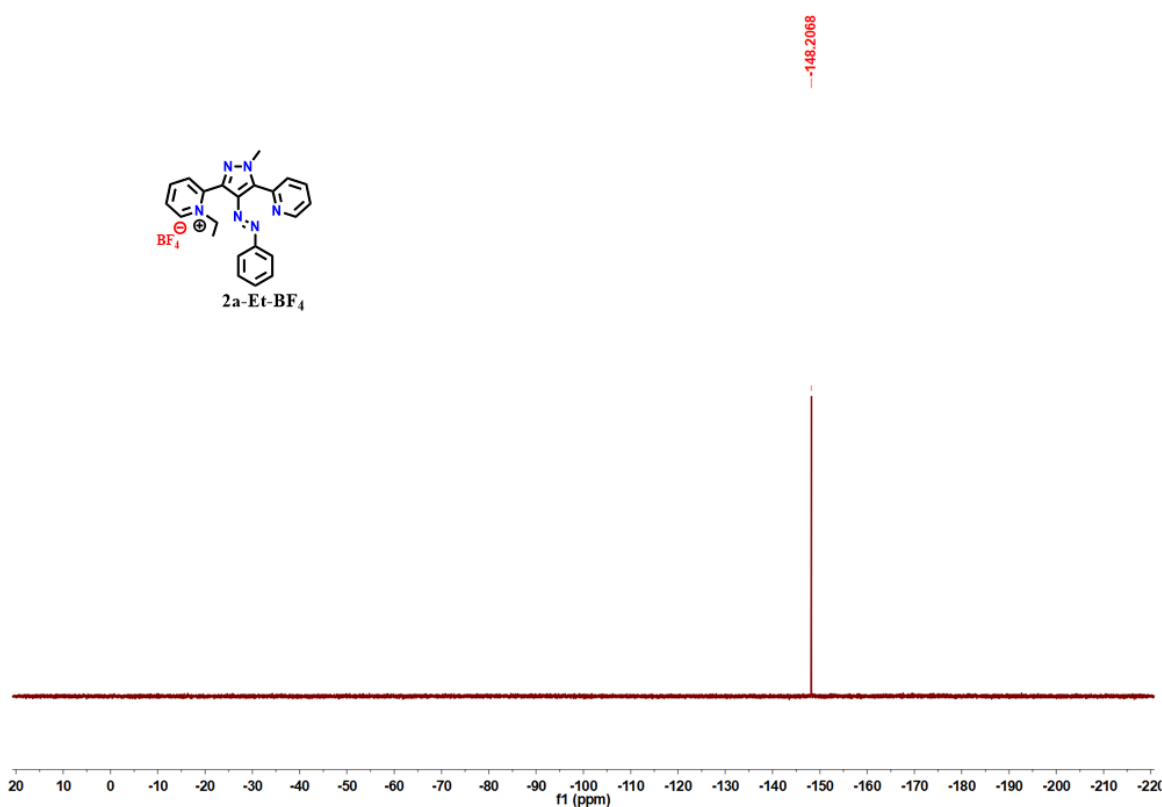


Figure S7.9. ¹⁹F NMR (376.5 MHz) data of **2a-Et-BF₄** in DMSO-*d*₆.

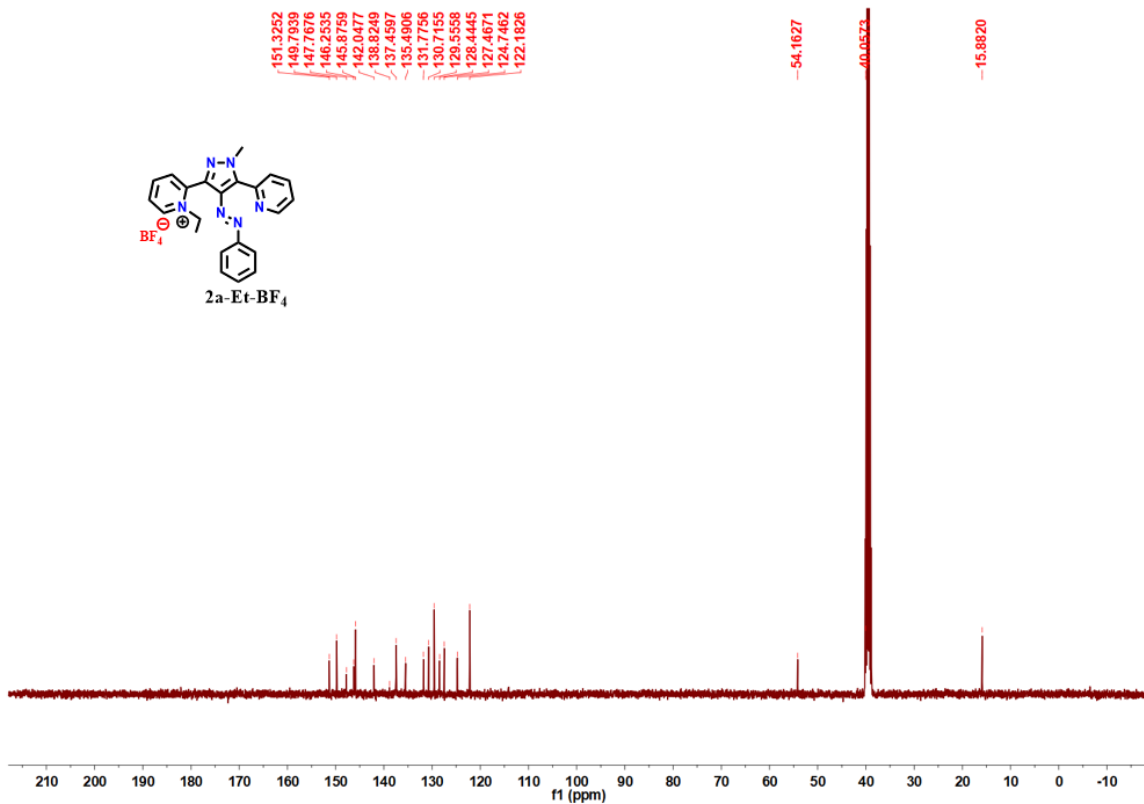


Figure S7.10. ¹³C{¹H} NMR (100 MHz) data of **2a-Et-BF₄** in DMSO-*d*₆.

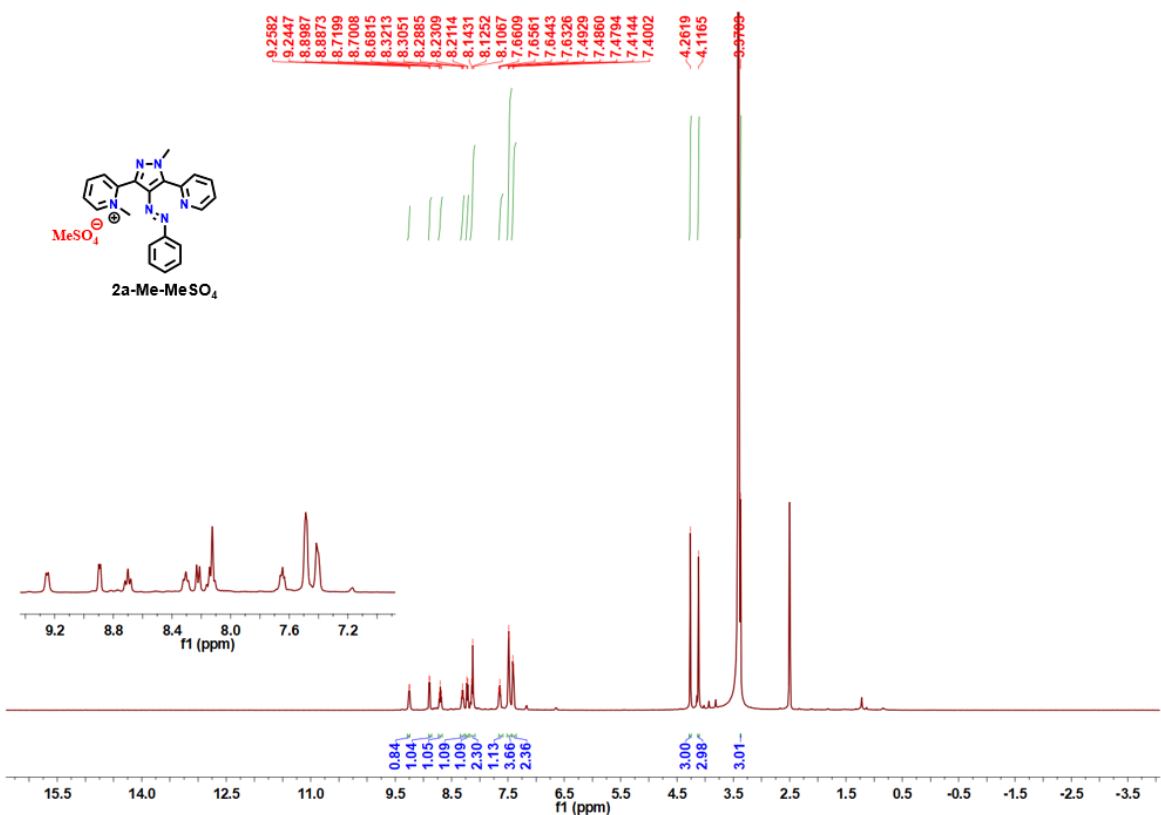


Figure S7.11. ^1H NMR (400 MHz) data of **2a-Me-MeSO₄** in $\text{DMSO}-d_6$.

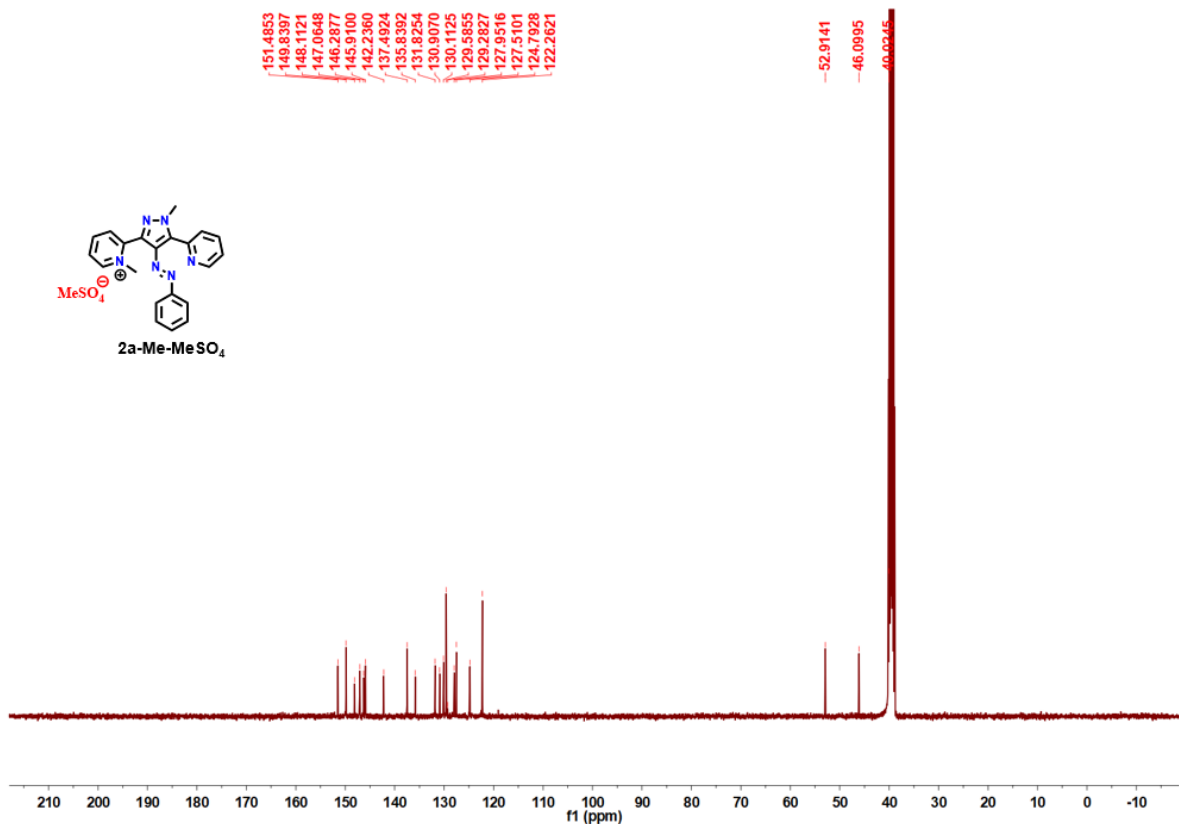


Figure S7.12. $^{13}\text{C}\{^1\text{H}\}$ NMR (100 MHz) data of **2a-Me-MeSO₄** in $\text{DMSO}-d_6$.

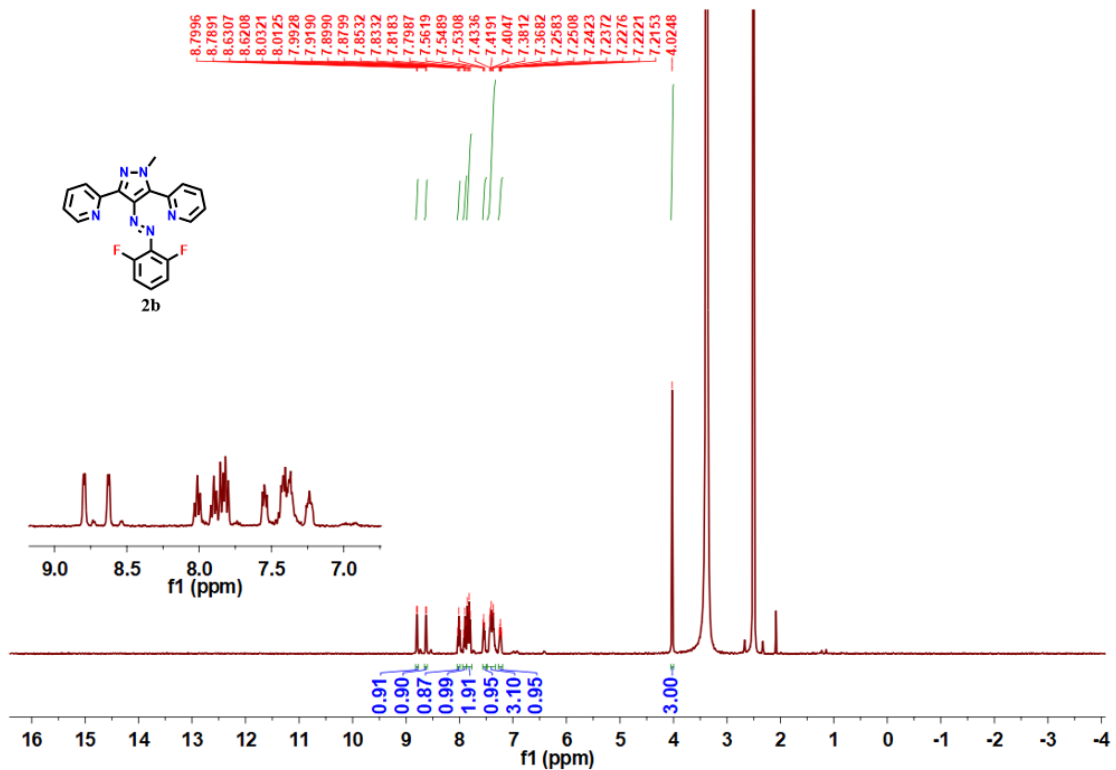


Figure S7.13. ^1H NMR (400 MHz) data of **2b** in $\text{DMSO}-d_6$.

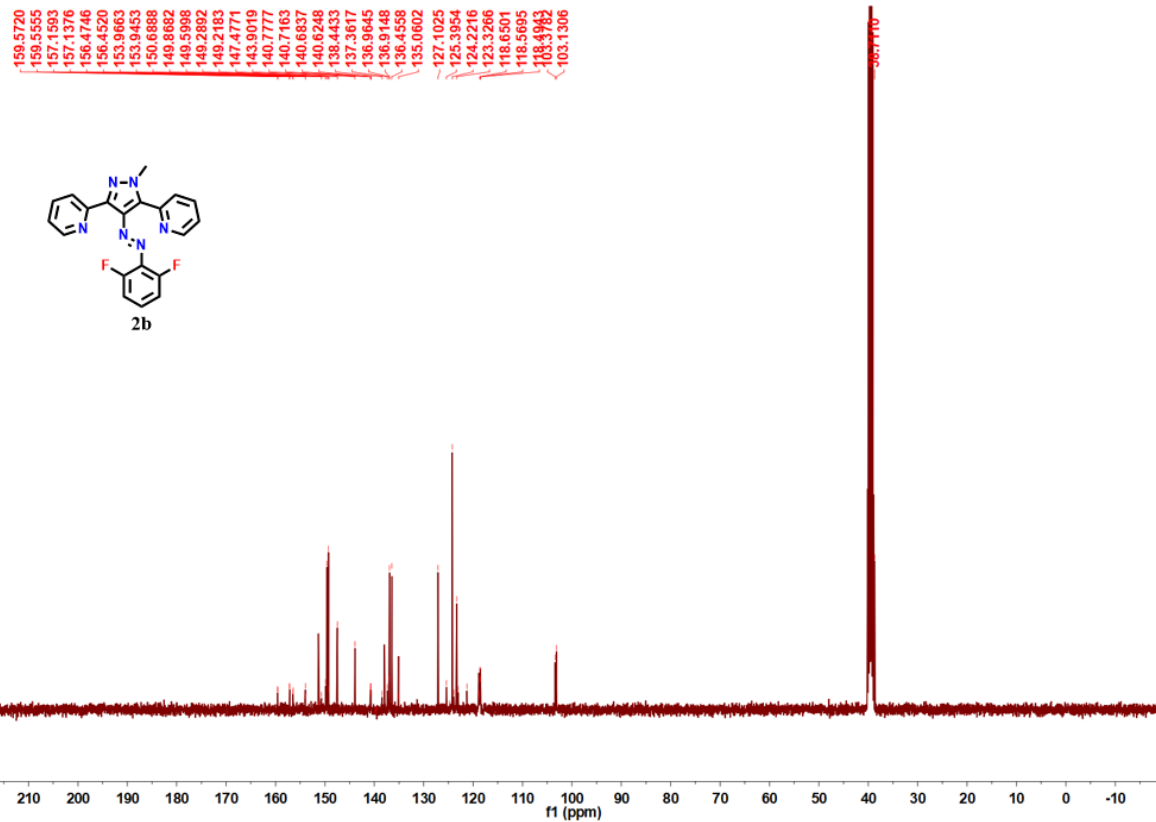


Figure S7.14. $^{13}\text{C}\{^1\text{H}\}$ NMR (400 MHz) data of **2b** in $\text{DMSO}-d_6$.

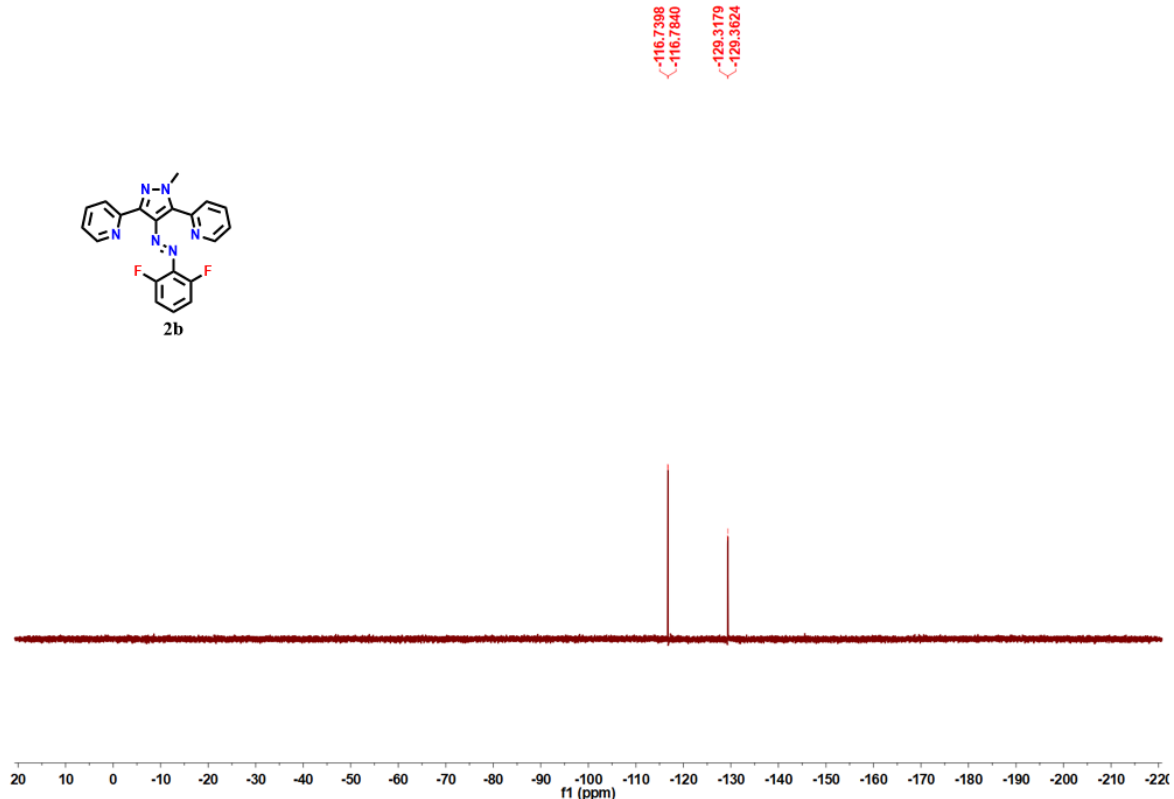


Figure S7.15. ¹⁹F NMR (376.5 MHz) data of **2b** in DMSO-*d*₆.

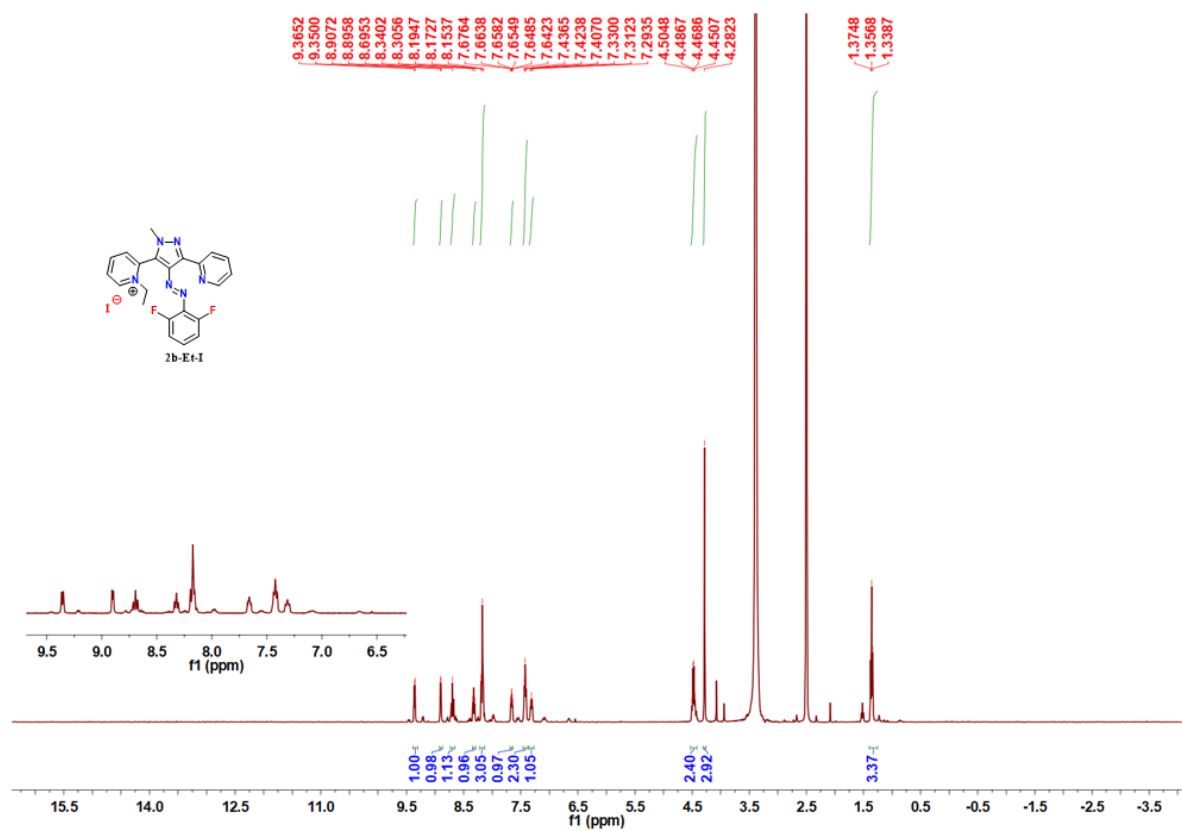


Figure S7.16. ¹H NMR (400 MHz) data of **2b-Et-I** in DMSO-*d*₆.

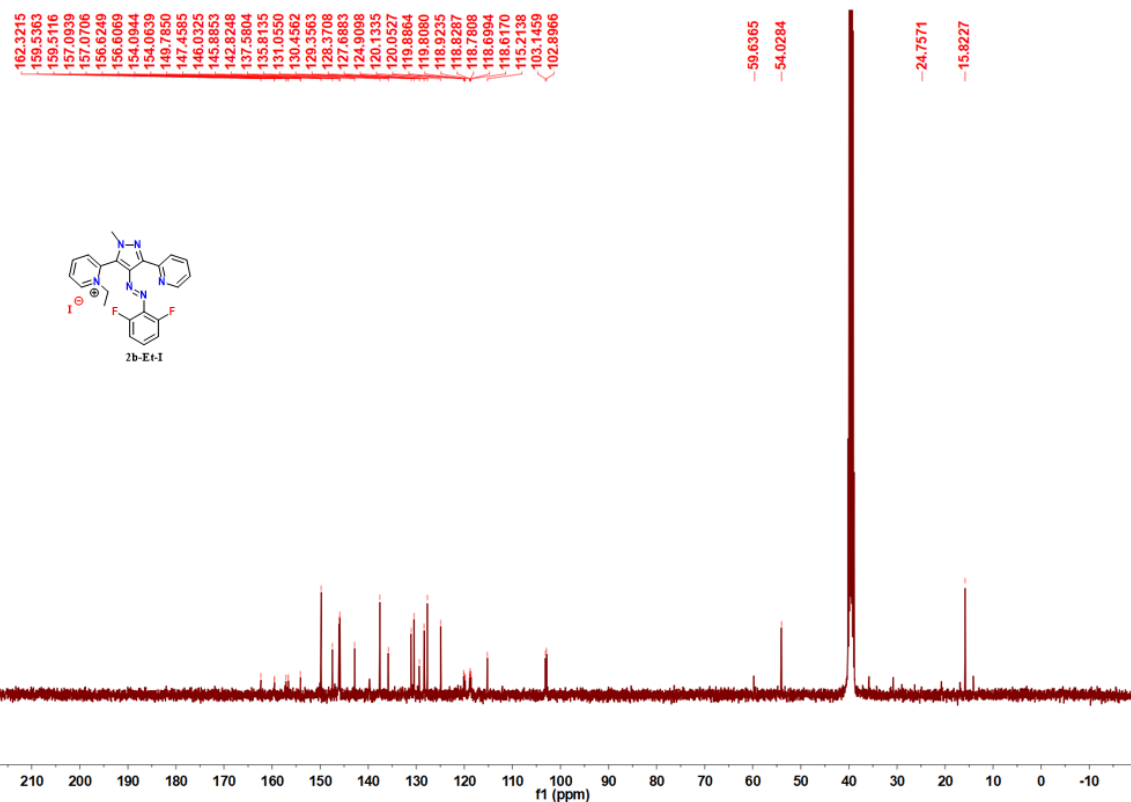


Figure S7.17. $^{13}\text{C}\{\text{H}\}$ NMR (100 MHz) data of **2b-Et-I** in $\text{DMSO}-d_6$.

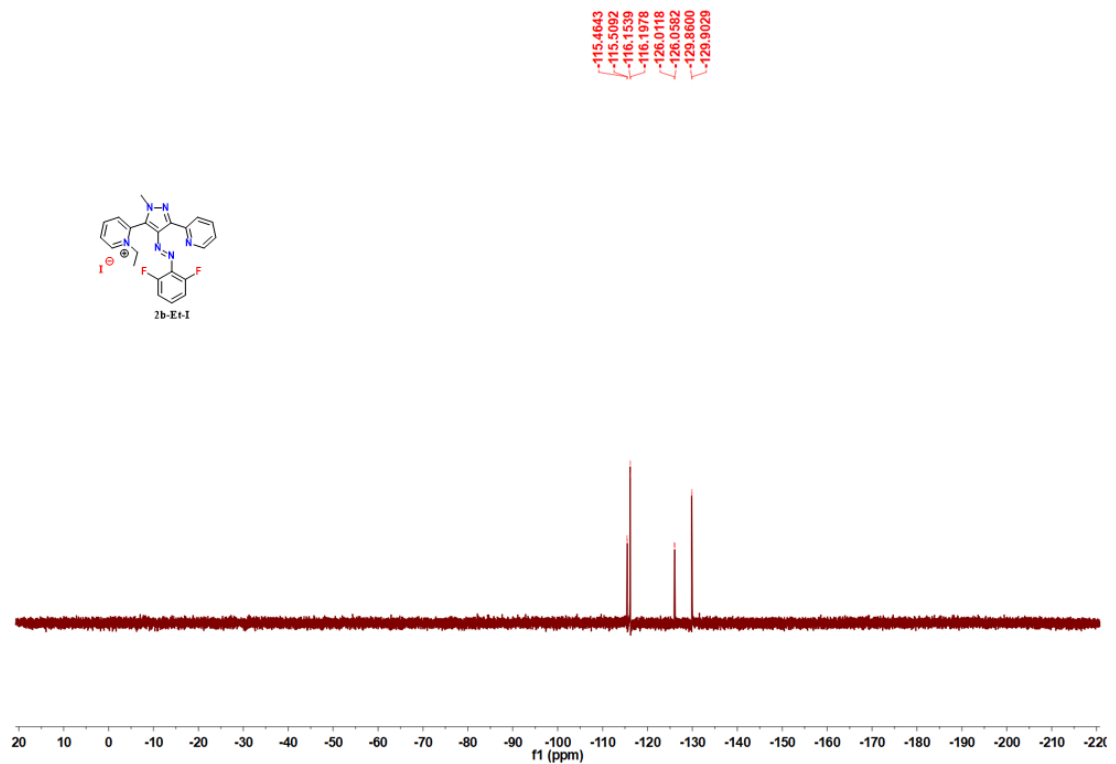


Figure S7.18. ^{19}F NMR (376.5 MHz) data of **2b-Et-I** in $\text{DMSO}-d_6$.

S8. References

1. a) A. K. Gaur, H. Kumar, D. Gupta, I. P. Tom, D. N. Nampoothiry, S. K. Thakur, A. Mahadevan, S. Singh, and S. Venkataramani, *J. Org. Chem.*, 2022, **87**, 10, 6541–6551.
2. a) A. K. Gaur, D. Gupta, A. Mahadevan, P. Kumar, H. Kumar, D. N. Nampoothiry, N. Kaur, S. K. Thakur, S. Singh, T. Slanina and S. Venkataramani, *J. Am. Chem. Soc.*, 2023, **145**, 10584–10594. b) J. Dai, K.Q. Zhao, B.Q. Wang, P. Hu, B. Heinrich and B. Donnio, *J. Mater. Chem. C.*, 2020, **8**, 4215–4225.
3. a) C. E. Weston, R. D. Richardson, P. R. Haycock, A. J. P. White, and M. J. Fuchter, *J. Am. Chem. Soc.*, 2014, **136**, 34, 11878–11881. b) S. R. Logan, *J. Chem. Educ.* 1997, **74**, 11, 1303.
4. R. Lin, P. K. Hashim, S. Sahu, A. S. Amrutha, N. M. Cheruthu, S. Thazhathethil, K. Takahashi, T. Nakamura, T. Kikukawa, N. Tamaoki, *J. Am. Chem. Soc.*, 2023, **145**, 16, 9072–9080.
5. M. J. Frisch, G. W. Trucks, H. B. Schlegel, G. E. Scuseria, M. A. Robb, J. R. Cheeseman, G. Scalmani, V. Barone, G. A. Petersson, H. Nakatsuji, X. Li, M. Caricato, A. V. Marenich, J. Bloino, B. G. Janesko, R. Gomperts, B. Mennucci, H. P. Hratchian, J. V. Ortiz, A. F. Izmaylov, J. L. Sonnenberg, D. Williams-Young, F. Ding, F. Lipparini, F. Egidi, J. Goings, B. Peng, A. Petrone, T. Henderson, D. Ranasinghe, V. G. Zakrzewski, J. Gao, N. Rega, G. Zheng, W. Liang, M. Hada, M. Ehara, K. Toyota, R. Fukuda, J. Hasegawa, M. Ishida, T. Nakajima, Y. Honda, O. Kitao, H. Nakai, T. Vreven, K. Throssell, J. A. Montgomery, Jr., J. E. Peralta, F. Ogliaro, M. J. Bearpark, J. J. Heyd, E. N. Brothers, K. N. Kudin, V. N. Staroverov, T. A. Keith, R. Kobayashi, J. Normand, K. Raghavachari, A. P. Rendell, J. C. Burant, S. S. Iyengar, J. Tomasi, M. Cossi, J. M. Millam, M. Klene, C. Adamo, R. Cammi, J. W. Ochterski, R. L. Martin, K. Morokuma, O. Farkas, J. B. Foresman, and D. J. Fox, Gaussian 16, Revision C. 01, Gaussian, Inc., Wallingford CT, 2016.
6. (a) A. D. Becke, *J. Chem. Phys.* 1993, **98**, 5648–5652; (b) C. Lee, W. Yang and R. G. Parr, *Phys. Rev. B*, 1988, **37**, 785–789; (c) S. H. Vosko, L. Wilk, M. Nusair and *Can. J. Phys.*, 1980, **58**, 1200–1211; (d) P.J. Stephens, F.J. Devlin, C.F. Chabalowski and M. J. Frisch, *J. Phys. Chem.*, 1994, **98**, 11623–11627.
7. S. Grimme, J. Antony, S. Ehrlich and H. Krieg, *J. Chem. Phys.*, 2010, **132**, 154104.
8. (a) P.C. Hariharan and J. A. Pople, *Theor. Chim. Acta*, 1973, **28**, 213–222. (b) M. M. Franci, W. J. Pietro, W. J. Hehre, J. S. Binkley, M. S. Gordon, D. J. DeFrees and J. A. Pople, *J. Chem. Phys.*, 1982, **77**, 3654–3665.
9. D. Andrae, U. Haußermann, M. Dolg, H. Stoll and H. Preuß, *Theor. Chim. Acta*, 1990, **77**, 123–141.
10. H. B. Schlegel, *J. Comp. Chem.*, 1982, **3**, 214–18.
11. J. Tomasi, B. Mennucci and R. Cammi, *Chem. Rev.*, 2005, **105**, 2999–3093.
12. R. F. W. Bader, *Acc. Chem. Res.*, 1985, **18**, 9–15.
13. T. Lu and F. J. Chen, *Comput. Chem.*, 2012, **33**, 580–592.
14. E. Espinosa, I. Alkorta, J. Elguero and J. Molins, *J. Chem. Phys.*, 2002, **117**, 5529.
15. W. Humphrey and A. Dalke K. Schulten, *J. Molec. Graphics*, 1996, **14**, 33–38.
16. R. E. Johnson, S. Keinan, P. Mori-Sánchez, J. Contreras-García, A. J. Cohen and W. J. Yang, *J. Am. Chem. Soc.*, 2010, **132**, 6498–6506.

17. a) C. E. Weston, R. D. Richardson and M. J. Fuchter, *Chem. Commun.*, 2016, **52**, 4521–4524. b) S. Samanta, A. Babalhavaeji, M. -x. Dong, and G. A. Woolley, *Angew. Chem. Int. Ed.*, 2013, **52**, 14127-14130.
18. M. W. Zemansky, *Heat and Thermodynamics*, 7th ed., McGraw Hill, New York, 1997.
19. K. S. Alongi and G. C. Shields, *Ann. Rep. Comp. Chem.*, 2010, **6**, 113-118.
20. a) A. V. Marenich, C. J. Cramer and D. G. Truhlar, *J. Phys. Chem. B* 2009, **113**, 6378-6396. (b) M. D. Liptak and G. C. Shields, *J. Am. Chem. Soc.*, 2001, **123**, 7314-7319; (c) A. V. Marenich, W. D. Ding, C. J. Cramer and D. G. Truhlar, *J. Phys. Chem. Lett.*, 2012, **3**, 1437-1442.

S9. Cartesian coordinates

| E-2a | Z-2a | TS1-2a |
|--|---------------------------------------|---------------------------------------|
| N -1.25081800 0.78875400 0.24136400 | N 0.46296300 -1.80758400 -1.20822600 | N 0.78661300 -1.39644400 0.08101500 |
| N -0.04224500 0.69761800 -0.09184100 | N -0.41838000 -0.94385600 -1.39068000 | N -0.41501400 -1.18420400 -0.02895100 |
| N 1.97004400 -2.20174200 0.08928600 | N -1.47099300 1.79754900 0.63951400 | N -2.21879300 1.86780800 -0.06601600 |
| N 4.11795600 -0.30761000 0.55562300 | N -4.03138000 0.47593900 0.72738400 | N -4.48426800 0.18677900 0.56518200 |
| N -2.28378400 -1.67470300 -1.09254900 | N 2.24072400 0.83589500 -1.67320100 | N 1.99533800 0.97998900 -1.20222000 |
| N 0.76743800 -2.82210600 0.09653400 | N -0.16314800 2.10576000 0.57822400 | N -0.97360300 2.40431500 -0.10834900 |
| C -0.15262900 -1.86833000 -0.00587300 | C 0.41881100 1.15458500 -0.15191100 | C -0.12459500 1.38527600 -0.16158600 |
| C 0.47515700 -0.58960200 -0.07975500 | C -0.54847500 0.20487700 -0.57513700 | C -0.84213000 0.15464100 -0.14463000 |
| C 1.85523500 -0.85185700 -0.03541000 | C -1.77230400 0.665527500 -0.06982200 | C -2.20052200 0.51005300 -0.08995200 |
| C -1.57916000 -2.23491100 -0.09977900 | C 1.85724300 1.21890400 -0.44719300 | C 1.33087300 1.61788900 -0.22874700 |
| C -1.78024900 2.10003100 0.22260600 | C 1.33119000 -1.79287900 -0.07072400 | C 2.07978300 -1.64828900 0.20973600 |
| C 2.99195800 0.07444500 -0.07032400 | C -3.11325700 0.07842400 -0.17038700 | C -3.39874600 -0.33558800 -0.03028600 |
| C -2.13137300 -3.15588500 0.79480400 | C 2.76099700 1.65977100 0.52588600 | C 1.95825100 2.46018200 0.69265200 |
| H -1.51242600 -3.58791400 1.57011600 | H 2.39654400 1.94708600 1.50275600 | H 1.37176100 2.95491500 1.45586800 |
| C -1.02821700 3.26442100 0.00664700 | C 0.85288800 -1.68910800 1.23978900 | C 2.75641100 -1.35336900 1.42328300 |
| H 0.03738800 3.17936200 -0.15844800 | H -0.20438200 -1.54613100 1.42021800 | H 2.19762400 -0.93452400 2.24995800 |
| C -3.15574100 2.19208000 0.45675800 | C 2.68624100 -2.03156400 -0.30462900 | C 2.82476200 -2.18204600 -0.87508500 |
| H -3.70788000 1.27569900 0.62332600 | H 3.02617900 -2.14433000 -1.32588300 | H 2.31621800 -2.39195600 -1.80641400 |
| C -3.56918900 -2.00514100 -1.20653900 | C 3.54111600 0.88520600 -1.96424200 | C 3.31493700 1.15170100 -1.27173000 |
| H -4.11072500 -1.53517200 -2.02283700 | H 3.81574900 0.56944000 -2.96673300 | H 3.82476700 0.60554100 -2.05828700 |
| C 5.16284200 0.52149100 0.53689500 | C -5.25848200 -0.04146500 0.65068400 | C -5.58395800 -0.56332700 0.64210200 |
| H 6.05228400 0.17634700 1.05597400 | H -5.96746300 0.30610900 1.39668000 | H -6.43816100 -0.10573600 1.13239500 |
| C 3.16696100 -3.02967800 0.15702300 | C -2.35021700 2.71290900 1.35829300 | C -3.35272100 2.78446200 -0.04967700 |
| H 2.83919500 -4.05413300 -0.00439300 | H -1.73857300 3.57349300 1.61969900 | H -2.95562700 3.76488800 -0.30242900 |
| H 3.65048600 -2.92643300 1.12714700 | H -2.75401100 2.23668700 2.24954800 | H -3.81978000 2.79750100 0.93359500 |
| H 3.87347900 -2.73124000 -0.61589800 | H -3.18140300 3.01500300 0.72330100 | H -4.09511400 2.47367500 -0.78247300 |
| C -3.47464000 -3.48879600 0.66500100 | C 4.11123900 1.70135100 0.20820800 | C 3.33557500 2.63074700 0.60574000 |
| H -3.93396900 -4.19417500 1.34805600 | H 4.83741400 2.02988200 0.94280500 | H 3.85478700 3.26835100 1.31196600 |
| C 2.88808100 1.30198400 -0.74226400 | C -3.40796900 -0.85923200 -1.17389500 | C -3.38991600 -1.62842600 -0.57337300 |
| H 1.96147800 1.56630500 -1.23006000 | H -2.63636100 -1.15913600 -1.86985900 | H -2.49319400 -2.01242100 -1.03652200 |
| C -4.21622000 -2.89850400 -0.35345100 | C 4.51636200 1.30648600 -1.06428300 | C 4.03300600 1.96039400 -0.39280800 |
| H -5.26663900 -3.12438900 -0.49139200 | H 5.55977500 1.32153100 -1.35467100 | H 5.10774700 2.04988100 -0.48880600 |
| C -1.65875000 4.50033200 0.02077000 | C 1.74322500 -1.77700200 2.30396200 | C 4.11644100 -1.59654800 1.52842400 |
| H -1.07922100 5.40245200 -0.14005600 | H 1.37155200 -1.70290100 3.31944000 | H 4.61177100 -1.37148100 2.46689700 |
| C -3.78235400 3.43452000 0.46299700 | C 3.57472000 -2.08234300 0.76289800 | C 4.19022600 -2.37432100 -0.74158700 |
| H -4.84951300 3.50139500 0.63952200 | H 4.63120300 -2.23350600 0.57556100 | H 4.74381600 -2.76287500 -1.58989500 |
| C 5.15006400 1.76176500 -0.09436000 | C -5.64266400 -0.97307300 -0.30846000 | C -5.66693500 -1.85943000 0.14056300 |
| H 6.02768500 2.39591400 -0.07471600 | H -6.65302900 -1.36251500 -0.32177100 | H -6.58562500 -2.42508600 0.23403800 |
| C -3.03604600 4.59068800 0.24520400 | C 3.10676800 -1.95453400 2.06969300 | C 4.85617000 -2.09364700 0.45341000 |
| H -3.52049000 5.56021300 0.25400300 | H 3.79773000 -2.00791300 2.90300300 | H 5.92138700 -2.26213000 0.54599700 |
| C 3.98402800 2.15239800 -0.74882300 | C -4.69024400 -1.38378500 -1.23872100 | C -4.54232000 -2.39643900 -0.48002700 |
| H 3.93107000 3.10559800 -1.26204200 | H -4.94257400 -2.10553200 -2.00688300 | H -4.56184300 -3.39973600 -0.88904900 |
| TS2-2a | E-2a-H⁺ | Z-2a-H⁺ |
| N -0.46092100 1.77496400 -0.86918900 | N 1.22048000 0.99288300 0.06939200 | N -0.11093500 -2.13014700 -0.50678600 |
| N 0.02637300 0.68054200 -0.58442600 | N -0.00492400 0.69277400 0.02381100 | N 0.78869000 -1.25718200 -0.57905800 |
| N 1.99479200 -2.03891100 0.39314500 | N -1.75138000 -2.35442400 0.06439400 | N 0.59125900 2.27685100 0.14251300 |
| N 4.25283300 -0.23345400 0.45387600 | N -3.97961800 -0.63101400 -0.59965800 | N -2.29507600 2.02268200 0.39848700 |
| N -2.23437800 -1.08496200 -0.85398900 | N 2.67740300 -1.24372500 0.03524500 | N 3.45963200 -1.16894600 -0.34462000 |
| N 0.80882400 -2.65724700 0.28982100 | N -0.52812700 -2.89702300 0.04346900 | N 1.89404200 2.02512300 0.28933200 |
| C -0.08316000 -1.73892600 -0.07320700 | C 0.34483600 -1.88995000 0.04463800 | C 2.03841700 0.72310600 0.04802600 |
| C 0.56899200 -0.46617700 -0.26479500 | C -0.36337600 -0.63376300 0.06755100 | C 0.77734900 0.10655700 -0.22538000 |
| C 1.94552400 -0.72101600 0.01182100 | C -1.72461500 -0.99614700 0.07929800 | C -0.14533200 1.16933400 -0.18138600 |
| C -1.49125300 -2.04543100 -0.27770200 | C 1.75794700 -2.23318100 0.00443800 | C 3.35792900 0.12238500 0.05603300 |
| C -1.61982100 2.17986100 -0.12252200 | C 1.53504000 2.36383000 -0.02110200 | C -1.35940600 -1.97356000 0.12155100 |
| C 3.07544800 0.19289300 -0.04662800 | C -2.92521300 -0.15080800 0.07916400 | C -1.59023800 1.23325400 -0.42707100 |
| C -2.03978300 -3.26979700 0.14138200 | C 2.20983400 -3.55687200 -0.06815200 | C 4.52672800 0.79781800 0.41782800 |
| H -1.39961200 -4.00903100 0.60412800 | H 1.47799000 -4.35102200 -0.09489700 | H 4.45175700 1.82900200 0.73256100 |
| C -2.12576600 1.47586300 0.97459400 | C 0.59876200 3.34867200 -0.37092900 | C -1.58682900 -1.23047700 1.28997100 |
| H -1.64214200 0.56160900 1.28914400 | H -0.41859800 3.05882100 -0.59554400 | H -0.78148700 -0.68372400 1.76034700 |
| C -2.22428600 3.36437700 -0.54533800 | C 2.86330300 2.71563500 0.24671700 | C -2.39156900 -2.74591400 -0.43124500 |
| H -1.79953300 3.88731200 -1.39415700 | H 3.57421400 1.94584600 0.52425200 | H -2.17169900 -3.36055300 -1.29529600 |
| C -3.53985500 -1.30945500 -0.101601300 | C 4.00458400 -1.46928900 -0.00724000 | C 4.62793000 -1.83595100 -0.41246800 |
| H -4.10477100 -0.50316200 -1.47478100 | H 4.63841000 -0.59318000 0.01676300 | H 4.57553000 -2.86216400 -0.74924000 |
| C 5.31033600 0.57255700 0.37302300 | C -5.08581500 0.11024600 -0.64478100 | C -3.61685200 2.06659400 0.24060700 |
| H 6.23521800 0.18309600 0.78984700 | H -5.91630000 -0.30508600 -1.20621500 | H -4.15909400 2.70893200 0.92689400 |

| | | |
|---|--|---|
| C 3.12604800 -2.83019100 0.86249100 H 2.74414000 -3.83733700 1.01441400 H 3.51852600 -2.41830800 1.79050400 H 3.92582800 -2.82784300 0.12400400 C -3.39365900 -3.49052100 -0.04929400 H -3.84377000 -4.42693800 0.26024600 C 2.94463200 1.46522200 -0.64075400 H 1.99779400 1.79414200 -1.04143200 C -4.16979700 -2.49057900 -0.63896500 H -5.23158300 -2.62384900 -0.80520300 C -3.24476400 1.96072000 1.63803700 H -3.64282600 1.42117000 2.48973700 C -3.35158100 3.83976500 0.11683000 H -3.83024000 4.75381100 -0.21451800 C 5.27462800 1.84162200 -0.19681700 H 6.16557300 2.45599300 -0.23019700 C -3.86231800 3.13867400 1.20889800 H -4.73776500 3.50985200 1.72917500 C 4.05940800 2.28540400 -0.71518400 H 3.97867000 3.26377300 -1.17470000 | C -2.90761100 -3.25277800 0.08927800 H -2.52869300 -4.23918400 0.34358500 H -3.39418400 -3.25753200 -0.88338600 H -3.61806200 -2.90925600 0.83802000 C 3.56944300 -3.81200500 -0.10619100 H 3.92279900 -4.83439900 -0.16175000 C -2.94696800 1.07736700 0.74884100 H -2.08064000 1.41853400 1.29614600 C 4.48965800 -2.75538700 -0.07692700 H 5.55571600 -2.93183200 -0.10877900 C 1.00200800 4.67303600 -0.43987700 H 0.28748500 5.43822700 -0.71776800 C 3.25594300 4.04700500 0.18137900 H 4.28114600 4.32086100 0.39687900 C -5.20078700 1.35134600 -0.01862600 H -6.12449400 1.91194000 -0.08572900 C 2.32644600 5.02658000 -0.16259100 H 2.63143800 6.06421900 -0.22120200 C -4.11034200 1.83712000 0.69416400 H -4.16459000 2.78985300 1.20685100 H 2.28107100 -0.24704600 0.08189100 | C 0.12842600 3.65819600 0.29029700 H 1.01701100 4.28366300 0.29808800 H -0.43563100 3.76484300 1.21396600 H -0.51421900 3.91773500 -0.54906200 C 5.73996300 0.13188000 0.36041500 H 6.64959100 0.64828300 0.64180900 C -2.17583400 0.49172600 -1.45566000 H -1.56560900 -0.10741900 -2.11840800 C 5.79920900 -1.20456000 -0.05860400 H 6.73669700 -1.74051000 -0.10658300 C -2.85305400 -1.22157200 1.85513700 H -3.02947300 -0.65644000 2.76193100 C -3.66547700 -2.69520800 0.11672800 H -4.46894700 -3.26907200 -0.32825400 C -4.29557000 1.33759400 -0.73604300 H -5.37329000 1.40357900 -0.81407500 C -3.89887800 -1.92998400 1.25876700 H -4.88729700 -1.90449600 1.70123000 C -3.55645900 0.54437400 -1.60566400 H -4.04382200 -0.02546700 -2.38691100 H 2.54396800 -1.59841700 -0.61912000 |
| TS1-2a-H⁺ N -0.57744400 -1.48884400 0.00900800 N 0.60467600 -1.15504800 -0.11331700 N 1.05822900 2.41494100 -0.02077800 N -1.83093100 2.43007800 0.70414800 N 3.33046400 -1.47867100 -0.02995200 N 2.32975300 2.00285800 0.03292500 C 2.27572900 0.66964300 -0.02316600 C 0.92766000 0.22412000 -0.10666600 C 0.15786100 1.39173800 -0.11542600 C 3.48024500 -0.13047600 0.01993800 C -1.84822100 -1.87615800 0.14792500 C -1.29543300 1.60681100 -0.21013300 C 4.77412600 0.38996000 0.10486000 H 4.89670200 1.46312000 0.14531300 C -2.68112400 -1.25519300 1.11441400 H -2.26959600 -0.47001700 1.73509700 C -2.38765400 -2.89116800 -0.68219300 H -1.74708600 -3.36545000 -1.41465800 C 4.36629200 -2.34079800 -0.00384600 H 4.11649700 -3.39190600 -0.04915500 C -3.14668700 2.64677900 0.65024400 H -3.55076000 3.31302100 1.40546200 C 0.77074600 3.84864700 0.01465600 H 1.71848800 4.36487900 -0.11091400 H 0.30707800 4.10732400 0.96462300 H 0.08981500 4.10171700 -0.97909300 C 5.85395300 -0.47685000 0.13442300 H 6.85966000 -0.08002100 0.20039500 C -2.04604000 0.98850600 -1.21210200 H -1.56823200 0.34247400 -1.93671900 C 5.65469700 -1.86362000 0.07949100 H 6.48519000 -2.55508100 0.10284200 C -3.98827700 -1.68316400 1.27185700 H -4.60646000 -1.23639600 2.04132000 C -3.72816900 -3.22501600 -0.57451300 H -4.14620200 -3.97190600 -1.23880700 C -3.98012300 2.06728500 -0.30574100 H -5.04220100 2.27676500 -0.30082800 C -4.52736400 -2.64582400 0.41466500 H -5.56282500 -2.94531100 0.51805300 C -3.41511100 1.22506800 -1.25632100 H -4.02677700 0.75660900 -2.01730100 H 2.34085300 -1.80876800 -0.09605400 | TS2-2a-H⁺ N 0.03052700 1.94209500 -0.60406900 N -0.26769900 0.73946200 -0.45386100 N -0.78266300 -2.65652900 0.25013000 N 2.13309900 -2.87865700 0.37856700 N -0.07947800 1.21089200 -0.28863200 N -0.03242300 -2.20088700 0.40816300 C -1.99617600 -0.90381100 0.10057500 C -0.64538400 -0.48871000 -0.19148000 C 0.11470800 -1.68786000 -0.08678200 C -3.18561000 -0.09883400 0.07522100 C 1.26132700 2.39465900 -0.05717000 C 1.54317300 -1.87231500 -0.29321100 C -4.46699900 -0.59321700 0.35783700 H -4.55925600 -1.62971400 0.64994600 C 2.03781700 1.64774600 0.84074000 H 1.71168700 0.66430800 1.15025500 C 1.65184400 3.68374400 -0.43897500 H 1.02222400 4.23863500 -1.12390400 C -4.14205500 2.04117700 -0.40425100 H -3.92026600 3.05538200 -0.70537700 C 3.45039200 -3.02103700 0.25829800 H 3.89376700 -3.84232600 0.81220900 C -0.54015000 -4.08704900 0.44685400 H -1.51567900 -4.56239100 0.50521100 H 0.03077300 -4.24465300 1.35904200 H 0.03004700 -4.47540600 -0.39490700 C -5.56375700 0.23987000 0.25553700 H -6.55209600 -0.14315000 0.47832000 C 2.25588700 -0.99320400 -1.12058500 H 1.74424700 -0.22579400 -1.68385100 C -5.40654100 1.58070900 -0.13554900 H -6.25240900 2.24777700 -0.22235300 C 3.21101500 2.19435100 1.33909300 H 3.81315100 1.63128600 2.04175300 C 2.83657500 4.21559600 0.05299500 H 3.15282700 5.20641600 -0.24849600 C 4.24793100 -2.18024500 -0.52218300 H 5.31658000 -2.34294300 -0.57989300 C 3.61503300 3.47240700 0.94152200 H 4.53397100 3.89160700 1.33330600 C 3.63388600 -1.15183800 -1.22533900 H 4.21263500 -0.48704400 -1.85478400 H -2.14923700 1.57055500 -0.50744400 | E-2a-N-Me⁺ N 1.17561900 0.84423800 -0.03880100 N -0.08489900 0.78809000 -0.02171000 N -0.206552700 -2.14317800 -0.04356100 N -4.24620700 -0.32261900 -0.56613800 N 2.30564800 -1.88576000 0.91518200 N -0.85854900 -2.74050200 -0.08653900 C 0.04057300 -1.76223300 -0.02564500 C -0.60293300 -0.49150800 0.03969700 C -1.97846200 -0.78598600 0.02613700 C 1.46270800 -2.10389400 -0.13312200 C 1.73514700 2.13372000 -0.13920400 C -3.13306600 0.12013900 0.04017600 C 1.96523500 -2.70243700 -1.28585000 C 1.27674600 -2.89444900 -2.09644800 C 0.98633600 3.31421200 -0.26982300 H -0.09285200 3.25645900 -0.31028800 C 3.13370900 2.18904500 -0.10778800 H 3.69017000 1.26291400 -0.02213300 C 3.62439500 -2.17220700 0.82272400 H 4.22069900 -1.94875900 1.69564200 C -5.30933700 0.48041300 -0.59091700 H -6.18951400 0.09133800 -1.09249200 C -3.25447000 -2.99720700 -0.05139700 H -2.90617200 -4.01147500 0.12680600 H -3.76324100 -2.92037100 -1.00943000 H -3.93772500 -2.68239600 0.73457400 C 3.31150300 -3.01703100 -1.38626400 H 3.70011800 -3.47324800 -2.28824800 C -3.05145400 1.37726700 0.65056100 H -2.13678600 1.69186900 1.13137000 C 1.79359000 -1.29163200 2.16665500 H 1.64936300 -0.22406100 2.00362300 H 2.52057600 -1.46379500 2.95577100 H 0.84847300 -1.76347400 2.42335700 C 4.15923500 -2.73136300 -0.31625800 H 5.21747100 -2.95014700 -0.35281800 C 1.64482200 4.53072400 -0.35749100 H 1.07378400 5.44537800 -0.46246000 C 3.78597300 3.41376900 -0.19460400 H 4.86792100 3.45649600 -0.17066300 C -5.32204300 1.75167500 -0.01851000 H -6.21397900 2.36321500 -0.06780800 C 3.04228600 4.58549900 -0.31795200 H 3.54652600 5.54160600 -0.38910500 C -4.16926700 2.20250200 0.61560400 H -4.14105100 3.18020200 1.08134200 |
| Z-2a-N-Me⁺ N 0.46298700 1.50749500 1.48820300 N -0.45818300 0.66162400 1.49037000 | TS1-2a-N-Me⁺ N -0.70389900 -1.46919600 -0.11714500 N 0.50530800 -1.26394600 -0.09955200 | TS2-2a-N-Me⁺ N -0.08534200 -1.59508000 -0.52843600 N -0.68981200 -0.53332100 -0.39786600 |

| | |
|--|---|
| N -1.59434400 -1.60872700 -1.02694500 N -4.12553300 -0.25447400 -0.86351100 N 2.32229800 -1.36524200 1.22350200 N -0.29557000 -1.92928100 -1.05338500 C 0.30083000 -1.13649600 -0.15848400 C -0.64737700 -0.27172600 0.44886300 C -1.87972200 -0.62143300 -0.11925500 C 1.75009600 -1.21492800 -0.00604100 C 1.29550200 1.76184200 0.35440900 C -3.21356700 -0.04348200 0.09833900 C 2.57678300 -1.13815200 -1.12773400 H 2.10251600 -1.03163000 -2.09192800 C 0.80700400 1.90639000 -0.95161900 H -0.24510800 1.76495000 -1.15947300 C 2.63936100 2.02700600 0.63464900 H 2.97648700 1.98653800 1.66356900 C 3.67127000 -1.36516500 1.36801900 H 4.03655000 -1.47005900 2.37958400 C -5.34571000 0.25652700 -0.69796800 H -6.05432500 0.06711900 -1.49780700 C -2.49990400 -2.36949000 -1.89277000 H -1.90668200 -3.17591700 -2.31653000 H -2.90275200 -1.72513000 -2.66997300 H -3.32615300 -2.76457200 -1.30610400 C 3.95247700 -1.15985900 -0.99107800 H 4.58878400 -1.08643400 -1.86387900 C -3.49346300 0.69154200 1.25748400 H -2.72762600 0.84774800 2.00485600 C 1.49947300 -1.56627400 2.44084900 H 1.25290900 -0.60404400 2.88643200 H 2.07092000 -2.17117500 3.14017400 H 0.58628900 -2.08666900 2.16695300 C 4.51014100 -1.25667200 0.28545900 H 5.57997100 -1.26100800 0.44175100 C 1.68019800 2.26605000 -1.97022100 H 1.30132600 2.40134800 -2.97619000 C 3.51330600 2.34982700 -0.39793100 H 4.55651400 2.54495600 -0.18036900 C -5.72012900 0.99645400 0.42176000 H -6.72499100 1.39034000 0.50521200 C 3.03599000 2.46862600 -1.70210500 H 3.70851900 2.75117600 -2.50296800 C -4.77158400 1.21293900 1.41621900 H -5.02058600 1.78155100 2.30399400 | N -3.04612700 1.96327300 0.23997800 N -5.02641100 -0.16292400 0.23533800 N 1.43756600 2.06455800 -0.69047400 N -1.95275400 2.71095100 0.29001300 C -0.90881100 1.90287500 0.03405600 C -1.38161800 0.55842700 -0.21386000 C -2.79883700 0.65332100 -0.10646300 C 0.43648000 2.41436300 0.17267400 C 0.74215700 -2.02435700 0.54488300 C -3.79632800 -0.39280200 -0.26528300 C 0.74581800 3.27704100 1.23243100 H -0.05999800 3.56259400 1.89277400 C 0.73689700 -1.42672500 1.81094400 H 0.06710200 -0.60044000 2.01551300 C 1.59770600 -3.08519700 0.24737200 H 1.59513700 -3.49035200 -0.75523600 C 2.72334000 2.43648000 -0.46658700 H 3.45420300 2.03186500 -1.15397100 C -5.95947000 -1.10242400 0.08489100 H -6.93531100 -0.87137500 0.50266900 C -4.33233400 2.62047400 0.45541500 H -4.11335800 3.67774700 0.58523700 H -4.82266600 2.20649000 1.33331500 H -4.98137700 2.46477400 -0.40509000 C 2.04275200 3.70648800 1.43581700 H 2.27306800 4.36290800 2.26617800 C -3.48130000 -1.59193700 -0.93450700 H -2.49576100 -1.75692300 -1.34399000 C 1.16830300 1.31123700 -1.93695300 H 1.37174800 0.25323500 -1.79167400 H 1.84325700 1.68613700 -2.70218100 H 0.13747300 1.48426900 -2.23363800 C 3.05492700 3.25608300 0.58515800 H 4.09096100 3.52623200 0.73220500 C 1.60308500 -1.90111500 2.78007500 H 1.61475700 -1.45097400 3.76564900 C 2.48134200 -3.53718700 1.21933600 H 3.18530700 -4.32497500 0.98446300 C -5.73665000 -2.31912400 -0.55320100 H -6.53103800 -3.04969700 -0.63794400 C 2.48127400 -2.94946500 2.48124800 H 3.17594500 -3.29744100 3.23672300 C -4.46659300 -2.55717300 -1.07435600 H -4.24433500 -3.48473800 -1.58879400 |
| E-2a-Me-MeSO₄ N -0.40793200 0.84032800 -0.34427700 N -1.66966300 0.83275800 -0.32269000 N -3.61994300 -2.09709800 0.16977400 N -5.89579300 -0.31841900 0.25720500 N 0.83549500 -1.98435700 0.11038300 N -2.44454100 -2.69044600 -0.12670000 C -1.57155800 -1.70575900 -0.31628500 C -2.19814200 -0.44059000 -0.15001600 C -3.53610000 -0.73389200 0.15918800 C -0.20189100 -2.00484100 -0.77453200 C 0.21995900 2.07261400 -0.58668600 C -4.65632800 0.17547600 0.41923000 C 0.04972100 -2.32565800 -0.209763600 H -0.78517000 -2.35114700 -2.78368200 C -0.44327300 3.22408900 -1.04552900 H -1.50861800 3.18816500 -1.23259300 C 1.60117500 2.08661500 -0.36231800 H 2.09210700 1.19884000 0.01477400 C 2.09724200 -2.23773900 -0.28525600 H 2.86643900 -2.15770800 0.46421400 C -6.93158800 0.49219600 0.47330900 H -7.91534100 0.05497300 0.33083300 C -4.75786000 -2.95941400 0.47511600 H -4.36071200 -3.96831200 0.55888000 H -5.50385200 -2.89879500 -0.31441100 H -5.21908100 -2.65083400 1.41155300 | Z-2a-Me-MeSO₄ N 0.56089600 1.60655900 0.66232000 N 1.50742900 1.38645600 -0.12235000 N 3.46963300 -1.51449500 -0.83193200 N 5.75304800 0.07787800 -0.11046900 N -0.96852200 -0.85151900 -1.45219700 N 2.25927200 -2.07712200 -0.95415700 C 1.36838900 -1.12120300 -0.67609500 C 2.03213900 0.09290200 -0.35981300 C 3.39931600 -0.18801000 -0.49499900 C -0.05236700 -1.49731500 -0.67326700 C 0.02726000 0.60941800 1.53340600 C 4.56315000 0.68010900 -0.27413000 C -0.47176900 -2.56855600 0.10465600 H 0.26506800 -3.06296700 0.71884300 C 0.83510500 -0.19117900 2.35356100 H 1.91340300 -0.10727900 2.30818800 C 1.36448600 0.55664000 1.63177100 H -1.97368900 1.19526800 1.00386800 C -2.26478300 -1.23113900 -1.46466100 H -2.93575600 -0.66518600 -2.09057400 C 6.82709100 0.84200200 0.09086100 H 7.76754600 0.31486100 0.22113100 C 4.63431800 -2.34872200 -1.12080300 H 4.24286200 -3.29010500 -1.49923100 H 5.22289700 -2.50321100 -0.21943600 H 5.26459300 -1.86732800 -1.86589600 |

| | | |
|---|---|--|
| C 1.35305100 -2.57353500 -2.52556100 H 1.54876100 -2.79436900 -3.56783900 C -4.42267400 1.50284000 0.80919600 H -3.41074300 1.86267300 0.92303600 C 0.60129600 -1.60244000 1.51899500 H 0.14133400 -0.61617100 1.52086800 H 1.56573100 -1.53714000 2.01318600 H -0.05440900 -2.33660200 1.98479500 C 2.39062500 -2.51899200 -1.60779500 H 3.43035600 -2.65141400 -1.87088100 C 0.29163500 4.37697900 -1.27051500 H -0.20416100 5.26938700 -1.63548100 C 2.32909700 3.25061000 -0.58641300 H 3.39720600 3.23070700 -0.41000600 C -6.79840500 1.82486500 0.85485600 H -7.67573300 2.43893400 1.01504600 C 1.67487000 4.39269700 -1.04127900 H 2.23757400 5.30041600 -1.22802600 C -5.51392600 2.33355800 1.02430500 H -5.36156500 3.36337000 1.32509100 C 7.06787200 -0.05793100 1.43067800 H 7.65061100 -0.17171800 2.34416300 H 7.24941000 0.92579100 0.99056900 H 7.33679000 -0.84066000 0.71610000 O 5.69725800 -0.18700100 1.82779100 S 4.59569700 -0.05346200 0.59305300 O 4.85788900 -1.20578900 -0.30475000 O 4.81930900 1.26360500 -0.02258600 O 3.31301400 -0.18491800 1.33014400 | C -1.80737000 -2.94933000 0.11956000 H -2.13183600 -3.76141400 0.75803000 C 4.41897200 2.07564300 -0.23808400 H 3.44202800 2.52064200 -0.36799300 C -0.62661200 0.33722700 -2.26421200 H -0.97891300 1.22055500 -1.73250600 H -1.15217600 0.26024100 -3.21297600 H 0.44443700 0.37051500 -2.43139400 C -2.71845700 -2.26857600 -0.67644400 H -3.77772100 -2.48219100 -0.68918900 C 0.23204300 -1.06883000 3.24555800 H 0.84870800 -1.67413800 3.90034300 C -1.95759500 -0.35921200 2.49566100 H -3.03908800 -0.41006800 2.51595500 C 6.78266500 2.23228900 0.14043700 H 7.68640500 2.80394000 0.31032100 C -1.16146100 -1.16704500 3.30544200 H -1.62198300 -1.86057100 3.99998100 C 5.54902600 2.85445800 -0.03135600 H 5.46488100 3.93441700 -0.00309200 C -6.89679800 1.87377500 0.24083100 H -7.41258400 2.81278400 -0.43755900 H -6.97414100 1.61745900 0.81861100 H -7.32716900 1.07563100 -0.85135800 O -5.52884200 2.10286900 -0.60419700 S -4.52578600 0.80286900 -0.41050000 O -5.01847800 -0.24427300 -1.33929500 O -4.61077500 0.41785300 1.01203800 O -3.21492200 1.36678300 -0.81377800 | C -1.65148100 2.21499000 2.21480100 H -1.88071600 3.26186800 2.36236900 C 4.32824500 -0.36717200 -1.88481800 H 3.35403500 -0.22313600 -2.32806000 C -0.76996000 -1.87236200 1.50912800 H -1.71651200 -2.40514000 1.51251200 H -0.08990600 -2.22980300 2.27823000 H -0.33343600 -1.96733000 0.51793200 C -2.65505600 1.25652500 2.23876100 H -3.69177100 1.51631600 2.39753900 C -1.68366900 4.35644800 -0.66398200 H -1.67306200 5.42183100 -0.45932100 C -2.88015100 2.31736300 -1.11828900 H -3.79892000 1.75636200 -1.24149800 C 6.70712000 -0.61785800 -2.04523700 H 7.62368800 -0.68217400 -2.61819100 C -2.89431600 3.68915800 -0.84059600 H -3.83226500 4.22605800 -0.77130500 C 5.47414300 -0.44266000 -2.66603400 H 5.40215700 -0.36931400 -3.74458300 C -5.60315700 -0.06379900 -1.61705100 H -5.82341300 -3.78716500 -2.40110800 H -6.20869000 -2.16468700 -1.75422600 H -5.80246500 -3.50282900 -0.63601100 O -4.20932500 -2.75767100 -1.75654100 S -3.61277800 -1.68059100 -0.65432300 O -3.75933900 -2.34063800 0.67495000 O -4.42774400 -0.45627100 -0.77554900 O -2.20684400 -1.53932500 -1.08072300 |
| T52-2a-Me-MeSO₄ | E-2a-Me-BF₄ | Z-2a-Me-BF₄ |
| N -0.99402600 -1.84219000 0.04267100 N -1.66622200 -0.97963800 0.02198300 N -3.94276200 1.85021300 -0.21342500 N -6.07561400 -0.09249300 -0.19034300 N 0.60391800 1.44930700 -0.57101500 N -2.78999200 2.55051000 -0.21386400 C -1.80698900 1.66218800 -0.13028900 C -2.33839300 0.31514800 -0.11241600 C -3.75150400 0.49934300 -0.19915600 C -0.42648200 2.06556400 0.08267100 C 0.21825000 -1.78919900 0.79557900 C -4.79911600 -0.51605100 -0.24614000 C -0.11670900 3.00714500 1.06393800 H -0.94034000 3.49629500 1.56454300 C 0.47596500 -0.81438800 1.76939300 H -0.29934100 -0.10670500 2.03650100 C 1.18486400 -2.74346700 0.46859300 H 0.95244600 -3.48445900 -0.28673200 C 1.89298000 1.66028700 -0.21406100 H 0.26250300 1.06891900 -0.75510900 C -7.04925900 -0.99847100 -0.26603900 H -8.06285500 -0.61151500 -0.21636400 C -5.18436900 2.61879300 -0.26879600 H -4.88816800 3.66478600 -0.29772600 H -5.79484600 2.40747000 0.60625800 H -5.75469700 2.35252100 -1.15648500 C 1.20295500 3.25386300 1.41657900 H 1.42813200 3.97263400 2.19534500 C -4.47061700 -1.87805500 -0.37492100 H -3.43986900 -2.19761200 -0.41437300 C 0.41373200 0.57376500 -1.75442300 H 0.78417100 -0.42132600 -1.51991700 H 0.10110000 0.98250200 -2.56729000 H -0.63305800 0.55406000 -2.03360200 C 2.22320800 2.53975700 0.79250700 H 3.26887000 2.62272200 1.05482000 C 1.72194200 -0.77471200 2.37488800 H 1.93872900 -0.02096400 3.12250000 C 2.44360700 -2.67093000 1.05269800 H 3.23700700 -3.33374000 0.73698300 C -6.82063000 -2.36559400 -0.39813700 | N 0.20530100 0.82299200 -0.57779500 N -1.04245900 0.79432900 -0.39765700 N -3.00650400 -2.12095200 0.06712000 N -5.24802600 -0.29021800 0.14525400 N 1.43501200 -0.20858000 0.05970600 N -1.84260000 -2.72762800 -0.24723600 C -0.95460600 -1.75354100 -0.42391800 C -1.55914400 -0.48152000 -0.23061700 C -2.89855900 -0.76131400 0.08643200 C 0.41723700 -2.08452000 -0.84537100 C 0.76559400 2.09404500 -0.80667000 C -4.00265600 0.15966500 0.37474400 C 0.68512600 -2.49694600 -2.14038000 H -0.13752900 -2.55269100 -2.83901000 C 0.00684000 3.24795100 -1.06858900 H -0.107173900 3.17571400 -1.11420000 C 2.16262000 2.15438600 -0.76641000 H 2.73429400 1.26299400 -0.54604200 C 2.70236700 -2.32559500 -0.29071300 H 3.44771800 -2.22299300 0.48661900 C -6.26913200 0.53214700 0.38634800 H -7.25895800 0.13253700 0.18720300 C -4.15964500 -2.96663600 0.36098800 H -3.78045200 -3.98245000 0.44400100 H -4.89890200 -2.89051800 -0.43367600 H -4.62131600 -2.65379900 1.29577100 C 1.98779000 -2.80636500 -2.52024300 H 2.19935400 -3.11225000 -3.53756900 C -3.74643800 1.44997700 0.86090200 H -2.72956200 1.77220200 1.02963900 C 1.17305300 -1.56812200 1.44261200 H 1.02303700 -0.49010800 1.41384100 H 2.05062000 -1.77673700 2.04597700 H 0.29259100 -2.08091500 1.82238900 C 3.00670500 -2.71140200 -1.58397400 H 4.03766300 -2.92117300 -1.83160300 C 0.65708100 4.45294700 -1.27909700 H 0.08195100 5.34715400 -1.49053200 C 2.80238300 3.37406800 -0.96508000 H 3.88279800 3.42210900 -0.90818600 C -6.11329500 1.83221200 0.86098200 | N 0.12694900 -1.24264800 -1.28226700 N 1.04917700 -1.25890100 -0.44190700 N 2.87537000 1.25756600 1.30587700 N 5.21928500 0.04273000 0.16832000 N -1.56811300 0.39993000 1.42783900 N 1.64756600 1.74237100 1.54006700 C 0.79391700 0.92754000 0.91407300 C 1.50068000 -0.11243500 0.25231700 C 2.85287900 0.11777900 0.54891200 C -0.63132300 1.27771700 0.96386400 C -0.46829200 -0.03672600 -1.76387600 C 4.05122100 -0.61949000 0.12327000 C -1.03372200 2.54806600 0.57442400 H -0.27755900 3.22730500 0.21182600 C 0.29422800 1.02020900 -2.27788900 H 1.37567500 0.97328500 -2.25369100 C -1.86310000 -0.01849500 -1.84500100 H -2.43195900 -0.85946800 -1.46834000 C 2.87610700 0.73486300 1.47303800 H -3.55201700 -0.03600000 1.82043900 C 6.32522500 -0.59976000 -0.20908800 H 7.24710400 -0.02796000 -0.16074500 C 4.00584500 1.95232900 1.91871100 H 3.57668200 2.69511900 2.58703900 H 4.62145200 2.42134400 1.15464500 H 4.62115000 1.24691400 2.47356600 C -2.37459300 2.90546900 0.61850000 H -2.68457700 3.88951600 0.28973800 C 3.95957200 -1.95171900 -0.30609300 H 2.99681500 -2.44248700 -0.33905300 C -1.20176500 -0.96735400 1.87250700 H -1.26340300 -1.64491800 1.02293900 H -1.93172500 -1.28626300 2.61065300 H -0.20227300 -0.94528100 2.29700700 C -3.30747100 1.98073000 1.06510700 H -4.36707200 2.19117500 1.08931700 C -0.35429600 2.11144600 -2.84353300 H 0.22922800 2.92254000 -3.26396700 C -2.49957500 1.09986800 -2.37310900 H -3.58218300 1.12032900 -2.39871100 C 6.33389100 -1.92099300 -0.64711000 |

| | | |
|---|---|---|
| H -7.65099400 -3.05831800 -0.45151000 C 2.71421800 -1.68584900 1.99957100 H 3.70987400 -1.60889300 2.41486600 C -5.50046500 -2.80436800 -0.45562700 H -5.27132800 -3.85824200 -0.56022400 C 7.18556800 0.10723900 -1.17389400 H 7.79329600 0.42798600 -2.01962100 H 7.53021000 -0.86465700 -0.81214700 H 7.24788600 0.84584700 -0.36943200 O 5.84655900 0.01358000 -1.67177300 S 4.71157800 -0.45799300 -0.54939600 O 4.65184400 0.64617500 0.44322700 O 5.18581100 -1.73710700 -0.00109900 O 3.49077700 -0.53482900 -1.38887000 | H -6.97931400 2.45772200 1.03765300 C 2.05501800 4.51997100 -1.22262500 H 2.55457700 5.46869200 -1.38210700 C -4.82246400 2.29357400 1.10209600 H -4.65379800 3.29557800 1.47847800 F 4.30105400 -1.31191100 2.01737800 F 3.16007400 0.68932200 1.93505700 F 4.31504300 -0.05573000 0.08849500 F 5.47417300 0.68874200 1.94949900 B 4.33871400 0.03512500 1.51897600 | H 7.26160900 -2.39331700 -0.94487800 C -1.74996200 2.16120900 -2.87842700 H -2.24776800 3.01820800 -3.31744300 C 5.12216900 -2.60507300 -0.69140900 H 5.07979400 -3.63554400 -1.02369000 F -4.44733200 -1.74043800 1.74166200 F -3.13644900 -2.31513400 -0.06224800 F -4.68149200 -0.62542000 -0.26267700 F -5.39700700 -2.82130800 -0.07646200 B -4.44726400 -1.90653000 0.31805000 |
| TS1-2a-Me-BF₄ | TS2-2a-Me-BF₄ | E-2a-Me-Cl |
| N -0.27980700 1.71540100 0.62079600 N -1.42452600 1.27789100 0.65205600 N -2.91149000 -1.28174700 -1.33206500 N -5.40324200 -0.33056500 -0.21672400 N 1.37673600 -1.17555600 -1.17496900 N -1.67292500 -1.33730300 -1.86892300 C -0.94852200 -0.42579200 -1.22944100 C -1.73858500 0.22954700 -0.24555300 C -3.01235500 -0.35198500 -0.34330200 C 0.47431700 -0.22278200 -1.55405700 C 0.94506300 2.23789700 0.51233100 C -4.24318500 -0.06852600 0.40737400 C 0.92486100 0.90786500 -2.21506400 H 0.20267200 1.65710300 -2.50540000 C 1.11523000 3.48688600 -0.13537700 H 0.24457400 4.03076400 -0.47913400 C 2.07991200 1.53396300 0.98200400 H 1.97017100 0.57025300 1.46127200 C 2.69613100 -1.02103800 -1.40943400 H 3.34015500 -1.80346800 -1.03313900 C -6.53872600 -0.07397500 0.43285700 H -7.45541100 -0.29645500 -0.10466500 C -3.92097500 -2.20102800 -1.85232600 H -3.38790700 -2.92682600 -2.46175800 H -4.65638000 -1.66079900 -2.44464100 H -4.43142100 -2.69445200 -1.02772200 C 2.28191100 1.08371900 -2.46079400 H 2.63208600 1.98769200 -2.94105900 C -4.18545300 0.45386000 1.70602100 H -3.23073000 0.65626100 2.16852200 C 0.91830000 -2.40197100 -0.47392800 H 0.37106900 -2.10725400 0.41845600 H 1.79472800 -2.96544800 -0.17234800 H 0.27719300 -2.96784000 1.14595300 C 3.17620300 0.10703200 -0.204844300 H 4.24334900 0.21184700 -2.17977200 C 2.39959100 3.97993300 -0.33645100 H 2.51677900 4.92780700 -0.85083200 C 3.33949100 2.07993900 0.80196400 H 4.18870300 1.50872000 1.15617900 C -6.58282400 0.45107800 1.72228000 H -7.53432500 0.64151200 2.20271100 C 3.51916200 3.29364600 0.13007100 H 4.51287800 3.69689000 -0.01907300 C -5.37860700 0.71722200 2.36655900 H -5.36541500 1.12127500 3.37172500 F 3.80761800 -2.99579400 0.58558300 F 2.53506100 -1.49834500 1.78588400 F 4.55916300 -0.84523500 0.89791400 F 4.50466800 -2.31139900 2.69016700 B 3.87795700 -1.91608000 1.52915000 | N -0.08534200 -1.59508000 -0.52843600 N -0.68981200 -0.53332100 -0.39786600 N -3.04612700 1.96327300 0.23997800 N -5.02641100 -0.16292400 0.23533800 N 1.43756600 2.06455800 -0.69047400 N -1.95275400 2.71095100 0.29001300 C -0.90881100 1.90287500 0.03405600 C -1.38161800 0.55842700 -0.21386000 C -2.79883700 0.65332100 -0.10646300 C 0.43648000 2.41436300 0.17267400 C 0.74215700 -2.02435700 0.54488300 C -3.79632800 -0.39280200 -0.26528300 C 0.74581800 3.27704100 1.23243100 H -0.05999800 3.56259400 1.89277400 C 0.73689700 -1.42672500 1.81094400 H 0.06710200 -0.60044000 2.01551300 C 1.59770600 -3.08519700 0.24737200 H 1.59513700 -3.49035200 -0.75523600 C 2.72334000 2.43648000 -0.46658700 H 3.45420300 2.03186500 -1.15397100 C -5.95947000 -1.10242400 0.08489100 H -6.93531100 -0.87137500 0.50266900 C -4.33233400 2.62047400 0.45541500 H -4.11335800 3.67774700 0.58523700 H -4.82266600 2.20649000 1.33331500 H -4.98137700 2.46477400 -0.40509000 C 2.04275200 3.70648800 1.43581700 H 2.27306800 4.36290800 2.26617800 C -3.48130000 -1.59193700 -0.93450700 H -2.49576100 -1.75692300 -1.34399000 C 1.16830300 1.31123700 -1.93695300 H 1.37174800 0.25323500 -1.79167400 H 1.84325700 1.68613700 -2.70218100 H 0.13747300 1.48426900 -2.23363800 C 3.05492700 3.25608300 0.58515800 H 4.09096100 3.52623200 0.73220500 C 1.60308500 -1.90111500 2.78007500 H 1.61475700 -1.45097400 3.76564900 C 2.48134200 -3.53718700 1.21933600 H 3.18530700 -4.32497500 0.98446300 C -5.73665000 -2.31912400 -0.55320100 H -6.53103800 -3.04969700 -0.63794400 C 2.48127400 -2.94946500 2.48124800 H 3.17594500 -3.29744100 3.23672300 C -4.46659300 -2.55717300 -1.07435600 H -4.24433500 -3.48473800 -1.58879400 F 4.40274700 0.34072300 -1.77582500 F 2.82750500 -1.33788900 -1.90451200 F 3.14122100 -0.19864800 0.07028700 F 4.75769700 -1.67399900 -0.67761500 B 3.80793400 -0.74578300 -1.07032200 | N 0.69955100 0.95693800 -0.11903100 N -0.55265000 0.82745200 -0.17632700 N -2.36655700 -2.21180900 -0.03728700 N -4.70802100 -0.53225700 -0.27585200 N 1.99707900 -2.01176600 0.63836900 N -1.13212600 -2.73930700 -0.17895700 C -0.28743700 -1.71150600 -0.21855200 C -0.99581700 -0.48387700 -0.10401900 C -2.34848000 -0.84919300 0.00577700 C 1.14702100 -1.98433000 -0.43765700 C 1.18114300 2.27538300 -0.25717100 C -3.53984100 -0.00315800 0.12705400 C 1.62205500 -2.32898600 -1.68191300 H 0.93342800 -2.32857700 -2.51447700 C 0.37672800 3.36867600 -0.62439700 H -0.67391500 3.21100300 -0.82910400 C 2.54839300 2.44562100 -0.01646300 H 3.15829100 1.59001900 0.26323000 C 3.30529200 -2.32593000 0.49649300 H 3.88249300 -2.40865300 1.39819100 C -5.80477500 0.22068200 -0.19130200 H -6.72704400 -0.24329000 -0.52819200 C -3.49273500 -3.13368200 0.06898100 H -3.06407700 -4.12445900 0.20075300 H -4.10536200 -3.09181800 -0.82935900 H -4.11271800 -2.86855900 0.92356400 C 2.97097600 -2.68158800 -1.84575800 H 3.34341700 -2.95075300 -2.82648400 C -3.44328100 1.30104200 0.63531700 H -2.48460300 1.68943500 0.94524200 C 1.54567200 -1.51738400 1.94823900 H 1.50900800 -0.42877800 1.89610600 H 2.27298300 -1.81281200 2.69860800 H 0.56628300 -1.93031000 2.17886400 C 3.80733600 -2.69302000 -0.75351400 C 4.85576300 -2.94165300 -0.82937300 C 0.94947400 4.62552800 -0.73383400 H 0.33929400 5.47353700 -1.02362500 C 3.10833500 3.71618100 -0.12330000 H 4.16603500 3.84587600 0.07193000 C -5.80523200 1.52757000 0.28948600 H -6.72656600 2.09479600 0.33327100 C 2.31552600 4.80350600 -0.47977500 H 2.75467900 5.79080100 -0.56867800 C -4.59527300 2.07190600 0.71065800 H -4.54823200 3.08282400 1.09817900 CI 4.68879000 -0.09023800 1.06463800 |
| Z-2a-Me-Cl | TS1-2a-Me-Cl | TS2-2a-Me-Cl |
| N -0.24167000 -1.64305500 1.05106300 N 0.63934800 -0.78249500 1.25661500 N 2.07948700 1.71938700 -0.85629500 N 4.59328500 0.37386400 -0.44227000 | N 0.28281100 1.62496100 0.09618700 N -0.91598100 1.36896900 0.14366500 N -2.55971100 -1.69015500 -0.67117800 N -5.00995900 -0.20358700 -0.31806500 | N 0.28281100 1.62496100 0.09618700 N -0.91598100 1.36896900 0.14366500 N -2.55971100 -1.69015500 -0.67117800 N -5.00995900 -0.20358700 -0.31806500 |

| | | |
|---|--|--|
| N -2.08435700 1.50655300 0.84554900 N 0.79060300 2.06006700 -1.00765700 C 0.08195900 1.17847100 -0.29762500 C 0.94494100 0.24267600 0.32624100 C 2.24135500 0.63513400 -0.03289900 C -1.38537000 1.28115600 -0.31439000 C -0.90112400 -1.79035600 -0.20760400 C 3.53186900 0.02256800 0.30329300 C -2.06797200 1.21215900 -1.50976900 H -1.50083000 1.03809100 -2.41117600 C -0.20651700 -1.83946800 -1.42399600 H 0.86804200 -1.71293700 -1.44506100 C -2.27745500 -2.02144600 -0.16239900 H -2.80053500 -1.97751700 0.78714600 C -3.43794100 1.58417000 0.84665700 H -3.90100000 1.84151400 1.78126100 C 5.77653500 -0.17014500 -0.15544100 H 6.06035700 0.13943000 -0.78397500 C 3.08083400 2.55177400 -1.51820000 H 2.53737100 3.38970400 -1.94865800 H 3.59800800 1.98430700 -2.28872800 H 3.81627300 2.90099600 -0.79606000 C -3.46334900 1.32919300 -1.53124400 H -3.99526000 1.26387400 -2.47217200 C 3.63245600 -0.89226800 1.36352000 H 2.75355600 -1.15123700 1.93822800 C -1.43183500 1.53431800 2.16696400 H -1.60324600 0.56817900 2.64492800 H -1.89964200 2.31508400 2.76368400 H -0.37324400 1.74123100 2.05254700 C -4.14800400 1.51840800 -0.35147100 H -5.22521600 1.59038300 -0.31199000 C -0.90852700 -2.07881600 -2.59873800 H -0.37422800 -2.13668500 -3.54012100 C -2.97308000 -2.21910200 -1.35061800 H -4.04682700 -2.35878300 -1.31370500 C 5.97332500 -1.08394500 0.87567800 H 6.95660500 -1.49732600 1.06195300 C -2.29475200 -2.25185400 -2.56738900 H -2.83671400 -2.43021200 -3.48917800 C 4.87283400 -1.44513700 1.64871500 H 4.97685100 -2.15076400 2.46452800 Cl -4.22554600 -0.57544200 2.25422200 | N 1.73722000 -1.66259200 -0.10595100 N -1.30107700 -2.05963000 -1.00231700 C -0.52971600 -1.00875200 -0.75339500 C -1.30604800 0.06402500 -0.23952600 C -2.62640800 -0.41196000 -0.20607400 C 0.92150800 -1.03847100 -1.00563900 C 1.58725100 1.90224500 0.00260200 C -3.86500400 0.25872800 0.21068700 C 1.47982200 -0.42827100 -2.11475200 H 0.82374100 0.07301900 -2.81222400 C 2.05774500 2.71762500 -1.05687500 H 1.34696100 3.15211100 -1.74810300 C 2.51403100 1.34909300 0.91889600 H 2.18701300 0.70918900 1.72811100 C 3.07846200 -1.69056100 -0.27128300 H 3.64846900 -2.11875900 0.55150200 C -6.15032400 0.39210600 0.03051500 H -7.05354500 -0.00889400 -0.41919300 C -3.62142900 -2.68043600 -0.83476700 H -3.12512500 -3.63126600 -1.01358600 H -4.26409900 -2.41349700 -1.67101800 H -4.22654700 -2.72767600 0.06828400 C 2.86028600 -0.43591900 -2.29683800 H 3.29617100 0.06850100 -3.14946100 C -3.82996600 1.33241100 1.11070900 H -2.88662800 1.67927700 1.50603800 C 1.18852100 -2.30187400 1.11351800 H 1.97227500 -2.25582100 1.87815600 H 0.90446300 -3.32784900 0.88073700 H 0.31305400 -1.74688800 1.43976800 C 3.66347100 -1.07691300 -1.36693300 H 4.74081100 -1.08566500 -1.45059200 C 3.42438700 2.92276800 -1.20255400 H 3.77239400 3.53092400 -2.03074700 C 3.86492500 1.61098100 0.76666300 H 4.54004400 1.14568500 1.47586300 C -6.21546600 1.46832600 0.91229400 H -7.16998000 1.91563200 1.15977400 C 4.33819500 2.38130200 -0.29962100 H 5.39950200 2.56014500 -0.41827000 C -5.02756200 1.94290300 1.45989300 H -5.03085800 2.77554500 2.15311900 Cl 4.01992300 -1.38562400 2.68296100 | N 1.73722000 -1.66259200 -0.10595100 N -1.30107700 -2.05963000 -1.00231700 C -0.52971600 -1.00875200 -0.75339500 C -1.30604800 0.06402500 -0.23952600 C -2.62640800 -0.41196000 -0.20607400 C 0.92150800 -1.03847100 -1.00563900 C 1.58725100 1.90224500 0.00260200 C -3.86500400 0.25872800 0.21068700 C 1.47982200 -0.42827100 -2.11475200 H 0.82374100 0.07301900 -2.81222400 C 2.05774500 2.71762500 -1.05687500 H 1.34696100 3.15211100 -1.74810300 C 2.51403100 1.34909300 0.91889600 H 2.18701300 0.70918900 1.72811100 C 3.07846200 -1.69056100 -0.27128300 H 3.64846900 -2.11875900 0.55150200 C -6.15032400 0.39210600 0.03051500 H -7.05354500 -0.00889400 -0.41919300 C -3.62142900 -2.68043600 -0.83476700 H -3.12512500 -3.63126600 -1.01358600 H -4.26409900 -2.41349700 -1.67101800 H -4.22654700 -2.72767600 0.06828400 C 2.86028600 -0.43591900 -2.29683800 H 3.29617100 0.06850100 -3.14946100 C -3.82996600 1.33241100 1.11070900 H -2.88662800 1.67927700 1.50603800 C 1.18852100 -2.30187400 1.11351800 H 1.97227500 -2.25582100 1.87815600 H 0.90446300 -3.32784900 0.88073700 H 0.31305400 -1.74688800 1.43976800 C 3.66347100 -1.07691300 -1.36693300 H 4.74081100 -1.08566500 -1.45059200 C 3.42438700 2.92276800 -1.20255400 H 3.77239400 3.53092400 -2.03074700 C 3.86492500 1.61098100 0.76666300 H 4.54004400 1.14568500 1.47586300 C -6.21546600 1.46832600 0.91229400 H -7.16998000 1.91563200 1.15977400 C 4.33819500 2.38130200 -0.29962100 H 5.39950200 2.56014500 -0.41827000 C -5.02756200 1.94290300 1.45989300 H -5.03085800 2.77554500 2.15311900 Cl 4.01992300 -1.38562400 2.68296100 |
| E-2a-Me-I | Z-2a-Me-I | TS1-2a-Me-I |
| N -0.03138300 1.72659400 -0.83712900 N 0.37783700 0.59326100 -0.57373200 N 2.31119400 -2.09351600 0.55916500 N 4.58247200 -0.29591600 0.48570000 N -1.94028100 -1.86175600 -1.04160000 N 1.11646900 -2.68815400 0.54602000 C 0.23326200 -1.78424100 0.11444500 C 0.90322900 -0.54664800 -0.19884200 C 2.27855600 -0.80863000 0.06504500 C -1.19042900 -2.09515000 0.08579300 C -0.98309400 2.30819600 0.05007700 C 3.42146300 0.07695400 -0.08949900 C -1.81154900 -2.63172000 1.19971900 H -1.20437700 -2.83295400 2.07009300 C -1.46502300 1.67688100 1.20153900 H -1.14736600 0.66979600 1.43662100 C -1.41486600 3.58856400 -0.29955000 H -1.03118300 4.03548700 -1.20847000 C -3.29519600 -1.96608900 -1.01704900 H -3.79831100 -1.80439500 -1.95324200 C 5.64989600 0.48605900 0.33177700 H 6.56155300 0.14256700 0.81281800 C 3.45260800 -2.87734400 1.01954000 H 3.06500000 -3.86865500 1.24374300 H 3.89405600 -2.42011800 1.90257000 H 4.21508900 -2.92834400 0.24393500 C -3.18876700 -2.88309800 1.18891800 | I 4.32328700 -1.41707900 -0.24548300 N -0.30329500 -1.32143900 1.09715200 N -1.19823800 -1.30125100 0.22628600 N -3.12121500 1.35641100 -1.19352400 N -5.43998200 -0.03276200 -0.20385500 N 1.29823800 0.53987600 -1.59152600 N -1.90153400 1.87328600 -1.40579900 C -1.02828600 1.00597700 -0.88698000 C -1.71258400 -0.10131200 -0.32306000 C -3.07255500 0.14156800 -0.56137100 C 0.40079900 1.34908700 -0.93835900 C 0.16766000 -0.14251900 1.75140100 C -4.24786200 -0.65233400 -0.18176800 C 0.84349500 2.53312800 -0.38571300 H 0.12231100 3.15900600 0.11679300 C -0.69003400 0.82154300 2.29851100 H -1.76258700 0.72134300 2.19483900 C 1.54755000 -0.05698200 1.94263000 H 2.19792600 -0.82196400 1.53388300 C 2.61556000 0.85945600 -1.65129200 H 3.2 | |

| | | |
|--|--|--|
| | C 2.19754100 2.88166100 -0.44895300 H 2.53973800 3.80446100 0.00196900 C -4.11137400 -1.99979400 0.18695200 H -3.13298100 -2.46044900 0.19682200 C 0.91662000 -0.76223200 -2.16692600 H 1.23571800 -1.54744400 -1.47757200 H 1.44069700 -0.88774700 -3.11207900 H -0.15519400 -0.79441400 -2.33015800 C 3.08625400 2.03616000 -1.08091100 H 4.14561000 2.24224100 -1.13585700 C -0.14802600 1.89300300 2.99737500 H -0.80648900 2.63165600 3.43991300 C 2.08053800 1.04322500 2.60530100 H 3.15584000 1.11950300 2.71339300 C -6.48673400 -2.07104700 0.51400100 H -7.39804400 -2.58966900 0.78407300 C 1.23718300 2.01699400 3.13632600 H 1.65122000 2.86113600 3.67579300 C -5.25076600 -2.71190300 0.53436300 H -5.17222500 -3.75448500 0.81908100 | C 1.96278000 0.98040100 -2.57313800 H 2.27634100 1.88724700 -3.07293000 C -4.44106500 0.53353800 1.69557600 H -3.49210200 0.81671600 2.12608300 C 0.79730300 -2.49647300 -0.46475200 H 1.64966700 -2.70395800 0.18680100 H 0.59250300 -3.32622200 -1.14057400 H -0.08105400 -2.29542900 0.13957000 C 2.87936000 -0.00115000 -2.24635600 H 3.93294000 0.09955800 -2.46433700 C 1.95471300 4.14976200 -0.63089100 H 2.01769000 5.07899300 -1.18704300 C 3.00732800 2.34054700 0.55653000 H 3.88794600 1.82176400 0.91697300 C -6.83716400 0.45224800 1.72889300 H -7.79297800 0.66044500 2.19316000 C 3.11555600 3.53309500 -0.16520000 H 4.08622900 3.97299900 -0.35662600 C -5.64022200 0.82450500 2.33304700 H -5.63730000 1.33252100 3.29002800 |
| TS2-2a-Me-I I 3.59717400 0.84205500 0.05042100 N -0.00684900 1.13427300 1.07266600 N -0.66575200 0.13254700 0.78626200 N -2.63363500 -2.54093300 -0.34634300 N -4.85420100 -0.65369600 -0.41797000 N 1.77561100 -2.11956900 0.83204900 N -1.42879000 -3.09053900 -0.45838900 C -0.54305500 -2.19862600 0.00289300 C -1.22145100 -0.97382500 0.36549400 C -2.59542000 -1.24367700 0.11655600 C 0.88612000 -2.43829400 -0.16559800 C -0.12161600 2.26181800 0.20562800 C -3.72553400 -0.35116900 0.25876000 C 1.37413400 -3.00047900 -1.33338900 H 0.66065700 -3.26875300 -2.09869000 C -1.01499100 2.32972000 -0.87035600 H -1.68355000 1.50281900 -1.07096200 C 0.75156300 3.31513200 0.48510600 H 1.45331600 3.20330600 1.30065500 C 3.11302200 -2.14145300 0.60243800 H 3.73921300 -1.84324600 1.42608200 C -5.87559100 0.19713500 -0.35568200 H -6.76395000 -0.08846300 -0.91224800 C -3.80210500 -3.37108400 -0.61540500 H -3.42758000 -4.37064000 -0.82338800 H -4.36141800 -2.97472300 -1.45961100 H -4.45697500 -3.38426100 0.25625800 C 2.74845400 -3.17903800 1.51721900 H 3.11950200 -3.62700600 -2.43048900 C -3.62198300 0.81741500 1.03846100 H -2.73268000 1.01791000 1.61745800 C 1.34198300 -1.59638600 2.13649600 H 1.45787300 -0.51044400 2.13601500 H 1.97590700 -2.03632200 2.90490100 H 0.30842800 -1.87823400 2.31170400 C 3.62434300 -2.71881200 -0.55458800 H 4.69622900 -2.75238700 -0.68579100 C -1.03315100 3.46869500 -1.66164300 H -1.72229900 3.53731400 -2.49513600 C 0.73020500 4.44910400 -0.31803100 H 1.41633800 5.26339400 -0.12045000 C -5.84859400 1.39359800 0.35939500 H -6.70813800 2.05166700 0.36272300 C -0.16106100 4.52704300 -1.38696400 H -0.17571500 5.41106100 -2.01397800 C -4.69250700 1.69904200 1.07209500 H -4.62667400 2.60835100 1.65802400 | | |